Analysis of Cellular Transcriptomic Changes Induced by Merkel Cell Polyomavirus miRNA

Pouria AKHBARI

Submitted for the degree of

Doctor of Philosophy

Centre for Skin Sciences

School of Chemistry and Biosciences

Faculty of Life Sciences

University of Bradford

2017

Abstract

Pouria Akhbari

Analysis of Cellular Transcriptomic Changes Induced by Merkel Cell Polyomavirus miRNA

Keywords: Virus, Cancer, miRNA

Merkel cell carcinoma (MCC) is a highly aggressive skin cancer with rising global incidence. Merkel cell polyomavirus (MCV) was discovered in 2008 in 80% of MCC samples and since then a causal link between MCV and the majority of MCC cases has been established. microRNAs (miRNA, miR) are a family of small non-coding RNAs which play a key role in post-transcriptional regulation of gene expression and are considered significant players in disease and development in many species. Whilst the focus of MCV research has thus far been on the oncogenic MCV early proteins, large tumour (LT) and small tumour (sT) antigens, there is a knowledge gap regarding MCV miRNA and its functional significance in MCV pathogenesis. Given the emerging importance of viral miRNAs in virus-host interaction and pathogenesis, the aim of this doctoral research project was to investigate alterations in host cell transcripts induced by MCV miRNA and determine any functional significance these might have on virus-host cell interaction. RNA sequencing (RNA-Seq) in the presence and absence of MCV miRNA uncovered a multitude of downregulated cellular transcripts. Gene ontology analysis revealed that MCV miRNA targets transcripts associated with multiple cellular processes, however, regulation of immune response was overrepresented in our datasets. Validation of RNA-Seq data using MCV

miRNA mimics and a synthetic, fully replicative MCV genome (MCVSyn) confirmed RNA-Seq data at mRNA and protein expression level for several targets, including the cytokine stimulating gene, SP100, and the neutrophil stimulator chemokine, CXCL8. Moreover, dual luciferase assays revealed that SP100 and MAPK10 (a member of mitogen-activated protein kinases (MAPK) family which is involved in regulation of CXCL8 expression) are directly and specifically targeted and downregulated by MCV miRNA. The MCV miRNA-dependent dysregulation of CXCL8 secretion is associated with impaired neutrophil migration, suggesting that the virus miRNA may be implicated in evasion of the host immune response.

Acknowledgements

I would like to thank my first supervisor, Dr. Jim Boyne, for his patient support, meticulous and constructive advice and feedback on my work throughout this project. I would also like to thank Dr. Boyne for the encouragement and the opportunity he gave me to work in his laboratory before and during my PhD project.

I would like to thank my second supervisor, Prof. Desmond Tobin, for his kind advice and support during this doctoral project.

I would also like to thank the following members of staff for their kind help and support during my project; Dr. Stephen Sikkink, Mr Richard Baker, Mr Emtiaz Aziz and Mr Lasty Sibanda.

Special thanks to Dr. Sally Fairweather (Saint James's Hospital, Leeds) for training on RNA-Seq and Dr. Krzysztof Poterlowicz for initial RNA-Seq data analysis.

I would like to say a huge thank you to my lovely wife Azi for her patience and support during my postgraduate studies.

Contents

List of Figures

List of Tables

Abbreviations

3'UTR	3'untranslated region
5'UTR	5'untranslated region
4E-BP1	eIF4E–binding protein 1
ADP	adenosine diphosphate
ADRA1D	alpha-1D adrenergic receptor
AGO, Ago	Argonaute
AJCC	American Joint Committee on Cancer
ALTO	Alternate frame of the Large T Open reading frame
AMBRA1	Activating Molecule In Beclin-1-Regulated Autophagy protein 1
Arg	arginine
ATM	Ataxia telangiectasia mutated
Atoh1	atonal homolog 1
ATP	adenosine triphosphate
BCLAF1 / BTF	BCL2-associated transcription factor 1
BKV	BK polyomavirus
BLV	bovine leukaemia virus
bp	basepair
BPCV	bandicoot papillomatosis carcinomatosis virus
Brd4	Bromodomain-containing protein 4
BrdU	Bromodeoxyuridine
BSA	bovine serum albumin
C/EBP	CCAAT-enhancer-binding protein

CAF1	CCR4-associated factor 1
CCL2	C-C motif ligand 2
CCNE2	cyclin E2
CCR4	C-C chemokine receptor type 4
CD	cluster of differentiation
cDNA	complementary deoxyribonucleic acid
CGRP	calcitonin gene-related peptide
CK	cytokeratin
CLLs	chronic lymphocytic leukaemias
cm	centimetre
CNS	central nervous system
CR1	conserved region 1
CXCL8	C-X-C motif ligand 8
CYB5R2	cytochrome b5 reductase 2
DAVID	Database for Annotation, Visualization and Integrated Discovery
DDR	DNA damage response
DDX6	DEAD-box helicase 6
DHFR	dihydrofolate reductase
DLA	dual luciferase assay
DMSO	dimethyl sulfoxide
dscDNA	double-stranded complementary deoxyribonucleic acid
dsDNA	double-stranded deoxyribonucleic acid
dsRBD	dsRNA-binding-domain
dsRNA	double-stranded ribonucleic acid

DTS	digital transcriptome subtraction
EBV	Epstein-Barr Virus
EDTA	ethylenediaminetetraacetic acid
EGF	epidermal growth factor
eIF4E	eukaryotic translation initiation factor 4E
ELISA	enzyme-linked immunosorbent assay
EXP5	exportin-5
Ezh	enhancer of zeste homolog
FBS	fetal bovine serum
FBW7	F-box and WD repeat domain-containing 7
Fluc	firefly luciferase
FOX2	RNA Binding Protein, Fox-1 Homolog 2
GAPDH	Glyceraldehyde 3-phosphate dehydrogenase
GDP	guanosine diphosphate
GGR	global genomic repair
GO	gene ontology
GTP	guanosine triphosphate
h	hour
HAART	highly active antiretroviral therapy
HBP1	HMG-box transcription factor 1
HIV	human immunodeficiency virus
HPV	human papillomavirus
HSC70 / HSPA8	heat shock 70 kDa protein 8
HSV	herpes simplex virus
ICP0	infected cell polypeptide 0

IE	immediate-early protein
IFI30	interferon, gamma-inducible protein 30
IFIH1	interferon induced with helicase C domain 1
IFN	interferon
IkB	inhibitors of κB
IKK	IκB kinase
ISG	interferon-stimulated gene
JCV	JC polyomavirus
JNK3	c-Jun N-terminal kinase 3
kb	kilobase
KLLN	killin
KSHV	Kaposi's sarcoma-associated herpesvirus
LSD	LT stabilising domain
LT Ag	Large tumour antigen
Lys	lysine
m7G	7-Methylguanosine
MAPK	mitogen-activated protein kinases
MAPK10	mitogen-activated protein kinase 10
MAVS	mitochondrial antiviral-signalling protein
MC	Merkel cell
MCC	Merkel cell carcinoma
MCV, MCPyV	Merkel cell polyomavirus
MDA5	Melanoma Differentiation-Associated protein 5
MECP2	Methyl-CpG Binding Protein 2
miRISC	complex of miRNA and RISC

miRNA, miR	microRNA
MM	Master mix
mM	millimolar
mRNA	messenger ribonucleic acid
MT	middle T Ag
mTOR	mechanistic target of rapamycin
MuPyV	murine polyomavirus
MUR	MCV T antigen unique region
Mut, mut	mutant
NCCR	Non-coding Control Region
NCRR	Non-coding Regulatory Region
NEMO	NF-κB essential modulator
NF-H	heavy chain neurofilament
NF-κB	nuclear factor kappa-light-chain-enhancer of activated B cell
ng	nanogram
NLS	nuclear localisation signal
nm	nanometre
NOT1	negative regulator of transcription 1
NRT	no reverse transcriptase control
NS	no significance
nt	nucleotide
NTC	no template control
o/n	overnight
OBD	origin binding domain

ORI	origin of replication
OSR1	odd-skipped related 1
p.t.	post-transfection
PABP	poly(A)-binding protein
PAMP	pathogen-associated molecular pattern
PAR-CLIP	Photoactivatable-Ribonucleoside-Enhanced Crosslinking and Immunoprecipitation
PAZ	PIWI–AGO–ZWILLE
PBS	phosphate-buffered saline
PCNA	proliferating cell nuclear antigen
PHO2	Phosphate 2
PI3K	phosphoinositide 3-kinase
PIK3CD	Phosphatidylinositol-4,5-Bisphosphate 3-Kinase Catalytic Subunit Delta
PKB	protein kinase B
PML-NB	promyelocytic leukaemia nuclear bodies
Pol II	RNA polymerase II
PP2	protein phosphatase 2
pRb, RB	retinoblastoma protein
PRC	polycomb repressive complex
pre-miRNA	precursor miRNA
pri-miRNA	primary miRNA
PRR	pattern recognition receptor
PSME3	Proteasome Activator Subunit 3
PUMA	p53 upregulated modulator of apoptosis

RAET1G	Retinoic acid early transcript 1G
RAN.GTP	GTP-binding RAs-related Nuclear protein
RE	response element
RFC	Replication factor C
RIIIDa	RNase III domain
RISC	RNA-induced silencing complex
RLC	RISC loading complex
RLCV	Rhesus Lymphocryptovirus RLCV
Rluc	*Renilla* luciferase
RNAi	RNA interference
RPA70	replication protein A 70
rpm	revolutions per minute
RT	room temperature
RTA	replication and transcription activator
RUNX1	Runt Related Transcription Factor 1
SCF	SKP1, CUL1 and F-box containing complex
SCLC	small cell lung cancer
SDS	sodium dodecyl sulfate
SELPLG	selectin P ligand
siRNA	small interfering RNA
SNP	single nucleotide polymorphisms
Sox2	sex determining region Y box 2
ssDNA	single-stranded deoxyribonucleic acid
ssRNA	single-stranded ribonucleic acid
sT Ag	Small tumour antigen

SV40	simian virus 40
T Ag	Tumour antigen
t.p.	time point
TAE	Tris Acetate EDTA
TANK	TRAF family member-associated NF-kappa-B activator
TBS	Tris-buffered saline
TGF-β	transforming growth factor beta
TLR9	Toll-like receptor 9
TNF-α	tumour necrosis factor alpha
TRAF	TNF receptor associated factor
TRBP	trans-activation response RNA-binding protein
TRIM28	tripartite motif-containing 28
TUT	terminal uridylyl transferase
ULBP3	UL16 binding protein 3
UR	uranaffin reaction
UVB	Ultraviolet B
v/v	volume/volume
VP1	viral capsid protein 1
w/v	weight/volume
Wnt	Wingless-related integration site
WT, wt	wild type
ZTA	bZip transcription transactivator
µg	microgram
µM	micromolar
µl	microlitre

CHAPTER 1

Introduction

1. Introduction

1.1. Background

Merkel cell polyomavirus (MCV or MCPyV) was identified in 2008 in 80% of Merkel cell carcinoma (MCC) samples via digital transcriptome subtraction (DTS) (Feng *et al.* 2008). MCC is a rare but aggressive skin cancer that typically occurs in immunocompromised individuals. However, the rising incidence of MCC especially in the ageing population (Hodgson 2005) and implication of MCV in the majority of MCC cases has prompted extensive research on the life cycle and virus-host interaction of MCV as well as mechanisms leading to MCV infection and MCC tumourigenesis. Thus far, the central role of LT and sT antigens of MCV in cell transformation, maintenance of cancerous state and metastasis has been described (Houben *et al.* 2010; Shuda *et al.* 2015). MCV T antigens also play an important role in virus immune evasion by targeting host innate immune ligands TLR9 (Toll like receptor 9) and nuclear factor kappa-light-chain-enhancer of activated B cells (NF-κB) essential modulator (NEMO) (Griffiths *et al.* 2013; Shahzad *et al.* 2013). These immune evasion and oncogenesis properties have been described in other polyomaviruses and herpesviruses. Murine polyomavirus (MuPyV) and bandicoot papillomatosis carcinomatosis virus (BPCV) have been directly implicated in the aetiology of cancer (Stewart *et al.* 1958; Woolford *et al.* 2007). BK and JC polyomaviruses establish persistent infection in their host by targeting UL16 binding protein 3 (ULBP3) via an identical virus-encoded miRNA (Bauman and Mandelboim 2011; Bauman *et al.* 2011) and Epstein-Barr Virus (EBV) and Kaposi's sarcoma-associated herpesvirus (KSHV) manipulate host immune response

in order to establish latent/persistent infection (Li *et al.* 2016; Piedade and Azevedo-Pereira 2016; Sun *et al.* 2016). Despite significant differences in terms of genome size and complexity (~5kb versus >120kb), polyomaviruses and herpesviruses share several common features including, a double-stranded DNA (dsDNA) genome, the ability to code for miRNAs and the capacity to establish latent and persistent infection in their host (Arvin *et al.* 2007; Cann 2012). Of particular relevance to this thesis is the emerging role of viral miRNAs in immune evasion and carcinogenesis, as described in tumorigenic herpesviruses, such as KSHV and EBV (Pfeffer and Voinnet 2006; Boss *et al.* 2011; Suffert *et al.* 2011; Kincaid and Sullivan 2012). In addition, as mentioned above, BK and JC polyomaviruses encode an identical miRNA that is implicated in virus persistence and immune evasion (Bauman *et al.* 2011). Reduced susceptibility of wild type (WT) simian virus 40 (SV40) polyomavirus to cytotoxic T-cells compared to miRNA-mutant virus suggests a role for SV40 miRNA in host immune evasion (Sullivan *et al.* 2005). Similarly, a miRNA-deficient MCV loses its ability to establish long term infection (Theiss *et al.* 2015). Whilst these observations are indicative of a role for SV40 and MCV miRNAs in host immune evasion it is yet to be determined whether the miRNA exerts such effect solely by downregulating its cognate target, the virus LT antigen or, like BK and JC viruses, via direct targeting of transcripts encoding components of the host cell immune system. The aim of this thesis was to determine if MCV miRNA (MCV-miR-M1) modulates the expression of cellular transcripts and the functional impact of any observed alteration on MCV and host cell interactions.

1.2. Merkel Cells

Merkel cells (MCs) are 10-15µm oval shape cells, located in basal layer (*stratum basale*) of the epidermis, the hair follicle external sheath (Lucarz and Brand 2007), ectoderm-derived mucosa (Halata *et al.* 2003) and may also be found in the dermis (Mahrle and Orfanos 1974; Moll *et al.* 1986) (Figure 1.1). Merkel cells are defined as slowly adapting type 1 (SA1) mechanoreceptors and are involved in sense of touch, predominantly found in areas of skin with acute sensory perception such as finger tips, and form mechanoreceptors in synaptic contact with discoid axon terminals while simultaneously binding to keratinocytes via desmosomes (Ross and Wojciech 2010). It has been shown that elimination of MCs via atonal homolog 1 (Atoh1) knockout results in loss of light touch sense in the mice skin (Maricich *et al.* 2009). A model has been proposed in which activation of mechanosensitive receptors leads to MC depolarisation followed by opening of voltage-gated calcium channels and calcium-induced Ca++ release in MCs. This results in release of thus far unidentified neurotransmitters which in turn triggers action potential in SA1 afferent nerves (Nakatani *et al.* 2015).

MCs are most prevalent in the palm of hands, the feet and plantar surface of the toes (Hartschuh and Grube 1979). They are also more abundant in sun-exposed skin compared to covered skin (Lucarz and Brand 2007). Morphologically, MCs are characterised by their oval shape with protrusions, a large lobulated nucleus and dense core granules near their junction with nerve terminals (Figure 1.2) (Halata *et al.* 2003). Hair follicle MCs generally lack nerve association and it is suggested that they may contribute to hair development by paracrine activity (Lucarz and Brand 2007), however, it is

postulated that unlike nerve terminal-associated MCs, hair follicle MCs are considered immature (undifferentiated) cells because of the absence of nerve connection (Uchigasaki *et al.* 2004). In addition, Merkel cell-like cells are located in the skin with suggested neuroendocrine but not mechanoreceptor functions (Halata *et al.* 2003; Lucarz and Brand 2007). These cells usually reside in the same area as MCs, however, they can be distinguished by a pale oval nucleus, non-lobulated nucleus, skin surface-facing dense-core granules, lack of contact with nerve endings and lack of cytoplasmic processes (Figure 1.3). Halata *et al.* conclude that, based on the available data, it is not certain whether MC-like cells and MCs are from different origins with different functions or they both stem from the same origin but adopt different forms and functions (Halata *et al.* 2003). Unless stained by specific markers, MCs are difficult to identify and hardly recognisable via light microscopy. In electron microscopy, MCs characteristically appear as cells bearing 80-140nm dense-core granules near the cells nerve terminal junction site, with nuclear lobules and microvilli protruding into neighbouring cells (Figure 1.4).

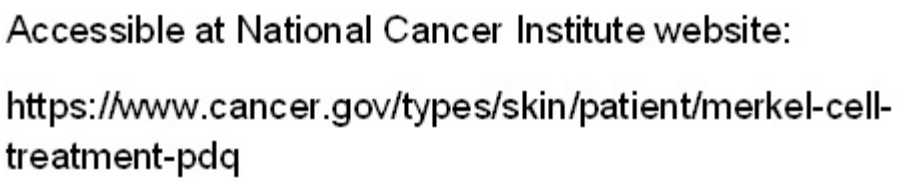

Figure 1.1. Location of Merkel cells in the skin. Taken from National Cancer Institute (General Information About Merkel Cell Carcinoma 2016).

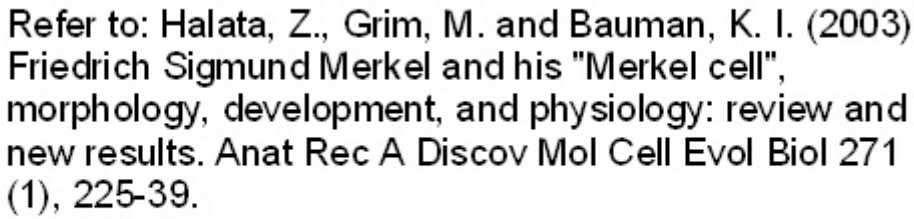

Figure 1.2. Merkel cells in the skin of the eyelid. A Merkel cell (M) surrounded by nerve terminals (T) and glial cells (S) and in contact with an epidermal keratinocyte (K) (A and B); cytoplasmic protrusions of Merkel cells are marked by asterisks (B). Taken from (Halata *et al.* 2003).

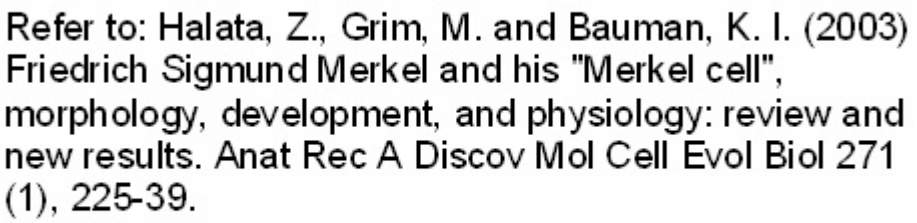

Figure 1.3. Merkel cell-like cells (N) with oval shape and non-lobulated nucleus and without cytoplasmic protrusions or contact with nerve endings. Dense-core granules are mainly located towards the skin surface (Right, larger magnification). K, keratinocyte; F, fibroblast. Taken from (Halata *et al.* 2003).

MCs also form desmosomes (intercellular junctions responsible for providing adhesion between cells (Garrod and Chidgey 2008)) with surrounding keratinocytes and might similarly bear small numbers of melanosomes (Lucarz and Brand 2007). With regards to their cytoskeleton, MCs express epithelial type cytokeratin (CK) filaments such as CK8, CK18, CK19 and CK20. Similarly, both MCs and MCCs express neuroendocrine markers such as synaptophysin and chromogranin A, while NF-H, a heavy chain neurofilament has also been reported in adult human scalp MCs (Moll *et al.* 2005). A variety of markers have been used to identify MCs. In light microscopy, CK20 is the most specific marker for cutaneous MCs (Boot *et al.* 1992; Moll *et al.* 1995). Specificity and sensitivity of CK20 has also been used for diagnosis of MCC and differential diagnosis of MCC with other

neoplasms such as melanoma (Scott and Helm 1999). Uranaffin reaction (UR) is a specific staining for neurosecretory (NS) granules of the neuroendocrine system (Beiras *et al.* 1986) and electron microscopy-based detection of uranaffin has been used for identification of MCs (Munde *et al.* 2013). Other neuropeptides such as Calcitonin gene-related peptide or CGRP (Garcia-Caballero *et al.* 1989) and vasoactive intestinal polypeptide or VIP (Alvarez *et al.* 1988) have been detected in dense-core granules of MCs.

Refer to: Lucarz, A. and Brand, G. (2007) Current considerations about Merkel cells. Eur J Cell Biol 86 (5), 243-51.

Figure 1.4. Schematic presentation of the ultrastructure of a mechanoreceptor Merkel cell. MCs contain dense-core granules (G) located near the nerve junction (NJ) site, melanosomes (me) and a lobulated nucleus (N). P, cytoplasmic protrusions (or microvilli); m, mitochondria; go, Golgi apparatus; D, desmosome; A, axon; BL, basal lamina; HD, hemidesmosome; if, intermediate filaments; K, keratinocyte. Taken from (Lucarz and Brand 2007).

The developmental origin of MCs has been a matter of controversy and both the neural crest and epidermis have been proposed as the origin of MCs. The neural crest hypothesis is supported by the observation that avian MCs migrate, along with melanocytes and glial cells, from neural crest (Grim and Halata 2000), however, it is noteworthy that Grandry cells, the avian equivalent of MCs, reside in the dermis rather than epidermis (Lucarz and Brand 2007). The evidence for neural crest origin of mammalian MCs comes from the observation that whisker pad MCs express β-galactosidase under the control of Wnt1 promoter in R26R double transgenic mice. Given that Wnt1 is specifically and transiently expressed in neural crest and some cells of the embryonic central nervous system (CNS), the authors conclude that β-galactosidase-positive MCs are of neural crest descent (Szeder *et al.* 2003). However, most recent studies provide strong evidence for the epidermal origin of mammalian MCs. It has been shown that MCs express the transcription factor Atoh1 and require its expression for their formation (Ben-Arie *et al.* 2000; Maricich *et al.* 2009). Using conditional ablation of Atoh1 from the skin or neural crest, Morrison *et al.* showed that MCs are absent in the skin of epidermal but not the neural crest mouse lineage (Morrison *et al.* 2009). Atoh1-dependent differentiation of MCs from epidermal progenitor cells was independently confirmed via another *in vivo* mouse study (Van Keymeulen *et al.* 2009), further strengthening the epidermal origin hypothesis. Van Keymeulen *et al.* showed that Atoh1 conditional ablation renders MCs undetectable via both ultrastructural investigation and immunoreactivity of markers such as CK18, CK20 and Rab3c in newborn and adult mice (Van Keymeulen *et al.* 2009). Finally, most recently it has

been shown that Atoh1 is directly activated by SRY (sex determining region Y)-box 2 (Sox2) transcription factor, whilst Sox2 itself is repressed by the polycomb repressive complex (PRC) histone-lysine N-methyltransferases Enhancer of zeste homolog 1 (Ezh1) and Ezh2 in epidermal stem cells (Bardot *et al.* 2013). Bardot *et al.* described a Sox2 binding site in the Atoh1 enhancer and demonstrated a significant upregulation in Atoh1 mRNA following overexpression of Sox2 in cultured epidermal progenitor cells. Ezh1/Ezh2 ablation resulted in Sox2 upregulation and MC differentiation whilst Sox2 ablation led to the loss of MCs in the epidermis of all tested body regions in the mice, suggesting that Sox2 is repressed by Ezh1 and Ezh2 preventing it from driving differentiation of epidermal progenitor cells to MCs (Bardot *et al.* 2013). While our understanding of Merkel cell physiology and differentiation has increased in recent years, the mechanisms underlying transformation of MCs to cancerous state remain largely unknown. However, the identification of MCV and its key role in most MCC cases is shedding light on MCC pathophysiology.

1.3. Merkel cell carcinoma

Merkel cell carcinoma is a rare, aggressive skin tumour with increasing incidence (Hughes *et al.* 2014) and a mortality rate higher than malignant melanoma (Becker 2010).

First described as a trabecular skin carcinoma (Toker 1972), MCC was subsequently reclassified as a neuroendocrine cancer following discovery of neurosecretory granules in MCs (Gould *et al.* 1985; Becker 2010). However, as discussed above, more recent findings are predominantly in favour of an

epidermal origin for MCs. Around 33% of MCC patients exhibit distant metastases and outcome for these patients is poor due to the lack of effective chemotherapy in metastatic and recurrent cases (Hughes *et al.* 2014). Importantly, regression of MCC following improvement in immune response (Burack and Altschuler 2003) and association of higher incidence of MCC with T-cell dysfunction i.e. in solid organ transplant receivers (5-10 fold), AIDS patients (11-13 fold) and chronic lymphocytic leukaemia patients (Becker 2010), accentuate the significance of the immune system in MCC (Hughes *et al.* 2014). Similar features have been reported in malignancies associated with viruses such as KSHV where tumour incidence demonstrates positive and negative association with immune compromise and immune reconstitution, respectively (Bihl *et al.* 2007; Hislop and Sabbah 2008; Giffin and Damania 2014). These similarities suggest involvement of an infectious component in the MCC aetiology.

In a retrospective population-based study using data gathered over more than three decades, it was revealed that MCC was more prevalent in men (61.5%) than women (38.5%). Women also had a higher ten-year relative survival rate than men (65% versus 50.5%, respectively) (Albores-Saavedra et al. 2010). In addition, the study demonstrated a higher prevalence for MCC in 60-85 year old white compared to black patients. MCC is predominantly located in the head and neck while the most common non-cutaneous sites include lips, salivary glands and lymph nodes, nasal cavity and oesophagus, vulva and vagina. The cancer stage was also determined as the best prediction factor for survival, where local stage defined as lesions confined to the dermis and regional involved the underlying musculoskeletal tissues.

Regional lymph nodes were classified as head and neck, trunk (lower and upper), extremities (lower and upper) and NOS (not otherwise specified). Distant stage comprised metastases and lymph nodes distant from the primary tumour site (Albores-Saavedra *et al.* 2010). Local lesions demonstrated the highest relative ten-year survival at 71% whereas distant stage showed the poorest rate at 21%. Unknown and regional stages reported 40.5% and 47.8% survival rates, respectively (Albores-Saavedra et al. 2010).

Patients refer to medical services due to the rapidly growing painless lesions in sun-exposed skin. Indeed, the positive correlation between UVB exposure and MCC incidence suggests that sun exposure, especially in fair skinned individuals, is a risk factor for MCC (Agelli *et al.* 2010), although unexposed skin might be affected too (Hughes *et al.* 2014). Recent data suggest an increase in the annual incidence of MCC by up to 10% in the US (1992-2001) and 8% in Australia (1986-2001). It should be noted, however, that part of this increase in the reported incidence is due to improvement in the diagnosis of MCC during 1980s and 1990s driven by CK20 staining (Agelli *et al.* 2010). Nevertheless, a more recent study of MCC cases between 2004 and 2013 in the east of England noted that the overall age-adjusted incidence of MCC has increased by three-fold within ten years, with a concurrent rising incidence in other areas of the UK (Goon *et al.* 2016). This study also reported the male to female ratio of MCC incidence in England as 2:3, which is contrary to the Agelli *et al.*'s report regarding gender risk factor. However, it must be noted that the sample size in Goon *et al.*'s study was significantly

smaller (73 versus 3870 cases) and therefore might not be a true representative of the actual ratio.

Inefficient or suppressed immune system is associated with increased risk of cancer. This correlation has been proved by multitude of reports about increased MCC incidence in transplant recipients and autoimmune patients which, as part of their treatment, receive long term and often potent immunosuppressants (Lentz *et al.* 1993; Gooptu *et al.* 1997; Penn and First 1999; Buell *et al.* 2002; Lillis *et al.* 2005; McLoone *et al.* 2005; Satolli *et al.* 2005; Nemoto *et al.* 2008). In a case report of an HIV-positive and MCC-positive patient, sustained remission of MCC was observed following highly active antiretroviral therapy (HAART) and use of interleukin-2 (IL-2) (Burack and Altschuler 2003). This report along with evidence for greater risk of developing MCC in HIV patients (Engels *et al.* 2002; Izikson *et al.* 2011) further underscores the link between an undermined immune system and onset of MCC. Based on these observations and the similarity with Kaposi's sarcoma, another common virus-driven malignancy of transplant and HIV patients, Feng *et al.* embarked on their search for an infectious element in MCC cases, a study which led to the discovery of MCV.

1.3.1. Diagnosis of MCC

MCC predominantly presents as an asymptomatic and rapidly growing red or pink cyst or acneiform lesion with an initially non-ulcerated appearance (Figure 1.5) and median size of 1.8cm at the time of diagnosis (Heath *et al.* 2008).

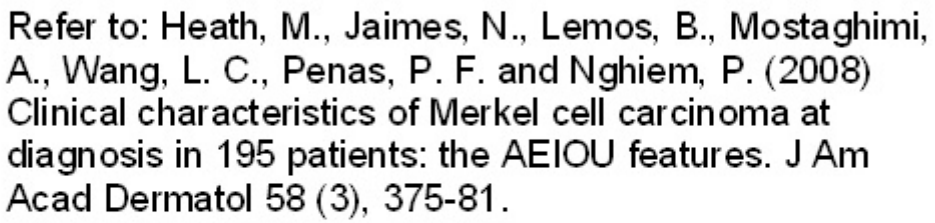

Figure 1.5. Examples of MCC clinical presentation on the eyelid (A), buttock in an HIV patient (B), finger (C) and arm (D). Taken from (Heath *et al.* 2008).

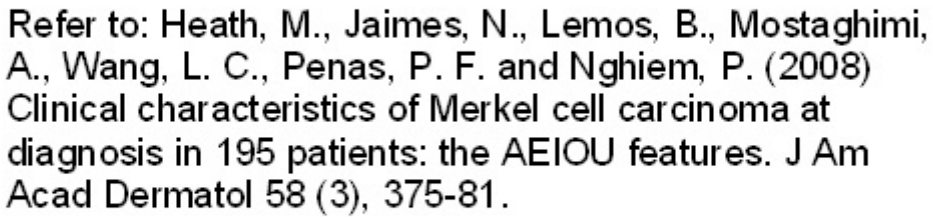

Figure 1.6. Body site distribution of primary MCC and MCC in lymph nodes with unidentified primary. Taken from (Heath *et al.* 2008).

Histopathological features of MCC include a solid nodular and dermal or subcutaneous lesion (Figure 1.7). Cells typically appear as uniform, highly mitotic and undifferentiated, often apoptotic and occasionally necrotic with scant cytoplasm, large oval/round lobulated nuclei, which stain blue on haematoxylin.

Refer to: Kuwamoto, S. (2011) Recent advances in the biology of Merkel cell carcinoma. Hum Pathol 42 (8), 1063-77.

Figure 1.7. Histologic presentation of MCC with dermal and subcutaneous solid nodular lesion (A), small-blue-round-cell on haematoxylin (B) and paranuclear dot-like staining (CK20), characteristic of MCC (C). Taken from (Kuwamoto 2011).

Infiltration of cells to the surrounding stroma and lack of capsule are common features of MCC (Kuwamoto 2011). In immunohistochemistry, MCC is identified by both epithelial (such as CK20 and AE1/AE3 cytokeratins) and neuroendocrine (neuron-specific enolase or NSE, synaptophysin and chromogranin A) markers (Table 1.1). NSE is also expressed in other neuroendocrine tumours such as small cell lung cancer (SCLC) (Kuwamoto 2011). CK20 immunohistochemistry results in a paranuclear dot-like staining (Figure 1.7 C) and is currently considered the best marker for differential diagnosis of MCC from other tumours (Kuwamoto 2011; Lebbe *et al.* 2015). MCV T antigen staining has also been used for identification of MCV-positive MCCs (Shuda *et al.* 2009).

Table 1.1. Immunohistochemistry markers for MCC diagnosis and differential diagnosis. Adapted from (Becker *et al.* 2013). SCLC, Small cell lung cancer.

	MCC	**Lymphoma**	**Melanoma**	**SCLC**
CK20	+	−	−	−
Neuron-specific-enolase (NSE)	+	−	−	+/−
Chromogranin A (CgA)	+/−	−	−	+/−
Huntingtin interacting protein 1 (HIP1)	+	+/−	−	−
Vimentin	−	+	+	−
Melan-A/MART-1	−	−	+	−
Leucocyte common antigen (LCA)	−	+	−	−
Thyroid transcription factor-1 (TTF-1)	−	−	−	+

1.3.2. Prognosis of MCC

The European consensus-based interdisciplinary guideline recommends clinical/histological features, distant tissue involvement and American Joint Committee on Cancer (AJCC) staging system be employed for prognostic classification of MCC (Lemos *et al.* 2010; Lebbe *et al.* 2015). Male gender, primary tumour size of more than 2cm and head, neck and trunk tumour locations are considered as unfavourable predictors. As mentioned earlier, female MCC patients have a higher 10-year survival rate (~65%) compared to males (~50%). Upper limb primary skin MCCs have a better 10-year survival rate (~61%) compared to skin of unknown site (~38%), trunk (~54%), head and lower limbs (~57%) MCCs. It must be noted, however, that the difference in survival rates were only statistically significant between head and upper limbs and between trunk and upper and lower limbs. Tumour size of more than 2cm also has a poorer 10-year survival rate (61% versus ~40%).

Differences in 10-year survival rates were most noticeable when the degree of primary tumour spread was taken into account. Localised MCCs showed the highest survival rate by 71%, followed by regional and unknown tumours with ~48% and ~40%, respectively. The poorest prognosis was identified for distant spreads with ~20% survival rate. Interestingly, no significant difference in the survival rate was observed between three different age groups of 0 to 49, 50 to 69 and 70 to 85 plus (Albores-Saavedra *et al.* 2010).

Histologically, thus far, no robust prognostic marker has been identified for MCC, however, T-cell tumour infiltration and lack of lymphatic system

invasion have been reported as favourable indicators for MCC prognosis (Sihto *et al.* 2012; Sihto and Joensuu 2012; Lebbe *et al.* 2015).

AJCC classification of MCC staging is based on three indicators of TNM, as defined by T for size and invasiveness of primary tumour, N for degree of lymph node involvement and M for metastatic state of MCC. Each of these criteria are classified to provide a scale for tumour staging and therefore for MCC prognosis. According to this staging system, the best 5 year survival rate is 79% for stage IA where primary tumour is =<2cm in diameter, there is no node involvement in pathologic examination and no distant metastasis. Concordant with the Albores-Saavedra *et al.* analysis, survival chance correlates negatively with tumour size (stages IB to IIC), however, the prognosis is poorer, regardless of primary tumour size, when nodal metastasis is present (stages IIIA and IIIB). When distant metastasis is present, the 5-year survival rate plummets to 18% and tumour size and nodal involvement are no longer a determinant of survival (Lemos *et al.* 2010; Lebbe *et al.* 2015). For a detailed TNM-based staging for MCC prognosis, refer to Table 1.2.

Table 1.2. MCC staging criteria based on TNM system to evaluate the 5 year survival rate of MCC patients outlined by AJCC. TIS, tumour in situ (tumour has not invaded the host organ supporting tissues, such as basement membrane and stroma (Young *et al.* 2000)); T1, primary tumour <2 cm; T2, primary tumour 2-5 cm; T3, primary tumour more than 5 cm; NO, absence of regional node metastasis; cNO, clinically detectable node, no pathologic examination; pNO, nodes negative clinically and pathologically; N1a, micrometastasis; N1b, macrometastasis; N2, transit metastasis; M1, distant metastasis. Adapted from (Lemos *et al.* 2010).

Stage	**T**	**N**	**M**	**% of 5-year survival**
O	TIS	N0	M0	
IA	T1	pN0	M0	79
IB	T1	cN0	M0	60
IIA	T2/T3	pN0	M0	58
IIB	T2/T3	cN0	M0	49
IIC	T4	N0	M0	47
IIIA	Any T	N1a	M0	42
IIIB		N1b/N2	M0	26
IV		Any N	M1	18

Overall, MCC treatment includes standard therapeutic approaches used for other malignancies, which routinely include surgical excision, chemotherapy and radiation therapy. One of the challenges in the treatment of MCC is the

sensitivity of the elderly to toxic side effects of the drugs, and to date there is no standardised systemic treatment protocol for MCC (Becker *et al.* 2013).

1.3.3. Treatment of MCC

Chemotherapy remains the main therapeutic approach for advanced MCC, however, several studies have reported a low rate of efficacy and high rate of mortality (Voog *et al.* 1999; Tai *et al.* 2000). Other treatment methods have been proposed against several therapeutic targets. It has been shown that a higher MCC survival rate is positively associated with infiltration of CD8+ lymphocytes into the tumour (Paulson *et al.* 2011). In another study, Afanasiev *et al.* also showed that MCV-specific T-cells increase or decrease alongside tumour progression or treatment-associated regression (Afanasiev *et al.* 2013). Moreover, the authors demonstrated that these T-cells expressed high levels of programmed death-1 (PD1) and T-cell immunoglobulin and mucin-domain (Tim-3). PD1 and Tim-3 are known as markers of T-cell exhaustion and functionality failure (Sakuishi *et al.* 2010) and several studies have shown that targeting PD1 and Tim-3 pathways can be a promising and safe therapeutic approach for cancer, including MCC (Sakuishi *et al.* 2010; Ngiow *et al.* 2011; Brahmer *et al.* 2012; Topalian *et al.* 2012). Dysregulated signalling pathways have been suggested as another therapeutic target for MCC. Specifically, studies have shown that phosphoinositide 3-kinase (PI3K) is upregulated in MCC (Hafner *et al.* 2012; Nardi *et al.* 2012). Both groups reported that phosphorylation of protein kinase B (PKB or AKT) occurs independently of MCV status in MCC. In this regard, the activated PI3K/AKT pathway in MCC has been suggested as a potential target for MCC treatment. Successful application of tumour necrosis

factor alpha (TNF-α) (Hata *et al.* 1997), anti-CD56 antibodies (Shah *et al.* 2016) and interferons (Wahl *et al.* 2016) have been reported, however, these alternative methods require further trial at larger scales. Finally, presence of MCV in the majority of MCCs and the central role of MCV T antigens in virus tumourigenesis may hold promise for novel therapeutic approaches in the majority of MCCs (Schrama and Becker 2011). MCV oncogenesis is discussed in detail in section 1.4.1.

1.4. Virology of MCV

Given that MCC is predominantly detected in immunosuppressed individuals and the elderly, Feng *et al.* hypothesised that an infectious agent is involved in the onset of MCC, a hypothesis that led to MCV discovery in 80% of MCCs using a novel technique called digital transcriptome subtraction (Feng et al. 2008). Briefly, the authors generated cDNA libraries from four MCC tumour samples and aligned them to human genome sequences. 'Subtracting' the human genome sequences, a sequence with high homology to African green monkey lymphotropic polyomavirus (LPyV) and human BK polyomavirus appeared. However, being sufficiently distinct from previously identified polyomaviruses the novel sequence was assigned a new place in this virus family and termed Merkel cell polyomavirus due to its association with MCC (Feng et al. 2008). Following this discovery, Feng *et al.* showed that MCV sequence is clonally integrated into the genome of tumour samples from 8 out of 10 MCC patients, indicating MCV as the aetiological agent of most MCC cases.

1.4.1. MCV genome structure

Merkel cell polyomavirus is an ~40nm non-enveloped double-stranded DNA (dsDNA) virus of the polyomaviridae family (Collier *et al.* 2010). The small circular genome of polyomaviruses (~5kb, Figure 1.8) is efficiently organised via the association with host cell histones H2A, H2B, H3 and H4, enabling the packaging of the virus genome into the capsid in a chromatin-like form (Cann 2012). The MCV genome contains early and late regions which code for the viral oncoproteins, LT and sT and viral capsid proteins VP1 and VP2/3, respectively (Feng *et al.* 2008; Cann 2012). These regions are under the control of a Non-coding Regulatory Region (NCRR) or Non-coding Control Region (NCCR), which separates the early and late region and functions as a virus origin of replication (ORI).

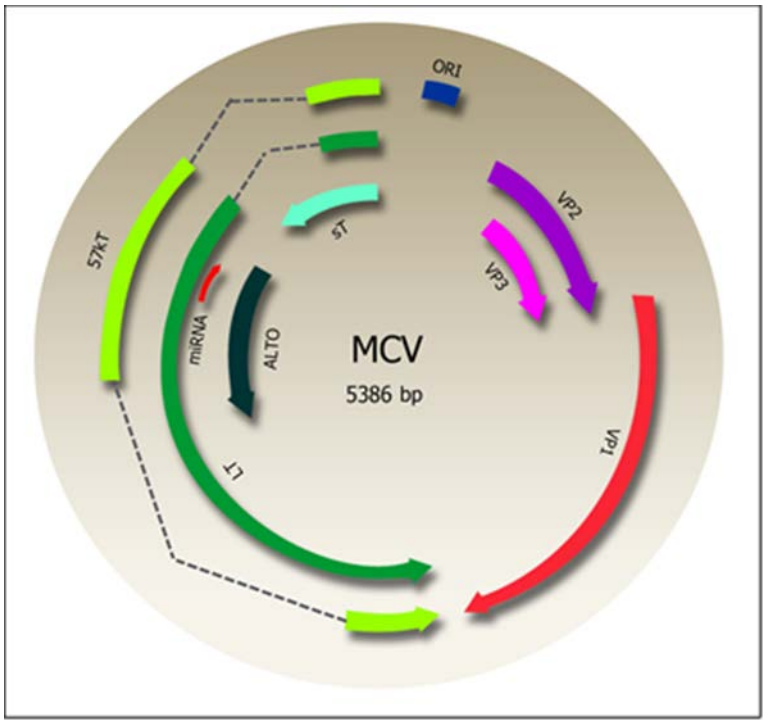

Figure 1.8. Schematic presentation of MCV genome with products of early (LT, sT, 57kT and ALTO) and late region (VP1, VP2, VP3 and miRNA).

This replication origin contains early and late promoters and is composed of ten pentanucleotide sequences, eight of which perfectly match LT-binding sequence 5'-GAGGC-3'. It has been shown that a minimum core ORI of 71 base pairs (bp) is sufficient for efficient LT-mediated DNA replication of MCV (Kwun *et al.* 2009). LT, the largest of all the early proteins, is transcribed from two exons and is translated to produce a protein 816 amino acids (aa) in length (Stakaityte *et al.* 2014). Several MCV LT domains are conserved among polyomavirus T antigens, including retinoblastoma (pRb, pRB) protein-binding (pRb-binding) motif or LXCXE, DnaJ, conserved region 1 (CR1), origin binding domain (OBD) and helicase/ATPase domain, highlighting a number of conserved functions for MCV LT in the virus life cycle (Feng *et al.* 2008).

The helicase domain is required for efficient DNA binding activity of LT, since lack of this portion of LT results in a marked reduction of DNA recognition by LT (Kwun *et al.* 2009). Binding of ATP to ATP-binding site of LT stimulates the binding of OBD to the origin of replication (Borowiec and Hurwitz 1988). LT then forms a hexamer ring which binds to OBD and the movement of two LT hexamer rings in opposite directions unwinds the circular virus dsDNA genome from the origin of replication (Topalis *et al.* 2013). MCVs with a truncated LT lose their replication capacity in MCV-positive MCCs and it has been shown that truncated LT is a characteristic of MCV-positive MCC cell lines (Shuda *et al.* 2008; Houben *et al.* 2010). Nakamura *et al.* identified a conserved and functional Arg–Lys–Arg–Lys sequence between pRb-binding and OBD as a nuclear localisation signal (NLS) in MCV-positive MCCs and suggested that this plays an important role in oncogenesis of MCV by

providing LT with access to the nucleus and consequent binding to pRb (Nakamura *et al.* 2010). pRb is an inhibitor of cellular proliferation (Frolov and Dyson 2004) which is dysregulated in some cancers (Murphree and Benedict 1984). It has been shown that pRb associates with Histone deacetylase 1 (HDAC1) and recruits it to E2F, a regulator of cyclin E promoter, to repress cyclin E expression and hence inhibit cell cycle progression (Brehm *et al.* 1998). In SV40, the OBD and helicase sections of LT bind to the cellular proteins p53, p300 and CBP, which has been suggested to play a role in T antigen-mediated cell transformation. In this complex, SV40 LT Ag is acetylated and it has been shown that the acetylation site is conserved in JCV and BKV whose LT also interacts with p53 (Poulin *et al.* 2004). In MCV, a recent study showed that while full length MCV LT co-precipitates with p53, it does so at a significantly lower level compared to SV40 LT. Interestingly, the authors also showed that MCC-specific truncated MCV LT does not co-precipitate with p53 (Borchert *et al.* 2014), suggesting that similar to SV40, MCV LT OBD and helicase regions might interact with p53. Luciferase reporter assays also showed that while p53-dependent transcription is reduced by full length MCV LT, the truncated LT loses this ability too. In both NLS-containing and NLS-deficient truncated MCV LT, a significant portion of LT Ag localises to the cytoplasm. Interestingly, MCV LT truncations increase its Rb-binding affinity, leading to a significant cytoplasmic re-localisation of Rb (Borchert *et al.* 2014). In general, polyomavirus LT Ags can induce cell proliferation by binding to tumour suppressor proteins p53 and Rb and inactivating them (Topalis *et al.* 2013). MCV LT also contains MCV T antigen unique region (MUR), a 200-aa

sequence, between its first exon and OBD (Figure 1.9). MUR, conserved in MCC-derived MCVs, can bind to the lysosome clustering and fusion promoter protein, human Vam6p (hVam6p) and redistribute it to the nucleus (Liu *et al.* 2011). Liu *et al.* suggest that the disruption of lysosome clustering may play a role in un-coating or egress of MCV during replication.

Small T antigen is another product of alternative splicing of the T antigen locus, producing a 186aa peptide (Figure 1.9). In addition to CR1 and DnaJ domains, which are shared with LT and 57kT, sT also contains a protein phosphatase 2 (PP2, PP2A) binding domain at its carboxyl terminus (Kwun *et al.* 2009). PP2A-binding is a conserved characteristic of polyomavirus sT Ags and its importance has been shown in cell transformation ability of MuPyV and SV40 (Pallas *et al.* 1990). Interestingly, in MCV the transformation ability of sT is independent of PP2A and instead MCV sT exerts its transformation effect via several routes that include increasing the activity of eukaryotic translation initiation factor 4E (eIF4E) by promoting hyperphosphorylation of eIF4E–binding protein 1 (4E-BP1) (Shuda *et al.* 2011). In addition, MCV sT plays an important role in efficient MCV replication. It has been shown that while sT alone does not have any direct effect on MCV-driven replication, it is required for efficient replication activity of MCV LT. Details of how this mechanism operates can be found in section 1.4.2.2: Virus replication.

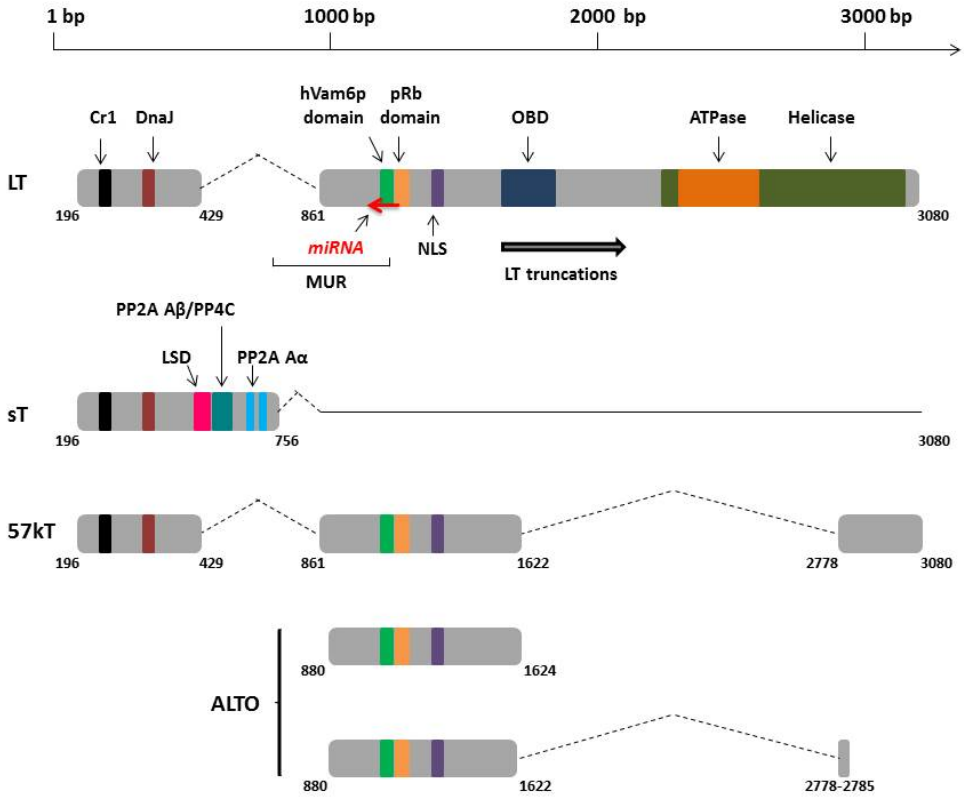

Figure 1.9. Schematic presentation of the T antigen (TAg) locus of MCV. Alternative splicing of the TAg locus gives rise to four different proteins, large T (LT), small T (sT), 57kT and ALTO. MCV LT contains conserved polyomavirus LT domains including, CR1, DnaJ, pRb-binding, nuclear localisation signal (NLS), origin binding domain (OBD), and helicase domain as well as MCV unique region (MUR) and human Vam6p-binding site. The thick black arrow depicts the MCC-specific mutation site. MCV miRNA, MCV-miR-M1, is located on the opposite strand of LT and is expressed late in the infection. sT shares the first exon of LT plus PP2A and PP4C binding site as well as LT stabilising domain (LSD). 57kT is identical to LT but with incomplete origin binding and helicase domains.

MCV sT has also been implicated in disruption of innate immunity, inflammatory signalling and MCC metastasis. NF-κB is a protein complex with various key roles in regulation of cell proliferation, inflammation, immunity and antiviral response (Richards and Macdonald 2011; Griffiths *et al.* 2013). NF-κB remains in a cytoplasmic inhibited state and bound to inhibitors of κB (IκB) until activated via a variety of stimuli such as cytokines, TNF-α and pattern recognition receptors (PRRs). Activation of TNF-α or PRRs (e.g. Toll like receptors, TLRs) triggers a signalling cascade, leading to activation of catalytic subunits of IκB kinase (IKK) complex, IKKα and IKKβ and the non-catalytic subunit IKKγ. IKK-mediated phosphorylation of IKB results in its rapid degradation and release of NF-κB, where NF-κB translocates to the nucleus and activates transcription of genes that are involved in antiviral response such as type I interferons. IKKγ, also called NF-κB essential modulator or NEMO, provides a platform for IKKα and β and a vehicle to link them to other components of the signalling complex (Griffiths *et al.* 2013). MCV sT has been shown to co-localise with NEMO and cellular protein phosphatases 4C (PP4C) and 2A (PP2A) Aβ subunits in cytoplasmic puncta preventing phosphorylation of IKKα and β (Griffiths *et al.* 2013). Given the role of PP4C and PP2A in dephosphorylation and inactivation of the IKK complex (Barisic *et al.* 2008; Brechmann *et al.* 2012) this suggests that sT interrupts eventual release and nuclear translocation of NF-κB by preventing IkB phosphorylation (Griffiths *et al.* 2013). Interestingly, PP4C has also been implicated in MCV sT-mediated cell migration and motility. Stathmin is a microtubule-associated protein which upon dephosphorylation indirectly leads to destabilisation of cellular microtubules (Jourdain *et al.* 1997).

Microtubules are key components of cellular shape and motility (Kaverina and Straube 2011; Etienne-Manneville 2013). Knight *et al.* reported that sT promotes stathmin-mediated microtubule destabilisation via PP4C and that this leads to increased cell motility/migration, suggesting a role for sT in MCC metastasis (Knight *et al.* 2014). In addition to disrupting NF-κB signalling, sT expression has been shown to downregulate the expression of several innate immunity-associated genes such as, TRAF family member-associated NF-kappa-B activator (TANK), Chemokine (C-C motif) ligand 2 (CCL2), Chemokine (C-X-C motif) ligand 8 and 9 (CXCL8 and CXCL9), suggesting yet another key role for sT in MCV life cycle and pathogenesis (Griffiths *et al.* 2013).

Further evidence for MCV manipulating innate immune response comes from the observation that MCV T antigen locus downregulates the expression of TLR9, a major component of innate immune system. TLR9 is an endosomal sensor of nonmethylated CpG motifs, a pathogen-associated molecular pattern (PAMP) characteristic of dsDNA viruses and bacteria (Beutler 2004; Leifer *et al.* 2004), which upon stimulation triggers NF-κB signalling and inflammatory response (Wagner 2004). Expression of MCV early region, particularly LT, has been shown to downregulate TLR9 via downregulation of TLR9 transactivator CCAAT-enhancer-binding protein β (C/EBPβ) (Shahzad *et al.* 2013), suggesting that LT too is involved in MCV immune evasion mechanism, however, the mechanistic detail and if this is via a direct interaction remains unclear.

In addition to its modulatory effect on the innate immunity, MCV LT plays a central role in virus-mediated oncogenesis. MCV-positive MCCs have been

shown to undergo apoptosis following LT knockdown, suggesting that LT expression is vital for the maintenance of cancerous state in these cells (Houben *et al.* 2010). In addition, inhibition of the oncoprotein survivin results in rapid cell death in MCV-positive MCC cells (Arora *et al.* 2012). Interestingly, it has been shown that pRb can repress survivin via interaction with its promoter (Jiang *et al.* 2004), therefore, LT binding and sequestration of pRb can upregulate survivin expression leading to promotion of cell proliferation. As previously mentioned, MCV LT affinity for p53 is significantly weaker than its SV40 homologue and it is lost upon LT truncation in tumours. In contrast, LT truncations boost LT binding affinity for pRb (Borchert *et al.* 2014). pRb regulates the cell cycle by binding to E2F, an activator of cyclin A, cyclin E and dihydrofolate reductase (DHFR). Phosphorylation of pRb disrupts pRb-E2F complex leading to E2F-mediated DNA synthesis and advancement of cell cycle. SV40 LT has been shown to interact with Heat shock 70 kDa protein 8 (HSC70, HSPA8) via its DnaJ domain, and in an ATP-dependent manner, leading to dissociation of Rb-E2F complex and subsequent cell transformation (Sullivan *et al.* 2000). Likewise, MCV LT binds to pRb and HSC70 and disrupts pRb-E2F complex (Shuda *et al.* 2008; Kwun *et al.* 2009) suggesting that MCV LT might contribute to cell proliferation through the same mechanism (Stakaityte *et al.* 2014). Concordantly, it has been shown that MCV-positive MCCs undergo cell cycle arrest when LT binding is lost via mutation in the pRb-binding domain (Houben *et al.* 2012). Moreover, pRb1 knockdown can rescue MCC growth arrest induced by LT knockdown and loss of pRb1 renders LT dispensable for MCC growth (Hesbacher *et al.* 2016).

In addition to clonal integration of MCV genome in to the host cell DNA, one characteristic feature of all MCV-positive MCCs is loss of essential replication domains, OBD and helicase (Figure 1.9). In contrast, those domains of LT implicated in tumourigenesis, such as DnaJ and pRb-binding, as well as the entire sT open reading frame are preserved. One explanation for the observed mutation pattern is that tumours may naturally select for replication-deficient MCV clones to prevent fatal replication fork collision arising from an otherwise actively replicating clone (Shuda *et al.* 2008). LT truncating mutation and viral genome amplification could precede or succeed the integration step (Figure 1.10). A preceding random integration will be naturally followed by truncating mutation in LT gene to disable any unlicensed virus replication. In this model, genome amplification occurs subsequent to integration, possibly via a similar mechanism to genome copy number amplification of cellular oncogenes such as *MYC* (DeCaprio and Garcea 2013). In contrast, in the second model, LT gene truncation occurs in the episomal MCV, leading to rolling circle amplification of the genome rather than normal bidirectional replication. As will be discussed in section 1.4.2.2 (Virus replication), polyomavirus genome replication is initiated by head-to-head binding of two LT hexamers to OBD which unwind the dsDNA genome and proceed in opposite directions (Figure 1.11 C). A ssDNA break in the episomal virus can suspend the associated LT hexamer and cease replication of the broken strand while the opposite LT hexamer continues replicating the intact strand. The elongated multimer of the mutated viral genome will eventually integrate in to the host genome, leading to the subsequent transformation events (DeCaprio and Garcea 2013).

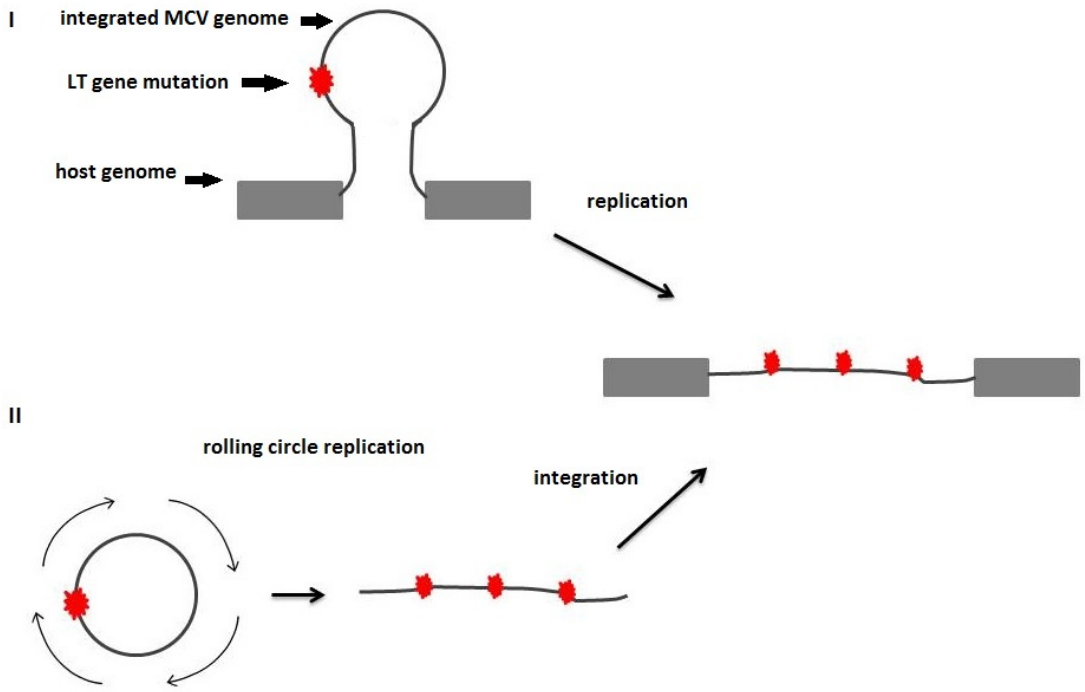

Figure 1.10. Proposed models for MCV LT truncating mutations and virus clonal integration in MCC. In the first model, integration precedes LT gene mutation and virus amplification (top) whereas in the second model, LT gene mutation occurs in the episomal MCV prior to elongation of the mutant virus and subsequent clonal integration (bottom).

Currently, the second model is thought to be the more likely, supported in part by evidence showing that expression of mutated LT impairs UV-induced DNA repair and hampers cell cycle arrest, leading to genomic instability of the host cell and subsequent integration of the virus (Demetriou *et al.* 2012). Interestingly, this study also shows that MCV-positive cell line MKL1 is more UV-sensitive and exhibits poorer global genomic repair (GGR) compared with

the MCV-negative UISO cell line, further corroborating the role of MCV in the host genomic instability.

To date and in contrast to MCV LT and sT no function has been identified for MCV 57kT, however, due to its highly conserved sequence in different MCV strains it has been suggested to be involved in the virus multiplication and survival (Kwun *et al.* 2009). Moreover, since 57kT is a homologue of SV40 17kT it is suggested to play a role in host cell proliferation (Zerrahn *et al.* 1993; Comerford *et al.* 2012). SV40 17kT has been demonstrated to stimulate hepatocyte proliferation in transgenic mice, however, unlike SV40 LT is incapable of inducing hepatic dysplasia and hepatocarcinogenesis (Comerford *et al.* 2012).

ALTO, unlike sT and 57kT, is transcribed from the second exon of LT and therefore does not share its N terminal with other MCV early proteins (Figure 1.9). Despite lack of sequence identity, ALTO is considered evolutionarily related to MuPyV middle T (MT) antigen and is assumed to play a role in manipulation of host cell signalling and transformation to cancerous state (Carter *et al.* 2013). However, it has been shown that ALTO is dispensable for proliferation of MCV-positive MCCs (Houben *et al.* 2014).

The late region of MCV genome codes for capsid proteins VP1, VP2 and probably VP3, however, the MCV-specific VP3 ORF is either not expressed or is non-functional (Spurgeon and Lambert 2013). While VP1 is involved in attachment and entry of MCV, VP2 is required for infectivity in some cell lines but not in others (Schowalter and Buck 2013; Spurgeon and Lambert 2013). Crystal structure of VP1 shows arrangement of five VP1 monomers around a

five-fold axis with unique interaction surfaces formed as a result of variable loops. The ratio of VP1 to VP2 has been determined as 5 to 2, i.e. two VP2 molecules for each VP1 pentamer (Neu *et al.* 2012). VP1 possesses an NLS at its N-terminus and localises as a diffuse nuclear pattern, moreover, its presence can shift VP2 localisation to the nucleus from an otherwise cytoplasmic state (Schowalter and Buck 2013). In keeping with other polyomaviruses, MCV also expresses a miRNA from the late region which is located opposite to the MUR region of LT that is able to auto-regulate MCV LT expression (Seo *et al.* 2009). This will be discussed in greater detail in the following sections.

1.4.2. MCV life cycle

As discussed above, MCV was initially identified in MCC as a clonally integrated virus genome (Feng *et al.* 2008). Later studies showed that MCV is a commensal virus chronically shed from the skin (Schowalter *et al.* 2010) with infections starting in childhood and persisting into adult life (Tolstov *et al.* 2011). However, the cellular tropism of MCV was not evident until recently, when dermal fibroblasts were shown to fully support MCV entry, transcription and replication, and therefore suggested as the major natural host of MCV (Liu *et al.* 2016). In this section, the life cycle of MCV from entry to egress will be discussed.

1.4.2.1. Virus cell surface binding and entry

Polyomaviruses bind various cell surface receptors before entering the cell. BKV, MuPyV and SV40 use different ganglioside receptors (Tsai *et al.* 2003; Low *et al.* 2006) while JCV has preferential binding for serotonin receptor

(Elphick *et al.* 2004). Virus entry mechanism is determined by attachment receptors, for instance, BKV, MuPyV and SV40 undergo caveolar endocytosis (Norkin *et al.* 2002; Eash *et al.* 2004; Gilbert and Benjamin 2004). Caveolar endocytosis depends on caveolin proteins and formation of flask-shape invaginations in the cell membrane called caveolae (Pelkmans and Helenius 2002), in which gangliosides accumulate (Sapp and Day 2009). Caveolae never join lysosomes and therefore viruses using this internalisation route avoid lysosomal degradation (Kiss and Botos 2009). Following attachment, SV40 virions move to caveolin 1-containing caveolae which will then depart from cell membrane and join pre-existing pH-neutral and cholesterol-rich stationary organelles called caveosomes (Pelkmans *et al.* 2001). A few hours after SV40 entry, caveosomes transform into long tubular membrane structures which no longer contain caveolin-1, detach from caveosomes and transport virions to smooth endoplasmic reticulum (ER) where SV40 accumulates and disassembles (Pelkmans *et al.* 2001; Norkin *et al.* 2002). A more recent study revealed that SV40 internalisation still occurs in caveolin-deficient cells, suggesting that caveolin-1 is not essential for membrane-to-ER transport (Stergiou *et al.* 2013). The authors also demonstrated that SV40 binding of integrins, a type of bidirectional signalling and adhesion receptor (Hynes 2002), triggers recruitment of PI3K (Phosphatidylinositol-4,5-bisphosphate 3-kinase) to the membrane, leading to de-phosphorylation of Ezrin, a member of ezrin-radixin-moesin (ERM) family (Stergiou *et al.* 2013), which are important regulators of membrane domains (Fehon *et al.* 2010). Stergiou *et al.* suggest that Ezrin de-phosphorylation has several consequences including disconnection of

cortical actin from plasma membrane and membrane tubulation, both of which are required for SV40 internalisation (Ewers *et al.* 2010; Stergiou *et al.* 2013). Inhibition of actin filaments with jasplakinolide resulted in reduced BKV infectivity, suggesting that BKV too utilises the actin cytoskeleton for virus infection (Eash and Atwood 2005).

Unlike other polyomaviruses, JCV utilises clathrin-dependent endocytosis (Pho *et al.* 2000), an endocytosis mode which involves formation of clathrin-coated pits and various adaptor proteins such as eps15 (epidermal growth factor receptor pathway substrate clone 15), adaptor protein complex 1 (AP1), AP2 and AP180 (Motley *et al.* 2003; Ungewickell and Hinrichsen 2007; Schelhaas 2010). Studies have shown that JCV infectious entry to glial cells requires clathrin, eps15 and activated tyrosine kinase signalling (Querbes *et al.* 2004). In addition, JCV infection of glial cells activates mitogen-activated protein kinases 1 (MAPK1) and MAPK2, probably to facilitate efficient virus internalisation, cellular trafficking and replication (Querbes *et al.* 2004).

MCV attachment and entry is comprised of two steps in which the virus sequentially binds to glycosaminoglycans and sialylated oligosaccharides before cell entry. The initial attachment occurs via binding of MCV capsid protein VP1 to heparan sulfate (HS) and chondroitin sulfate (CS) (Schowalter *et al.* 2011), then VP1 via its apical shallow binding site binds Neu5Ac-α2,3-Gal, a linear motif of N-acetyl neuraminic acid (Neu *et al.* 2012). Interestingly, while the sialylated oligosaccharides are not required for the initial entry they are indispensable for the follow-up infectious entry of the virus (Schowalter *et al.* 2011). To date, there is no data available for MCV internalisation route.

1.4.2.2. Virus replication

Like other polyomaviruses, MCV requires the expression of LT to initiate replication and is largely dependent on the host cell machinery for successful transcription and replication of its genome. Virus replication is a delicately coordinated process in polyomaviruses, which begins with transcription of the early region upon nuclear entry of the genome, followed by oligomerisation of LT antigen in the form of hexamers (DeCaprio and Garcea 2013). In SV40, binding of ATP to LT triggers interaction between two LT hexamers and ORI followed by movement of hexamers in opposite directions, which combined with helicase activity unwinds the viral genome and advances bi-directional genome replication (Borowiec and Hurwitz 1988; Wessel *et al.* 1992). As mentioned in section 1.4.1, a minimum core region of 71bp in the MCV ORI has been reported as sufficient for initiation of the virus replication. This core region is composed of ten G(A/G)GGC pentamer (P1 to P10) repeats, as recognition sites for LT OBD, and flanking AT-rich sites. As can be seen in Figure 1.11 B, LT OBD binds the central P1, P2 and P4 sites. In fact, these three sites, along with P7, are indispensable for origin replication, although P7 is located further and outside the origin centre (Harrison *et al.* 2011). OBD recognition of the essential pentanucleotides leads to binding of LT hexamers in an apex-to-apex orientation while wrapping around the dsDNA genome (Figure 1.11 C). It has been suggested that the flanking AT-rich sequences (Figure 1.11 A) allow for easier melting of the core origin and hence facilitates replication initiation (Kwun *et al.* 2009).

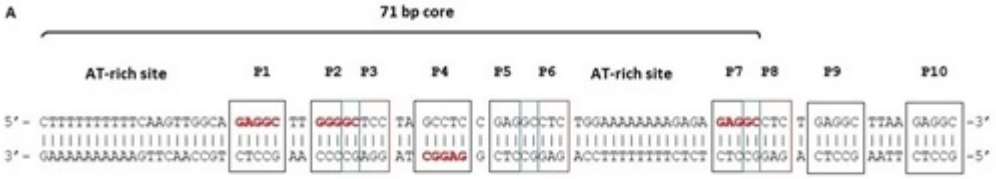

For part B refer to: Harrison, C. J., Meinke, G., Kwun, H. J., Rogalin, H., Phelan, P. J., Bullock, P. A., Chang, Y., Moore, P. S. and Bohm, A. (2011) Asymmetric assembly of Merkel cell polyomavirus large T-antigen origin binding domains at the viral origin. J Mol Biol 409 (4), 529-42.

For part C refer to: DeCaprio, J. A. and Garcea, R. L. (2013) A cornucopia of human polyomaviruses. Nat Rev Microbiol 11 (4), 264-76.

Figure 1.11. The minimum core region of MCV origin of replication required for efficient virus replication (A), schematic presentation of LT OBD binding to the central pentanucleotides P1, P2 and P4 based on X-ray crystallography (B) and LT hexamers binding, genome unwinding and replication initiation (C). The pentanucleotide repeats (P) are boxed and essential Ps are highlighted in red. Adapted from (Harrison *et al.* 2011) and (DeCaprio and Garcea 2013).

Other polyomaviruses such as BKV, JCV and SV40 have the same origin pentamer repeats, but unlike MCV, these are in a symmetrical arrangement with different inter-pentamer spacing. Moreover, while in BKV, JCV and SV40 the indispensable P1-P4 repeats are juxtaposed and show no overlapping, in MCV the essential P1, P2, P4 and P7 are separated by the second AT-rich site and the dispensable overlapped P5/P6 (Figure 1.11 A). The importance of such structural distinctions in the replication origins of polyomaviruses has

remained unexplained to date, however, what is clear is that despite perfect identity of the binding sites and noticeable identities among OBDs in MCV and SV40, cross replication does not occur by heterologous LTs (Harrison *et al.* 2011).

In tumour derived MCV, replication capacity is lost following a single point mutation in essential pentanucleotides (Kwun *et al.* 2009). Furthermore, consistent with the observation in MCV-positive MCC, loss of OBD and helicase domains renders MCV non-replicative (Shuda *et al.* 2008). Interestingly, whilst LT alone is sufficient for virus replication, efficient genome replication is achieved only in the presence of both sT and LT. In contrast, 57kT does not improve replication capacity of LT, and sT or 57kT alone cannot initiate or drive replication. As mentioned earlier, LT shares the first exon, and therefore some domains such as DnaJ with sT (Figure 1.9). DnaJ is a conserved motif in polyomaviruses and is required for efficient replication in SV40 (Sheng *et al.* 1997). It has been shown that, despite sharing the DnaJ domain, replication efficiency is significantly reduced following mutation in LT DnaJ whereas mutation of sT DnaJ does not alter the enhancing capacity of sT in LT-driven replication (Kwun *et al.* 2009). In contrast, a mutated sT PP2A domain does eliminate the replication enhancing capacity of sT, suggesting a role for sT and PP2A in efficient LT replication (Kwun *et al.* 2009). However, a later study revealed via domain mutation that any such effect is not mediated by sT PP2A, but rather by a domain located on the opposite side of PP2A termed LSD or LT-stabilisation domain (Kwun *et al.* 2013).

SCF (SKP1, CUL1 and F-box containing complex) is a conserved ubiquitin ligase complex and FBW7 (F-box and WD repeat domain-containing 7) is a subunit of SCF which regulates proto-oncogenes and proteins involved in cell division, growth and differentiation (Welcker and Clurman 2008). FBW7 dysregulation and mutation has been shown in several malignancies including T-cell acute lymphoblastic leukaemia/lymphoma (Maser *et al.* 2007), breast and colorectal cancers (Wood *et al.* 2007), cholangiocarcinomas and tumours of endometrium and stomach (Akhoondi *et al.* 2007). These studies suggest that FBW7 is an important tumour suppressor which promotes degradation of proto-oncogenes in a phosphorylation-dependent manner (Koepp *et al.* 2001; Strohmaier *et al.* 2001; Yada *et al.* 2004). Strikingly, LSD inhibits SCF^{FBW7}-mediated proteasomal degradation of LT, hence indirectly enhancing MCV replication by promoting the accumulation of LT. Interestingly, sT-mediated SCF^{FBW7} inhibition also reduces turnover of cellular proto-oncogenes c-Myc and Cyclin E (Kwun *et al.* 2013), a process which can promote cell transformation.

T antigen-mediated hijacking of cellular machinery in favour of virus replication is not limited to SCF^{FBW7}. DNA damage response (DDR) machinery governs the recognition and repair of DNA damage in the cell. Ataxia telangiectasia mutated (ATM) and ATM- and Rad3-related (ATR) kinases are two important components of DDR, which can mediate cell cycle arrest and apoptosis upon activation (Ciccia and Elledge 2010; Tsang *et al.* 2014). MCV LT has been shown to interact and co-localise with DDR elements in the nucleus in an ORI and replication-dependent manner. Furthermore, inhibition of DDR and elimination of ATM and ATR abolishes

MCV genome replication (Tsang *et al.* 2014), indicating the importance of DDR in MCV life cycle. This crucial role for DDR in the replication of polyomaviruses has also been described in SV40 (Sowd *et al.* 2013), MuPyV (Dahl *et al.* 2005), JCV (Orba *et al.* 2010) and BKV (Jiang *et al.* 2012). Another cellular protein contributing to MCV replication is bromodomain and extra terminal domain (BET) family member, Bromodomain-containing protein 4 or Brd4. Brd4 has been implicated in cell cycle progression to S phase (Mochizuki *et al.* 2008) and cancer (French *et al.* 2001; Zuber *et al.* 2011). It has also been associated with oncogenic viruses such as EBV, KSHV and papillomaviruses (Ottinger *et al.* 2006; Wu *et al.* 2006; Lin *et al.* 2008). Replication factor C (RFC) is a chaperone-like protein complex, which upon recognition of template-primer 3' ends, recruits and loads Proliferating cell nuclear antigen (PCNA) to DNA. PCNA is a DNA clamp which encircles and slides along DNA like a ring while acting as a tether for DNA polymerases (Moldovan *et al.* 2007). Wang *et al.* showed both *in vivo* and *in vitro* that MCV LT interacts with Brd4 at MCV replication sites and that this interaction is required for virus replication, since knockdown of Brd4 markedly reduces virus replication. Furthermore, similar to SV40 (Wold and Kelly 1988), MCV LT recruits replication protein A 70 (RPA70) to stabilise the nascent unwound viral ssDNA and prevent it from reannealing (Wold 1997). Directly interacting with LT, Brd4 then recruits RFC, PCNA and DNA polymerase delta to replication sites and facilitates viral DNA elongation (Wang *et al.* 2012).

Unlike the proteins described so far, hVam6p, which is a cellular vacuolar sorting protein, reduces MCV replication. hVam6p is part of HOPS or

homotypic fusion and protein sorting complex which modulates lysosome and late endosome fusion (Caplan *et al.* 2001). Direct interaction of MCV LT and hVam6p via a site near LT pRb-binding domain (Figure 1.9) re-localises hVam6p to the nucleus in an LT NLS-dependent manner and prevents lysosome clustering (Liu *et al.* 2011). While overexpression of hVam6p dramatically reduces MCV replication, loss of LT-hVam6p interaction enhances virion production by up to 6-fold (Feng *et al.* 2011). In addition, hVam6p isoforms have been shown to be involved in mechanistic target of rapamycin (mTOR) and transforming growth factor-β (TGF-β) signalling pathways, however, the interaction between MCV LT and hVam6p does not seem to affect these (Liu *et al.* 2011). Although further studies are required with regards to MCV dependence on hVam6p for cell growth and proliferation, current data suggest that MCV-driven tumourigenesis is not mediated by this cellular protein since mutation-driven loss of LT-hVam6p interaction does not affect cell viability or proliferation (Feng *et al.* 2011). Therefore, from a cellular point of view, the LT-hVam6p interaction might be important in the context of innate immunity, i.e. preventing persistent infection via disruption of MCV replication (Stakaityte *et al.* 2014). A second possibility is that MCV-mediated disruption of lysosome clustering might be important for virus uncoating or egress (Liu *et al.* 2011).

1.4.2.3. Virus assembly and egress

The mechanisms underpinning MCV assembly and egress are yet to be fully elucidated. In SV40, the major viral capsid protein, VP1, has been shown to self-assemble without the requirement of post-translational modifications (Salunke *et al.* 1986). So far, it has only been shown that prior to egress

MCV virions localise to the nuclear periphery (Neumann *et al.* 2011). SV40, BKV and JCV are known to code for a late protein called agnoprotein, which in case of SV40 facilitates virus particle formation and maturation via interaction with VP1 (Khalili *et al.* 2005). SV40 also codes for the very late protein, VP4, which is required for efficient propagation and timely lytic release of the progeny (Daniels *et al.* 2007). However, MCV does not encode either of these proteins or functional homologues. It has been proposed that, similar to other polyomaviruses, MCV might use a lytic mechanism or, depending on the host cell, be shed from the skin (Stakaityte *et al.* 2014). Interestingly, a recent study identified dermal fibroblasts as the natural host of MCV and the authors suggest that MCV might be released to the skin surface by fibroblasts residing adjacent to hair follicle and/or sebaceous and sweat glands, or alternatively, differentiating keratinocytes might function as the carrier for viruses released from dead infected dermal fibroblasts (Liu *et al.* 2016).

Virus replication is in fact a cascade of ordered events, from initiation of virus gene transcription to virus assembly and egress. In polyomaviruses, the importance of temporal organisation is highlighted by arrangement of the viral genome in to early and late regions. Extensive dependence of polyomaviruses on the host DNA replication and growth machinery presents the challenge of being detected and eliminated by the host immune system and therefore forcing the virus to a tightly coordinated replication process. Thus far, study of MCV replication using a synthetic virus has revealed that early gene expression begins with consecutive expression of LT, 57kT and sT followed by expression of the late protein VP1. Furthermore, eliminating

the replication capacity significantly attenuates 57kT and renders sT and VP1 undetectable. In contrast to the situation in SV40, this suggests that splicing of early transcripts and transcription of the late region is replication-dependent (Keller and Alwine 1984; Feng *et al.* 2011). A tightly regulated switch between early and late gene expression is therefore critical for efficient replication of polyomaviruses. Whilst the mechanism underpinning this vital process is not fully understood, it is possible that expression of the miRNA from the late region decelerates early gene transcription and viral replication to prepare for subsequent virus assembly and release (Seo *et al.* 2009). In addition to the auto-regulatory effect on viral transcripts, polyomavirus miRNAs might play an important role in virus latency/persistence in the host. Indeed, direct involvement of polyomavirus miRNAs in immune evasion has become evident in BKV and JCV (Bauman and Mandelboim 2011; Bauman *et al.* 2011) and preliminary data suggest that MCV-miR-M1 might similarly facilitate virus persistence (Theiss *et al.* 2015). The physiology of miRNAs and their significance in virus life cycle and pathogenesis will be discussed in the following sections.

1.5. miRNAs

Structurally, miRNAs are small 21-25 nucleotide (nt) non-coding single-stranded RNAs (ssRNA) which are functionally involved in a variety of cellular processes, including regulation of gene expression via post-transcriptional repression or degradation of their target mRNAs (Bartel 2009; Wahid *et al.* 2010; Lagatie *et al.* 2013). Generally, biogenesis of miRNAs includes canonical and non-canonical pathways, however, several alternative pathways have also been described. In this section, miRNA processing

pathways and mechanisms of miRNA-mediated RNA interference (RNAi) will be discussed.

1.5.1. Canonical miRNA processing pathway

In the canonical pathway, a miRNA-coding gene is transcribed by RNA polymerase II (PolII), spliced, and undergoes 5' capping and 3' polyadenylation (Cai *et al.* 2004). This primary miRNA (pri-miRNA) transcript is usually more than 1kb long and contains a stem-loop structure comprised of a terminal loop and a 33-35bp stem which embeds mature miRNA sequences at 5' and 3' sides (Ha and Kim 2014). Next, a miRNA processing (Microprocessor) complex of Drosha (nuclear RNase III RNASEN) and DGCR8 (DiGeorge syndrome critical region gene-8) recognises the ssRNA tails and stem-loop of pri-miRNA (Ha and Kim 2014). In this process, the C-terminus of DGCR8 binds to the middle region of Drosha whilst the RNA binding domains (RBD) of Drosha and DGCR8 interact with pri-miRNA (Yeom *et al.* 2006). The Microprocessor then measures ~11bp away from the intersect of ssRNA tail and dsRNA stem (basal junction) and ~22bp from the junction between dsRNA stem and the terminal loop of pri-miRNA (apical junction) (Ha and Kim 2014). Aligned to the stem, tandem RNase III domain a (RIIIDa) and RIIIDb of Drosha cleave pri-miRNA 3' and 5' strands, respectively, and generate a 2nt overhang at the 3' end (Blaszczyk *et al.* 2001; Han *et al.* 2004; Zhang *et al.* 2004). The resulting ~70-80nt hairpin-shape precursor miRNA (pre-miRNA) is then recognised via its 3' overhang and exported to the cytoplasm by complex of exportin-5 (EXP5) and GTP-binding Ras-related Nuclear protein (RAN.GTP). Crystallography studies have shown that pre-miRNA sits in a positively charged groove formed by

EXP5-RAN.GTP complex with pre-miRNA 3’ overhang placed in a tunnel-like structure at the bottom of the groove (Okada *et al.* 2009). Upon nuclear export, GTP hydrolysis triggers disassembly of the complex and cytosolic release of pre-miRNA (Bohnsack *et al.* 2004; Lund *et al.* 2004). Interestingly, it has been demonstrated that EXP5 gene knockdown reduces both nuclear export and nuclear accumulation of pre-miRNA suggesting that in addition to nuclear export EXP5 may also play a role in nucleolysis protection of pre-miRNA (Yi *et al.* 2003). Dicer is a cytosolic RNase III endoribonuclease whose N-terminus helicase domain interacts with pre-miRNA terminal loop (Tsutsumi *et al.* 2011). A conserved domain of Dicer called PAZ (PIWI–AGO–ZWILLE) has two basic pockets with a spatial arrangement which allows simultaneous binding to the phosphorylated 5’ end and 2nt 3’ overhang of pre-miRNA (Zhang *et al.* 2004; Macrae *et al.* 2006; Park *et al.* 2011; Tian *et al.* 2014). With PAZ located ~22bp away from catalytic domains, Dicer acts like a ‘molecular ruler’ and cleaves off the pre-miRNA terminal loop using its RIIIDa and RIIIDb domains, releasing a mature miRNA duplex (Zhang *et al.* 2002; Zhang *et al.* 2004; Macrae *et al.* 2006; Macrae *et al.* 2007). In *Drosophila,* longer miRNAs can be trimmed to ~22bp by a 3’-to-5’ exonuclease called Nbr (Nibbler) (Han *et al.* 2011). Dicer is associated with dsRNA-binding-domain (dsRBD)-containing cofactors including TRBP (trans-activation response RNA-binding protein) and Protein ACTivator of the interferon-induced protein kinase (PACT) (Chendrimada *et al.* 2005; Haase *et al.* 2005; Lee *et al.* 2013). It has been demonstrated that TRBP is not essential for pre-miRNA processing by Dicer, since the level of pre-miRNA processing is comparable for Dicer alone or Dicer-dsRBD complex (Lee *et al.*

2006). However, consistent with its *D. melanogaster* homologue, Loquacious (Loqs), it is suggested that TRBP which has three dsRBDs plays a role in efficient miRNA processing by stabilising Dicer (Fukunaga *et al.* 2012; Ha and Kim 2014). The role of PACT in miRNA processing is yet to be elucidated (Ha and Kim 2014).

The mature miRNA duplex, comprised of a guide and a passenger (star) strand, is then loaded onto Argonaute (AGO or Ago) protein to form RNA-induced silencing complex (RISC) (Hammond *et al.* 2001; Mourelatos *et al.* 2002). In *Drosophila* species, central base mismatches 9-10 lead miRNA duplex to AGO1 whereas siRNA (small interfering RNA) duplexes are loaded onto AGO2 (Tomari *et al.* 2007; Czech *et al.* 2009; Ghildiyal *et al.* 2010). In human, all four AGO proteins haphazardly associate with miRNA and siRNA duplexes, however with a preference for central (nts 8-11) mismatches (Liu *et al.* 2004; Meister *et al.* 2004; Yoda *et al.* 2010). The process of miRNA duplex loading is mediated by the HSC70-HSP90 chaperone complex which force a conformational opening in AGO proteins in an ATP-dependent manner (Iwasaki *et al.* 2010). Crystallography studies have shown that AGO proteins have a bilobal structure. The N-terminus lobe is composed of N-terminus domain and a PAZ domain whereas C-terminus contains a middle domain (MID) and a PIWI domain. Threaded along the two lobes of AGO, the guide strand 5’ monophosphate is firmly fixed in the MID-PIWI interface while its 3’ end binds PAZ domain in the opposite lobe (Song *et al.* 2004; Wang *et al.* 2008a; Wang *et al.* 2008b; Wang *et al.* 2009; Elkayam *et al.* 2012; Nakanishi *et al.* 2012; Schirle and MacRae 2012). It has been shown that an active site in the AGO PIWI domain governs cleaving of target mRNAs

between 10th and 11th nts relative to guide strand 5' end (Liu *et al.* 2004; Song *et al.* 2004; Parker *et al.* 2005). Interestingly, while all four human AGO proteins induce target mRNA repression and decay only AGO2 can cleave mRNAs with perfect miRNA complementarity (Liu *et al.* 2004).

In *D. melanogaster*, RISC loading complex (RLC) is composed of Dcr2 and R2D2 (contains two dsRBD (R2) and is associated with Dcr2 (D2)) which respectively bind the less stable and thermodynamically stable ends of duplexes to load siRNA onto AGO2 (Pham *et al.* 2004; Liu *et al.* 2009), whereas the role of RLC in AGO1 loading of miRNA duplexes is yet to be defined. In human, *in vitro* binding of Dicer–TRBP complex to siRNA duplexes and its role in pre-miRNA processing and target cleavage has been reported (Gredell *et al.* 2010; Noland *et al.* 2011; Liu *et al.* 2012). However, in Dicer-deficient murine embryonic stem cells siRNA-mediated repression is still detectable (Murchison *et al.* 2005), suggesting that Dicer is dispensable for AGO small RNA loading. Furthermore, Dicer is not necessary for determining the guide strand based on the thermodynamic asymmetry (asymmetric RISC assembly) of the strands of a small RNA duplex (Schwarz *et al.* 2003; Betancur and Tomari 2012). Therefore, RLC may not be essential for miRISC (miRNA-RISC complex) formation in *D. melanogaster* and human.

Following miRNA loading onto AGO proteins the passenger strand is removed to generate a mature miRISC. In siRNAs, absence of central base mismatches leads to cleavage of passenger strands by AGO2 (Rand *et al.* 2005; Leuschner *et al.* 2006) prior to their removal by C3PO (component 3 of promoter of RISC) endonuclease (Liu *et al.* 2009). However, due to lack of

cleaving activity in human AGO1, AGO3 and AGO4 and presence of central mismatches in most miRNA duplexes this mechanism is scarcely used in miRISC maturation process (Liu *et al.* 2004; Meister *et al.* 2004). Unlike loading process, the miRNA duplex unwinding is a passive ATP-independent event. It has been suggested that loading of a rigid miRNA duplex onto a force-opened AGO protein puts the duplex under a structural tension similar to a stretched rubber band. Therefore, with the guide strand firmly docked in place the unanchored passenger strand is easily ejected (Iwasaki *et al.* 2010). Base mismatches in seed (2-8) or 3'-mid (12-15) of guide strand have also been shown to promote duplex unwinding (Yoda *et al.* 2010).

An important event during the AGO loading step is selection of the guide strand. Thus far, two criteria have been described to determine the guide strand: lower relative thermodynamic stability (also referred to as thermodynamic asymmetry) at the 5' end (Schwarz *et al.* 2003) and preference of AGO proteins for a U at position 1 (Czech *et al.* 2009; Okamura *et al.* 2009; Ghildiyal *et al.* 2010). The MID domain of human AGO2 demonstrates a greater affinity for first A and U nts at 5' ends (Frank *et al.* 2010). However, strand selection is not a strict process since the less favoured strand may be incorporated into miRISC and, with less frequency, participate in silencing (Ha and Kim 2014). For instance, several mouse and fly pre-miRNAs have been shown to give rise to mature miRNAs from both guide and passenger strands *in vivo* (Aravin *et al.* 2003; Schwarz *et al.* 2003; Ro *et al.* 2007). Where structural elements favouring one strand are absent roughly equal amounts of both mature miRNAs accumulate *in vivo* as witnessed by *D. melanogaster* miR-10 and miR-10* (Schwarz *et al.* 2003).

Interestingly, tissue-dependent strand switching has also been reported. For example, study of mouse tissues revealed miR-142-5p as the dominant strand in brain, testes and ovaries whereas miR-142-3p was more frequently detected in newborn and embryonic samples (Chiang *et al.* 2010). Similarly, while mice miR-194-5p and -3p are co-expressed in uterus, ovaries, heart, lung and small intestine, other tissues including testes, brain, liver, spleen and stomach selectively express miR-194-5p (Ro *et al.* 2007). The strand switching phenomenon has been attributed to alterations in the relative thermodynamic stability of the strands due to alternative processing by Drosha-DGCR8 (Wu *et al.* 2009). These observations strongly suggest that miRNA strand selection is also determined by cell, tissue and developmental stage. miRNA maturation and turnover can be also affected by sequence or structural changes in the host RNA molecule. Examples of these changes include single nucleotide polymorphisms (SNPs), RNA 3'-end modification via uridylation and adenylation, RNA editing and RNA methylation.

CNNC is a conserved motif in bilaterian animals, located 17-18 nts downstream of the Drosha cleavage site of pri-miRNA (Auyeung *et al.* 2013). Splicing factor, arginine/serine-rich 3 (SFRS3 or SRp20) is a protein implicated in various RNA processing activities such as splicing (Zahler *et al.* 1993; Cavaloc *et al.* 1994) and translation initiation (Swartz *et al.* 2007). It has been shown that a C → T SNP in the 5' C of CNNC motif of human miR-16-1 abolishes recruitment of SFRS3 to CNNC, leading to downregulation of miR-16-1 (Auyeung *et al.* 2013) whose reduced expression has been associated with chronic lymphocytic leukaemia (Calin *et al.* 2002; Calin *et al.* 2005).

Uridylation of let-7 pre-miRNA (pre-let-7) has been shown to prevent Dicer processing and promote let-7 degradation, a process mediated by binding of LIN28 proteins to pre-let-7 terminal loop and recruitment of terminal uridylyl transferase 4 (TUT4) and TUT7 (Heo *et al.* 2008; Hagan *et al.* 2009). In contrast, in the absence of LIN28, monouridylation of group II pre-let-7 miRNAs by TUT7, TUT4 and TUT2 promotes biogenesis of let-7 miRNA (Heo *et al.* 2012). Similarly, adenylation can bring about both positive and negative regulation of the target miRNA. For instance, 3' adenylation of miR-122 after duplex unwinding by the cytoplasmic poly(A) polymerase GLD-2 (Germ Line Development 2) stabilises the mature miR-122 in human and mouse hepatocytes (Katoh *et al.* 2009), whereas polyadenylation of host cell miRNAs by the vaccinia virus VP55/VP39 heterodimeric poly(A) polymerase results in their degradation (Backes *et al.* 2012).

Adenosine Deaminases Acting on RNA (ADAR) are dsRNA-binding enzymes that are involved in RNA editing by catalysing the conversion of adenosine (A) to inosine (I), a process which can replace a Watson-Crick pair with a wobble pair (Wagner *et al.* 1989; Hough and Bass 1994). Such structural change in nucleotide positions -1 and +3 relative to 5' end of miR-151-3p has been demonstrated to prevent Dicer cleavage and drive accumulation of pri-miR-151 (Kawahara *et al.* 2007), whereas in the case of pri-miR-142, A → I conversion in nucleotide positions +4 and +5 relative to 5' end of miR-142-5p (Drosha cleaving site) inhibits Drosha-DGCR8 processing and results in degradation of pri-miR-142 by the nuclease enzyme Tudor-SN (tudor staphylococcal nuclease), a subunit of RISC (Caudy *et al.* 2003; Yang *et al.* 2006).

RNA methylation as a miRNA regulatory mechanism has also been described. An example of such intrinsic regulation is BCDIN3 domain containing RNA methyltransferase (BCDIN3D) which blocks Dicer access to 5' monophosphate of pre-miR-145 and thus prevents miR-145 biogenesis and maturation both *in vitro* and *in vivo* (Xhemalce *et al.* 2012). Importantly, expression of several miRNAs including miR-145 is deregulated in breast cancer (Iorio *et al.* 2005). It has been demonstrated that BCDIN3D depletion in breast cancer cells leads to concomitant reduction of pre-miR-145 and increased expression of mature miR-145. Consistent with this, malignancy phenotypes such as colony formation in soft agar (anchorage-independent growth assay) and penetration through basement membrane matrix (invasion assay) were also reduced (Xhemalce *et al.* 2012), suggesting that interruption of Dicer-dependent miRNA processing may be associated with tumourigeneis.

1.5.2. Non-canonical miRNA processing pathways

The major characteristic of non-canonical pathways is processing of miRNAs from the introns of protein-coding genes (mirtrons) in a Microprocessor-independent manner. Accordingly, the pri- to pre-miRNA step is instead processed in the spliceosome and gives rise to an intermediate lariat structure which after debranching by lariat debranching enzyme (Ldbr or DBR) forms a pre-miRNA-resembling hairpin (Okamura *et al.* 2007; Ruby *et al.* 2007). In some cases such as *Drosophila* spp. miR-1017, an exonuclease trimming step precedes dicing step to remove the 3' tail of the pre-miRNA (Flynt *et al.* 2010). The pre-miRNA export and miRNA maturation steps are shared between non-canonical and canonical pathways (Figure 1.12).

Alternative miRNA processing mechanisms have also been identified. Examples of these include miR-320 and miR-451 biogenesis pathways. Following Pol II-mediated transcription and 5' capping human and mouse pre-miR-320 are exported to the cytosol by EXP1 where Dicer cleaving selectively gives rise to miR-320-3p, presumably due to interference of 5' cap with Dicer interaction (Xie *et al.* 2013). In the case of miR-451, Drosha processing of pri-miR-451 generates an unusual 41-42nt pre-miR-451 with a 17nt stem and perfectly complement strands. Due to its short stem pre-miR-451 cannot be processed by Dicer and therefore is directly loaded onto and cleaved by AGO2, producing a 30nt intermediate RNA termed AGO-cleaved pre-miR-451 or ac-pre-miR-451 (Cheloufi *et al.* 2010; Cifuentes *et al.* 2010). Ac-pre-miR-451 is then trimmed down by poly(A)-specific ribo-nuclease (PARN) at its 3' end to give rise to mature miR-451 (Yoda *et al.* 2013).

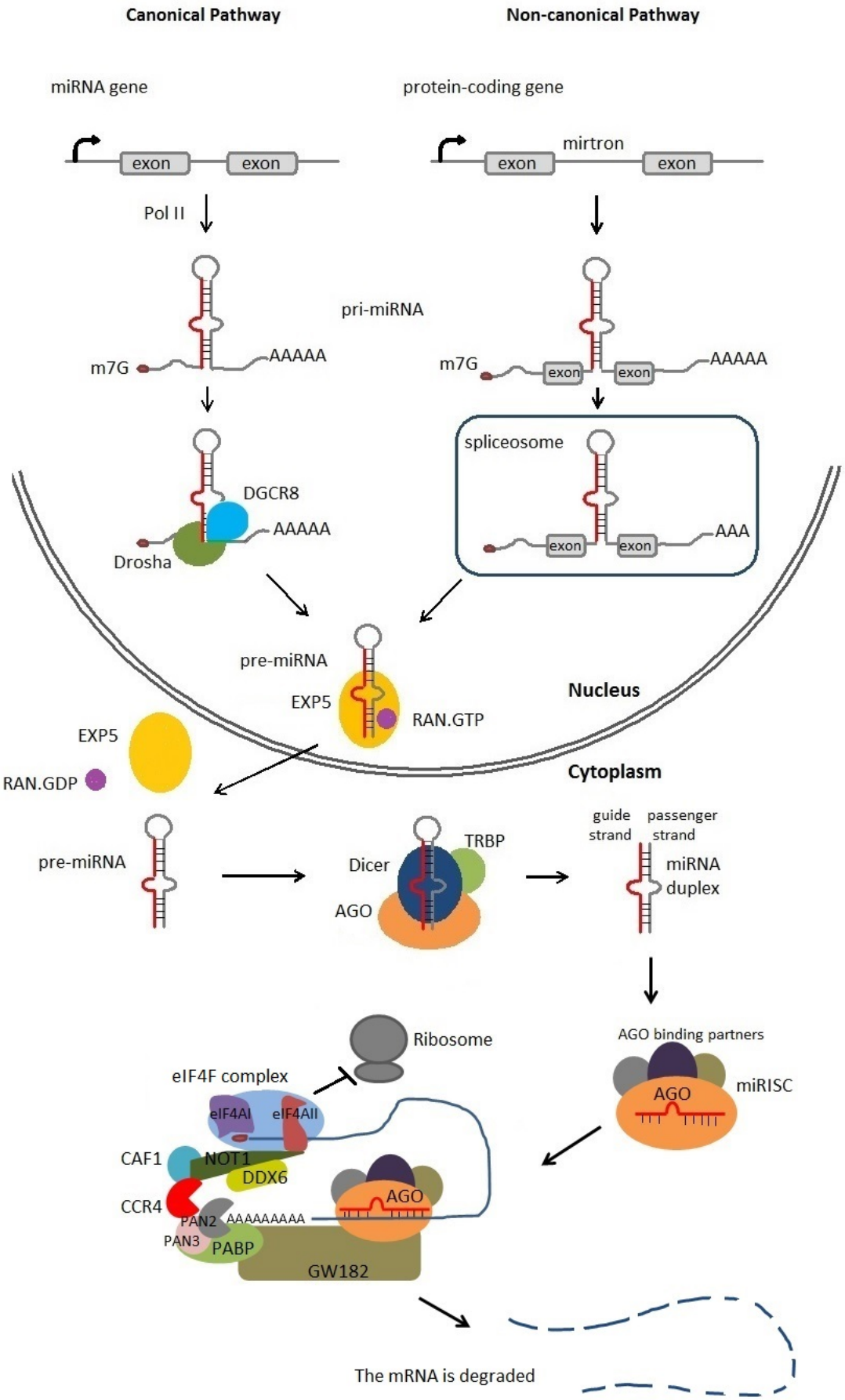
Canonical Pathway
Non-canonical Pathway
miRNA gene
protein-coding gene
exon
exon
mirtron
Pol II
pri-miRNA
m7G
AAAAA
spliceosome
DGCR8
Drosha
AAA
pre-miRNA
EXP5
RAN.GTP
Nucleus
RAN.GDP
Cytoplasm
guide strand
passenger strand
TRBP
Dicer
AGO
miRNA duplex
Ribosome
AGO binding partners
eIF4F complex
eIF4AI
eIF4AII
miRISC
CAF1
NOT1
DDX6
CCR4
PAN2
PAN3
PABP
GW182
The mRNA is degraded

Figure 1.12. Schematic presentation of animal miRNA biogenesis pathways and proposed model for miRNA-mediated inhibition of translation initiation. In canonical pathway, PolII-transcribed miRNA gene is 5' capped, 3' polyadenylated and folds on itself to form a dsRNA hairpin called pri-miRNA. Pri-miRNA is then cleaved at 5' and 3' ends by Drosha-DGCR8 complex to give rise to an ~70 nt stem loop structure known as pre-miRNA. This miRNA precursor is then recognised and exported to the cytoplasm by exportin 5, where Dicer-TRBP further process it into a miRNA duplex, containing a guide (red in this Figure) and passenger (grey) strand. Passenger strand is usually degraded and guide strand joins RISC complex to form miRISC. miRNA then guides the complex to target mRNAs for repression of translation or mRNA degradation. Non-canonical pathway is generally dedicated to miRNAs that occur in mirtrons (intronic regions of protein-coding genes) and therefore pri- to pre-miRNA conversion is processed in spliceosome. The remaining of the pathway is similar to the canonical pathway. GW182 co-localises with miRISC-bound mRNA and decapping and deadenylation factors in GW bodies. Recruitment of eIF4AII to 5'-cap by CCR4-NOT-CAF1 complex enforces a molecular conformation which inhibits initiation of translation by preventing 43S ribosomal subunit binding to the mRNA. CCR4-NOT-CAF1 complex also binds DDX6 and links decapping and deadenylation processes together to promote mRNA degradation. AGO, Argonaute protein; CAF1, CCR4-associated factor 1; CCR4, C-C chemokine receptor type 4; DDX6, DEAD-box helicase 6; eIF4F, eukaryotic initiation factor 4F; EXP5, exportin-5; RAN.GTP, GTP-binding RAs-related Nuclear protein; m7G, 7-Methylguanosine; NOT1, negative regulator of transcription 1; PABP,

poly(A)-binding protein, PAN2 & PAN3, PAB-dependent poly(A)-specific ribonuclease subunit 2 & 3; PolII, RNA polymerase II; pre-miRNA, precursor miRNA; pri-miRNA, primary miRNA; RISC, RNA-Induced Silencing Complex; miRISC, complex of miRNA and RISC; TRBP, trans-activation response RNA-binding protein.

1.5.3. miRNA-mediated RNA interference

Generally, miRNAs exert their effect via base pairing with binding sites in the 3'untranslated region (3'UTR) of the target messenger RNAs. Central to this interaction are nucleotides 2-8 of the mature miRNA, which constitute the seed region (Lewis *et al.* 2003) while nucleotides 13-17, which are located near the 3' end of the miRNA, can augment target recognition by providing 'supplementary' binding and hence are called 3'-supplementary sites (Grimson *et al.* 2007). In some cases, 3' supplementing can 'compensate' for seed region single nucleotide mismatches and thus called 3'-compensatory site (Yekta *et al.* 2004; Grimson *et al.* 2007). Examples of this include mammalian miR-196 targeting of Homeobox B8 (HOXB8) mRNA (Yekta *et al.* 2004) and *C. elegance* let-7 miRNA targeting of lin-41 mRNA (Lewis *et al.* 2003). These observations suggest that algorithm-based prediction of targets based solely on seed-sequence may be misleading.

Combined *in silico-in vitro* investigation has also identified other enhancing characteristics of target sites, including adjacent AU-rich regions and proximity to co-expressed miRNA sites. In addition, target sites located away

from the centre of and at least 15nt from the stop codon of 3'UTR demonstrate improved binding efficiency (Grimson *et al.* 2007).

It is generally accepted that partial miRNA-mRNA base pairing drives repression of mRNA translation whereas a perfect or near perfect pairing, e.g. in the case of siRNAs, can lead to cleavage of targeted mRNAs (Hutvagner and Zamore 2002; Zeng *et al.* 2002; Zeng *et al.* 2003; Bartel 2004; Bartel 2009). The process of miRNA-mediated regulation of gene expression has been subject to extensive investigation. Thus far, it has been established that RISC is central to the complex machinery of translation repression and mRNA degradation (Meijer *et al.* 2013; Wilczynska and Bushell 2015). A key component of the RISC is a protein complex of 182kD with multiple repeats of glycine (G)-tryptophan (W) called GW182 (Eystathioy *et al.* 2002). GW182 (Trinucleotide repeat-containing gene 6 or TNRC6 in human) contains an RNA recognition motif (RRM) and co-localises with mRNA degradation associated proteins Dcp1/Dcp2 (mRNA-decapping enzymes 1 and 2), LSm (Sm-like) proteins, 5'-3' exoribonuclease 1 (XRN1), Enhancer of mRNA-decapping protein 4 (EDC4 or Ge-1) and AGO2 in GW bodies (GWBs) (Ingelfinger *et al.* 2002; Eystathioy *et al.* 2003; Zee *et al.* 2008). GWBs are the mammalian homologue of eukaryotic processing bodies (P-bodies) which are involved in mRNA turnover and their loss upon GW182 knockdown suggests that GW182 is an indispensable component of this critical cellular domain (Yang *et al.* 2004). Importantly, a recent study using live imaging in *D. melanogaster* early embryos showed that GWBs and P-bodies are structurally and dynamically distinct and whereas P-bodies are mostly cytoplasmic, GWBs localise to both nucleus and the cytoplasm (Patel

et al. 2016). Several studies have shown that miRISC binding triggers deadenylation and decay of the target mRNAs. Poly(A)-binding protein (PABP) is an RNA-binding protein involved in eIF4G-mediated initiation of translation (Imataka *et al.* 1998) and mRNA poly(A) shortening by recruiting and stimulating PAB-dependent poly(A)-specific ribonuclease subunit 3 (PAN3) and its catalytic subunit PAN2 (Boeck *et al.* 1996; Brown *et al.* 1996; Uchida *et al.* 2004; Yamashita *et al.* 2005). C-C chemokine receptor type 4 (CCR4) is also an important deadenylase which along with CCR4-associated factor 1 (CAF1) and negative regulator of transcription 1 (NOT1) forms a poly(A)-nuclease complex (Tucker *et al.* 2001; Yamashita *et al.* 2005). Complex of AGO and GW182 has been shown to concert a rapid biphasic mRNA deadenylation by recruiting PABP-PAN3/PAN2 and CCR4-CAF1-NOT complexes, respectively, followed by DCP1/DCP2-mediated mRNA decapping (Tucker *et al.* 2001; Yamashita *et al.* 2005; Chen *et al.* 2009), a process which leads to the eventual degradation of miRNA-targeted mRNA by exoribonucleolytic activity of XRN1 (Arribas-Layton *et al.* 2013; Wahle and Winkler 2013). However, data from several studies suggest mRNA degradation may not be necessary for repression (Mathonnet *et al.* 2007; Fabian *et al.* 2009; Djuranovic *et al.* 2012; Meijer *et al.* 2013). In addition, it has been shown that translation repression of miRNA-targeted mRNAs precedes mRNA deadenylation and degradation (Bethune *et al.* 2012; Djuranovic *et al.* 2012) and that these two steps occur independently of each other (Zdanowicz *et al.* 2009). Consistent with this observation, deadenylation inhibition by protecting the poly(A) tail with a downstream non-poly(A) sequence does not prevent translation repression (Fukaya and

Tomari 2011; Bazzini *et al.* 2012; Mishima *et al.* 2012) and GW182 depletion restores expression of both polyadenylated and non-polyadenylated target reporters (Eulalio *et al.* 2008). Interestingly, it has also been demonstrated that 5’-cap-indepenedent translation is refractory to repression (Pillai *et al.* 2005; Meijer *et al.* 2013) and mRNA degradation even when an mRNA is bound by miRISC, suggesting that degradation of miRNA-targeted mRNAs is dependent on repression of translation (Meijer *et al.* 2013). Notably, however, translation repression does not always promote mRNA degradation and translation of miRNA-repressed mRNAs may be reactivated (Braun *et al.* 2011; Braun *et al.* 2013; Wilczynska and Bushell 2015). In addition to 5’-cap, secondary structure of an mRNA 5'UTR and the type of promoter from which it is transcribed determine the outcome and mechanism of translation repression, respectively. In an *in silico* study, the authors predicted secondary structure of the 5'UTR of human mRNAs deposited in RefSeq database using RNAfold web-based tool. When sorted these mRNAs based on presence or absence of TargetScan-predicted miRNA sites in their 3'UTR, a correlation was revealed between presence of secondary structures in 5'UTR and miRNA sites in 3'UTR of the mRNA. Interestingly, this correlation was stronger with shorter 5'UTRs (shorter than 100nt). According to authors, this is probably due to greater dependence of mRNAs with shorter 5'UTR on miRNA-mediated repression (Meijer *et al.* 2013). Moreover, an *in vitro* study demonstrated that translation of miRNA-targeted mRNAs transcribed from SV40 and TK (thymidine kinase) promoters is repressed at the initiation and post-initiation steps, respectively, suggesting that the mode of mRNA repression is determined by the coding gene promoter (Kong *et al.* 2008).

eIF4F is a 5’-cap-binding protein complex which plays an important role in promoting mRNA translation initiation and is comprised of eIF4A and eIF4E subunits and the scaffold subunit eIF4G (Grifo *et al.* 1983; Merrick 2015). eIF4A is an RNA helicase implicated in unwinding of secondary and tertiary structures of mRNA 5’-cap and 5'UTR which promotes binding of 43S ribosome subunit to the mRNA (Ray *et al.* 1985; Linder 2003). Using siRNA-knockdown studies it has been demonstrated that eIF4AII, an isoform of eIF4A, is the only component of eIF4F to be necessary for miRNA-mediated repression of translation (Meijer *et al.* 2013). DEAD-box RNA helicase 6 (DDX6) is a decapping factor whose involvement in miRNA-mediated gene silencing via interaction with CCR4-NOT complex has been described (Haas *et al.* 2010; Chen *et al.* 2014; Mathys *et al.* 2014; Rouya *et al.* 2014) . It has been suggested that CCR4-NOT-CAF1 interaction with eIF4AII and its associated factors enforces a structural conformation which can inhibit 43S binding and scanning of miRNA-targeted mRNAs whereas its association with DDX6 facilitates mRNA degradation by linking mRNA 5’ decapping and deadenylation (Basquin *et al.* 2012; Wilczynska and Bushell 2015).

The activity of miRNAs and the ultimate result of this activity should be considered in the context of the cell type and activity. Examples of such context-dependent miRNA-mediated gene regulation include tumour suppressor p27 and transcription factor Krüppel-like factor 4 (KLF4). P27 downregulation is required for cell cycle progression (Hengst and Reed 1996; Chu *et al.* 2008) and it has been shown that in quiescent cells, due to inaccessibility of its 3'UTR target sites, p27 and its inhibitors miR-221 and miR-222 are concurrently expressed at high levels. Pumilio homolog 1

(PUM1) is an RNA-binding protein which is upregulated upon growth factor induction. Strikingly, upregulation and phosphorylation of PUM1 triggers a conformational change in p27 3'UTR which allows miR-221 and miR-222 access to their cognate sites, resulting in p27 downregulation and consequent cell cycle entry (Kedde *et al.* 2010). KLF4 is also an important regulator of cell fate in cancer and development. It has been shown to act as a tumour suppressor in colorectal cancer (Dang *et al.* 2003; Zhao *et al.* 2004) while promoting malignancy in breast cancer (Foster *et al.* 2000; Pandya *et al.* 2004). Interestingly, KLF4 expression is upregulated by miR-206 in non-cancerous mammary epithelial cells whereas miR-206 downregulates KLF4 in breast cancer cells, suggesting that miRNA-mediated regulation of KLF4 is also determined by the cell type (Lin *et al.* 2011).

While the majority of miRNA target sites thus far identified reside in the 3'UTR of the mRNAs (Agarwal *et al.* 2015; Wilczynska and Bushell 2015), a few studies have reported functional miRNA binding sites within the 5'UTR of the target transcripts. For instance, an *in vitro* study demonstrated that association of miR-10a with 5'UTR of a set of ribosomal protein (RP) mRNAs promotes their translation (Orom *et al.* 2008). Similarly, binding of miR-122 to HCV mRNA 5'UTR is required for the activation of virus mRNA translation (Jopling *et al.* 2005; Roberts *et al.* 2011). Translation repression following 5'UTR binding of miRNAs has also been reported. Human cytomegalovirus (HCMV) miR-US25-1 has been demonstrated to downregulate expression of several genes associated with cell cycle control including cyclin E2 (CCNE2) and tripartite motif-containing 28 (TRIM28) via binding to their mRNA 5'UTR (Lytle *et al.* 2007; Grey *et al.* 2010). Finally, it is important to note that the

extent to which a given miRNA can modulate the expression of its target transcripts may be influenced by the abundance of its target sites in a certain cell type or during a certain phase of the cell growth, since competition between binding sites to recruit the miRNA can attenuate its regulatory effect (Seitz 2009). Indeed, such competing effect has been reported in *Arabidopsis thaliana* (*A. thaliana*) where IPS1 (Induced by Phosphate Starvation 1), a non-protein-coding gene, acts as a target for miR-399. IPS1-mediated sequestration of miR-399 results in accumulation of PHO2 (Phosphate 2) mRNA which is a protein-coding target of miR-399, resulting in reduced inorganic phosphate in the plants shoots (Bari *et al.* 2006; Franco-Zorrilla *et al.* 2007). In addition, artificial miRNA sponges which are routinely utilised in miRNA inhibition experiments exploit the phenomenon of competitive miRNA target binding (Ebert *et al.* 2007).

1.6. Viral miRNAs

The process of miRNA biogenesis initiates in the nucleus. Viral miRNAs, like their cellular counterparts, are dependent on the host cell miRNA processing machinery (Kincaid and Sullivan 2012). Given the requirement of host cell miRNA processing mechanisms, it is not surprising that almost all viral miRNAs thus far have been identified in DNA viruses, which replicate in the host-cell nucleus (Cann 2012). One notable exception is the retrovirus, bovine leukaemia virus (BLV) which, despite being a single stranded RNA virus, encodes five miRNAs. To avoid cleavage of its genome BLV circumvents the Drosha-mediated pri- to pre-miRNA stage of miRNA processing by coding for smaller miRNAs which are instead transcribed by RNA polymerase III (Pol III) (Kincaid *et al.* 2012). It has been demonstrated

that BLV-miR-B4 joins the RISC and downregulates expression of tumour suppressors HMG-box transcription factor 1 (HBP1) and peroxidasin homolog (PXDN) *in vitro* by specific binding to their 3'UTR luciferase reporters (Kincaid *et al.* 2012). Interestingly, while BLV-miR-B4 and miR-29a have an identical seed sequence (Kincaid *et al.* 2012), miR-29a overexpression in lymphocytes has been associated with downregulation of HBP1 and PXDN and induction of hyperproliferative malignancies in mouse and human (Han *et al.* 2010; Santanam *et al.* 2010). Importantly, nuclear access and a DNA genome do not guarantee the existence of viral miRNAs. Despite prediction of miRNAs for some papillomaviruses (Gu *et al.* 2011), in at least one papillomavirus, HPV31, no miRNA is present (Cai *et al.* 2006). Similarly, varicella zoster virus (VZV) is a non-miRNA-encoding herpesvirus (Umbach *et al.* 2009).

Viral miRNAs can be classified as host miRNA analogues or virus-specific miRNAs. As mentioned in section 1.5, the seed region of a miRNA plays a pivotal role in target recognition by miRISC. Therefore, virus-mediated translational regulation of host transcripts could be achieved via encoding virus miRNAs with seed region similarity to host miRNAs. Such a mechanism has been shown to exist in several herpesviruses and BLV. For example, KSHV-miR-K12-11 is an orthologue of human miR-155, sharing the same seed sequence as well as a common set of targets (Nair and Zavolan 2006; Gottwein *et al.* 2007; Skalsky *et al.* 2007). miR-155 is an important immune modulator which is involved in development of immune cells such as B and T-cells and macrophages in the haematopoietic system and its overexpression has been implicated in several lymphomas and other human

malignancies. Given that memory B cells are the natural reservoir of KSHV, mimicking this host miRNA can be of physiological significance to KSHV persistence (Grundhoff and Sullivan 2011). As explained earlier, BLV-miR-B4 is also a homologue of bovine miR-29a with identical seed sequence and common targets whose miR-29a-driven suppression has been associated with B cell-like malignancies, suggesting that BLV-miR-B4 may drive leukaemia by mimicking miR-29a (Kincaid *et al.* 2012).

One interesting question is whether host cell miRNAs exert an effect on viral transcripts, especially those cellular miRNAs with orthology to virus miRNAs. Currently, there is scant evidence for such a cellular miRNA effect, however, it has been shown that the human liver-expressed miR-122 targets the 5'UTR of hepatitis C virus genome and promotes viral replication (Jopling *et al.* 2005).

Cellular miRNAs are capable of targeting hundreds of mRNAs, therefore, mimicking host miRNAs provides a virus with a means to regulate large numbers of cellular transcripts. According to a gross estimate, almost a quarter of the identified human virus-miRNAs carry host-identical seed regions (Kincaid and Sullivan 2012). However, this estimate can be challenged by revisiting how these analyses were performed, i.e. based on hexameric or heptameric seed region, or by considering determinant factors other than seed matching and that some miRNAs might not be *bona fide* or functional (Grimson *et al.* 2007; Kincaid and Sullivan 2012). Nevertheless, encoding an endogenous miRNA provides considerable advantages to the virus, due to its small footprint on genome size and low immunogenicity. This is particularly important in herpesviruses, which express miRNAs

predominantly during the latent phase of the virus lifecycle. By employing such a strategy, herpesviruses can remain undetected by the host immune system, yet continue to regulate expression of host transcripts to their own advantage. Moreover, in γ-herpesviruses, such as EBV and KSHV, the latent state is associated with oncogenicity, raising an intriguing hypothesis that virus-encoded miRNAs may have a causal role in cancer and host cell transformation (Grundhoff and Sullivan 2011). The roles and functions of virus miRNAs are discussed in more detail below.

1.6.1. The functions of viral miRNAs

In addition to their regulatory role in virus replication and life cycle, viral miRNAs have been implicated in modulating host gene expression (Seo *et al.* 2009; Bauman *et al.* 2011). Three major functional roles have been assigned to viral miRNAs, based on their impact on the virus-host interaction and the associated outcomes: increasing host cell longevity, evasion of host-cell immune response and attenuation of lytic infection (Kincaid and Sullivan 2012). Below I consider each of these functional roles in more detail.

1.6.1.1. Increasing host cell longevity

Longer lifespan of the host cell is clearly beneficial to latent/persistent viruses. The regulatory role of cellular miRNAs in apoptosis, by targeting pro-apoptotic and anti-apoptotic genes, is well documented (Subramanian and Steer 2010). Interestingly, some γ-herpesviruses have managed to usurp the host-cell apoptosis regulatory system. For example, KSHV-miR-K12-1, miR-K12-3 and miR-K12-4-3p have been shown to specifically target 3'UTR of the pro-apoptotic gene caspase3 (casp3) mRNA and downregulate its

expression (Abend *et al.* 2010; Suffert *et al.* 2011). In EBV, it has been shown that the viral BART miRNAs miR-BART1, miR-BART3, miR-BART9, miR-BART-11 and miR-BART12 are able to prevent cell death by targeting and downregulating Bcl-2 interacting mediator of cell death (Bim) (Marquitz *et al.* 2011), whereas miR-BART5 downregulates p53 upregulated modulator of apoptosis (PUMA) (Choy *et al.* 2008). Marek's disease virus 1 (MDV1), a tumour-associated α-herpesvirus in chicken, downregulates the expression of the TGF-β signalling pathway protein, SMAD2, rendering the anti-cancer drug cisplatin ineffective (Xu *et al.* 2011). BCL2-associated transcription factor 1 (BCLAF1 or BTF) is a pro-apoptotic protein whose sustained overexpression has been shown to lead to apoptosis and it has been suggested to be a tumour suppressor (Kasof *et al.* 1999; Sarras *et al.* 2010). BTF has also been demonstrated to be a target for miRNAs of the above-mentioned herpesviruses as well as the β-herpesvirus, HCMV (Ziegelbauer *et al.* 2009; Lee *et al.* 2012; Riley *et al.* 2012).

Viral miRNAs are not only associated with derailing programmed cell death, there is also evidence supporting an association with oncogenesis. For instance, KSHV and MDV1, although infecting different species, encode miRNAs analogous to the host cell miR-155 (Boss *et al.* 2009; Du *et al.* 2011; Zhao *et al.* 2011) which when aberrantly expressed is associated with tumour formation (Faraoni *et al.* 2009; Tili *et al.* 2009). Interestingly, lack of miR-M4 expression (the orthologue of miR-155) or mutating the miR-M4 seed region in MDV1 renders the virus non-tumorigenic (Zhao *et al.* 2011). Although the exact mechanism of MDV1-miR-M4-mediated tumorigenesis has not been identified, Zhao *et al.* suggest that the virus miRNA exploits the host miR-155

pathway. C/EBPβ is a regulator of lymphoid and myeloid maturation whose miR-155-mediated downregulation has been associated with lymphoproliferative disorder in mice (Screpanti *et al.* 1995; Costinean *et al.* 2009). Interestingly, it has been demonstrated that while overexpression of miR-155 and KSHV-miR-K12-11 downregulates C/EBPβ, antagomir-mediated abolition of KSHV-miR-K12-11 in human primary effusion lymphoma cell lines leads to C/EBPβ derepression (Boss *et al.* 2011). These observations suggest a cardinal role for MDV1-miR-M4 and KSHV-miR-K12-11 in the oncogenic potential of the encoding virus. Furthermore, seed region similarities have been identified between cellular miRNAs and some other lymphotropic virus-encoded miRNAs. These include miR-BART1-3p of EBV, miR-rL1-6-3p of Rhesus Lymphocryptovirus (RLCV), and miR-M21 of MDV2 with seed similarities to miR-29 which has been shown to be overexpressed in human chronic lymphocytic leukaemias (CLLs) (Kincaid and Sullivan 2012). To date, there is no evidence for direct association of polyomavirus miRNAs with apoptotic or oncogenic states in their host cells.

1.6.1.2. Host immune evasion

Evading host immune detection and elimination is vital to persistence/latency-establishing viruses. As discussed earlier, miRNAs possess advantages over proteins in this regard, since their expression does not elicit an immune response and they occupy very little genomic real-estate (Kincaid and Sullivan 2012).

In vitro studies carried out on two members of the polyomavirus family, JC virus (JCV) and BK virus (BKV), demonstrated that these viruses

downregulate the immune ligand ULBP3 and as a result significantly reduce elimination of virus infected cells (Bauman *et al.* 2011). JCV and BKV cause severe life threatening diseases in immunosuppressed patients in the central nervous system and kidneys, respectively (Nickeleit *et al.* 1999; Jiang *et al.* 2009). It has been shown that SV40 miRNA is associated with reduced killing effect of cytotoxic T-cells (Sullivan *et al.* 2005). JCV and BKV also encode for a miRNA whose 3p strand is highly similar to SV40 miRNA 3p strand (Seo *et al.* 2008). Interestingly, the seed region of 5p strands of JCV and BKV miRNAs and their entire mature 3p strands are identical (Bauman *et al.* 2011) suggesting a common function. The JCV/BKV miRNA 3p strand was shown to map to a target site in the 3'UTR of ULBP3 and, despite an increase in the mRNA levels of ULBP3 following JCV infection, it was demonstrated that concurrent with increasing 3p expression, ULBP3 protein level was significantly reduced. This change in ULBP3 expression resulted in reduced efficacy of natural killer (NK) cytotoxic T-cells, an effect that was reversed following inhibition of 3p with a miRNA sponge. Bauman *et al.* suggest that the 3p strand of JCV miRNA exerts its regulatory effect on ULBP3 expression via inhibition of translation as well as other posttranscriptional mechanisms such as protein sequestration and degrading newly synthesised proteins (Bauman *et al.* 2011). They also conclude that since the ULBP3-mediated immune detection of infected cells is achieved via ULBP3 receptor NKG2D, a killer-cell receptor expressed by a variety of T-cells, JCV and BKV manage to remain undetected by adaptive as well as innate immune responses and hence establish a latent/persistent infection in immunologically healthy

individuals. To date, there is no evidence for similar activity of other polyomavirus miRNAs against host-cell immune-related transcripts.

1.6.1.3. Attenuating lytic replication

Viruses that establish a persistent infection avoid immune detection by downregulating the expression of antigenic viral proteins, host immune response proteins, or both. Therefore, if the host immune surveillance machinery is normally active and efficient, switching from lytic replication to a latent form is an effective strategy for evading host immune elimination. Virus-encoded miRNAs are predominantly found in viruses with a latent life-cycle, suggesting that their main evolutionary purpose is to enable the encoding virus to enter and maintain latency (Grundhoff and Sullivan 2011). In support of this hypothesis, the auto-regulation of viral immediate early transcripts has been predicted, *in silico*, to be the major role of some herpesvirus miRNAs (Murphy *et al.* 2008). The auto-regulatory effect of viral miRNAs against viral proteins has also been experimentally validated *in vitro* in several herpesviruses and polyomaviruses. KSHV miRNAs are able to negatively regulate the expression of the viral replication and transcription activator (RTA), a protein responsible for switching from latent to lytic replication (Sun *et al.* 1998). KSHV-miR-K12-9-5p directly targets the 3'UTR of RTA and reduces its expression. It has also been shown that antagomir-mediated inhibition of this interaction and mutation of miR-K12-9-5p seed match results in a significant increase in lytic state activation (Bellare and Ganem 2009). KSHV miRNAs can also stabilise latent infection indirectly and through cellular factors. Retinoblastoma-like protein 2 (Rbl2) is a repressor of DNA methyl transferases (DNMT) 3a and 3b. KSHV-miR-K12-4-5p directly

binds to the 3'UTR of Rbl2 leading to its translational repression and subsequently upregulation of DMNT3a, DMNT3b and DNMT1. This results in increased virus and host DNA methylation and inhibition of transcription (Lei *et al.* 2010; Lu *et al.* 2010b). In addition, KSHV-miR-K12-1-5p represses IkBα by targeting its 3'UTR, hence preventing lytic replication via NF-kB activation (Lei *et al.* 2010). Furthermore, it has been demonstrated that KSHV-miR-K12-3-5p downregulates nuclear factor I/B (NFIB) by directly targeting its 3'UTR. NFIB is an activator of RTA promoter, thus by suppressing NFIB, KSHV indirectly downregulates RTA, resulting in stabilisation of virus latency (Lu *et al.* 2010a). These mechanisms alongside RTA downregulation help KSHV maintain the latent state.

Similarly, EBV, HCMV and HSV (herpes simplex virus) miRNAs have also been demonstrated to target viral proteins which govern switching from latent to lytic replication. EBV-miR-BART-20-5p suppresses EBV immediate-early proteins ZTA (bZip transcription transactivator) and RTA by directly targeting 3'UTR of their transcripts, leading to stabilisation of latent infection (Jung *et al.* 2014). In HCMV, it has been shown that miR-UL112-1 downregulates expression of immediate-early (IE) proteins IE1, UL112/113 and UL120/121 by directly targeting their 3'UTR s in luciferase assays, indicating that HCMV-miR-UL112-1 may be involved in regulating viral replication (Murphy *et al.* 2008). Infected cell polypeptide 0 (ICP0) and ICP34.5 are key HSV-2 transactivator and neurovirulence factors. HSV-2 latency-associated transcript (LAT) encodes miR-I and miR-II which directly target ICP34.5 as well as miR-III which directly targets ICP0, leading to efficient downregulation of their expression and hence limiting HSV-2 lytic replication (Tang *et al.*

2008; Tang *et al.* 2009). The single miRNA of polyomaviruses is expressed from the late region and due to its perfect sequence complementarity against LT Ag can post-transcriptionally repress its expression (Lagatie *et al.* 2013). Thus far, the miRNA-mediated cleavage of LT transcripts has been described for SV40, JCV, BKV, MuPyV and MCV (Sullivan *et al.* 2005; Seo *et al.* 2008; Sullivan *et al.* 2009; Broekema and Imperiale 2013; Theiss *et al.* 2015). As described in section 1.4.1, polyomavirus LT antigens initiate viral genome replication, therefore their downregulation can restrict genome replication and subsequently limit virus detection by host immune surveillance (Seo *et al.* 2008). This has been confirmed by a recent study in BKV, which occurs naturally as both archetype and rearranged variants. Archetype BKV is the persistent variant and exhibits very low replication and T antigen levels, in contrast the rearranged variants are associated with lytic infection and renal disease (Gosert *et al.* 2008). In their novel study, Broekema and Imperiale showed that flipping the NCCR could reverse the mode of replication in both archetype and rearranged BKV virus (Broekema and Imperiale 2013). Archetype NCCR is comprised of five DNA sequence blocks (O (for origin of replication), P, Q, R and S) which act as enhancer and binding regions for transcription factors. The situation differs in rearranged variants where some sequence blocks have been deleted or duplicated. Interestingly, expression of early and late genes show opposite patterns, with rearranged variants exhibiting high early, low late region expression associated with high cytopathologic effects, whereas archetype variants are characterised by high late and low early region activity (Figure 1.13).

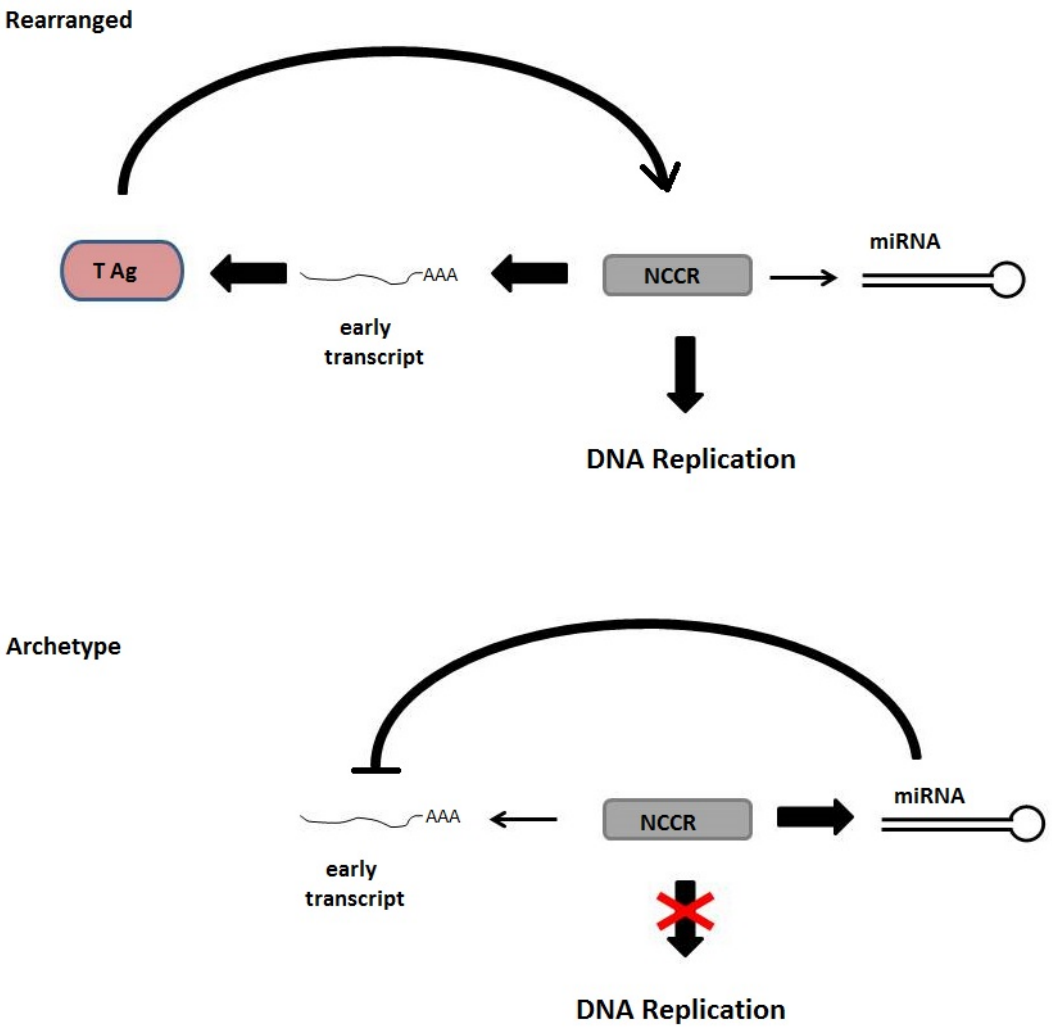

Figure 1.13. Suggested model for miRNA-mediated replication control. High activity of early promoter in rearranged variants results in high expression level of T Ag which in turn increases DNA replication by binding to replication origin (top). In archetype variants high miRNA expression level leads to early transcript degradation and abolishment of DNA replication (bottom). T Ag, Tumour antigen; NCCR, Non-coding control region.

As one would expect, in archetype BKV, miRNAs are generated before transcription of T Ag, readily directing cleavage of early transcripts, resulting in a very low replication rate. By flipping NCCR in both variants the activity of both regions under opposite conditions can be assessed, i.e. late region under late or early promoter and vice versa (Broekema and Imperiale 2013). This provided the first evidence that polyomavirus miRNAs can be expressed prior to virus DNA replication, suggesting a key role for BKV miRNA in virus persistence. Furthermore, the use of rearranged polyomavirus variants in previous studies may explain the failure to observe the regulatory role of viral miRNAs in virus replication. It remains to be determined if this mechanism is conserved in other polyomaviruses. In addition, it is not clear yet whether polyomavirus miRNAs can be, under certain cellular conditions, expressed independently from late proteins that would otherwise be immunogenic and in obvious opposition to miRNA-mediated persistence/latency. However, a recent study in MCV provided *in vitro* evidence for origin-independent expression of viral miRNA and its essential role in MCV establishment of persistent infection (Theiss *et al.* 2015).

Variations in the sequence of virus-encoded miRNA have also been described for several polyomaviruses. In JCV, miRNA polymorphisms have been reported in the 5p strand, although these fall outside the seed and loop regions of the pre-miRNA, suggesting that this may have limited functional effect (Lagatie *et al.* 2013). However, one must be cautious when making such assumptions as SV40 miRNA variants have been shown to target distinct host transcripts while their auto-regulatory effect against early genes remains unaltered (Chen *et al.* 2013).

Given the causal association of MCV with the majority of MCC cases, it is important to identify mechanisms underlying MCV pathogenesis and its role in cellular transformation. To date, the majority of MCV research has been focused on the role of viral T antigens in MCC, and to some degree, in immune modulation. Studies focused on MCV-miR-M1 have predominantly been limited to auto-regulation of LT Ag (Seo *et al.* 2009; Lee *et al.* 2011; Theiss *et al.* 2015). Using a synthetic MCV genome (MCVSyn) and its miRNA mutant (MCVSyn-hpko), an important recent study confirmed that miRNA-mediated downregulation of LT is sufficient to diminish episomal replication (Theiss *et al.* 2015). The authors also provided compelling *in vitro* evidence for the essential role of MCV-miR-M1 in establishing persistent infection (Theiss *et al.* 2015) by showing that MCVSyn-hpko episomes are cleared from cultured cells by four months post-transfection, whereas the wild type MCVSyn episome was retained and remained replication-competent six months post-transfection. However, this study did not investigate the mechanism by which MCV-miR-M1 drives latency/persistence. Therefore, a key outstanding question is whether the role of MCV-miR-M1 in persistent infection is solely due to downregulation of LT and genome replication or if MCV-miR-M1 modulation of cellular transcripts that regulate antiviral response also contribute to persistent infection of MCV.

1.7. Project aims

The underlying hypothesis of this PhD thesis is that MCV-miR-M1 may modulate the expression of cellular transcripts in order for MCV to evade the host immune response and establish persistent infection and latent replication. In this regard, the project aims can be summarised as follows:

- Generation and validation of tools required for expression of MCV-miR-M1 *in vitro*. This will be achieved by generating plasmid constructs and inducible cell lines incorporating MCV-miR-M1 sequence and validating MCV-miR-M1-5p and -3p expression in each system. In addition, MCV-miR-M1 mimics will be used as an alternative expression tool and MCV-miR-M1 relative expression will be compared to determine and use the most efficient expression system in follow-up experiments.
- Investigating global transcriptomic changes of the host cell induced by MCV-miR-M1 via RNA-Seq. This will be determined by deep sequencing of total RNA harvested from 293 cells expressing MCV-miR-M1, followed by *in silico* analysis of the data to identify the degree of MCV-miR-M1-induced modulation and cellular pathways affected by such changes.
- Validation of RNA-Seq data at mRNA and protein expression levels using qRT-PCR and western blotting, respectively.
- Identifying and validating MCV-miR-M1 specific targets in 3'UTR of altered transcripts. This will be assessed using dual luciferase assay in 293 cells transfected with luciferase response elements of putative targets and in the presence or absence of MCV-miR-M1.
- Investigating functional significance of MCV-miR-M1-induced changes.
- Confirming the data obtained from validation and functional studies in the context of MCV replication using wild type and miRNA-mutant MCV synthetic genomes.

CHAPTER 2

Materials and Methods

2. Materials and methods

2.1. Cell lines

Unless stated otherwise, cells were supplied from ATCC and maintained in Dulbecco's Modified Eagle Medium (DMEM). Growth media were supplemented with 10% fetal bovine serum (FBS) (PAA, The Cell Culture Company), 100 U/ml of penicillin and 100 µg/ml of streptomycin (PenStrep) (Thermo Fisher Scientific). Where indicated Zeocin, Blasticidin and Hygromycin B selection reagents (Thermo Fisher Scientific) were used at 100 µg/ml, 15 µg/ml and 100µg/ml, respectively. All cell lines were cultured at 37˚C and 5% CO2 and passaged at ~80% confluency. For a list of cell lines and growth media used in this study see Table 2.1.

Table 2.1. List of cell lines with growth media and supplements. DMEM, Dulbecco's Modified Eagle Medium; FBS, Fetal Bovine Serum; Pen Strep, Penicillin Streptomycin; Tet-Free, Tetracyclin-free; RPMI, Roswell Park Memorial Institute.

Cell line	Growth media and supplements
HEK293 (Human Embryonic Kidney cells)	DMEM, FBS, PenStrep
Flp-In™ T-REx™ 293	DMEM, Tet-Free FBS, PenStrep, Zeocin, Blasticidin (Thermo Fisher Scientific)
Flp-In™ T-REx™ 293 - MCV-LT	DMEM, Tet-Free FBS, PenStrep, Blasticidin, Hygromycin B
Flp-In™ T-REx™ 293-MCVmiR	DMEM, Tet-Free FBS, PenStrep, Blasticidin, Hygromycin B

2.2. Primers and oligonucleotides

Primers and oligonucleotides were designed using online primer design tools Primer-BLAST (National Center for Biotechnology Information, NCBI) and Primer3Plus (http://primer3plus.com/) and supplied by SIGMA-ALDRICH. miRNA primers were designed using miRNA Primer Design Tool accessible at http://genomics.dote.hu:8080/mirnadesigntool/ (Czimmerer *et al.* 2013). For a list of primers and oligonucleotides see Tables 2.2 to 2.5.

Table 2.2. List of oligonucleotides for qRT-PCR of MCV and cellular transcripts.

Target	Forward	Reverse
MCV LT	TTCCAGCAAAATATCCACAAGC	TGGATTGGGCCCATATTCGT
MCV sT	AAGTTGTCTCGCCAGCATTG	GCCACCAGTCAAAACTTTCCC
MCV VP1	AAAACACCCAAAAGGCAATG	GCAGAGACACTCTTGCCACA
ACTB	GGGAAATCGTGCGTGACATT	GACTCCATGCCCAGGAAGG
ADRA1D	CCGCTCGGCTCCTTGTTC	CACGCAGCTGTTGAAGTAGC
AMBRA1	ATTCACTCAGGAGGAGGCTG	TCTGTTGGTAGCGCATGGAG
C/EBPα	CTAGAGATCTGGCTGTGGGG	TCATAACTCCGGTCCCTCTG
C/EBPβ	CAGCGACGAGTACAAGAT	CTGCTCCACCTTCTTCTG
CCDC85A	GCCAGCCAGAATAGAAGGCA	AAGAACCCGGGAGAGTAGGC
CTSS	CACCACTGGCATCTCTGGAA	AGCACCACAAGAACCCATGT

CXCL8	ATGACTTCCAAGCTGGCCG	ACTGCACCTTCACACAGAGC
CYB5R2	AGACCAGACCAGACGAGTGA	AACATGGGTGTGATGCCTGT
DENND2D	CTTCGTTCTGACCAATGT	TGATGTCTCTTCTCCACTT
DMBT1	ACGACAGATTGGTGGCATCC	GTATGCAGGGTAGGATGGGC
DPP6	CCAACTTACACCGGCTCCAT	TGAGGATGGACACGTTCTGC
FOX2	ACCATCCCATTTCCACCACC	TGTGCTCCACCTTCTGTCTG
GAPDH	CGGAGTCAACGGATTTGGTC	GGATCTCGCTCCTGGAAGATG
IFI30	TACGGAAACGCACAGGAACA	CCCCATTGCACACTCCATGA
IFIH1	AGTGATTCAGGCACCATGGG	GCTGGGCAACTTCCATTTGG
KCNA1	CATCGCTGGTGTGCTAAC	GGTCACTGTCAGAGGCTAA
KLLN	CGAGGAGACCTAGGAGGGTT	ACCCCGAGCAAAGGAAGAAG
LILRB5	TTCCATCCACGGTGTATGACAG	GAGGGAGGGCTTCCTAGACA
LMO3	CACCAAGCCGAAAGGTTGTG	CCGTTACACCAAAGAGCCTCA
MAPK10	GGCTACAAGGAGAACGTGGA	TGGGCCGATTCTCCACATAG
MECP2	GGTAGCTGGGATGTTAGGGC	ATGTCTCTGCTTTGCCTGCC
OSR1	GGCCCTACACCTGTGACATC	AGTGAATATATCTGTGGTCTCGCA
PIK3CD	ATGTCACCGAGGAGGAGCA	CAGCAGGTAGAGCATCTGGG
RUNX1	AACAAGACCCTGCCCATCG	ACTTCGACCGACAAACCTGA
SCN1A	TCCTCCCCACACCAGTCTTT	TCGGGGCACAAACAAGGAAT

SELPLG	TCCTGTTGCTGATCCTAC	CTTTCTCGGCTTCATCTG
SOX10	TCTGGAGGCTGCTGAACGAA	CTTGTAGTGGGCCTGGATGG
SP100	AGCACTGTTCAGCGATGTCA	GTGGGGTTGTACCAGCATGA
TIGIT	GTGCCAGGTTCCAGATTCCA	GGGCTTTCTTCTTTCTAGTCAACG
TLR9	GGGCTGGGAAACCTCCGAGT	CGACCAGGCTCCCGAAGGAA
RAET1G (ULBP5)	GGGCAGAAGGAGTGCTAGAG	CAAAGAGAGTGAGGGTCGGC

Table 2.3. List of oligonucleotides for MCV-miR-M1 stem loop cDNA and stem loop qRT-PCR. F, forward; R, reverse.

Name	Sequence
MCV-miR-M1-5p stem loop primer	GTTGGCTCTGGTGCAGGGTCCGAGGTATTCGCACCAGAG CCAACAGTGTA
MCV-miR-M1-3p stem loop primer	GTTGGCTCTGGTGCAGGGTCCGAGGTATTCGCACCAGAG CCAACTTCAGG
GAPDH R (for stem loop cDNA)	CGTTCTCAGCCTTGACGGTG
MCV-miR-M1-5p	GTTTGGTGGAAGAATTTCTAGG
MCV-miR-M1-3p	GGGTGTGCTGGATTCTCTT
Universal reverse	GTGCAGGGTCCGAGGT
GAPDH F	CTCTGGTAAAGTGGATATTGT
GAPDH R	GGTGGAATCATATTGGAACA

Table 2.4. List of oligonucleotides for the cloning of pcDNA5/FRT/TO/MCVmiR and psiCHECK-2 constructs. Mutation sites of mutant psiCHECK-2-mcv-miR-concatemer oligonucleotide are underlined and marked in bold.

Name	Sequence
MCV-miR-M1 (BamHI)	GATCAGGTGCCATACGTTCTGGAAGAATTTCTAGGTACACTGGTTCCATTGGGTGTGCTGGATTCTCTTCCTGAATTGGTGGTCTCCTCTCTGC
MCV-miR-M1 (XhoI)	TCGAGCAGAGAGGAGACCACCAATTCAGGAAGAGAATCCAGCACACCCAATGGAACCAGTGTACCTAGAAATTCTTCCAGAACGTATGGCACCT
psiCHECK-2-MCV-miR-Concatemer (XhoI)	TCGAGAACCAGTGTACCTAGAAATTCTTCCAGAACGGAACCAGTGTACCTAGAAATTCTTCCAGAACGGATATCACCAATTCAGGAAGAGAATCCAGCACACCCAAACCAATTCAGGAAGAGAATCCAGCACACCCAAGC
psiCHECK-2-MCV-miR-Concatemer (NotI)	GGCCGCTTGGGTGTGCTGGATTCTCTTCCTGAATTGGTTTGGGTGTGCTGGATTCTCTTCCTGAATTGGTGATATCCGTTCTGGAAGAATTTCTAGGTACACTGGTTCCGTTCTGGAAGAATTTCTAGGTACACTGGTTC
Mutant psiCHECK-2-MCV-miR-Concatemer (XhoI)	TCGAGAACCAGTGTACCTAGAAATTC**CC**CCAGAACGGAACCAGTGTACCTAGAAATTC**CC**CCAGAACGGTCGACACCAATTCAGGAAGAGAATCCAG**AC**CACCCAAACCAATTCAGGAAGAGAATCCAG**AC**CACCCAAGC
Mutant psiCHECK-2-MCV-miR-Concatemer (NotI)	GGCCGCGCTTGGGTGGTCTGGATTCTCTTCCTGAATTGGTTTGGGTGGTCTGGATTCTCTTCCTGAATTGGTGTCGACCGTTCTGGGGGAATTTCTAGGTACACTGGTTCCGTTCTGGGGGAATTTCTAGGTACACTGGTTC
SP100 XhoI	CCGCTCGAGCGGTGAAGAGGATGAACAAGAGGAGGAA
SP100 NotI	ATAAGAATGCGGCCGCTAAACTATGAAGATTGCTAACCCAACACCAGC
CXCL8 XhoI	CCGCTCGAGCGGAAAAATTCATTCTCTGTGGTATCC
CXCL8 NotI	ATAAGAATGCGGCCGCTAAACTATTTACTTTGACAACAAATTATATTT
MAPK10 XhoI	CCGCTCGAGCGGTCATTTTCTTAGCACAGGTGCA

MAPK10 NotI	ATAAGAATGCGGCCGCTAAACTATGTGCCTGAAAACTGTTACCCAC
TLR9 XhoI	CCGCTCGAGCGGCCGTGAGCCGGAATCCTGCACGGT
TLR9 NotI	ATAAGAATGCGGCCGCTAAACTATGCCTTCGGTAGCATTTATTGAGTG
CYB5R2 XhoI	CCGCTCGAGCGGCACCAGGCCACACCCTGCCG
CYB5R2 NotI	ATAAGAATGCGGCCGCTAAACTATTGCTTTGTACTTGAGTTTATTTCA
KLLN XhoI	CCGCTCGAGCGGGACCTGAGACTCACTCCTTGCTCT
KLLN NotI	ATAAGAATGCGGCCGCTAAACTATTGGAGAATGTCTTAAAATTATCTT
OSR1 XhoI	CCGCTCGAGCGGTCAAGTGTCAAGAGTGTGGGAA
OSR1 NotI	ATAAGAATGCGGCCGCTAAACTATCAGAGAAACCTGGTCCTCTCCAA
SELPLG XhoI	CCGCTCGAGCGGGTAATTACTCCCCCACCGAGATGG
SELPLG NotI	ATAAGAATGCGGCCGCTAAACTATAAAGTGCTGGGATTACAGGCATGA
RAET1G (ULBP5) XhoI	CCGCTCGAGCGGTGGTTCCCTGGGCCCAGCTGTCTTTTCTTCCGTC
RAET1G (ULBP5) NotI	ATAAGAATGCGGCCGCTAAACTATGACGGAAGAAAAGACAGCTGGGCCCAGGGAACCA
C/EBPα PmeI	AGCTTTGTTTAAACGGCGCGCCGGGCCAGAGAGCTCCTTGGTCA
C/EBPα NotI	ATAAGAATGCGGCCGCTAAACTATGTGAGACTCTACGTTCTCCCC
C/EBPβ XhoI	CCGCTCGAGCGGTGCGGAACTTGTTCAAGCAG
C/EBPβ NotI	ATAAGAATGCGGCCGCTAAACTATGCCAATTACTGCCCCCAAAA

Table 2.5. List of site-directed mutagenesis oligonucleotides for the cloning of mutant psiCHECK-2 constructs.

	Forward	**Reverse**
SP100	CAACCATGTCTATTAGCTCCACA AAGCCAATC	AAGACTGACCTGGTACCTTGTCT ACACAG
MAPK10 5p	CTTCAACCAATGATGCTTACTACA GAAAG	ACCAAAGCAAGAGCAACTAGAAG TTAAATATAC
MAPK10 3p	ATCCAAAATTGTGTGTCTCTATCT TGCATC	GGGGCCACTGCACACCTTGTCAT GCCA

2.3. Plasmid propagation

All plasmids were propagated in NEB 5-alpha Competent *E. coli* (High Efficiency) (New England BioLabs, NEB). *E. coli* competent cells were transferred to ice from -80°C storage. After a gentle mix with a sterile and cold pipette tip 50µl of thawed cells per transformation were pipetted into an ice-cold 1.5ml microfuge tube and kept on ice. 100ng of plasmid DNA was transferred to transformation tube using an ice-cold pipette tip, the tube was flicked gently 5 times and incubated on ice for 30 minutes. Cells were then heat shocked at 42˚C for 30 seconds and returned to ice for a further 5 minutes. 950µl of room temperature SOC medium was added to each tube and cells were incubated at 37˚C in a shaking incubator at 250 revolutions per minute (rpm) for 60 minutes, prior to 100µl of cells being plated on 37˚C pre-warmed Luria-Bertani (LB) agar plates containing 100µg/ml ampicillin (SIGMA-ALDRICH) or 50µg/ml kanamycin (SIGMA-ALDRICH). Plates were incubated at 37˚C overnight (o/n). From the o/n LB agar cultures single colonies were transferred to sterile falcon tubes containing LB broth

supplemented with same concentration of ampicillin or kanamycin and incubated at 37˚C in a shaking incubator at 250rpm o/n. In every case, an LB agar plate was inoculated with pUC19-transformed *E. coli* and in the case of cloning or sub-cloning control plates for vector only and insert only were also included.

2.4. Plasmid isolation

Plasmid isolation was carried out in small scale and medium scale using PureLink Quick Plasmid Miniprep Kit (Thermo Fisher Scientific) and PureYield™ Plasmid Midiprep System (Promega), respectively.

2.4.1. Small scale plasmid isolation

Briefly, 1ml of o/n *E. coli* LB broth culture was pelleted at 13,000×g, resuspended in R3 resuspension buffer containing RNase A and lysed with L7 lysis buffer. Lysate was then precipitated with N4 precipitation buffer, homogenised by inverting several times and centrifuged at 13,000xg for 10 minutes. Supernatant was transferred to a binding column and centrifuged at 12,000xg for 1 minute, washed with W9 wash buffer containing 100% ethanol and centrifuged at 12,000xg for 1 minute two times. 50µl of TE elution buffer was added to the column in a new sterile microfuge tube, incubated at room temperature (RT) for 1 minute then centrifuged at 12,000xg for 2 minutes. Eluted plasmid was stored at -20°C.

2.4.2. Medium scale plasmid isolation

50ml of o/n culture was pelleted at 5,000xg for 10 minutes using a Beckman Avanti J25, resuspended in Cell Resuspension Solution then lysed by mixing with Cell Lysis Solution, inverting several times and incubating at RT for 3 minutes. Lysate was then neutralised by mixing with Neutralization Solution, inverted 5 times and incubated at RT for 3 minutes then centrifuged at 15,000xg for 15 minutes. Supernatant was transferred to a clearing column stacked on top of a binding column and connected to a vacuum manifold. Vacuum was applied until the entire liquid passed through both columns. Clearing column was discarded and binding column was washed by consecutive addition of Endotoxin Removal Wash and Column Wash Solution (contains 60% of 95% ethanol). Vacuum was applied for a further 30 seconds to allow the membrane to dry then 400µl nuclease-free water was added to the column, stacked on top of an Eluator™ Vacuum Elution Device and vacuum applied until all the liquid passed through the column and collected in a 1.5ml microfuge tube. For a list of plasmids and miRNA mimics see Table 2.6.

Table 2.6. List of plasmids, expression constructs and miRNA mimics.

Plasmid name	**Supplier**
pcDNA3.1	Thermo Fisher Scientific
pcDNA3.1/MCVmiR	Generated during this study
pcDNA5/FRT/TO	Thermo Fisher Scientific
pcDNA5/FRT/TO/MCVmiR	Generated during this study

pOG44	Thermo Fisher Scientific
pEGFP-C2	Clontech
pMK-MCVSyn and pMK-MCVSyn-hpko	Kindly provided by Prof. A. Grundhoff
MCV-miR-M1-5p mimic (ID:MC15405)	Thermo Fisher Scientific
MCV-miR-M1-3p mimic (ID:MC15468)	Thermo Fisher Scientific
mirVana miRNA mimic Negative Control #1	Thermo Fisher Scientific
psiCHECK-2	Promega
psiCHECK-2/wt-MCV-miR-concat	Generated during this study
psiCHECK-2/mut-MCV-miR-concat	Generated during this study
psiCHECK-2/SP100-3'UTR (WT and Mut)	Generated during this study
psiCHECK-2/CXCL8-3'UTR (WT and Mut)	Generated during this study
psiCHECK-2/TLR9-3'UTR (WT and Mut)	Generated during this study
psiCHECK-2/MAPK10-3'UTR (WT and Mut)	Generated during this study
psiCHECK-2/KLLN-3'UTR	Generated during this study
psiCHECK-2/RAET1G3'UTR	Generated during this study
psiCHECK-2/OSR1-3'UTR	Generated during this study
psiCHECK-2/SELPLG-3'UTR	Generated during this study
psiCHECK-2/CYB5R2-3'UTR	Generated during this study

2.5. Agarose gel electrophoresis

1% agarose (Thermo Fisher Scientific) gel was prepared in 100ml of 1x Tris Acetate EDTA (TAE) buffer (40mM Tris, 20mM acetic acid, 1mM EDTA pH 8.0) by boiling in microwave until completely dissolved. Ethidium bromide was added and thoroughly mixed at 5%v/v of gel (Thermo Fisher Scientific). DNA was electrophoresed at 120 Volt (v) for 45 minutes, visualised by Uvitec transilluminator and analysed using the Essential software package (UVItec Limited, Cambridge, United Kingdom).

2.6. DNA gel extraction

DNA fragments were extracted from agarose gel using PureLink Quick Gel Extraction Kit (Thermo Fisher Scientific). Briefly, the DNA fragment of interest was excised using a clean scalpel and transferred to pre-weighed nuclease-free microfuge tube. The tube was then re-weighed and the weight of the gel slice calculated. Gel Solubilisation Buffer L3 was added to the gel slice at a 3:1 ratio (w/v), tube was then incubated at 50°C for 10 minutes, inverting every 3 minutes to expedite dissolving the gel. Sample was incubated for a further 5 minutes and isopropanol added in 1:1 ratio (w/v) of the gel weight and mixed well. This solution was pipetted to a Quick Gel Extraction Column, centrifuged at 13000xg for 1 minute, flow-through discarded and 500µl of Wash Buffer W1 added to the column stack. Subsequent centrifugation at 13000xg for 1 minute and 15000xg for 2 minutes were performed with flow-through discarded after each spin. The Column was then transferred to nuclease-free microfuge tube and 50µl of elution buffer was added to the centre of the column stack prior to incubation at RT for 1 minute and elution

of the purified DNA fragment by centrifugation at 13000xg. DNA fragments were stored at -20°C.

2.7. Annealing of complementary oligonucleotides

Complementary oligonucleotides were diluted to 1µM concentration in T4 Polynucleotide Kinase Reaction Buffer (NEB) and mixed together in a 1:1 ratio at a final volume of 50µl prior to incubation in a T100 Thermal Cycler (BIO-RAD) as follows:

1. 95°C for 5 minutes
2. 95°C (-1°C/cycle) 1 minute for 70 cycles
3. 4°C for 30 minutes

Annealed oligonucleotides were stored at -20°C.

2.8. Cloning of plasmid constructs

Cloning of plasmid constructs was carried out as described below. Appropriate restriction enzyme sites were designed into 5' end of complementary oligonucleotides or oligonucleotides from which the DNA sequences of interest (insert sequence) were PCR amplified. PCR-amplified DNA or annealed complementary oligonucleotides and plasmid vectors (parent vectors) were digested with appropriate restriction enzymes (NEB) at the recommended temperature for 1h in the presence of CutSmart buffer (NEB). If required, restriction enzymes were deactivated at 65°C for 20 minutes. Digestion reactions were run on 1% agarose gel to confirm digestion and to gel-purify digested DNA prior to ligating the insert and vector using Instant Sticky-end Ligase Master Mix (NEB). Up to a total of 100ng of vector and insert DNA were mixed at a range of molar ratios from 1:3 to 1:6

and reaction volume adjusted to 5µl with nuclease-free water. 5µl of Ligase Master Mix was added to this vector-insert mixture, mixed by gently pipetting up and down 10 times and used immediately for transforming competent *E. coli*. For subcloning, insert sequence was obtained by digesting the plasmid construct containing the sequence and the new parent vector with same enzymes prior to ligating the insert and vector as described above.

2.8.1. Site-directed mutagenesis

miRNA recognition site mutated psiCHECK-2 constructs of cellular 3'UTRs were generated using Q5® Site-Directed Mutagenesis Kit (NEB). Briefly, back to back site mutation primers were designed with nucleotide replacements in miRNA seed and 3'UTR sequence matches (Table 2.5). Using WT psiCHECK-2-3'UTR constructs as template site mutated constructs were PCR amplified prior to degrading WT templates using DpnI for 5 minutes at RT. *E. Coli* competent cells were immediately transformed using 1µl of DpnI-treated reactions as described in section 2.3 and site mutated constructs were purified as described in section 2.4.1 All plasmid constructs generated during this study were confirmed via sequencing at DNA Sequencing facility, University of Dundee, Dundee, UK. For a list of plasmid constructs see Table 2.6.

2.9. Cell transfection

Lipofectamine 3000 Reagent (Thermo Fisher Scientific) was used for nucleic acid transfection. Briefly, plasmid DNA (250ng/1x10^5 cells) or miRNA mimics (30pmoles) were diluted in recommended volumes of 100, 50, 25 and 12.5µl of antibiotic and serum free growth medium for 6, 12, 24, and 48 well plates,

respectively. P3000 Reagent was added at 2µl/µg of diluted DNA and mixed well. Lipofectamine 3000 Reagent was diluted at the same concentration and in growth medium, mixed with DNA master mix at 1:1 ratio, incubated at RT for 5 minutes and added to cells at ~80% confluency. To determine transfection efficiency, pEGFP-C2 was transfected into HEK293 cells grown on poly-L-lysine (SIGMA-ALDRICH) coated 22x22x0.17mm glass coverslips (Thermo Fisher Scientific) as follows. Glass coverslips were soaked in 95% ethanol, left to air-dry, covered with poly-L-lysine (0.1% (w/v) in H2O) and incubated at 37˚C for 1h. Next, coverslips were placed in a 6-well plate, cells were seeded at $3x10^5$ cells per well and grown on glass coverslips. Cells were transfected 24h (hour) later at 80% confluency with 500ng of pEGFP-C2 and incubated for a further 24h. Transfected cells were then fixed using 4% formaldehyde in PBS for 15 minutes, washed with PBS and treated with 1% Triton-X 100 for 15 minutes. After a final PBS wash coverslips were mounted on glass slides in mounting medium for fluorescence with DAPI (Vector Laboratories, USA) and visualised using a Nikon ECLIPSE 80i fluorescent microscope. Transfection efficiency was calculated by scoring the number of GFP-positive cells and determined to be over 80%.

2.10. Cell proliferation assays (BrdU Cell Proliferation ELISA Kit)

BrdU (bromodeoxyuridine) cell proliferation assay was carried out to determine the impact of MCV-miR-M1 overexpression or MCVSyn replication on cell proliferation using Abcam colorimetric BrdU Cell Proliferation ELISA Kit. BrdU is a thymidine analogue which replaces thymidine by incorporating into DNA of replicating cells and can be detected using specific antibodies (Crane and Bhattacharya 2013). Briefly, 100µl of 293 cells were seeded in a

96 well plate at $1x10^5$/ml concentration and 24h later were either transfected with MCV-miR-M1 and scramble mimics or MCVSyn and MCVSyn-hpko or mock transfected. BrdU was added to the transfected cells and medium only wells 24h prior to fixing the cells with 200µl/well of fixing solution for 30 minutes at RT. The wells were then washed three times using supplied Wash Buffer and blotted dry prior to 1h RT incubation with 100µl/well of anti-BrdU monoclonal Detector Antibody. After a second wash and dry step, 100µl/well of 1:2000 Peroxidase Goat Anti-Mouse IgG Conjugate in Conjugate Diluent was added and plate was incubated for 30 minutes at RT prior to final wash and dry step. Next, the plate was exposed to 100µl/well TMB Peroxidase substrate for 30 minutes in the dark followed by 100µl/well of Stop Solution. The absorbance was recorded at 450/550nm dual wavelength. Cell proliferation was evaluated by plotting BrdU positive absorbance versus transfection condition at each time point. In addition, data was analysed by normalising BrdU positive to BrdU negative absorbance for each transfection condition.

2.11. Total RNA extraction

Total RNA was extracted from $1x10^6$ cells in 6-well plates using Aurum Total RNA Mini Kit (BIO-RAD). Briefly, after washing cells with sterile PBS, 350µl of lysis buffer (supplemented with 1% β-mercaptoethanol) was added to each well and cells were homogenised by pipetting. 350µl of 70% ethanol was added to cell lysate and pipetted up and down until the viscous lysate mixed thoroughly with alcohol and formed a non-viscous homogenous liquid. Lysates were transferred to an RNA binding column stacked on top of a cap-less wash tube and centrifuged at 13000xg for 30 seconds. Flow through

(collected in wash tube) was discarded, 700µl of low stringency solution was added to column and centrifuged at 13000xg for 30 seconds. 80µl of 1:15 (v/v) diluted DNase1 in DNase1 dilution solution was pipetted to the centre of column and incubated at RT for 15 minutes. Column was washed by consecutive addition of 700µl of high stringency solution and low stringency solution and centrifugation at 13000xg for 30 seconds. Column was centrifuged for a further 60 seconds and wash tube was discarded. Column was transferred to a nuclease-free 1.5ml microfuge tube, 80µl of elution buffer was pipetted to the centre of column and incubated at RT for 1 minute prior to centrifuging for 2 minutes at 13000xg at RT. Extracted total RNA was quantified (see section 2.12) and was immediately used for first strand cDNA synthesis. For smaller plates the amount of reagents used was scaled down accordingly.

2.12. Quantification of RNA and DNA

DNA and RNA concentrations were measured by NanoPhotometer P330 (Implen GmbH, Munich, Germany). Briefly, after programing the instrument to measure the concentration at 0.2mm path length, 1µl of reference sample (elution buffer or nuclease-free water) was pipetted onto the centre of measuring window, concentration was measured with Lid 50 and the instrument was blanked. Reference sample was wiped off and concentration of DNA or RNA was measured and recorded as ng/µl. A260/280 absorbance was read and recorded for each sample.

2.13. First strand cDNA synthesis

cDNA was generated using iScript Select cDNA Synthesis Kit (BIO-RAD). Briefly, reactions were set up in a nuclease-free 200µl PCR tube by mixing 5x iScript select reaction mix (4µl), Oligo(dT)20 primer or random primer mixes (2µl), nuclease-free water (up to 20µl), RNA (500ng) and iScript reverse transcriptase (1µl). In reverse transcriptase negative (NRT) reactions, reverse transcriptase was replaced with 1µl of water. Reactions were incubated as follows,

Primed with Oligo(dT)20

1. 42˚C for 30 minutes
2. 85˚C for 5 minutes

Primed with random primer mix

1. 25˚C for 5 minutes
2. 42˚C for 30 minutes
3. 85˚C for 5 minutes

cDNA samples were stored at -20˚C.

2.14. Stem loop cDNA synthesis

Stem loop cDNA was synthesised for detection of MCV-miR-M1 expression. Reactions were set up using iScript Select cDNA Synthesis Kit (BIO-RAD) by mixing 5x iScript select reaction mix (4µl), MCV-miR-M1-5p or -3p stem loop primer (500nM), gene specific primer enhancer solution (2µl), nuclease-free water (up to 20µl), RNA (500ng) and iScript reverse transcriptase (1µl). Reactions were incubated as follows,

1. 42˚C for 30 minutes
2. 85˚C for 5 minutes

2.15. Quantitative Real Time PCR (qRT-PCR)

qRT-PCR reactions were set up for two different quantitative assays as follows.

2.15.1. qRT-PCR for stem loop cDNA

qRT-PCR reactions were set up for detection of MCV-miR-M1-5p and -3p expression (Czimmerer *et al.* 2013) using SsoAdvanced Universal Probes Supermix (BIO-RAD) and ProbeLibrary probe #21 (Roche). Master mixes (MM) were prepared by mixing components in a sterile nuclease-free 0.5ml microfuge tube according to the following scale, 2x SsoAdvanced Universal Probes Supermix (10µl), MCV-miR-M1-5p or -3p forward primer (400nM), universal reverse primer (400nM), Universal ProbeLibrary probe #21 (200nM), nuclease-free water (up to 20µl). 5µl of each stem loop cDNA was added to 15µl of MM in each well of a BR Clear 96-well PCR plate (BIO-RAD), briefly mixed and centrifuged and incubated in a CFX Connect Real-Time PCR Detection System (BIO-RAD) as follows,

1. Initial denaturation and polymerase activation at 95°C for 30 seconds, 1 cycle
2. Denaturation at 95°C for 15 seconds followed by annealing and extension at 60°C for 30 seconds, 40 cycles with plate read
3. 65-95°C (+0.5°C increments, 5 seconds/increment) with plate read for melting curve

2.15.2. qRT-PCR for first strand cDNA

qRT-PCR reactions were set up for expression analysis of genes of interest using iTaq Universal SYBR Green Supermix (BIO-RAD). Briefly, reaction MMs were prepared according to the following scale, 2x iTaq Universal SYBR Green Supermix (10µl), forward and reverse primers (300nM each), nuclease-free water (up to 20µl). 1µl of first strand cDNA was added to 19µl of each MM in each well of a BR Clear 96-well PCR plate (BIO-RAD). Reactions were briefly mixed and centrifuged and incubated in a CFX Connect Real-Time PCR Detection System (BIO-RAD) as follows,

1. Initial denaturation and polymerase activation at 95°C for 30 seconds, 1 cycle
2. Denaturation at 95°C for 5 seconds followed by annealing and extension at 62°C for 30 seconds, 40 cycles with plate read
3. 65-95°C (+0.5°C increments, 5 seconds/increment) with plate read for melting curve

For both real time qRT-PCR assays data were viewed and analysed using BIO-RAD CFX Manager software (version 3). Gene expression was analysed using ΔΔCT (normalised expression) method.

2.16. Dual luciferase assay (DLA)

Luciferase assay was performed using Dual-Luciferase Reporter Assay System (Promega) and analysed using a TECAN infinite M 200 plate reader (Tecan, Männedorf, Switzerland) and data was obtained using Magellan software (Version 6.6). Briefly, $3x10^5$ 293 cells were seeded per well of a 6-

well plate and after 24h were co-transfected in triplicates according to following conditions,

1. For MCVmiR plasmid construct assays, either of pcDNA3.1 (control) or pcDNA3.1/MCVmiR plus either psiCHECK-2/wt-MCV-miR-concat or psiCHECK-2/mut-MCV-miR-concat
2. For MCV-miR-M1 mimics assays, either of 5p, 3p or control mimics plus either psiCHECK-2/wt-MCV-miR-concat or psiCHECK-2/mut-MCV-miR-concat

24h after transfection cells were washed with sterile PBS and lysed with 1x Passive Lysis Buffer (PLB) for 30 minutes on a plate shaker. Cell lysates were transferred to sterile microfuge tubes. 100µl of Luciferase Assay Reagent II (LAR II) and 20µl of cell lysates were manually pipetted to the wells of a 96-well flat bottom black microplate (Thermo Fisher Scientific). After measuring firefly luciferase (Fluc) activity, 100µl of Stop & Glo Reagent was dispensed to each well and activity of *Renilla* luciferase (Rluc) was measured. Data were exported to an Excel sheet and analysed as follows. Luciferase activity was normalised by dividing each Rluc value by corresponding Fluc value. Relative luciferase activity was calculated by dividing mean average of normalised Rluc values of MCV miRNA-transfected cells by that of control cells.

2.17. Generation of stable cell line (SCL) for inducible expression of MCV-miR-M1-5p and MCV-miR-M1-3p (Flp-In™ T-REx™ 293-MCVmiR)

Stable cell lines were generated according to Flp-In™T-REx™ Core Kit guidelines (Thermo Fisher Scientific). Flp-In™T-REx™293 cells were seeded

in 500µl of complete DMEM containing 100µg/ml Zeocin and 15µg/ml Blasticidin in a 24-well plate at $2x10^5$ cell/well concentration. At 70% confluency the cells were exposed to Hygromycin B in duplicate wells at 0, 10, 50, 100, 150, 200, 250, 300, 350, 400, 450 and 500µg/ml concentrations. Growth media was replaced with fresh DMEM containing the same amount of selection reagent every 3 days for 2 weeks. The minimum concentration at which all cells were dead after one week was determined as 50µg/ml. Flp-In™T-REx™293 cells were seeded in a 6-well plate with 15µg/ml Blasticidin but without Zeocin and co-transfected with pOG44 (a plasmid expressing Flp recombinase) and pcDNA5/FRT/TO/MCVmiR at 9:1 ratio using Lipofectamine 3000. Non-transfected and pcDNA5/FRT/TO/MCVmiR only (no pOG44) transfected wells were included as negative and positive controls, respectively. Cells were washed with sterile PBS after 24h and growth media was replaced. 48h post transfection cells were washed again, trypsinised and reseeded at 30% confluency. Hygromycin B was added to cells at 100µg/ml concentration and media was replaced every 3 days with fresh DMEM containing Hygromycin and Blasticidin until cell foci emerged. Cell foci were then transferred to new plates and tested for Zeocin sensitivity and Hygromycin resistance. Zeocin sensitive, Hygromycin resistant cells were expanded and maintained in complete DMEM containing 100µg/ml Hygromycin and 15µg/ml Blasticidin. Expression of MCV-miR-M1-5p and -3p was assessed via stem loop qRT-PCR as explained in section 2.15.1.

2.18. Construction of MCVSyn and MCVSyn-hpko

WT and miRNA-mutant Synthetic consensus MCV genome (MCVSyn and MCVSyn-hpko, respectively) were constructed as described previously

(Neumann *et al.* 2011). Briefly, pMK-MCVSyn and pMK-MCVSyn-hpko (a kind gift of Prof. Adam Grundhoff, Heinrich-Pette-Institute, Leibniz Institute for Experimental Virology, Hamburg, Germany) were digested with SacI (NEB) at 37°C for 1h followed by enzyme inactivation at 65°C for 20 minutes. The larger of the two DNA fragments was gel purified and recircularised using T4 DNA Ligase (Thermo Fisher Scientific) by mixing 5x Ligase Reaction Buffer at 1:5 ratio and DNA and T4 DNA Ligase at final concentrations of 1ng/µl and $5x10^{-3}$U/µl, respectively with sterile nuclease-free water, then incubated at 24°C for 1h. DNA was purified from ligation reaction using PureLink® PCR Purification Kit (Thermo Fisher Scientific) and stored at -20°C.

2.19. RNA sequencing

Total RNA samples were sequenced as described below at the Next Generation Sequencing facility based at Leeds Institute of Molecular Medicine (Saint James's University Hospital) under the supervision of Dr Sally Fairweather. Total RNA samples were assessed via the following steps prior to RNA sequencing.

2.19.1. Assessing RNA quality

RNA quality was assessed using RNA 6000 Nano Chip (Agilent Technologies, USA). Briefly, room temperature Agilent RNA 6000 Nano gel matrix was spin filtered at 4000rpm for 10 minutes. RNA 6000 Nano dye concentrate was thoroughly mixed with filtered gel at 1:65 ratio and centrifuged at 14000rpm for 10 minutes. On chip priming station 9µl of gel-dye mix was added to the well of the chip marked as black G, pressurised for 30 seconds and 9ul of gel-dye mix was added to other G wells. 5µl of RNA

6000 Nano marker was added to the rest of the wells prior to addition of 1µl of RNA samples to sample wells and 1µl of RNA ladder to ladder well. Loaded chip was vortexed at 2400rpm for 60 seconds then placed in an Agilent 2100 Bioanalyzer and RNA quality was analysed using 2100 expert software according to the supplier's guidelines.

2.19.2 RNA quantification

RNA samples were quantified using Qubit RNA Broad Range Assay Kit (Thermo Fisher Scientific) as follows. To prepare Qubit® working solution, Qubit® RNA BR Reagent and Qubit® RNA BR Buffer were mixed at 1:200 ratio. Standards were prepared by mixing each Qubit® RNA BR Standard (#1 and #2) with working solution at 1:19 ratio. 1-20µl of each RNA sample was added to 199-180µl of working solution, respectively, vortexed and incubated at RT for 2 minutes. Standards and samples were analysed consecutively using a Qubit® 2.0 Fluorometer (Thermo Fisher Scientific). Concentration of samples was calculated using the equation below,

Sample concentration=QF value × 200/V

(QF value: the value (µg/ml) obtained from Qubit® 2.0 Fluorometer; V: volume (µl) of the sample).

2.19.3. Preparation of total RNA library

Total RNA libraries were prepared using TruSeq Stranded Total RNA Sample Prep Kit (Illumina, USA) as follows.

2.19.3.1. Ribosomal RNA (rRNA) removal and RNA fragmentation

Total RNA was diluted with ultrapure nuclease-free water to a final volume of 10µl then mixed with 5µl of rRNA binding buffer and 5µl of Ribo-Zero rRNA removal mix by pipetting up and down prior to denaturation in a pre-heated T100™ Thermal Cycler (BIO-RAD) at 68˚C for 5 minutes. Denatured RNA was thoroughly mixed with 35µl of rRNA removal beads in a new tube and incubated at RT for 1 minute then placed on a magnetic stand for 1 minute and supernatant was transferred to a new tube. rRNA removal was repeated twice then 99µl of RNAClean XP beads was added to the sample, gently mixed and incubated at RT for 15 minutes followed by 5 minutes on magnetic stand. Supernatant was removed and discarded. Without disturbing the beads, 200µl fresh 70% ethanol was gently added to the tube on magnetic stand and incubated at RT for 30 seconds. Supernatant was removed and discarded and beads were left to air-dry for 15 minutes. After removing from magnetic stand, 11µl of Elution Buffer was gently mixed with beads and incubated at RT for 2 minutes. Tube was placed on magnetic stand for 5 minutes then 8.5µl of supernatant and 8.5µl of Elute, Prime, Fragment High Mix were mixed in a new tube and incubated as follows, 94˚C for 8 minutes then 4˚C on hold. At 4˚C, sample was removed from thermal cycler and immediately proceeded to the next step.

2.19.3.2. Synthesis of first and second strand cDNA

SuperScript II was gently mixed with First Strand Synthesis Act D Mix at 1:9 ratio then 8µl of mix was added to fragmented RNA sample, gently pipetted up and down 6 times and incubated in a T100™ Thermal Cycler as follows,

1. Lid pre-heat, 100˚C
2. 25˚C for 5 minutes
3. 42˚C for 15 minutes
4. 70˚C for 15 minutes
5. Hold at 4˚C

At 4˚C, sample was removed from thermal cycler and 5µl of Resuspension Buffer plus 20µl of Second Strand Marking Master Mix was added to tube, gently mixed and incubated in pre-heated thermal cycler at 16˚C for 1h.

2.19.3.3. Double-stranded cDNA (dscDNA) clean up

90µl of thoroughly dispersed room temperature AMPure XP beads was gently mixed with 50µl of dscDNA and incubated at RT for 15 minutes then placed on magnetic stand for 5 minutes and 135µl of supernatant was removed and discarded. Without disturbing the beads, 200µl fresh 80% ethanol was added to tube and incubated at RT for 30 seconds prior to discarding the supernatant. Ethanol wash was repeated twice and tube was left on magnetic stand for a further 15 minutes to air-dry, then removed from stand and 17.5µl of Resuspension Buffer was added and gently mixed with beads followed by incubating at RT for 2 minutes. Tube was placed on magnetic stand for 5 minutes then 15µl of supernatant was transferred to a new tube.

2.19.3.4. Verification of dscDNA presence

Prior to proceeding to adenylation step, presence of dscDNA was confirmed using High Sensitivity DNA 1000 Tape (Agilent Technologies, USA) as follows. Briefly, 2µl of High Sensitivity D1000 Sample Buffer was mixed with

2µl High Sensitivity D1000 Ladder and 2µl of dscDNA in separate tubes. 2µl of each mix was loaded onto a High Sensitivity D1000 ScreenTape, placed in Agilent 2200 TapeStation system, run and analysed using Agilent 2200 TapeStation Software.

2.19.3.5. Adenylation of 3' ends

Briefly, 2.5µl of Resuspension Buffer and 12.5µl of A-Tailing Mix was added to dscDNA and gently mixed by pipetting up and down 10 times then incubated in a pre-heated thermal cycler as follows,

1. Lid pre-heat, 100˚C
2. 37˚C for 30 minutes
3. 70˚C for 5 minutes
4. Hold at 4˚C

2.19.3.6. Adapter ligation

Immediately after adenylation and at 4˚C, dscDNA was gently mixed with 2.5µl of each of Resuspension Buffer, Ligation Mix and an RNA Adapter Index (Table 2.7) then incubated in a thermal cycler at 30˚C for 10 minutes (with lid pre-heat at 100˚C) prior to mixing with 5µl of Stop Ligation Buffer. 42µl of AMPure XP beads was added and thoroughly mixed with ligation reaction then incubated at RT for 15 minutes. Tube was placed on magnetic stand for 5 minutes and 79.5µl of supernatant was removed and discarded. Then 200µl fresh 80% ethanol was added to the tube without disturbing the beads and incubated for 30 seconds. Supernatant was discarded and ethanol wash was repeated twice prior to leaving beads to air-dry on

magnetic stand. Tube was removed from stand and beads were resuspended in 52.5µl Resuspension Buffer by gentle pipetting and incubated at RT for 2 minutes then placed back on magnetic stand for 5 minutes and 50µl of supernatant was transferred to a new tube. 50µl of mixed AMPure XP beads was added to each tube for a second clean up (as explained above but 95µl supernatant was removed and discarded before ethanol wash). Following third ethanol wash and removal, beads were air-dried, tube was removed from magnetic stand and 22.5µl of Resuspension Buffer was added and gently mixed with beads by pipetting and incubated at RT for 2 minutes. Tube was placed back on magnetic stand for 5 minutes and 20µl of supernatant was transferred to a new tube for PCR amplification.

Table 2.7. RNA Adapter Indices used in adapter ligation step.

Sample ID	Index No.	Index Sequence
Control 1	2	CGATGT
Control 2	4	TGACCA
Control 3	5	ACAGTG
3p1	6	GCCAAT
3p2	7	CAGATC
3p3	12	CTTGTA
5p1	14	AGTTCC
5p2	15	ATGTCA
5p3	19	GTGAAA

2.19.3.7. PCR amplification of adapter ligated samples

Adapter ligated dscDNA was amplified via PCR as follows. 5µl of PCR Primer Cocktail and 25µl of PCR Master Mix was added to dscDNA and mixed gently then incubated in a thermal cycler as follows,

1. Lid pre-heat, 100˚C
2. 98˚C for 30 seconds
3. 15 cycles of
    a. 98˚C for 10 seconds
    b. 60˚C for 30 seconds
    c. 72˚C for 30 seconds
4. 72˚C for 5 minutes
5. Hold at 4˚C

Following PCR run, 50µl of AMPure XP beads was added to tube and gently mixed then proceeded to clean up step as explained above, but 95µl supernatant was removed and discarded before ethanol wash. Following third ethanol wash and removal and an air-dry step, tube was removed from magnetic stand and 32.5µl of Resuspension Buffer was added and gently mixed then incubated at RT for 2 minutes. Tube was returned to magnetic stand for 5 minutes and30µl of cleaned up PCR product was transferred to a new tube.

2.19.3.8. Verification of final libraries

Final libraries were verified using DNA 1000 Chip (Agilent Technologies, USA) as follows. Briefly, 25µl of room temperature DNA dye Concentrate was added to a vial of DNA Gel Matrix, mixed well and transferred to a spin filter then centrifuged at 2300xg for 15 minutes. On chip priming station 9µl of gel-dye mix was pipetted to the well of DNA chip marked with black G and pressurised for 60 seconds. After releasing the pressure, 9µl of gel-dye mix was pipetted to the other two wells marked as G. To the rest of the wells 5µl of marker, to ladder well 1µl of DNA ladder, and to sample wells 1µl of final

library (or deionised water to unused wells) was added. After vortexing for 1 minute at 2400rpm, DNA chip was run in Agilent 2100 Bioanalyzer, DNA sizes were read and analysed using 2100 expert software.

2.19.3.9. Quantification of final libraries

Final libraries were quantified using Quant-iT™ PicoGreen ® dsDNA Kit (Thermo Fisher Scientific) as follows. Quant-iT™ PicoGreen® reagent working solution was prepared by diluting the reagent in 1xTE buffer at 1:200 ratio in a plastic container and protected from light, 5 serial dilutions of dsDNA in TE were prepared according to Table 2.8. To each dilution, 1ml of Quant-iT™ PicoGreen® reagent working solution was added, mixed well and incubated in the dark at RT for 5 minutes. Fluorescence was measured for dilutions at standard fluorescein wavelengths (480nm excitation, 520nm emission), normalised by subtracting the fluorescence value of the blank from that of each of the dilutions and a standard curve was plotted for fluorescence versus DNA concentration. dscDNA was diluted in TE to a final volume of 1ml, mixed with 1ml of Quant-iT™ PicoGreen® reagent working solution and incubated in the dark at RT for 5 minutes. Fluorescence was measured and normalised as above and concentration of dscDNA was determined using standard curve.

Table 2.8. Protocol for preparing standard curve for final library quantification. Volumes are in µl.

TE volume	Volume of 2µg/ml DNA Stock	Volume of Diluted Quant-iT PicoGreen Reagent	Final Concentration of DNA in Quant-iT PicoGreen Assay
0	1000	1000	1µg/ml
900	100	1000	100ng/ml
990	10	1000	10ng/ml
999	1	1000	1ng/ml
1000	0	1000	blank

Libraries were normalised to 10nM using Tris-Cl 10mM, pH 8.5 (with 0.1% Tween 20) and 10µl of each was pooled for sequencing on an Illumina HiSeq 2500 platform.

2.20. Enzyme-linked immunosorbent assay (ELISA)

ELISA was carried out for CXCL8 using Human IL-8 ELISA Ready-SET-Go! (2nd Generation) (eBioscience) according to the supplier's protocol. Briefly, ELISA was performed for growth media of transfected 293 cells as follows. Growth media of TNF-α stimulated (10ng/µl) or non-stimulated 293 cells were included as positive and negative controls, respectively. A 96-well Nunc Maxisorp ELISA plate (SIGMA-ALDRICH) was coated overnight at 4°C with 100µl/well of Anti-Human IL-8 capture antibody in Coating Buffer followed by 3x wash with 270µl/well Wash Buffer. The plate was blotted on absorbent paper prior to blocking with 200µl/well of 1x ELISA/ELISPOT Diluent for 1h, then washed once. To the appropriate wells was added 100µl/well of the following in technical duplicates, Human IL-8 top standard diluted with

ELISA/ELISPOT Diluent in 2-fold serial dilutions for 8 dilution points including diluent only as blank, samples including positive and negative controls. Plate was sealed and incubated at RT for 2h prior to 5x wash. After blotting on absorbent paper, to each well was added 100µl of Anti-Human IL-8 Biotin detection antibody diluted in 1X ELISA/ELISPOT Diluent, sealed and incubated at RT for 1h, then washed 5x and 100µl/well of Avidin-HRP diluted in 1X ELISA/ELISPOT Diluent was added to the plate. After a final 5x wash and blotting, the plate was incubated with 100µl/well of 1X TMB Solution for 15 minutes at RT, then 50µl/well of Stop Solution was added to the plate and absorbance was recorded immediately at 450nm using a TECAN infinite M 200 plate reader. A standard curve was plotted using absorbance versus concentration of the 8-point top standard dilutions and the concentration of samples was calculated using the obtained standard curve formula.

2.21. Western blotting

SDS-PAGE and western blotting was carried out to determine and quantify the expression of MCV-miR-M1 target genes at protein level. Briefly, 293 cells were transfected with MCV-miR-M1 mimics and control miRNA or WT and mutant MCVSyn. Cells were lysed using Radioimmunoprecipitation assay (RIPA) buffer (SIGMA-ALDRICH) containing protease inhibitor (cOmplete Protease Inhibitor Cocktail, Roche) for 30 minutes on ice. Whole cell lysates (WCL) were then centrifuged at 15000rpm at 4°C for 20 minutes and supernatants were transferred to fresh microcentrifuge tubes prior to protein quantification (see section 2.21.1). Laemmli buffer was added to each sample at 1x final concentration and samples were boiled at 100°C for 5 minutes prior to being aliquoted and stored at -20°C. 20µg of total protein

were loaded on to sodium dodecyl sulfate (SDS) polyacrylamide gel and run at 100V for 2h then transferred to a polyvinylidene fluoride (PVDF) membrane (BIO-RAD) prior to blocking with 5% dry low fat milk or bovine serum albumin (BSA) in TBST (Tris-buffered saline (TBS) and 0.1% Tween 20) for 1h at RT. Blocked membranes were then washed 3x5 minutes with TBST, incubated with 1:500 or 1:2000 of primary antibody in blocking solution overnight at 4°C on a shaker. Membranes were washed again using TBST prior to incubating with 1:1000 or 1:2000 of secondary antibodies for 1h at RT. Finally, membranes were washed 3x5 minutes with TBST, incubated with Clarity™ Western ECL Substrate (BIO-RAD) for 5 minutes at RT and visualised and pictured using a Gel Doc XR+ imager (BIO-RAD). Images were analysed using Image Lab™ Software (BIO-RAD). Where required, membranes were stripped using Restore™ Western Blot Stripping Buffer (Thermo Fisher Scientific) and reprobed with appropriate Ab's. For a list of antibodies and dilutions used refer to table 2.9.

Table 2.9. List of primary and secondary antibodies with dilution ratios.

Antibody (supplier)	**Dilution ratio (v/v)**
GAPDH (mouse monoclonal, 2mg/ml, abcam)	1:2000
CM2B4 (mouse monoclonal, 200µg/ml, Santa Cruz), a kind gift of Prof. A. Whitehouse (University of Leeds)	1:500
SP100 (rabbit polyclonal, 200µg/ml, Santa Cruz)	1:500
TLR9 (rabbit polyclonal, 200µg/ml, Santa Cruz)	1:500
Goat Anti-Mouse IgG (H+L)-HRP Conjugate (BIO-	1:1000 and 1:2000

RAD)	
Goat Anti-Rabbit IgG (H+L)-HRP Conjugate (BIO-RAD)	1:1000

2.21.1 Protein quantification

Protein quantification was carried out using Pierce® Microplate BCA Protein Assay Kit (Thermo Fisher Scientific). Briefly, protein standards were prepared as 8 point serial dilutions of BSA in RIPA buffer (0, 125, 250, 500, 750,1000, 1500 and 2000µg/ml). 9µl of protein standards and total protein samples were transferred to the wells of a clear 96 well plate in duplicates. BCA Working Reagents (WR) A and B were mixed at 50:1 ratio and 260µl of WR mix was added to each well, mixed with protein samples for 1 minute on a shaker prior to incubation at 37ºC for 30 minutes. The plate was then cooled at RT for 5 minutes prior to recording the absorbance at 562nm on a TECAN infinite M 200 plate reader. Using RIPA buffer absorbance (0µg/ml of BSA protein standard) as blank, a standard curve was plotted for absorbance versus concentration of protein standards. Concentration of total protein samples was calculated using formula of the standard curve and concentrations were normalised to 1µg/µl using Laemmli buffer prior to aliquoting and storing at -20ºC.

2.22. *In silico* identification of MCV-miR-M1 putative matches in 3'UTR of cellular transcripts

RNAhybrid online tool (Rehmsmeier *et al.* 2004) was utilised to identify putative seed matches of MCV-miR-M1-5p and MCV-miR-M1-3p in 3'UTR of qRT-PCR-validated targets. Briefly, 3'UTR sequences of interest and MCV-miR-M1-5p or -3p sequences were copied in FASTA format into the 'target sequence(s)' and 'miRNA sequence(s)' boxes of RNAhybrid tool, respectively, prior to proceeding to select 'hits per target' and '3utr-human' option. Finally, predicted MCV-miR-M1 matches were obtained and downloaded via 'start calculation' tab which included predicted matches, minimum free energy (mfe) and miRNA seed match position relative to 5' end of the 3'UTR.

2.23. Neutrophil isolation from peripheral blood

Neutrophils were isolated from peripheral blood as previously described (Lau and Hunstad 2013). Briefly, fresh blood was obtained from University of Bradford Ethical Tissue Bank (Ethical Tissue, REC Ref 07/H1306/98+5). Equivalent volumes of blood and 3% dextran (w/v) in 0.9% NaCl were mixed in a sterile conical tube prior to RT incubation for 20 minutes. The upper layer was carefully transferred to a new tube and cells were pelleted at 300xg for 10 minutes prior to resuspending in 0.9% NaCl. Equivalent volume of density centrifugation solution was carefully layered under cell suspension, to preserve the interphase, and centrifuged at 400xg for 30 minutes. To lyse red blood cells (RBC), supernatant was discarded and cell pellet underwent several rounds of consecutive resuspension in equivalent volumes of cold

0.2% NaCl (30 seconds) and 1.6% NaCl followed by 6 minute centrifugation at 300xg until cell pellet appeared RBC-free. Cell pellet was resuspended in appropriate volume of DMEM containing 10% FBS and 1% PenStrep prior to counting cells with haemocytometer. Neutrophil purity was confirmed by Giemsa smear staining as described by Bain *et al.* (Bain *et al.* 2012) and determined as 90 percent. Briefly, a smear was prepared from cell suspension on a glass slide and air dried prior to methanol fixation for 30 seconds followed by immersing in Giemsa stain for 20 minutes. Slide was flushed with water, air dried and examined under light microscope using immersion oil.

2.24. Transwell migration assay

In vitro neutrophil migration was measured using transwell (Boyden) chambers (BD Falcon Cell Culture Inserts, BD Biosciences) as described previously (Alfaro *et al.* 2016). Briefly, neutrophils were seeded ($2x10^6$ neutrophils in 500µl DMEM) into the top chamber and migration stimuli (cell growth media) were placed in the lower chamber. Where appropriate, CXCR2 antagonist SB265610 (SIGMA-ALDRICH) was added to the top chamber at 1000nM final concentration. Plate was incubated at 37ºC and 5% CO2 for 2h prior to mixing the lower chamber contents with equal volume of CellTiter-Glo® 2.0 reagent (Promega). The mixtures were then transferred to the wells of a 96-well plate (100µl in technical triplicates) and luminescence was recorded for each sample using a TECAN infinite M 200 plate reader. The chemotactic index was measured as the ratio of luminescence in the presence to that of the absence of MCV-miR-M1.

CHAPTER 3

Generation and Validation of MCV-miR-M1 Expression Tools

3. MCV-miR-M1 expression tools

3.1. Generation and validation of tools required for expression of MCV-miR-M1

When this project commenced in October 2013 there were no MCV-miR-M1 expression constructs described in the literature. This necessitated the development of several MCV-miR-M1 expression tools for use in subsequent screening experiments to examine the functional consequences of MCV-miR-M1 on cellular mRNA transcripts.

3.1.1. Construction of tools

3.1.1.1. Construction of pcDNA5/FRT/TO/MCVmiR and pcDNA3.1/MCVmiR for expression of MCV-miR-M1

With a view to promote the transcription of pre-miRNA loop, the full predicted MCV-miR-M1 pre-miRNA sequence was cloned into pcDNA5/FRT/TO and pcDNA3.1 which would then be processed by cellular miRNA pathways to produce the mature MCV miRNA. To this end, pcDNA5/FRT/TO/MCVmiR was constructed by inserting MCV-miR-M1 sequence into HindIII/XhoI site of pcDNA5/FRT/TO. Briefly, pcDNA5/FRT/TO was digested with HindIII and XhoI enzymes at 37˚C for 1h, run on agarose gel and gel extracted. Forward MCV-miR-M1 and reverse MCV-miR-M1 oligonucleotides (incorporating a HindIII and a XhoI compatible overhang, respectively) were annealed and ligated into the digested pcDNA5/FRT/TO vector. *E. coli* competent cells were transformed with the ligation products and recombinant plasmid was selected via antibiotic resistance and plasmid DNA extracted. The extracted plasmid was digested with HindIII + XhoI and run on agarose gel along with

undigested plasmid. Presence of the insert was confirmed by observing a 94bp fragment in HindIII/XhoI digested plasmid (Figure 3.1 A). DNA sequencing verified presence of MCV-miR-M1 sequence prior to using pcDNA5/FRT/TO/MCVmiR to generate Flp-In™ T-REx™ 293-MCVmiR cell line for inducible expression of MCV-miR-M1 (see section 3.1.1.2).

To generate a tool for transient expression of MCV-miR-M1 a plasmid construct was generated by subcloning MCV-miR-M1 into pcDNA3.1. Briefly, pcDNA3.1 and pcDNA5/FRT/TO/MCVmiR were digested with KpnI + XhoI and run on agarose gel. Digested pcDNA3.1 and the smaller DNA fragment (102bp) from pcDNA5/FRT/TO/MCVmiR were gel-purified, ligated and used for transformation of *E. coli* competent cells. Plasmid construct was extracted from the cells, digested with KpnI + XhoI and run on agarose gel along with undigested plasmid and pcDNA3.1. In addition to size difference with the undigested plasmid and parent vector (pcDNA3.1), a 102bp fragment was observed in the digested construct lane. pcDNA3.1/MCVmiR was verified via DNA sequencing. For a map of pcDNA5/FRT/TO/MCVmiR and pcDNA3.1/MCVmiR see Figure 3.1.

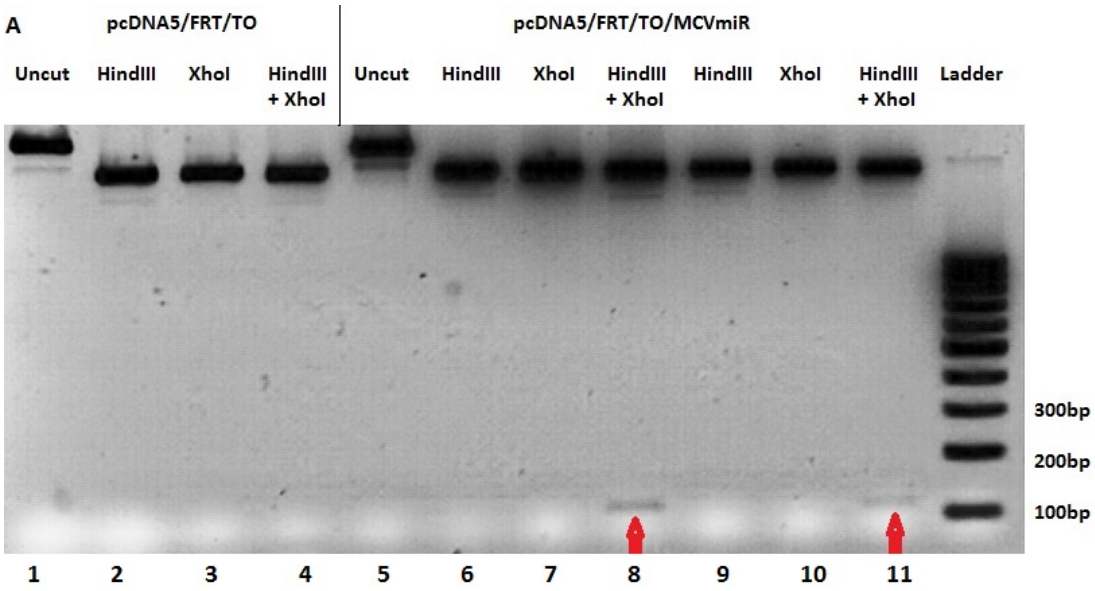
A
pcDNA5/FRT/TO
pcDNA5/FRT/TO/MCVmiR
Uncut
HindIII
XhoI
HindIII + XhoI
Uncut
HindIII
XhoI
HindIII + XhoI
HindIII
XhoI
HindIII + XhoI
Ladder
300bp
200bp
100bp
1
2
3
4
5
6
7
8
9
10
11

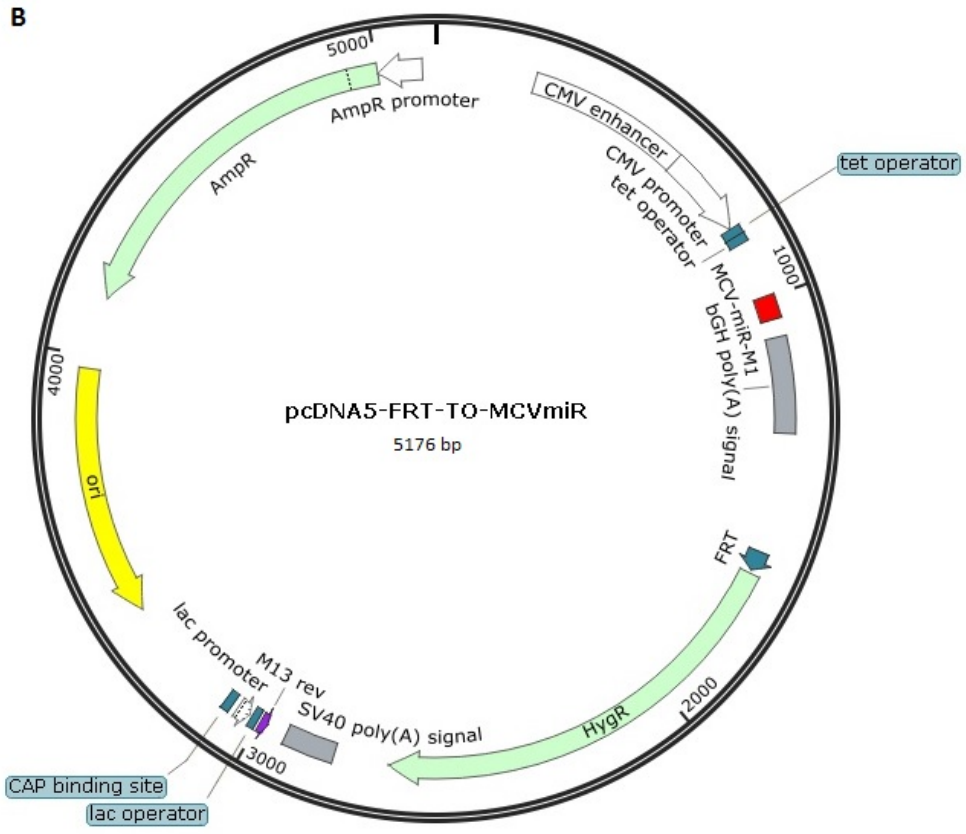
B
5000
AmpR promoter
AmpR
CMV enhancer
CMV promoter
tet operator
tet operator
1000
MCV-miR-M1
bGH poly(A) signal
4000
pcDNA5-FRT-TO-MCVmiR
5176 bp
ori
FRT
lac promoter
M13 rev
SV40 poly(A) signal
HygR
2000
3000
CAP binding site
lac operator

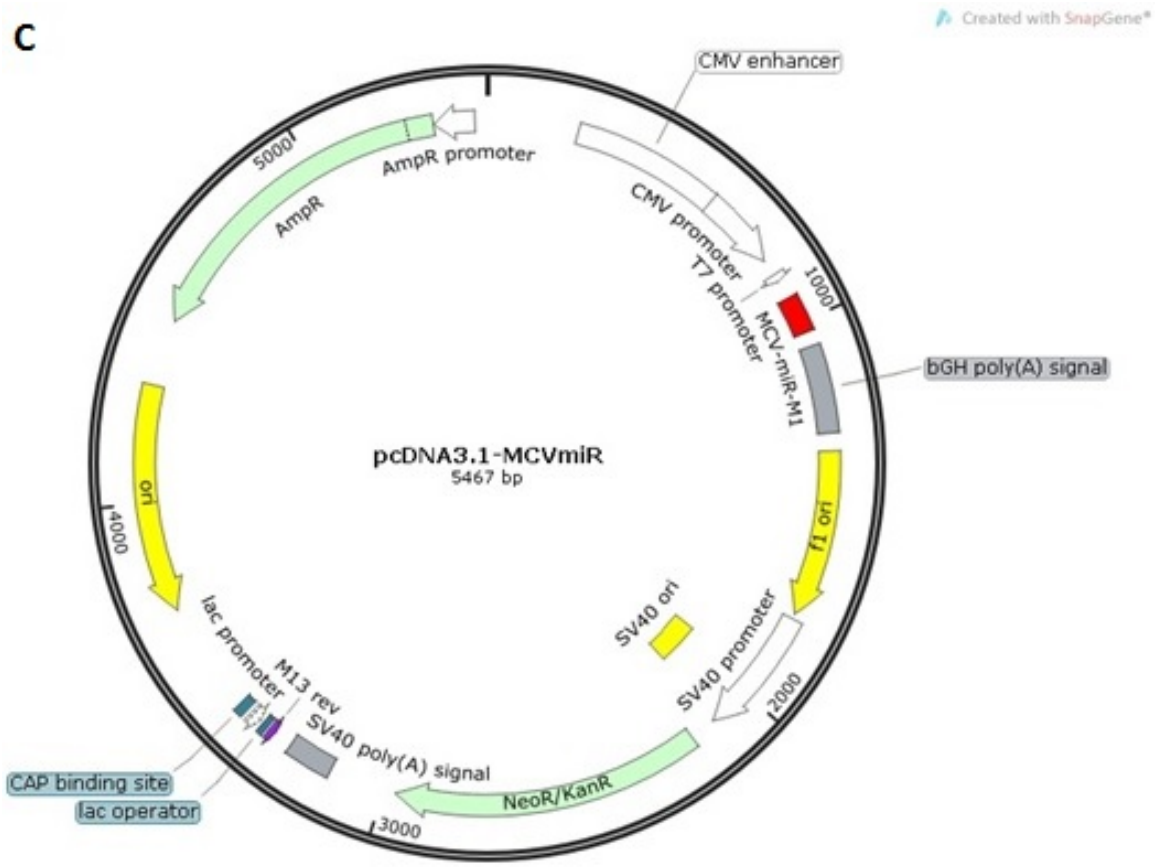

Figure 3.1. Generation of MCV-miR-M1 plasmid constructs. (A) pcDNA5/FRT/TO and putative pcDNA5/FRT/TO/MCVmiR construct were digested with HindIII, XhoI and HindIII + XhoI. A 94bp fragment (red arrows, lanes 8 and 11) was observed only in HindIII + XhoI digested construct. Lanes 9-11 were loaded with lower concentration of digested construct. (B and C) Schematic representation of pcDNA5/FRT/TO/MCVmiR and pcDNA3.1/MCVmiR (generated by SnapGene software).

3.1.1.2. Generation of Flp-In™ T-REx™ 293-MCVmiR cell line for inducible expression of MCV-miR-M1

In addition to pcDNA3.1/MCVmiR, it was desirable to generate a stable cell line that would allow inducible expression of MCV-miR-M1 from the integrated MCV pre-miRNA (MCV-miR-M1) sequence. This would not only eliminate the need for plasmid transfection and facilitate the quantitative expression of the virus miRNA, but also would have the benefit of assessing the effect of an endogenously expressed MCV-miR-M1 on cellular transcripts. Flp-In™T-REx™293 cells were co-transfected with pOG44 and pcDNA5/FRT/TO/MCVmiR and integrants selected for via Hygromycin B resistance and Zeocin sensitivity. Six Hygromycin-resistant Zeocin-sensitive cell foci were expanded and assessed for MCV-miR-M1 expression via stem-loop qRT-PCR (See section 3.1.2.1).

3.1.1.3. Construction of MCVSyn

When studying functional significance of miRNA targets it is necessary to assess the miRNA expression at endogenous levels. In addition, it is important to assess the effect of polyomavirus miRNAs on host cell transcripts in the context of virus replication due to their modulatory effect on virus early transcripts and replication (Lagatie *et al.* 2013). However, one of the challenges in the field of MCV research (until very recently) is the lack of a permissive virus cell line to facilitate analysis of MCV replication and virus-host cell interactions. During the lifetime of this project novel tools were published that permitted the generation of miRNA-positive and -negative synthetic virus genomes, termed MCVSyn and MCVSyn-hpko, respectively

(Theiss *et al.* 2015). Therefore, to assess the impact of MCV-miR-M1 expression on host cell transcripts in a virus-relevant context a collaboration was established with Prof. Adam Grundhoff (Heinrich Pette Institute, Hamburg). MCVSyn and MCVSyn-hpko were generated from parental pMK-MCVSyn and pMK-MCVSyn-hpko, respectively, as detailed in section 2.18. Briefly, pMK-MCVSyn and pMK-MCVSyn-hpko were digested with SacI and the larger of the two linear DNA fragments (5387bp) was gel extracted and recircularised with T4 DNA ligase prior to purification. To confirm the generation of MCVSyn, purified DNA was digested with EcoRI and run on agarose gel. As can be seen in Figure 3.2, a 5387bp band representing MCVSyn was observed, this contrasts with what would be expected if the MCVSyn genome was in a linear form where two bands of 3599bp and 1788bp would be detected. 293 cells were transfected with 250ng/1x10^5 cells of the recircularised MCVSyn or MCVSyn-hpko vector and virus gene expression, including MCV-miR-M1 expression, assessed.

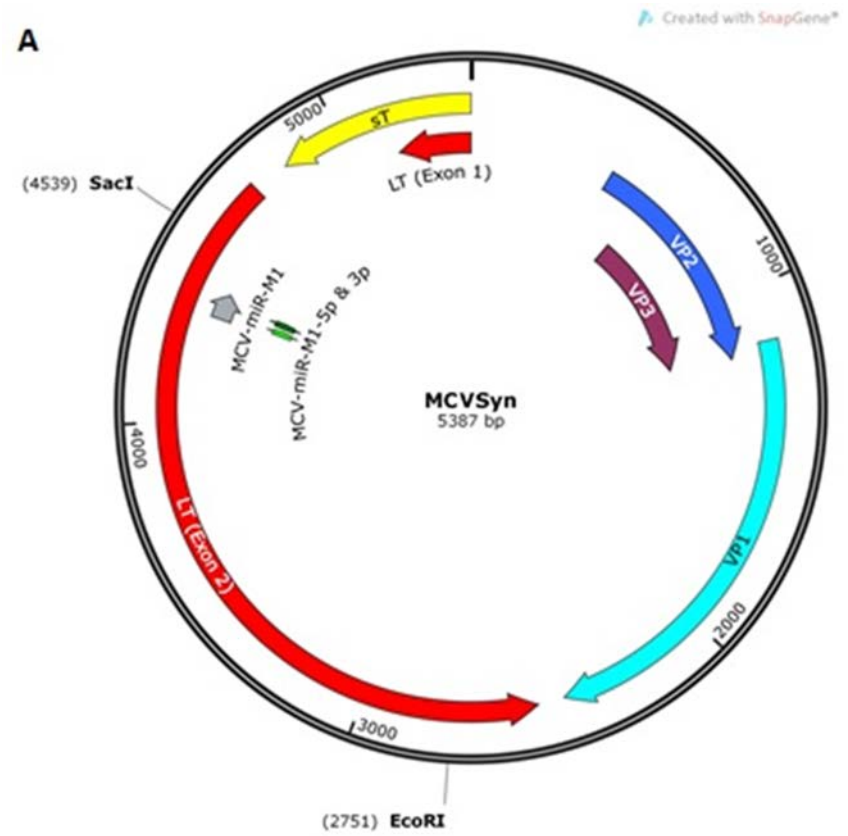
A
Created with SnapGene®
5000
sT
LT (Exon 1)
(4539) SacI
1000
VP2
VP3
MCV-miR-M1
MCV-miR-M1-5p & 3p
MCVSyn
5387 bp
4000
LT (Exon 2)
VP1
2000
3000
(2751) EcoRI

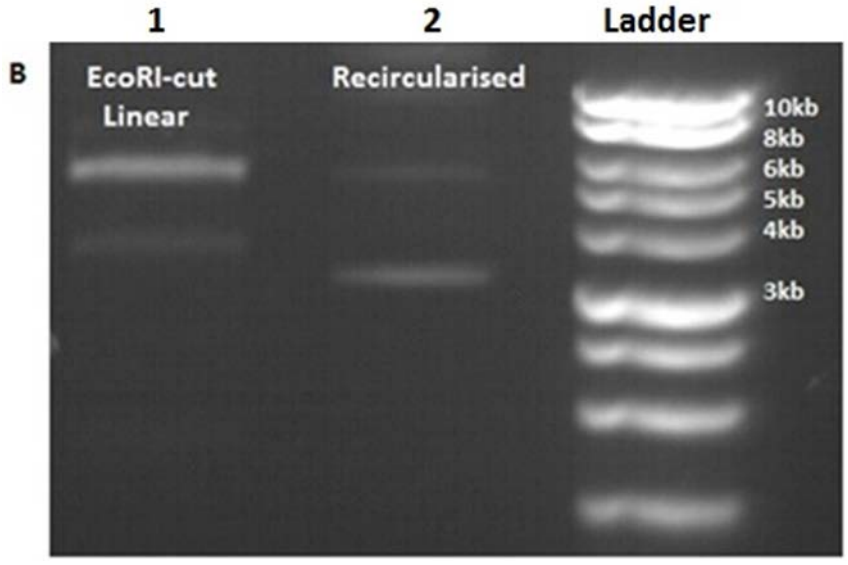
1
2
Ladder
B
EcoRI-cut
Linear
Recircularised
10kb
8kb
6kb
5kb
4kb
3kb

Figure 3.2. The synthetic MCV consensus construct, MCVSyn. (A) Schematic representation of MCVSyn as described by Neumann *et al.* (B) Size difference between the EcoRI digested and un-digested recircularised MCVSyn. The upper bands in both lanes correspond to the expeceted 5387bp size of MCVSyn. The lower bands in lanes 1 and 2 represent linear and supercoiled forms of MCVSyn, respectively.

3.1.2. Validation of tools

3.1.2.1. Detecting the expression of MCV-miR-M1-5p and -3p via stem loop qRT-PCR for plasmid constructs, stable cell lines, and MCV-miR-M1 mimics

To determine if MCV-miR-M1 was expressed from pcDNA3.1/MCVmiR, 293 cells were transfected with pcDNA3.1/MCVmiR or pcDNA3.1 as described in section 2.9. Expression of both strands was confirmed via stem loop qRT-PCR in pcDNA3.1/MCVmiR (Figure 3.3 A) whereas no MCV-miR-M1 expression was detected in pcDNA3.1-transfected, NTC and NRT controls. In addition, expression of MCV-miR-M1 was assessed in uninduced and doxycycline-induced Flp-In™ T-REx™ 293-MCVmiR cell line. Expression of MCV-miR-M1-5p and -3p was confirmed in induced but not uninduced cells (Figure 3.3 B). To test the specificity of miRNA detection system, stem loop qRT-PCR for each strand was performed using stem loop cDNA and forward primer of the other strand, i.e. 5p stem loop cDNA as a template for 3p primer, and vice versa. Stem loop cDNA and forward primer of 5p could only detect expression of MCV-miR-M1-5p and not that of MCV-miR-M1-3p.

Similarly, MCV-miR-M1-3p was only detectable with 3p stem loop cDNA and 3p forward primer but not with those of the 5p strand. These results indicate specificity of the stem loop qRT-PCR for detection of each of the MCV-miR-M1 strands.

miRNA mimics are routinely used for overexpression of endogenous cellular miRNAs and due to more stable modified chemical structure and more efficient expression are a suitable substitute for plasmid constructs. In addition, the mirVana™ miRNA Mimics used in this study display excellent specificity for the chosen guide strand due to inactivation of the star strand by proprietary chemical modifications. Moreover, unlike MCVSyn, Flp-In™ T-REx™ 293-MCVmiR and pcDNA3.1/MCVmiR, miRNA mimics would allow identification of specific targets and exclusive study of each of the MCV miRNA strands, this was highly desirable given that the JC/BK-encoded miRNA is reported to exert major function in host-immune evasion via the 3p strand (Bauman et al. 2011). To confirm specific expression of MCV-miR-M1 mimics in our 293 transfection system, MCV-miR-M1-5p, -3p and scramble control mimic were transfected into 293 cells. Exclusive expression of either the 5p or 3p strands was confirmed in the corresponding MCV-miR-M1-5p or -3p mimic samples via stem loop qRT-PCR (Figure 3.3 C). Comparison of the relative expression of MCV-miR-M1 revealed significantly lower levels in Flp-In™T-REx™293-MCVmiR SCLs compared to pcDNA3.1/MCVmiR and MCV-miR-M1 mimics (Figure 3.3 D). Given such low levels of expression, the decision was taken to exclude the Flp-In™T-REx™293-MCVmiR SCL from further analysis and instead focus on the other expression systems.

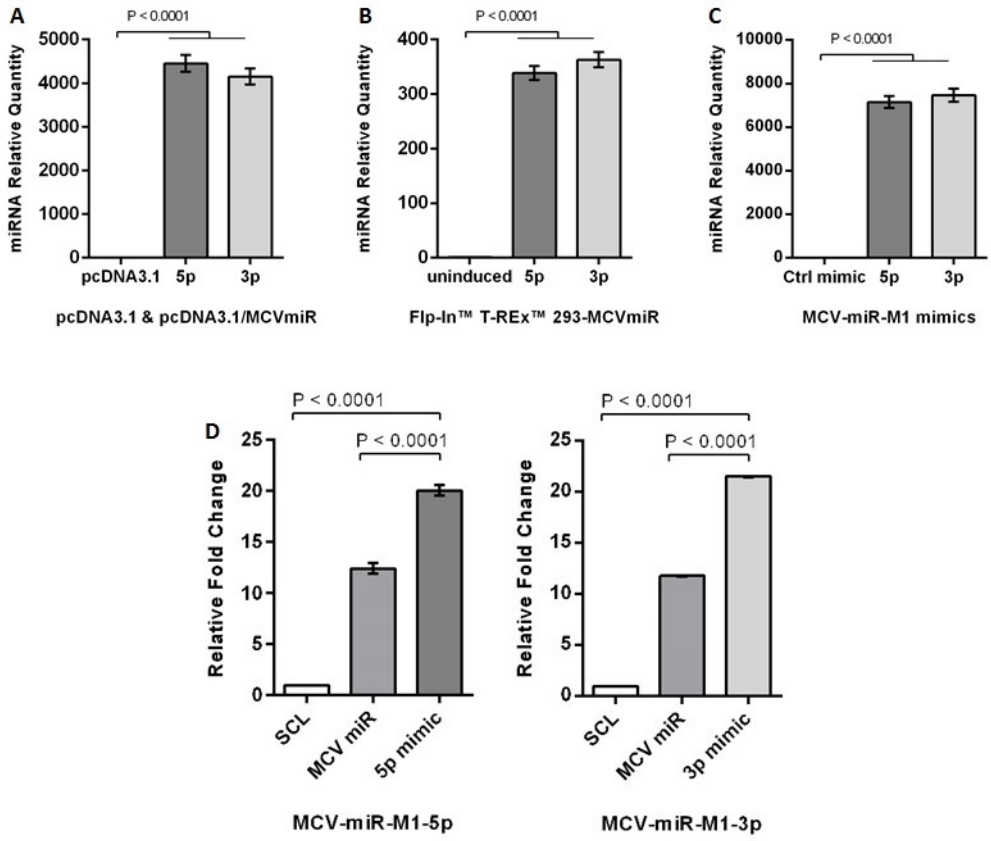

Figure 3.3. Relative expression of MCV-miR-M1-5p and -3p in pcDNA3.1/MCVmiR (MCV miR)-transfected 293 cells (A), Flp-In™ T-REx™ 293-MCVmiR stable cell lines (SCL) (B), MCV-miR-M1-5p and -3p mimics-transfected 293 cells and comparison of MCV-miR-M1 expression between the three systems (D).

3.1.2.2. Assessing the regulatory effect of MCV-miR-M1 on MCV LT transcripts in Flp-In™ T-REx™ 293-MCV-LT stable cell line (LT SCL)

Having confirmed the expression of MCV-miR-M1-5p and MCV-miR-M1-3p via stem-loop qRT-PCR in a variety of different systems, it was important to confirm the functionality of MCV-miR-M1 by assessing their effect on the expression of their cognate target, the MCV LT transcript. To achieve this, an

inducible Flp-In™T-REx™293-MCV-LT stable cell line (a kind gift of Prof. Adrian Whitehouse, University of Leeds) that expresses MCV LT under a regulatable promoter was used. Since MCV-miR-M1 is encoded from the opposite strand of LT one of the challenges in the study of MCV LT is concomitant expression of MCV-miR-M1 (Figure 3.4 A). Therefore, to assess the regulatory effect of MCV-miR-M1 against MCV LT necessitated MCV-miR-M1 overexpression in Flp-In™T-REx™293-MCV-LT cells. Data shown in Figure 3.3 demonstrate that the highest expression of MCV-miR-M1 is achieved via transient transfection of mimics. Moreover, the use of mimics also enables the exclusive assessment of the regulatory effect for each strand. MCV-miR-M1 was overexpressed by transfecting MCV-miR-M1 mimics into induced (1µg/ml doxycycline) and uninduced Flp-In™T-REx™293-MCV-LT cells. Expression of MCV-miR-M1 and MCV LT was assessed via qRT-PCR and normalised against GAPDH. As can be seen in Figure 3.4 B, in induced Flp-In™T-REx™293-MCV-LT cells, MCV LT expression shows a small but statistically significant downregulation (less than 2-fold, p-value<0.0001) in MCV-miR-M1-5p and -3p mimics versus control mimic. Although MCV LT expression was detectable in uninduced Flp-In™T-REx™293-MCV-LT cells, it was significantly lower compared to induced LT cell line (up to 60-fold, Figure 3.4 B). In addition, relative expression level of endogenous MCV-miR-M1-3p was higher than that of MCV-miR-M1-5p by 2-fold (Figure 3.4 A) which is reflected in relatively lower LT expression in 3p- versus 5p-transfected induced LT SCL (Figure 3.4 C). These results confirm that both MCV-miR-M1-5p and -3p are able to negatively regulate the MCV LT expression.

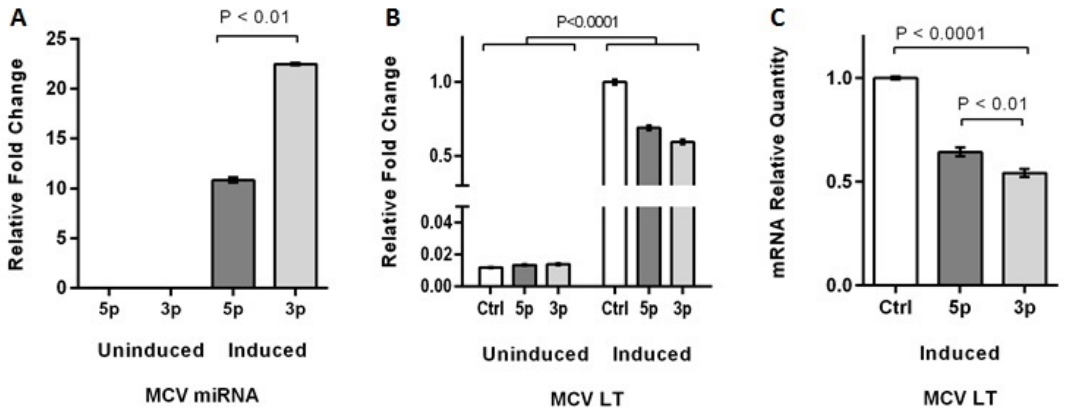

Figure 3.4. Expression of MCV-miR-M1 in induced and uninduced Flp-In™T-REx™293-MCV-LT stable cell line (LT SCL) (A). MCV LT expression in MCV-miR-M1 mimic-transfected induced and uninduced LT SCL. MCV LT mRNA level in uninduced LT SCL is significantly lower than that of induced cells (B). MCV LT is downregulated following transfection of MCV-miR-M1 mimics in induced (C). 5p and 3p, MCV-miR-M1-5p and -3p mimics; Ctrl, control mimic; NS, no significance.

3.1.2.3. MCV-miR-M1 directly targets MCV LT recognition sequence in dual luciferase assay

MCV-miR-M1 is located antisense to MCV LT second exon and therefore exhibits perfect complementarity to the LT transcript (Figure 1.9). To confirm that MCV-miR-M1 directly targets MCV LT recognition sequence in our 293 system, wild type psiCHECK-2/wt-MCV-miR-concat reporter plasmid construct was generated by inserting a concatemerised sequence of MCV LT complementary to MCV-miR-M1-5p and -3p into psiCHECK-2 and 3'UTR of *Renilla* luciferase. For negative control, a mutant (Mut) construct (psiCHECK-

2/mut-MCV-miR-concat) was also generated by substituting two nucleotides in the seed region of each miRNA binding site (see Table 2.4) as described by Bauman *et al.* (Bauman *et al.* 2011). 293 cells were co-transfected with psiCHECK-2/wt-MCV-miR-concat and either pcDNA3.1/MCVmiR or pcDNA3.1 parental control. As can be seen in Figure 3.5 A, relative luciferase activity was decreased 40% (p-value<0.05) in cells co-transfected with pcDNA3.1/MCVmiR versus control. This assay was then repeated using MCV-miR-M1 mimics and relative luciferase activity compared with cells transfected with a control scramble mimic. We observed a striking reduction in relative luciferase activity of around 50- and 20-fold (p-value<0.0001) in cells transfected with MCV-miR-M1-5p and -3p mimics, respectively (Figure 3.5 B).

To confirm that the effect of MCV-miR-M1 in our DLA reporter system was specific, the assays were repeated with the mutant construct, psiCHECK-2/mut-MCV-miR-concat. In contrast to cells co-transfected with the WT construct, cells expressing psiCHECK-2/mut-MCV-miR-concat showed no statistically significant change in normalised luciferase activity when co-transfected with either pcDNA3.1/MCVmiR or MCV-miR-M1 mimics (Figure 3.5 A & B). Together these data confirm that MCV-miR-M1 tools generated are able to downregulate MCV LT and that this occurs via direct targeting of the MCV LT recognition sequence.

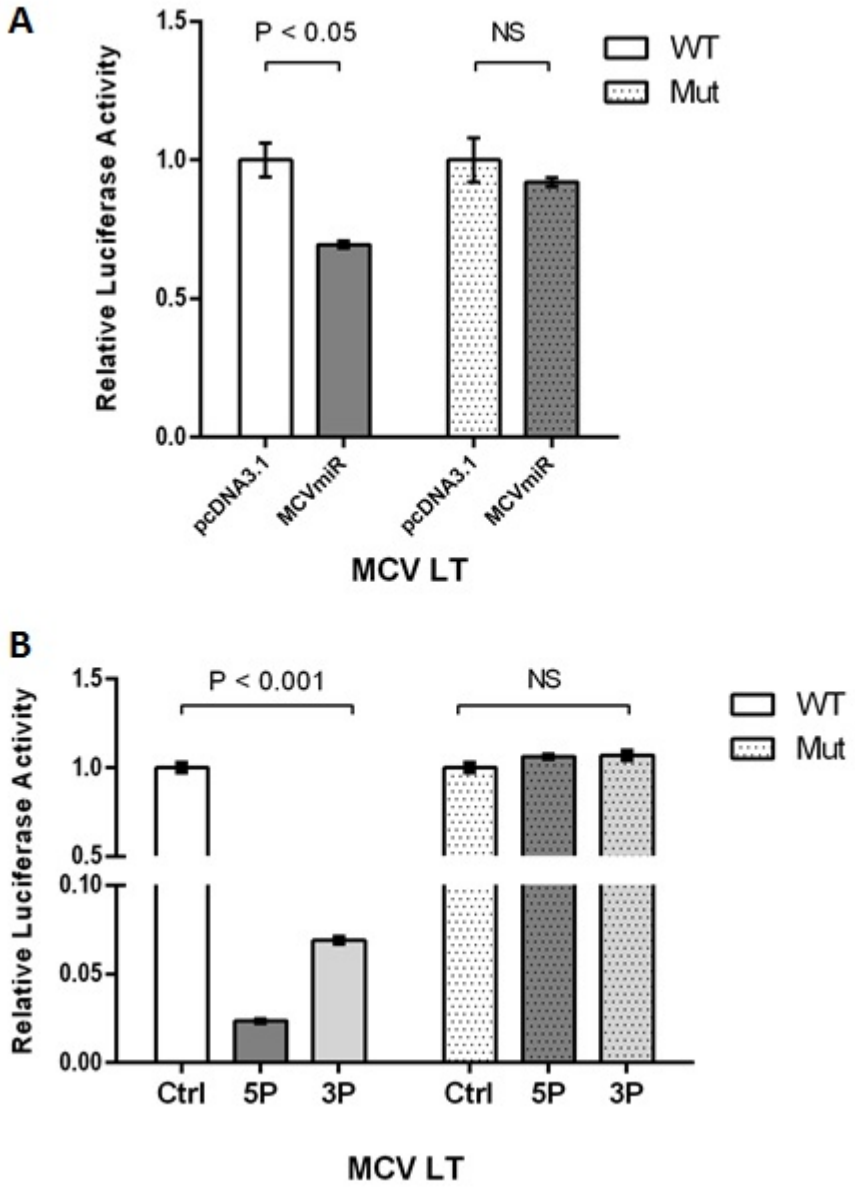

Figure 3.5. Assessing functionality of MCV-miR-M1 using dual luciferase assay (DLA). WT and Mut psiCHECK-2/MCV-miR-concat were co-transfected with either pcDNA3.1 and pcDNA3.1/MCVmiR (A) or with MCV-miR-M1 and control mimics (B). Normalisation of *Renilla* luciferase activity to that of firefly luciferase showed a significant reduction in luminescence in WT construct in the presence of MCV-miR-M1 (A & B, WT) whereas in Mut construct luminescence signal remains unchanged in the presence and absence of MCV-miR-M1 (A & B, Mut).

3.1.2.4. Assessing the effect of MCV-miR-M1 on cell proliferation

As part of the functional assessment, it was of interest to determine if MCV-miR-M1 affected cell proliferation. In this regard, 293 cells were mock-transfected or transfected with MCV-miR-M1 and control miRNA mimics prior to adding BrdU to the cells. Analysis of BrdU incorporation into the DNA of 293 cells, as described in section 2.10, revealed that overexpression of MCV-miR-M1-5p and -3p mimics did not alter cell proliferation when compared to control miRNA mimic and mock 24h post-transfection.

In addition, BrdU assay was repeated for MCVSyn and MCVSyn-hpko. Similarly to MCV-miR-M1 mimics, no difference was observed in terms of cell proliferation between MCVSyn-, MCVSyn-hpko- and mock-transfected cells at 24, 48 and 72h post-transfection. These data indicate that cell proliferation is not affected by MCVSyn replication or MCV-miR-M1 expression within the tested time period (Figure 3.6).

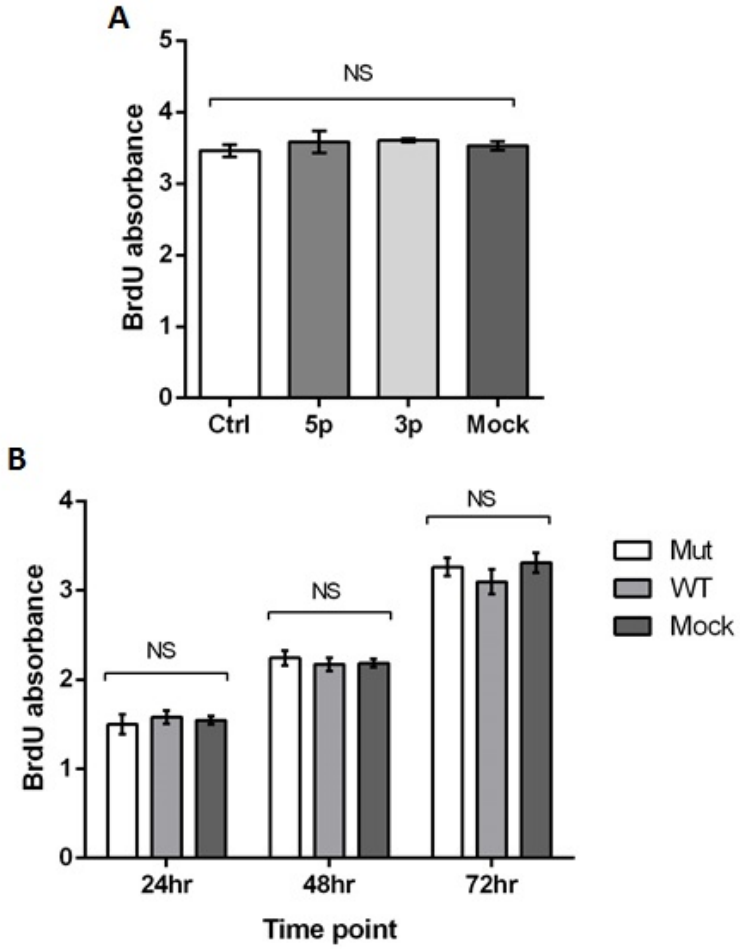

Figure 3.6. BrdU cell proliferation assay in 293 cells mock transfected or transfected with MCV-miR-M1 and control mimics (A) and MCVSyn and MCVSyn-hpko at 24h to 72h time points (B). BrdU absorbance remained unchanged across transfection conditions at each time point for mock- or MCVSyn-transfected cells as well as MCV-miR-M1 and control miRNA mimics.

3.1.2.5. Expression of MCV early and late transcripts in MCVSyn

MCV-miR-M1 mimics are a powerful tool for the study of MCV-miR-M1-dependent modulation of host cell transcripts, however, given the high expression levels of mimics it was important to validate mimic-dysregulated

transcripts in a virus-relevant context. To address this, I took advantage of the MCVSyn system, which I go on to describe in detail below. However, it is important to state that MCV-miR-M1 mimics remain crucial for subsequent validation and functional studies, as in addition to any direct effect it might have on host cell mRNA, MCV-miR-M1 also regulates expression of MCV LT and by extension virus DNA replication (Seo *et al.* 2009; Theiss *et al.* 2015). This is potentially problematic as the MCV T Ags have themselves been associated with changes in host cell proliferation and immune response (Griffiths *et al.* 2013; Shahzad *et al.* 2013). This necessitates careful scrutiny of any observed MCV-miR-M1-related phenotypic effects and while investigating such effects in the context of virus replication is ideal, the importance of attributing any observed miRNA effects as direct, as opposed to modulation of its cognate target, LT, must be considered.

MCVSyn is a synthetic MCV clone generated based on the consensus MCC sequences to facilitate *in vitro* study of the biology and replication of MCV (Neumann *et al.* 2011). Efficient DNA replication, early and late gene expression and virus particle production of MCV was shown by Neumann and colleagues in human cell lines including 293 cells. In a more recent study, MCVSyn-hpko was generated by disrupting the hairpin structure of MCV-miR-M1 (hpko: hairpin knockout) and it was shown that MCVSyn-hpko fails to establish long term persistence in PFSK cells (Theiss *et al.* 2015). Whilst MCV-miR-M1-exclusive alterations in the host cell transcripts could be monitored via MCV-miR-M1 mimics, MCVSyn and MCVSyn-hpko allow investigation of such changes in the absence of MCV-miR-M1 but presence of other MCV components. Therefore, not only can MCVSyn be used to

validate MCV-miR-M1 mimics data in the context of virus replication but also by comparing the data from MCVSyn and MCV-miR-M1 mimic experiments it is possible to identify any synergy or antagonism between MCV-miR-M1 and MCV T Ags. With this view, following confirmation of MCVSyn recircularisation via agarose gel electrophoresis (Figure 3.2 B), 293 cells were transfected with MCVSyn and MCVSyn-hpko in a 48-well plate, RNA was extracted at 24h intervals for 3 days and stem loop and oligo(dT) cDNAs generated prior to analysis of MCV-miR-M1, MCV LT, sT and VP1 expression via stem loop qRT-PCR and qRT-PCR, respectively (Figure 3.7). In cells harbouring MCVSyn, MCV-miR-M1 expression increased over the course of MCV replication, by ~200-fold and ~3-fold for 5p and 3p strands, respectively (Figure 3.7 A). In contrast, no MCV-miR-M1 expression was detected in MCVSyn-hpko at any time point (data no shown). In addition, MCV-miR-M1-5p was identified as the dominant strand with increasing expression (up to 8-fold) compared to MCV-miR-M1-3p (Figure 3.7 B). Consistent with MCV-miR-M1 expression, MCV LT showed a mild but steady and significant (p-value<0.05) downregulation and upregulation in MCVSyn and MCVSyn-hpko, respectively, over 72h (Figure 3.7 C). MCV sT expression demonstrated a fluctuating trend in cells harbouring MCVSyn with a nominal decrease in expression at 48h and similar expression levels at 24h and 72h p.t. Interestingly, MCV sT was steadily upregulated in cells harbouring MCVSyn-hpko over the duration of the time course (Figure 3.7 D). MCV VP1 transcripts showed increasing amounts over the time course in cells harbouring both MCVSyn and MCVSyn-hpko, however, this increase was more pronounced in MCVSyn-hpko (Figure 3.7 E).

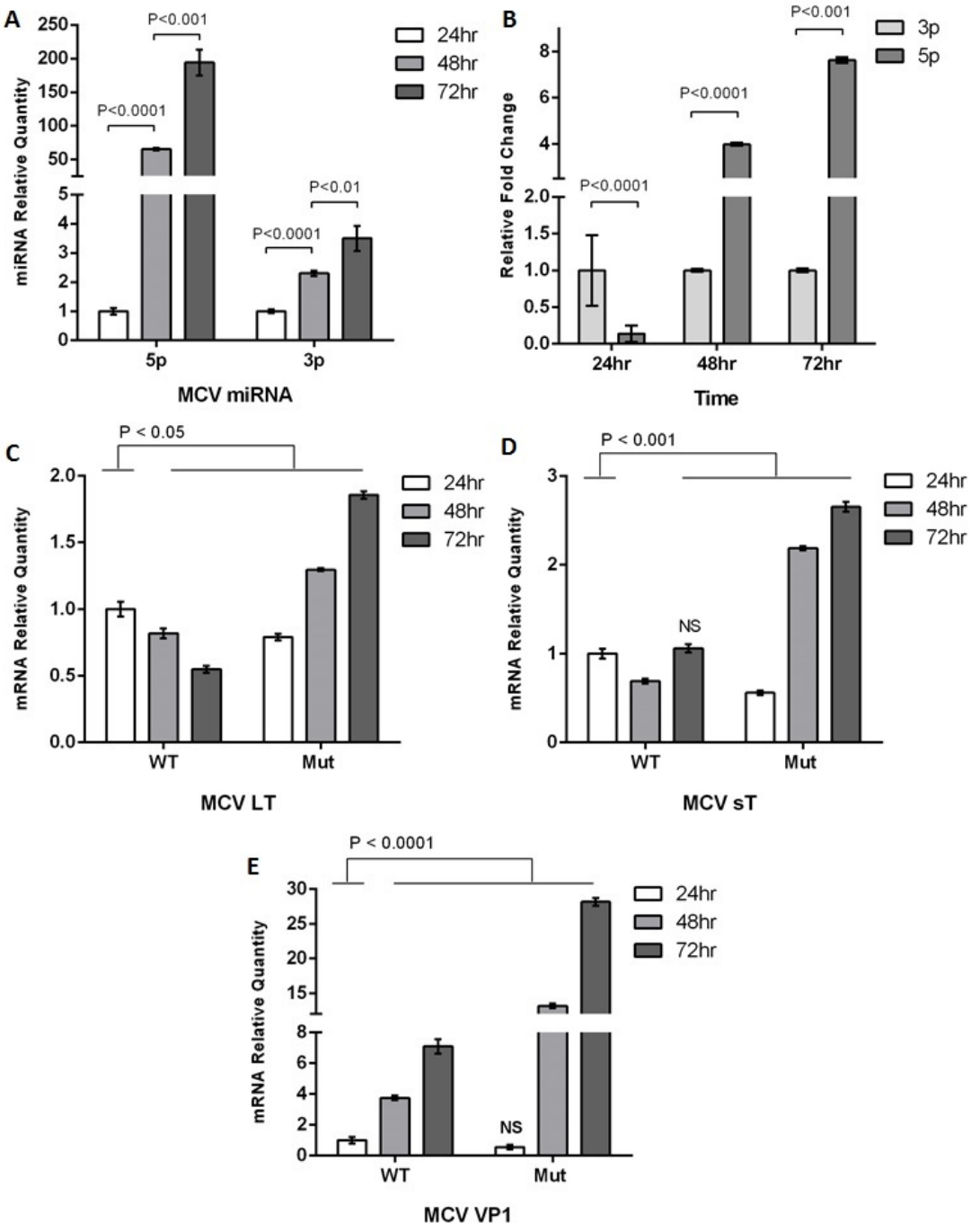
A
miRNA Relative Quantity
P<0.001
P<0.0001
P<0.01
P<0.0001
24hr
48hr
72hr
5p
3p
MCV miRNA
B
Relative Fold Change
P<0.001
P<0.0001
P<0.0001
3p
5p
24hr
48hr
72hr
Time
C
mRNA Relative Quantity
P < 0.05
24hr
48hr
72hr
WT
Mut
MCV LT
D
mRNA Relative Quantity
P < 0.001
NS
24hr
48hr
72hr
WT
Mut
MCV sT
E
mRNA Relative Quantity
P < 0.0001
NS
24hr
48hr
72hr
WT
Mut
MCV VP1

Figure 3.7. Detection of MCV early and late transcripts in MCVSyn and MCVSyn-hpko. 293 cells were transfected with MCVSyn or MCVSyn-hpko, stem loop and oligo(dT) cDNAs were generated using 1µg of total RNA of 24 to 72h time points and used as template in stem loop qRT-PCR or qRT-PCR reactions. MCV-miR-M1-5p and -3p expression increased by 200- and 3-fold over 72h, respectively (A). 5p was identified as dominant strand with 8 fold upregulation relative to 3p at 72h p.t. (No MCV-miR-M1 was detected in MCVSyn-hpko at any time point) (B). MCV LT was steadily downregulated in MCVSyn and upregulated in MCVSyn-hpko over 72h p.t. (C). MCV sT mRNA expression in MCVSyn showed a small drop at 48h, but at 72h returned to levels similar to 24h p.t. whereas in MCVSyn-hpko it was steadily upregulated over the 72h time course (D). MCV VP1 demonstrated a steady increase in both MCVSyn and MCVSyn-hpko, however with more pronounced upregulation in MCVSyn-hpko (E).

3.2. Assessing the effect of MCV-miR-M1 on cellular transcripts

An early *in silico* study predicted several cellular transcripts as putative targets of MCV-miR-M1-5p, including AMBRA1, FOX2, MECP2, PIK3CD, PSME3 and RUNX1 (Lee *et al.* 2011). Therefore, in order to determine whether MCV-miR-M1 targets mRNA of the predicted genes, 293 cells were transfected with either pcDNA3.1 or pcDNA3.1/MCVmiR. Relative normalised expression of *in silico* predicted transcripts showed either no change (AMBRA1, MECP2, PSME3) or less than 1.2 fold upregulation (FOX2, RUNX1) in cells expressing MCV-miR-M1. Only PIK3CD transcript showed a

significant downregulation and this was nominal (~1.5-fold) (Figure 3.8). Given the inconsistency between *in silico*-predicted cellular targets of MCV-miR-M1 and my qRT-PCR analysis of these cellular transcripts in cells expressing MCV-miR-M1 it is clear that an unbiased and global approach is required to identify if any cellular transcripts are modulated by MCV-miR-M1. This is described in detail in the chapter 4.

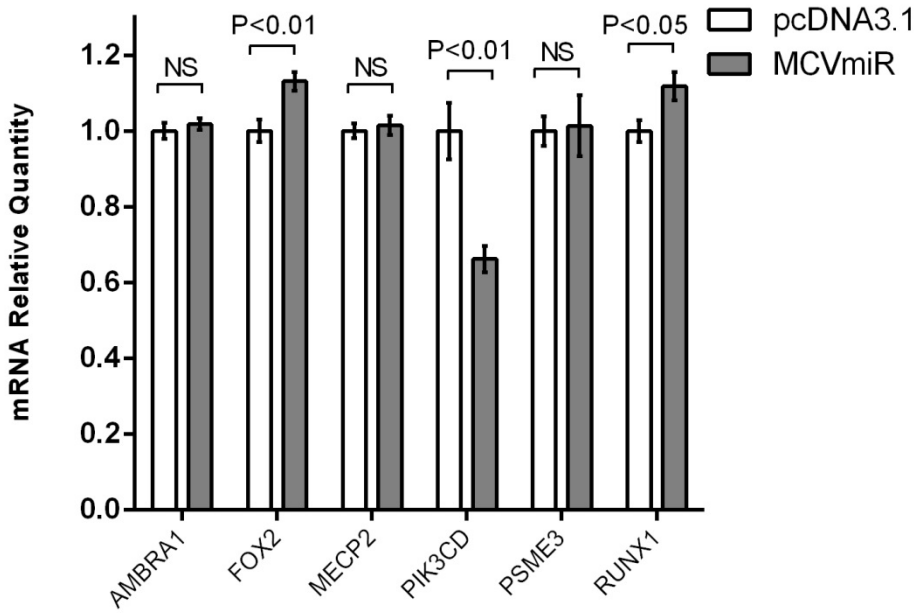

Figure 3.8. Relative normalised expression of *in silico*-predicted targets of MCV-miR-M1-5p in the presence and absence of MCV-miR-M1 in 293 cells. Of the six predicted targets only PIK3CD shows a small but statistically significant downregulation (1.5 fold, p-value<0.01) in qRT-PCR analysis.

3.3. Discussion

Since the discovery of MCV and its causal link with the majority of MCC cases extensive research has been carried out to delineate various aspects of MCV life cycle and pathogenesis. The majority of research has focused on

two major early proteins LT and sT, however, far less is understood about how other MCV genome transcripts regulate infection and contribute to disease pathogenesis. In recent years, there has been mounting evidence for the important role of viral miRNAs in various aspects of virus-host interaction (Kincaid and Sullivan 2012). While the majority of these data have been obtained from herpesviruses (Kincaid and Sullivan 2012), several studies have provided insights into the key role of polyomavirus miRNAs in virus pathogenesis (Broekema and Imperiale 2013) and evasion of host immune response (Sullivan *et al.* 2005; Bauman *et al.* 2011; Chen *et al.* 2013; Theiss *et al.* 2015). Importantly, a recent study demonstrated that MCV miRNA is required for establishment of long-term infection in the host cell (Theiss *et al.* 2015), however, a mechanistic explanation delineating how MCV miRNA contributes to the virus persistent infection and pathogenesis is still lacking. To facilitate how MCV-miR-M1 expression affects the levels of cellular transcripts, a range of tools were generated and tested for expression of MCV-miR-M1 including, MCV-miR-M1 mimics, pcDNA3.1/MCVmiR and Flp-In™T-REx™293-MCVmiR inducible cell line (see sections 3.1.1.1 and 3.1.1.2). With respect to higher expression (Figure 3.3) and having the advantage of assessing the specific effect of each strand of MCV-miR-M1 individually it was decide to use MCV-miR-M1-5p and MCV-miR-M1-3p mimics in the follow-up experiments. Whilst there have been concerns over off-target effects of miRNA mimics it has been shown that this effect can be eliminated by chemical modification of passenger strand as demonstrated by Thomson and colleagues (Thomson *et al.* 2013).

In contrast to directly transfected miRNA mimics, the levels of mature MCV-miR-M1 detected via stem-loop qRT-PCR in pcDNA3.1/MCVmiR-transfected cells and induced Flp-In™ T-REx™ 293-MCVmiR cells were ~2-fold and ~20-fold lower, respectively (Figure 3.3). In Flp-In™ T-REx™ 293-MCVmiR cells one possible explanation for this could be inefficient processing of MCV-miR-M1-5p and -3p from MCV-miR-M1. Several studies have demonstrated that flanking sequences at 5' and 3' ends of pre-miRNAs play a critical role in efficient expression of miRNAs (Chen *et al.* 2004; Zhou *et al.* 2005; Chang *et al.* 2006; Fukuda *et al.* 2006) and are a key factor in pri-miRNA transcript processing by Drosha (Zeng and Cullen 2005; Rumi *et al.* 2006). Therefore, it might have been beneficial to include a flanking region in MCV-miR-M1 clones for generation of Flp-In™ T-REx™ 293-MCVmiR cells. Similar to Flp-In™ T-REx™ 293-MCVmiR SCL, MCV-miR-M1 shows very low expression in MCV-positive MCC cell lines (Lee *et al.* 2011). Interestingly, in MCC where the MCV genome has undergone integration and truncation but retained the MCV-miR-M1 expression cassette only very low levels of miRNA expression are detected (Lee *et al.* 2011; Theiss *et al.* 2015). While the underlying mechanisms of low level MCV-miR-M1 expression from integrated MCV sequences is yet to be elucidated, a recent study demonstrated that transcription initiation sites upstream of MCV-miR-M1 locus are required for efficient MCV-miR-M1 expression (Theiss *et al.* 2015). Therefore, it is possible that inefficient expression of MCV-miR-M1 in induced Flp-In™ T-REx™ 293-MCVmiR SCL is due to random insertion of MCV-miR-M1 sequence into the genome of Flp-In™ T-REx™ 293 cells and lack of

upstream sequences required for efficient processing and biogenesis of mature MCV miRNA.

qRT-PCR based miRNA expression analysis is unable to discriminate between RISC-bound and non-RISC-bound miRNA pools, therefore, miRNA reporter assays such as DLA are important complementary techniques in miRNA functional studies (Thomson *et al.* 2013; Thermo Fisher Scientific 2014). DLA for concatemerised MCV LT response element (termed psiCHECK-2/wt-MCV-miR-concat) and its site mutated version (termed psiCHECK-2/mut-MCV-miR-concat) demonstrated that co-expression of MCV-miR-M1-5p and -3p mimics resulted in 50-fold and 20-fold downregulation, respectively (Figure 3.5). MCV-miR-M1 functionality was also assessed in induced and uninduced Flp-In™T-REx™293-MCV-LT SCL using MCV-miR-M1-5p and -3p mimics. qRT-PCR analysis revealed some basal expression of MCV LT in uninduced Flp-In™T-REx™293-MCV-LT, which can be attributed to the 'leakiness' of the T-Rex system (Campeau *et al.* 2009). In induced Flp-In™T-REx™293-MCV-LT a much smaller (but statistically significant, p-value<0.0001) downregulation of MCV LT expression was observed in the presence of MCV-miR-M1-5p and -3p mimics (36% and 46% downregulation, respectively, Figure 3.4 C). Regarding the discrepancy in the degree of MCV LT downregulation in induced Flp-In™T-REx™293-MCV-LT (less than 2-fold, Figure 3.4 C) and MCV LT DLA (more than 50-fold, Figure 3.5 B), I investigated MCV-miR-M1 expression in Flp-In™T-REx™293-MCV-LT 24h post induction. Interestingly, whilst I could not detect any MCV-miR-M1 expression in uninduced cells, MCV-miR-M1-5p and -3p expression was confirmed in induced cells, with

MCV-miR-M1-3p demonstrating 12-fold higher expression relative to MCV-miR-M1-5p (Figure 3.4 A). This observation suggests that MCV LT is downregulated by endogenous MCV-miR-M1 expressed from MCV LT locus, however, transfected MCV-miR-M1-5p and -3p mimics exert an extra level of downregulation which is manifested as a small decrease in MCV LT mRNA. Assuming equivalent expression levels of MCV-miR-M1-5p and -3p mimics in induced Flp-In™T-REx™293-MCV-LT the 10% further downregulation of MCV LT with MCV-miR-M1-3p can be explained by the higher levels of endogenous MCV-miR-M1-3p (see Figures 3.4 A & C). Furthermore, relative higher levels of MCV-miR-M1-3p in 24h post induction Flp-In™T-REx™293-MCV-LT is consistent with relative higher expression of MCV-miR-M1-3p in MCVSyn at 24h p.t. (see section 3.1.2.5 and Figure 3.7 B).

Recently, an article was published by Theiss *et al.* (Theiss *et al.* 2015), describing the generation of a synthetic MCV genome and corresponding mutant that lacks the MCV-miR-M1 transcript. This system enabled the study of MCV replication and infection that more closely resembled native conditions. Measuring the expression of MCV transcripts revealed increasing levels of MCV LT in MCVSyn-hpko-transfected cells over the 72h period whereas in MCVSyn-transfected cells a decreasing trend was observed (Figure 3.7 C). Similarly, MCV LT protein expression was upregulated in MCVSyn-hpko (see Figure 4.7). This trend is consistent with increasing levels of MCV-miR-M1 in MCVSyn and its lack in MCVSyn-hpko (Figure 3.7 A).

In addition to temporal expression of MCV-miR-M1 in MCVSyn, these data reproduced MCV LT functional data obtained from MCV-miR-M1-5p and -3p

mimics. Moreover, whilst both MCV-miR-M1-5p and -3p demonstrated a steady increase during 72h MCVSyn genome replication their relative and temporal expression varied significantly. Where MCV-miR-M1-3p expression relative to MCV-miR-M1-5p showed 5-fold upregulation at 24h p.t. this trend was reversed at 48h and 72h p.t. by respective 4-fold and 8-fold upregulation of MCV-miR-M1-5p relative to -3p (Figure 3.7 B).

Although MCV-miR-M1 is expressed from late region of MCV genome a recent study has shown that low levels of MCV-miR-M1 pre-miRNA and mature MCV miRNA are expressed upon transcription initiation from MCV early region (Theiss *et al.* 2015). The authors describe an MCV early region intrinsic promoter upstream of the MCV-miR-M1 locus which can activate MCV-miR-M1 expression independent of MCV NCCR. My expression analysis of MCV-miR-M1 in MCVSyn revealed an initial higher expression of MCV-miR-M1-3p relative to -5p 24h p.t. However, with more efficient expression of MCV-miR-M1 following transcription initiation of the late region, relative higher levels of MCV-miR-M1-5p accumulate 48h and 72h p.t. Whether activation of this promoter region can lead to changes in the expression of MCV-miR-M1-3p relative to MCV-miR-M1-5p within the first 24h p.t. is to be elucidated. If so, this can explain the MCV-miR-M1 temporal expression pattern where both MCV-miR-M1-5p and -3p demonstrate increasing levels during MCVSyn replication, but MCV-miR-M1-5p shows a more substantial temporal upregulation compared to MCV-miR-M1-3p (Figures 3.7 A & B). Nevertheless, an accurate explanation of distinct MCV-miR-M1-5p and -3p expression patterns warrants further investigation within longer time periods of MCV genome replication.

In addition to MCV LT and MCV-miR-M1, I also investigated expression of MCV sT and MCV VP1 mRNAs in MCVSyn and MCVSyn-hpko. Whilst no direct correlation was observed between MCV-miR-M1 expression and MCV sT or MCV VP1 mRNA levels, as expected both transcripts showed a more significant increase in the absence of MCV-miR-M1 in MCVSyn-hpko due to LT upregulation and increased genome replication (Figures 3.7 D & E). These data are consistent with previous studies that suggest MCV miRNA can restrict MCV genome replication via direct targeting and downregulation of MCV LT (Theiss *et al.* 2015).

Having established and functionally validated a miRNA mimic-based expression system for MCV-miR-M1, I revisited work by Lee *et al.* that postulated a number of potential cellular targets for MCV-miR-M1, based on seed-sequence (Lee *et al.* 2011). All but one of Lee *et al.*'s *in silico*-predicted targets showed no significant downregulation in the presence of pcDNA3.1/MCVmiR (Figure 3.8). One possible explanation for this is the MCV-miR-M1 seed-sequence used by Lee *et al.* in target algorithms as more recent miRNA-Seq fine mapping of mature MCV-miR-M1 describes a different seed sequence for MCV-miR-M1-5p (Theiss *et al.* 2015), suggesting that these targets were based on the incorrect seed matching and further strengthening the remit for an unbiased and global approach to identify true cellular MCV-miR-M1 targets.

CHAPTER 4

MCV-miR-M1 Target Identification and Validation

4. MCV-miR-M1 cellular targets

4.1. RNA sequencing (RNA-Seq)

To date, there are no published studies investigating the cellular targets of MCV-miR-M1. Moreover, while studies exist detailing cellular targets for other polyomavirus miRNAs (Bauman *et al.* 2011), no one has investigated how human polyomavirus miRNAs affect the global transcriptional landscape. To address this question in MCV, it was decided to express MCV-miR-M1 in 293 cells and to this end, several MCV-miR-M1 expression tools including pcDNA3.1/MCVmiR, Flp-In™T-REx™293-MCVmiR inducible cell line and commercially available MCV-miR-M1-5p and -3p mimics were assessed and validated, as described in chapter 3. Comparison of these MCV-miR-M1 expression tools via stem loop qRT-PCR revealed highest expression levels of MCV-miR-M1 in MCV-miR-M1-5p and -3p mimic-transfected 293 cells (Figure 3.3). Importantly, this increased level corresponded with an active pool of miRNA, as evidenced by DLA experiments, demonstrating that of the three expression systems miRNA mimics were the most robust in terms of both expression and activity. Moreover, MCV-miR-M1-5p and -3p mimics provide the additional advantage of target specification for each strand of the MCV-miR-M1, an important consideration as previously demonstrated for the BK and JC polyomaviruses 3p miRNA (Bauman *et al.* 2011). For these reasons, to identify the effect of MCV-miR-M1 expression on the levels of cellular transcripts, RNA-Seq was carried out on total RNA extracted from 293 cells transfected with MCV-miR-M1-5p and -3p mimics and control mimic in biological triplicates.

4.1.1. Assessment of MCV-miR-M1 expression in total RNA samples

Prior to proceeding to the sequencing pipeline, it was crucial to confirm the expression of MCV-miR-M1-5p and -3p in the mimic-transfected 293 cells. Therefore, stem loop cDNA was generated from total RNA samples as described in section 2.15. As can be seen in Figure 4.1, expression of MCV-miR-M1-5p and MCV-miR-M1-3p was confirmed via stem loop qRT-PCR in 5p and 3p mimic transfected cells, but not in control mimic, NTC and NRT samples.

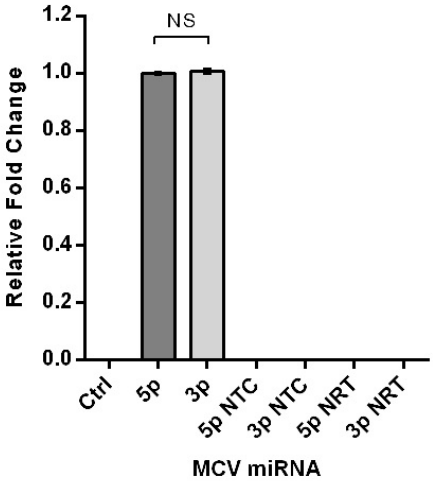

Figure 4.1. Expression of MCV-miRNA-M1-5p and MCV-miR-M1-3p in MCV-miR-M1 mimic- and control mimic-transfected 293 cells for RNA-Seq. NTC, no template control; NRT, no reverse transcriptase control.

4.1.2. Quality control (QC) of RNA-Seq RNA samples

To ensure that the total RNA samples were of a sufficient quality for library production and sequencing, QC of the samples was assessed using the Agilent 2100 Bioanalyzer system, as described in section 2.19.1. All RNA

samples passed the QC assay by RNA Integrity Number (RIN) with 8 of the samples scoring a RIN of 10 and the remaining sample a RIN of 9.8 (Figure 4.2). RIN scores of 10 and 1 indicate an intact RNA and a completely degraded RNA, respectively (Schroeder *et al.* 2006) with a RIN score >8 representing a sample of suitable quality for RNA-Seq (Gallego Romero *et al.* 2014).

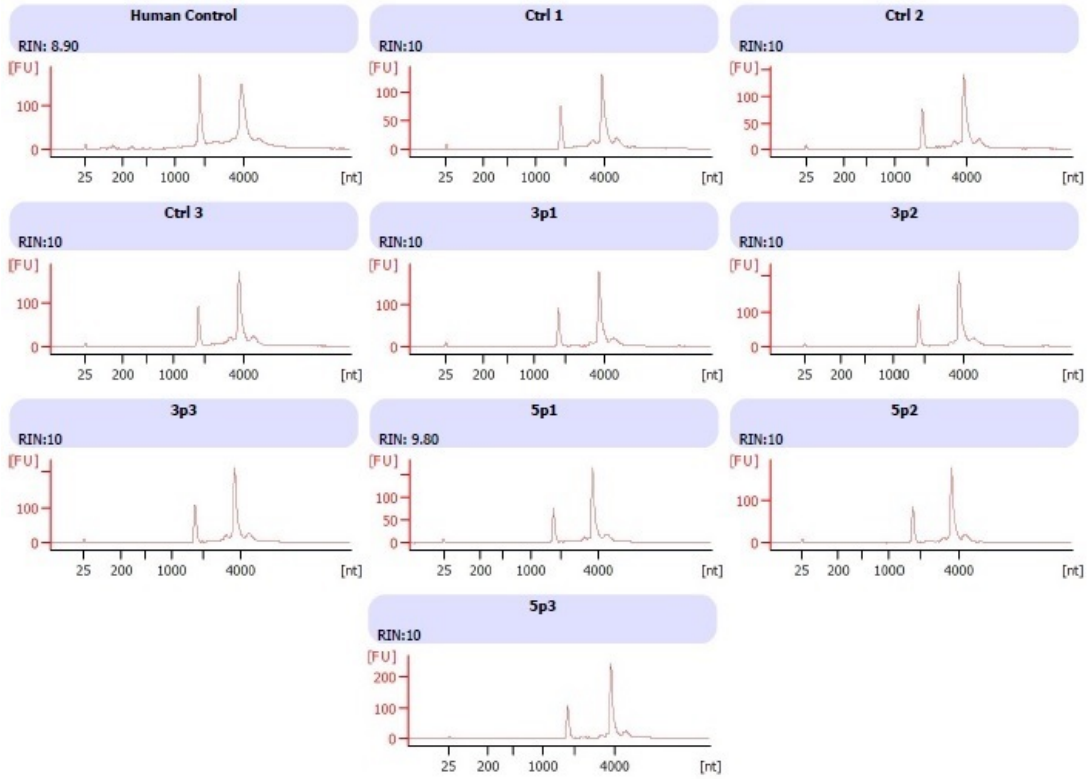

Figure 4.2. RNA QC assay results are represented by RNA Integrity Number (RIN). All of the total RNA samples passed the QC assay by highest possible score of RIN=10 (for 5p1 RIN=9.80).

4.1.3. Assessment of dscDNA samples

To prepare RNA-Seq libraries for hybridisation onto the flow cell, each library undergoes three consequtive steps: adenylation, adapter ligation and PCR

amplification. Addition of a single ‘A’ nucleotide to the 3’ ends of each dscDNA provides an overhang for a ‘T’ nucleotide at the 3’ end of adapters and prevents the blunt ends of dscDNAs from ligating to one another. Adapters in turn act as primer for PCR enrichment of dscDNAs and as an adapter to hybridise to surface of the flow cell. Therefore, since all subsequent steps depend on formation of dscDNA, it was crucial to confirm the presence of dscDNAs prior to proceeding to adenylation, adapter ligation and PCR enrichment steps. To this end, following dscDNA clean-up samples were loaded and run on a High Sensitivity DNA 1000 Tape and the presence of dscDNAs was verified as ~140-160bp products (Figure 4.3).

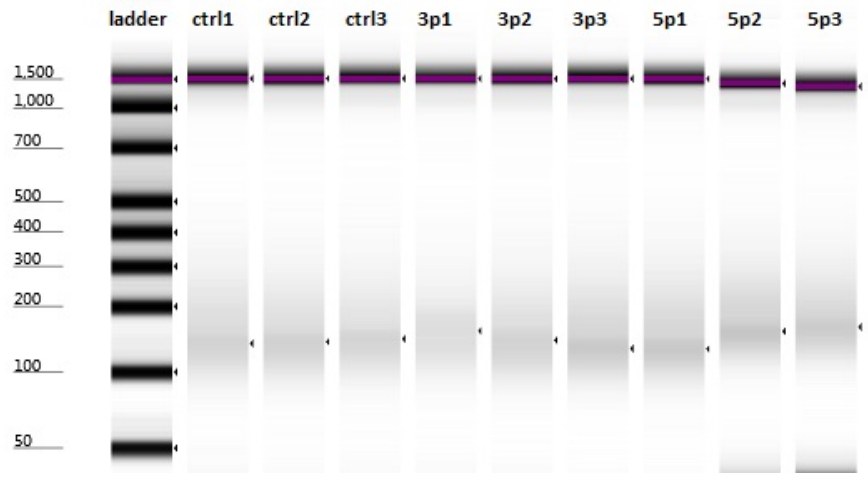

Figure 4.3. Gel image of verified double-stranded cDNAs before adenylation and adapter ligation steps of sequencing. The dscDNAs are marked by small dark arrows corresponding to ~140-160bp sizes.

4.1.4. Quality control of RNA-Seq libraries

After PCR enrichment, samples were loaded onto the flow cell for cluster generation and sequencing. Cluster generation includes denaturaion, hybridisation to flow cell surface, second strand generation and clonal amplification of second strand. The amplified strands are then sequenced. Consequently, the validity of sequencing results depends on the validity of final libraries and any primer dimer or non-specific PCR products can produce unreliable results. Therefore, validation of RNA-Seq libraries via quality control is a crucial step in the RNA sequencing workflow. To this end, prior to pooling and loading the flow cell, the final libraries were loaded into a DNA 1000 chip as described in section 2.19.3.8 and analysed using an Agilent 2100 Bioanalyzer and 2100 expert software. The final libraries were verified as ~240-360bp products (Figure 4.4).

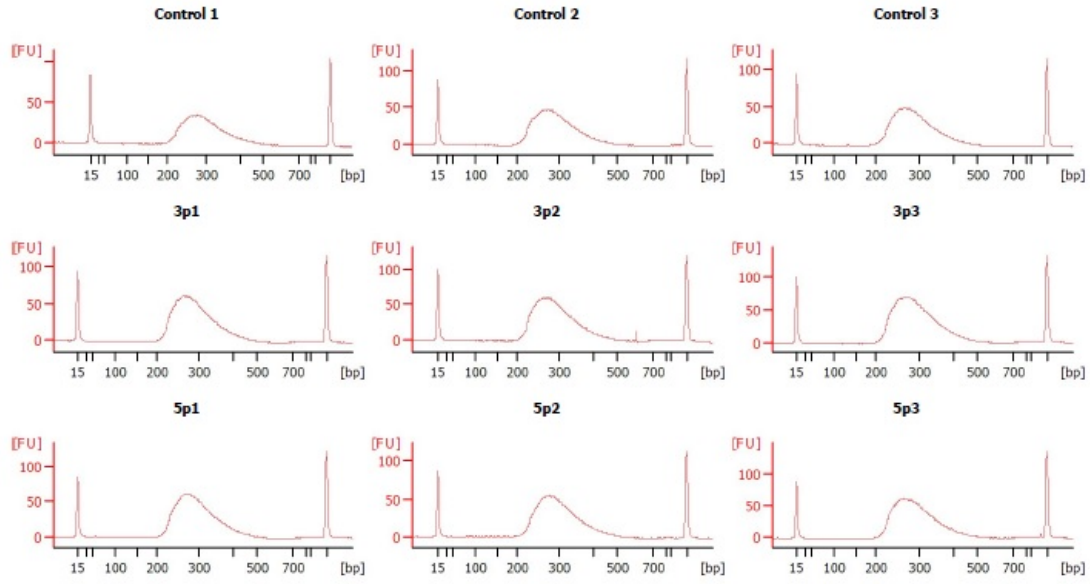

Figure 4.4. Electropherogram summary of the final libraries. The final libraries are represented as short curves of ~240-350bp size between the two spike-shape lower (15bp) and upper markers (1500bp).

4.1.5. RNA-Seq and data analysis

The TruSeq cDNA libraries described above were analysed via Illumina HiSeq2500 paired end 100bp run. To remove the least reliable data, often derived from overlapping clusters, raw data was filtered using the Illumina chastity filter and data analysed using TopHat (Institute of Genetic Medicine, Johns Hopkins University) which aligns RNA-Seq reads using the ultra-high-throughput short read aligner Bowtie. These data were then analysed using 'edgeR' (Bioconductor) which facilitates differential expression analysis of RNA-Seq profiles with biological replication via empirical Bayes estimation and exact tests based on the negative binomial distribution. Gene expression analysis revealed 69 and 110 transcripts with minimum 2-fold downregulation and statistical significance for MCV-miR-M1-5p and -3p, respectively (see Appendix). Gene ontology analysis carried out using The Database for Annotation, Visualization and Integrated Discovery (DAVID) highlighted various pathways downregulated by MCV-miR-M1, among which immune regulation, cell-cell signalling and regulation of cell proliferation pathways were of particular interest to this project (Figure 4.5 A & B).

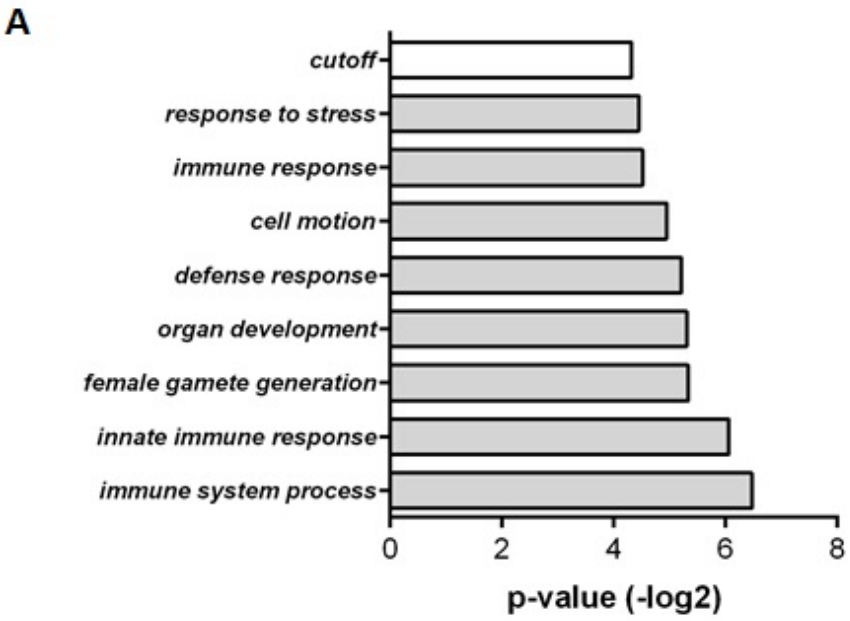
A
cutoff
response to stress
immune response
cell motion
defense response
organ development
female gamete generation
innate immune response
immune system process
0
2
4
6
8
p-value (-log2)

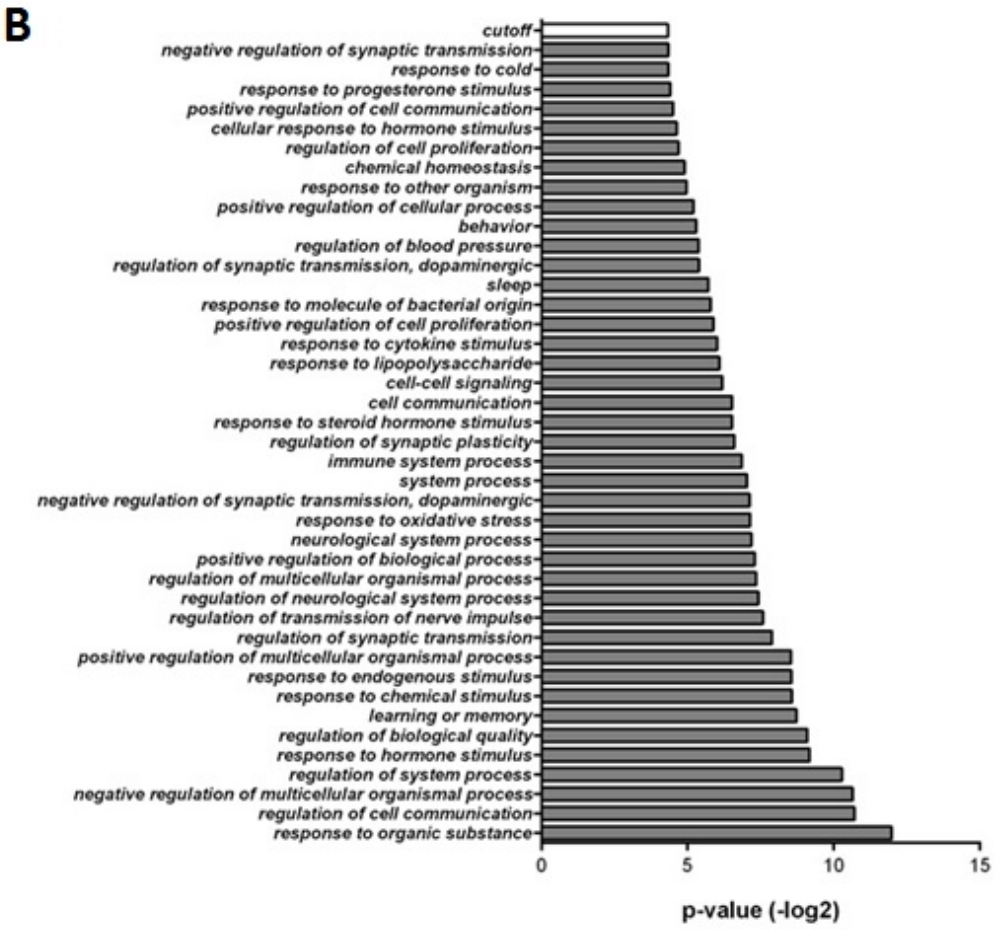
B
cutoff
negative regulation of synaptic transmission
response to cold
response to progesterone stimulus
positive regulation of cell communication
cellular response to hormone stimulus
regulation of cell proliferation
chemical homeostasis
response to other organism
positive regulation of cellular process
behavior
regulation of blood pressure
regulation of synaptic transmission, dopaminergic
sleep
response to molecule of bacterial origin
positive regulation of cell proliferation
response to cytokine stimulus
response to lipopolysaccharide
cell-cell signaling
cell communication
response to steroid hormone stimulus
regulation of synaptic plasticity
immune system process
system process
negative regulation of synaptic transmission, dopaminergic
response to oxidative stress
neurological system process
positive regulation of biological process
regulation of multicellular organismal process
regulation of neurological system process
regulation of transmission of nerve impulse
regulation of synaptic transmission
positive regulation of multicellular organismal process
response to endogenous stimulus
response to chemical stimulus
learning or memory
regulation of biological quality
response to hormone stimulus
regulation of system process
negative regulation of multicellular organismal process
regulation of cell communication
response to organic substance
0
5
10
15
p-value (-log2)

Figure 4.5. Gene ontology (GO) of MCV-miR-M1-3p (A) and -5p (B) RNA-Seq-identified targets base on - log2 of p-value. The bars represent - log2 p-values of each GO. Cut off, p-value=0.05.

4.2. Validation of RNA-Seq data

4.2.1. qRT-PCR validation of RNA-Seq-identified targets of MCV-miR-M1

Following gene expression analysis of the RNA-Seq data, transcripts with minimum 2-fold downregulation and statistical significance (p-value<0.05) were identified for MCV-miR-M1-5p and -3p. However, due to the large number of transcripts and time and budget limitations of the project it was necessary to prioritise targets for validation. With this view, targets of MCV-miR-M1-5p and -3p were selected for further analysis based on a combination of their frequency in GO analysis and their identified role in relation to virus-host cell interaction as discussed in section 1.6.1, i.e. increasing host-cell longevity and evasion of host-cell immune response. Furthermore, although not identified via RNA-Seq, several other transcripts were considered for qRT-PCR validation due to existing evidence in the literature regarding their role in innate immunity and reported MCV T Ag locus-mediated downregulation, given the co-expression of MCV-miR-M1 with LT (Shahzad *et al.* 2013).

To validate RNA-Seq data, 293 cells were transfected with MCV-miR-M1-5p, MCV-miR-M1-3p or control miRNA mimics (see section 2.9). Following stem loop qRT-PCR confirmation of MCV-miR-M1-5p and -3p expression in respective RNA samples, qRT-PCR of selected transcripts consistently and

universally corroborated all downregulated cellular targets identified via RNA-Seq (Table 4.1 and Figure 4.6).

As discussed in section 3.1.2.5, it was crucial to confirm miRNA mimics data in a system more akin to the replicative MCV. In this regard, 293 cells were transfected with MCVSyn and MCVSyn-hpko and expression of MCV-miR-M1-5p and -3p was confirmed in MCVSyn. qRT-PCR validated RNA-Seq and MCV-miR-M1 mimics data in MCVSyn, suggesting that the observed changes in the expression of cellular transcripts are reproducible in the context of MCV replication. For a list of qRT-PCR validated targets refer to Table 4.1.

Table 4.1. List of cellular transcripts tested for qRT-PCR validation of RNA-Seq results using MCV-miR-M1 mimics and MCVSyn. Targets marked with asterisk (*****) were not identified via RNA-Seq analysis. N/A, not applicable.

Transcript name	Downregulated by (RNA-Seq fold change)	Validated by (MCV-miR-M1 expression system)	
ADRA1D	5P (15 folds)	MCV miR mimic	MCVSyn
CXCL8	3P (16 folds)	MCV miR mimic	MCVSyn
IFI30	5P (5 folds) 3P (2.5 folds)	MCV miR mimic	MCVSyn
IFIH1	3P (2.5 folds)	MCV miR mimic	MCVSyn
MAPK10	3P (2 folds)	MCV miR mimic	MCVSyn
RAET1G (ULBP5)	5P (2.3 folds)	MCV miR mimic	MCVSyn
SELPLG	3P (32 folds) 5P (4.5 folds)	MCV miR mimic	MCVSyn
SP100	5P (18 folds)	MCV miR mimic	MCVSyn
CYB5R2	3P (32 folds)	MCV miR mimic	MCVSyn

KLLN	3P (2 folds)	MCV miR mimic	MCVSyn
OSR1	3P (19 folds)	MCV miR mimic	MCVSyn
TLR9*****	N/A	MCV miR mimic	MCVSyn
C/EBPα*****	N/A	MCV miR mimic	MCVSyn
C/EBPβ*****	N/A	MCV miR mimic	MCVSyn

The validated targets can be generally classified as immune-related and tumour-related transcripts, however, regarding their appearance in various pathways some transcripts give rise to multifunctional proteins with distinct or associated roles in different pathways. These targets and their downregulation (p-value<0.05) in cells expressing MCV-miR-M1 are described in more detail below.

4.2.1.1. Immune-related transcripts

ADRA1D (alpha-1D adrenergic receptor) has been implicated in the activation of signalling pathways crucial to lymphocyte activation and migration (Tybulewicz and Henderson 2009; Kennedy *et al.* 2012) as well as inducing MAPK1/3 signalling through transactivation of epidermal growth factor (EGF) (Chen *et al.* 2006). ADRA1D was highlighted in several downregulated pathways such as, regulation of cell communication, cell-cell signalling and regulation of cell proliferation. qRT-PCR confirmed significant ADRA1D downregulation by more than 2-fold in the presence of MCVSyn and MCV-miR-M1-5p mimic (Figure 4.6 A).

CXCL8 (C-X-C motif ligand 8), also known as interleukin 8 (IL-8) is a cytokine with chemoattractant activity for neutrophils and monocytes (Holmes *et al.* 1991; Chuntharapai *et al.* 1994; Seely *et al.* 2002). Pathway analysis put

CXCL8 in most 3p-downregulated pathways including immune system process, organ development, defense response, cell motion, immune response and response to stress. qRT-PCR confirmed RNA-Seq data with both MCV-miR-M1-3p mimic and MCVSyn (Figure 4.6 B).

IFI30 (interferon, gamma-inducible protein 30) or GILT (Gamma-interferon-inducible lysosomal thiol reductase) plays an important role in MHC (Major Histocompatibility Complex) class I- and MHC class II-restricted antigen processing by facilitating degradation of endocytosed antigens via disulfide bond reduction (West and Cresswell 2013). Appearing in immune system process and regulation of cell proliferation pathways, IFI30 showed 5- and 1.6-fold downregulation in MCV-miR-M1-5p mimic and MCVSyn qRT-PCR (Figure 4.6 C).

IFIH1 (interferon induced with helicase C domain 1) or MDA5 (Melanoma Differentiation-Associated protein 5) is a pattern recognition receptor and plays an important role in innate antiviral response by inducing type I IFNs via mitochondrial antiviral-signalling protein (MAVS) (Xu *et al.* 2005; Lei *et al.* 2015). Similar to CXCL8, IFIH1 appeared in the majority of MCV-miR-M1-3p-affected pathways including, immune system process, innate immune response, defense response, immune response and response to stress. qRT-PCR validation showed ~2-fold downregulation of IFIH1 by MCV-miR-M1-3p mimic, whereas IFIH1 mRNA was absent even after 45 cycles in the presence of MCVSyn, resulting in three order of magnitude downregulation relative to MCVSyn-hpko (CT≈33) (Figure 4.6 D).

MAPK10 (Mitogen-activated protein kinase 10) or JNK3 (c-Jun N-terminal kinase 3) is a member of MAPK signalling pathway and has been shown to stimulate TNF-α (Kanehisa *et al.* 2016e) and mediate CXCL8 secretion in response to DNA damage (Biton and Ashkenazi 2011). MAPK10 showed 3-fold and ~1.5-fold downregulation with MCV-miR-M1-3p mimic and MCVSyn, respectively (Figure 4.6 E) in qRT-PCR and was highlighted in response to stress pathway.

RAET1G (Retinoic acid early transcript 1G) or ULBP5 (UL16 binding protein 5) is a cell surface ligand for NKG2D, an immunoreceptor found on various immune cells such as macrophages, CD8(+) alphabeta T-cells and gammadelta T-cells (Cosman *et al.* 2001; Raulet 2003; Obeidy and Sharland 2009). ULBPs are related to MHC class I molecules and play an important role in antiviral immunity by stimulating cytokine and chemokine production in natural killer (NK) cells (Cosman *et al.* 2001). qRT-PCR confirmed RAET1G RNA-Seq results by 57-fold and 69-fold downregulation in MCV-miR-M1-5p mimic and MCVSyn, respectively (Figure 4.6 F).

SELPLG (selectin P ligand) is expressed on neutrophils, monocytes and some T-cells (Kansas 1996) and is involved in recruitment of leukocytes to sites of inflammation and injury (Somers *et al.* 2000; Hubert *et al.* 2014). Selectin P mediates adhesion of neutrophils and monocytes to activated platelets and endothelium (Larsen *et al.* 1989; Geng *et al.* 1990) leading to the leukocyte tissue migration (Somers *et al.* 2000). SELPLG, by 32-fold and 4.5-fold downregulation in 3p and 5p RNA-Seq targets, respectively, appeared in immune system process and cell motion GOs. qRT-PCR

validation showed more than 2-fold downregulation in the presence of MCV-miR-M1-3p and -5p mimics and MCVSyn (Figure 4.6 G).

SP100 (Speckled protein of 100 kDa), a component of promyelocytic leukaemia nuclear bodies (PML-NB), has been implicated in antiviral innate immunity via co-activation of interferon-stimulated gene (ISGs) and cytokines (Tavalai *et al.* 2011; Scherer and Stamminger 2016). In addition, a recent study suggests that SP100 can negatively regulate DNA replication in MCV (Neumann *et al.* 2016). SP100 was one of the top ten downregulated targets in the RNA-Seq dataset, exhibiting ~18-fold downregulation, qRT-PCR validation confirmed this and showed 11-fold and 5-fold downregulation in the presence of MCV-miR-M1-5p mimic and MCVSyn, respectively (Figure 4.6 H). In pathway analysis, SP100 was highlighted in pathways such as, response to cytokine stimulus, response to chemical stimulus and immune system process.

4.2.1.2. Tumour-related transcripts

As discussed above, MCV-miR-M1 is expressed at very low levels in MCC, suggesting that the miRNA is unlikely to impact on the cancer phenotype. However, several transcripts associated with pathways to cancer were identified by RNA-Seq analysis and several of these were investigated further.

CYB5R2 (cytochrome b5 reductase 2) is a member of cytochrome b-type NAD(P)H (Nicotinamide Adenine Dinucleotide Phosphate Hydrogen) oxidoreductases which have been implicated in a range of biological processes such as, biosynthesis of fats and oxidative burst (Zhu *et al.* 1999).

Oxidative or respiratory burst is a phenomenon in phagocytes during which elevated oxygen consumption is followed by oxygen reduction to superoxide (SO) and other reactive oxygen intermediates which are then used to destroy engulfed pathogens within phagolysosomes (Bose *et al.* 2014). In addition, CYB5R2 inactivation by promoter hypermethylation has been demonstrated in nasopharyngeal (Xiao *et al.* 2014) and prostate cancer (Devaney *et al.* 2013). CYB5R2 exhibited a 32-fold downregulation in RNA-Seq datasets and was identified as the top 3p target, in terms of downregulation. qRT-PCR validation showed a significant ~2-fold downregulation in cells expressing MCV-miR-M1-3p mimic and MCVSyn (Figure 4.6 I).

KLLN (killin, p53-regulated DNA replication inhibitor) is a high-affinity DNA-binding protein which negatively regulates DNA and RNA synthesis and has been demonstrated to be necessary and sufficient for P53-induced apoptosis (Cho and Liang 2008; Qiao *et al.* 2015). KLLN-mediated tumour suppression has been reported in breast and prostate cancers (Wang *et al.* 2013a; Wang *et al.* 2013b). KLLN RNA-Seq data was qRT-PCR-validated and showed more than 4-fold downregulation in the presence of MCV-miR-M1-3p mimic and MCVSyn (Figure 4.6 J).

OSR1 (odd-skipped related 1) is a transcription factor and tumour suppressor gene the overexpression of which has been associated with cell cycle arrest and induction of apoptosis in gastric cancer cell lines, where its knockdown promotes cell growth in normal gastric cells (Otani *et al.* 2014). qRT-PCR confirmed OSR1 RNA-Seq results with more than 2-fold downregulation with MCV-miR-M1-3p mimic and MCVSyn (Figure 4.6 K).

4.2.1.3. Transcripts not identified via RNA-Seq (Miscellaneous transcripts)

A recent study showed that MCV T Ag locus mediates downregulation of TLR9 promoter activity by downregulating C/EBPα and C/EBPβ and subsequent reduced binding to TLR9 promoter (Shahzad *et al.* 2013), however, the authors did not specify the mechanism by which C/EBPα and C/EBPβ are downregulated. Therefore, to address the possibility of miRNA-mediated downregulation of their transcripts, TLR9, C/EBPα and C/EBPβ were also included in MCV-miR-M1 qRT-PCR assays.

qRT-PCR analysis confirmed TLR9 downregulation in the presence of MCV-miR-M1-5p and -3p mimics and MCVSyn (Figure 4.6 L), suggesting that TLR9 downregulation is MCV-miR-M1-dependent. C/EBPα was downregulated by more than 2-fold in the presence of MCV-miR-M1-5p and -3p mimics while showing increased levels with MCVSyn (Figure 4.6 M). C/EBPβ was upregulated with both MCV-miR-M1 mimics and MCVSyn (Figure 4.6 N). Accordingly, whilst these data suggest a positive correlation between MCV-miR-M1 and C/EBPβ mRNA expression, C/EBPα expression presents a more complex association with MCV-miR-M1.

i. Immune-related transcripts

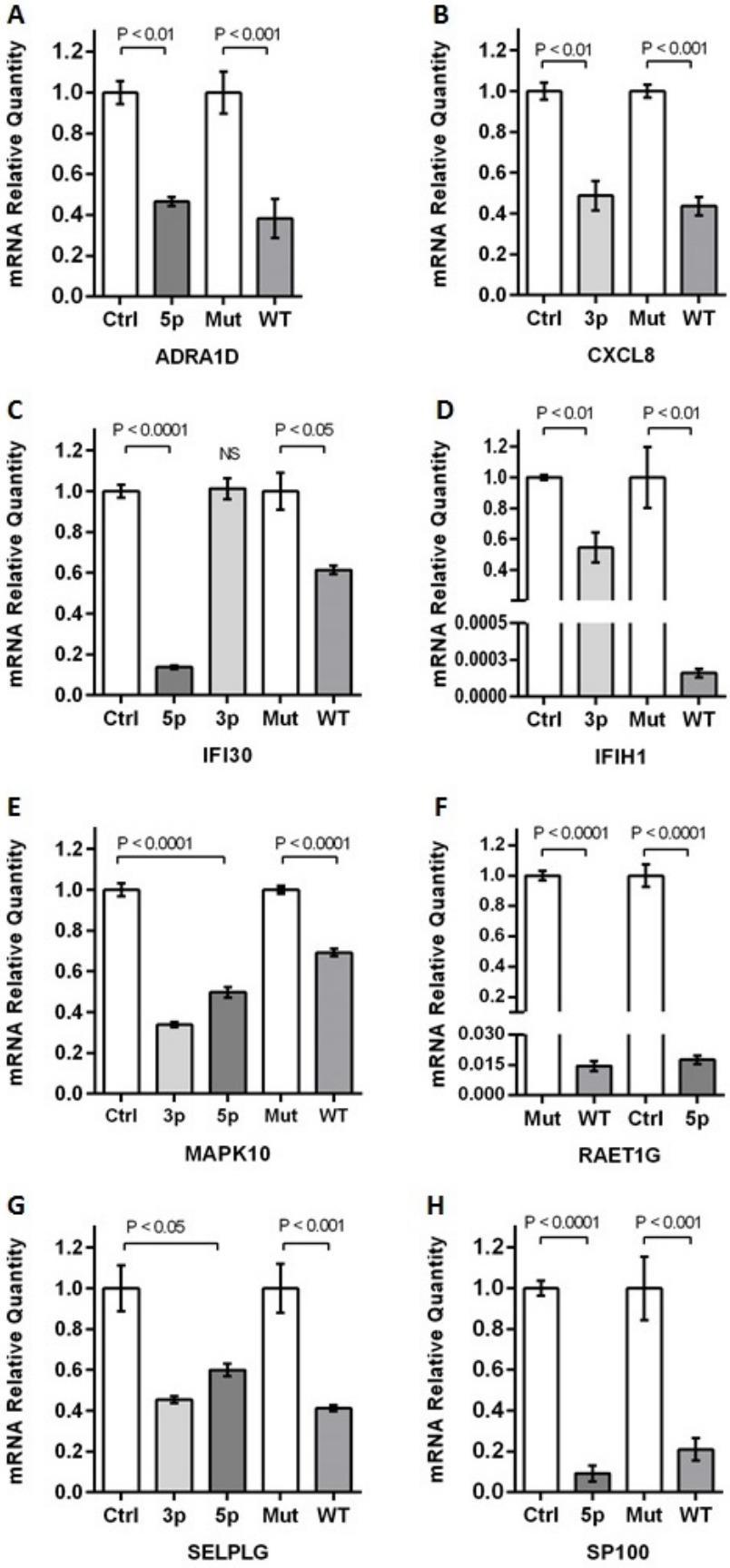

ii. Tumour-related transcripts

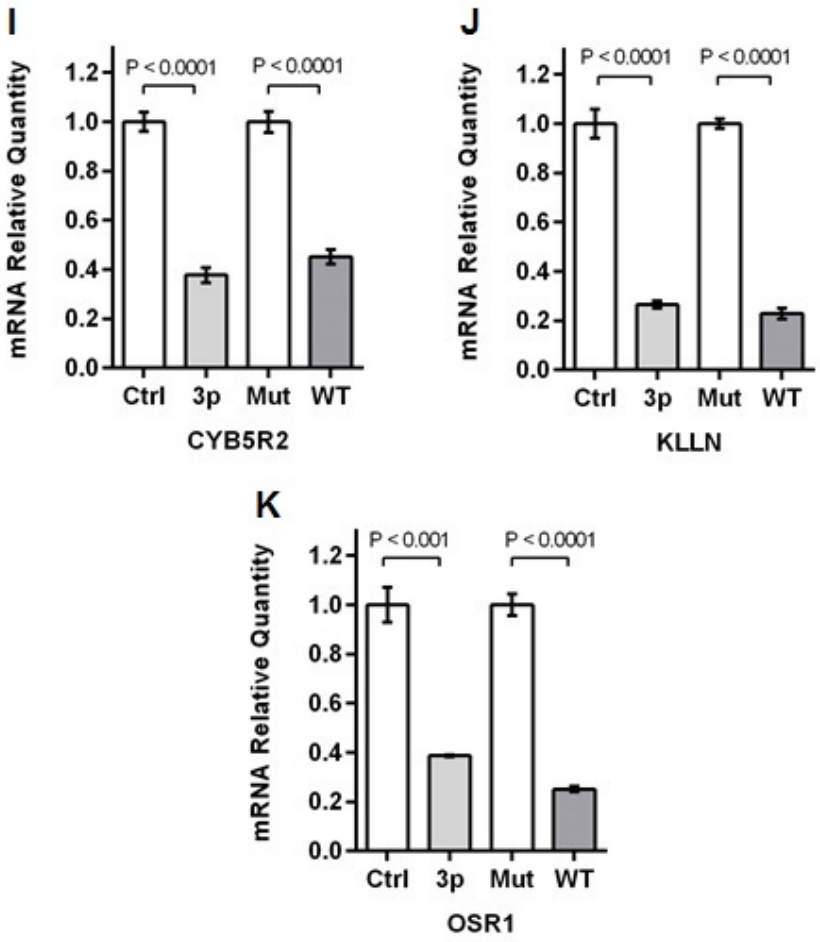

iii. Miscellaneous transcripts

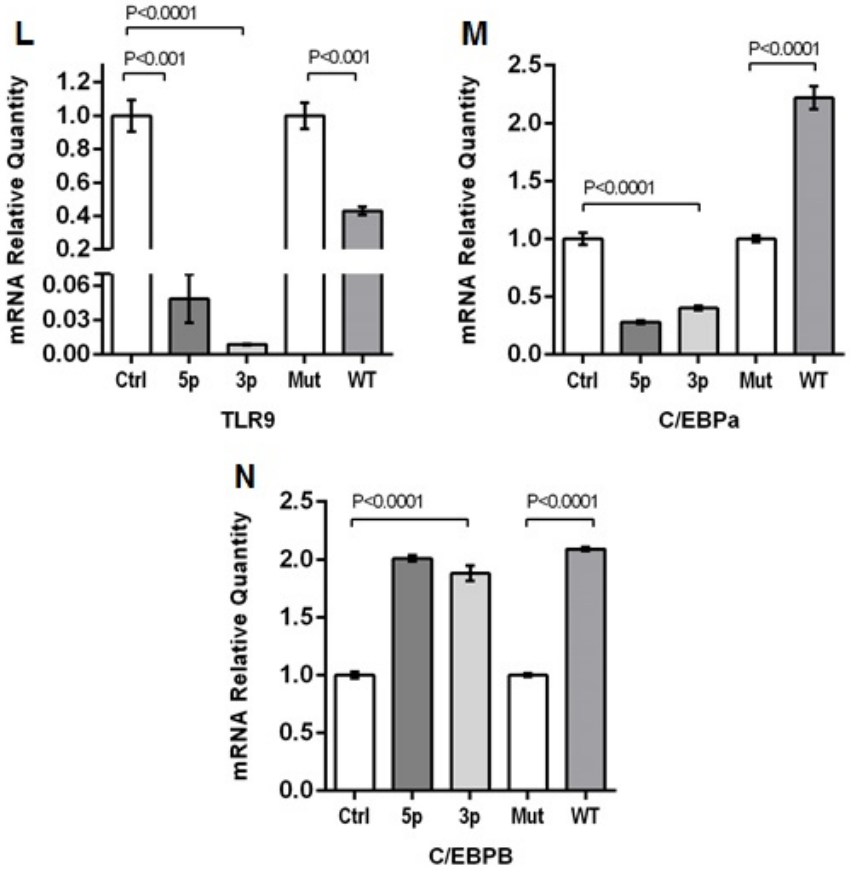

Figure 4.6. Panel i: Immune-related RNA-Seq-identified cellular transcripts. Panel ii: Tumour-related RNA-Seq-identified cellular transcripts. Panel iii: Miscellaneous transcripts downregulated by MCV T Ag locus (Shahzad *et al.* 2013). Downregulation of these transcripts was qRT-PCR validated using cDNA of 293 cells transfected with MCV-miR-M1-5p, MCV-miR-M1-3p and a scramble miRNA mimic or with MCVSyn and MCVSyn-hpko. Expression of MCV-miR-M1 was confirmed via stem loop qRT-PCR. Due to higher relative expression of MCV-miR-M1, MCVSyn experiments were carried out using cDNAs of 72h time point. 5p and 3p, MCV-miR-M1-5p and -3p mimics; Ctrl, control (scramble) miRNA mimic; WT, MCVSyn; Mut, MCVSyn-hpko.

4.3. Investigating protein expression of MCV-miR-M1 targets

Due to the limited consumables budget associated with the project, unfortunately it was not possible to investigate protein expression by western blot for all the qRT-PCR-validated transcripts. Therefore, it was decided to choose targets with the most functional relevance to MCV pathogenesis and life cycle, namely, CXCL8, SP100 and TLR9. As explained in section 4.2.1, CXCL8 is an important leukocyte chemoattractant whose downregulation may help MCV remain hidden from host immune surveillance. SP100 has also been implicated in cell antiviral response and a recent study has showed that SP100 expression is absent in a large proportion of cells with active MCV replication (Neumann *et al.* 2016), supporting existing data for the important role of SP100 in innate antiviral immunity. TLR9 was initially identified as a ligand for unmethylated CpG motif of bacterial DNA (Hemmi *et al.* 2000; Bauer *et al.* 2001) and has been implicated in immune recognition of dsDNA viruses such as herpesviruses (Krug *et al.* 2004), papillomaviruses (Hasan *et al.* 2007) and MCV (Shahzad *et al.* 2013). Moreover, SP100 and TLR9 have been linked to interferon and cytokine signalling pathways (Grotzinger *et al.* 1996; Krug *et al.* 2003; Lund *et al.* 2003; Krug *et al.* 2004; Scherer and Stamminger 2016). Given the role of MCV miRNA in virus persistence (Theiss *et al.* 2015), significant MCV-miR-M1-dependent downregulation of CXCL8 and SP100 in RNA-Seq analysis and MCV-driven downregulation of SP100 and TLR9, I embarked to investigate if MCV miRNA is undermining innate immune response by modulating protein expression of CXCL8, SP100 and TLR9. Initially, it was important to confirm the effect of MCV-miR-M1 on the protein expression of MCV LT. To this end,

293 cells were mock-transfected or transfected with MCVSyn and MCVSyn-hpko and western blotting was carried out for total protein of transfected cells using an MCV LT-specific antibody, CM2B4. Consistent with data for mRNA expression (Figure 3.7 C), MCV LT protein showed a steady and significant increase in MCVSyn-hpko versus MCVSyn over 72h, with no expression in mock (Figure 4.7), confirming functionality of MCV-miR-M1 in our 293 system at protein expression level.

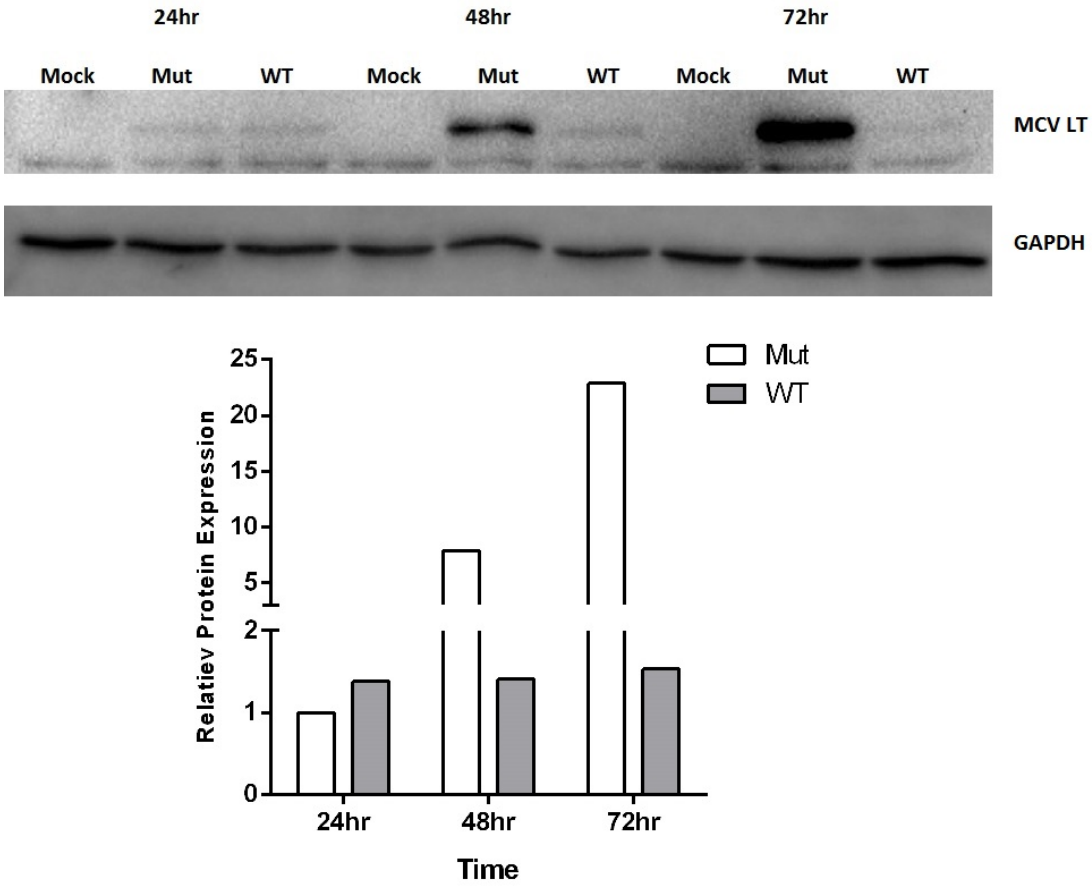

Figure 4.7. Protein expression of MCV LT Ag in total protein of mock- and MCVSyn-transfected 293 cells. Densitometry analysis revealed more than 5-fold and 22-fold increase in LT expression in MCVSyn-hpko versus MCVSyn at 48h and 72h time points, respectively.

Having confirmed that MCV-miR-M1 can negatively regulate its direct viral transcript at the level of protein expression, 293 cells were transfected with MCV-miR-M1-5p, -3p and control miRNA mimics to investigate whether MCV-miR-M1-5p and -3p can also downregulate protein expression of their identified cellular targets.

Previous studies have shown that TLR9 is downregulated by a number of viruses and viral proteins including, hepatitis B virus (HBV) (Vincent *et al.* 2011), human papillomavirus type 16 (HPV16) E6 and E7 proteins (Hasan *et al.* 2007), EBV latent membrane protein 1 (LMP1) (Fathallah *et al.* 2010) and BGLF5 (van Gent *et al.* 2011) as well as MCV T Ag locus (Shahzad *et al.* 2013). This is not surprising given the important role TLR9 plays in innate immunity (Wagner 2002; Krug *et al.* 2004). In MCV, TLR9 expression is impaired by T Ag locus, however, it is not clear whether this effect is miRNA-mediated or T Ag-mediated or both. My initial investigation revealed that TLR9 mRNA is significantly downregulated by MCV-miR-M1-5p and -3p and in the presence of MCVSyn (Figure 4.6 L). Therefore, to investigate whether TLR9 protein expression is also reduced by MCV-miR-M1 expression, western blotting was carried out for total protein of MCV-miR-M1-5p, -3p and control miRNA mimic-transfected 293 cells. As seen in Figure 4.8 A, densitometry analysis of TLR9, normalised to GAPDH protein levels, demonstrated 1.7-fold decrease in the presence of MCV-miR-M1-3p mimic. To test whether TLR9 protein level is also downregulated following expression of MCV-miR-M1 in MCVSyn, 293 cells were mock-transfected or transfected with MCVSyn and MCVSyn-hpko and total protein was extracted 72h p.t. The 72h time point was chosen due to higher levels of MCV-miR-M1

expression and larger degree of MCV LT downregulation at 72h compared to earlier time points (Figures 3.7 A & 4.7). Consistent with mimic data, TLR9 protein expression demonstrated 2-fold increase in MCVSyn-hpko versus MCVSyn and mock at 72h p.t. (Figure 4.8 B), suggesting that reduced TLR9 protein expression was MCV-miR-M1-dependent.

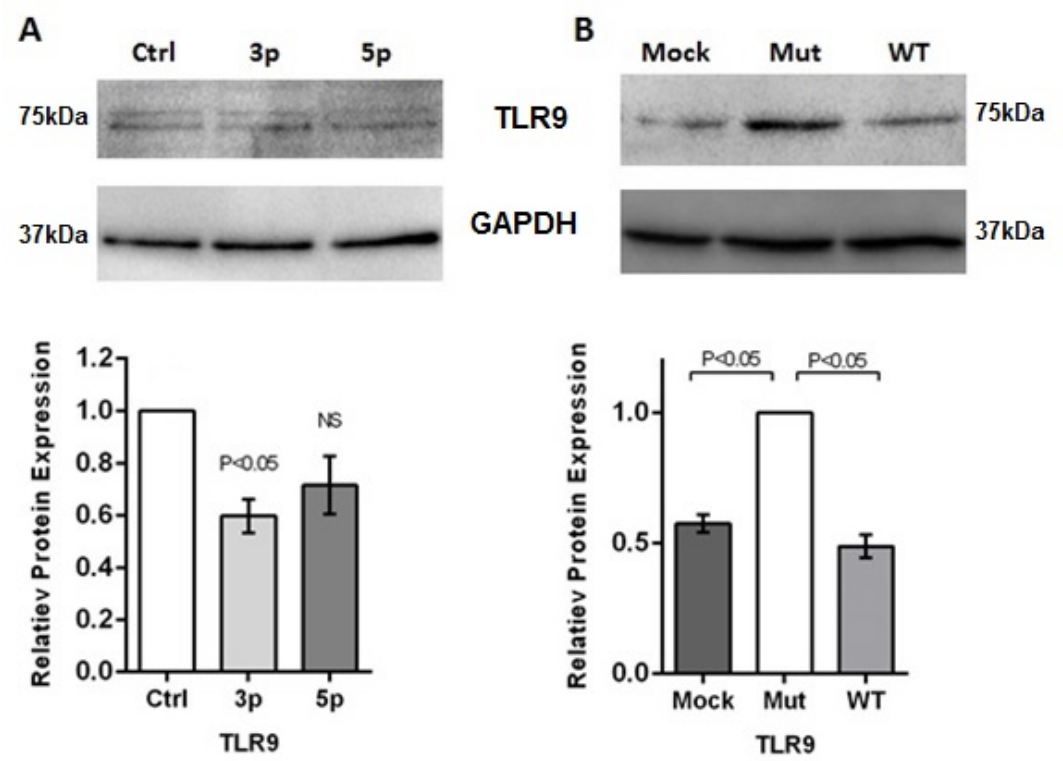

Figure 4.8. Protein expression of TLR9 in total proteins of MCV-miR-M1-5p, -3p and control mimic-transfected (A) and mock-, MCVSyn- and MCVSyn-hpko-transfected (B) 293 cells. Densitometry analysis revealed 1.7-fold downregulation of TLR9 with MCV-miR-M1-3p mimic and 2-fold upregulation in MCVSyn-hpko versus MCVSyn and mock at 72h p.t. (p-value<0.05). NS, no significance. Immunoblots are representative of three independent biological repeats.

SP100 is an IFN-stimulated gene (Grotzinger *et al.* 1996) whose alternative splicing gives rise to four isoforms including, SP100A (Szostecki *et al.* 1990), SP100B (Dent *et al.* 1996), SP100C (Seeler *et al.* 2001) and SP100-HMG (Guldner *et al.* 1999). Importantly, SP100B has been demonstrated to repress transcription of cellular and viral promoters (Wilcox *et al.* 2005) and preferentially bind to unmethylated CpG, hence targeting foreign DNA such as viral genomes (Isaac *et al.* 2006). SP100 has been implicated in immune response against dsDNA viruses such as HCMV (Kim *et al.* 2011; Tavalai *et al.* 2011; Wagenknecht *et al.* 2015), HSV-1 (Negorev *et al.* 2006; Negorev *et al.* 2009), HPV18 (Stepp *et al.* 2013) and MCV (Neumann *et al.* 2016). Further evidence for the important role of SP100 in host cell antiviral response comes from downregulation or loss of SP100 by several herpesvirus proteins including, HSV-1 ICP0 (Chelbi-Alix and de The 1999), VZV ORF61p (Kyratsous *et al.* 2009), HCMV IE1 (Tavalai and Stamminger 2009) and Murine Gamma-Herpesvirus 68 (MHV-68) ORF75c (Tavalai and Stamminger 2009). A recent study has also shown that EBV BART1-miR-3p directly targets 3'UTR of SP100 in DLA (Skalsky *et al.* 2012), suggesting direct involvement of EBV miRNAs in modulation of host cell antiviral response, cell survival and proliferation. Importantly, SP100-mediated antiviral response against MCV gains support from a very recent study where authors showed an increase in MCV genome replication following SP100 depletion in H1299 cells (Neumann *et al.* 2016). However, thus far there is no published data as to whether and how MCV counteracts SP100 by modulating its downregulation or depletion. To address this question, I demonstrated downregulation of SP100 mRNA via RNA-Seq and confirmed

this data via qRT-PCR with MCV-miR-M1-5p mimic and MCVSyn (Section 4.2.1, Table 4.1 and Figure 4.6 H). To verify MCV-miR-M1-5p-dependent downregulation of SP100 at protein expression level, western blotting was carried out for total protein of MCV-miR-M1-5p, -3p and control mimic transfected-293 cells using SP100-specific antibody. Importantly, in Bauman *et al.*'s study of JCV and BKV miRNA-mediated downregulation of ULBP3 (see section 1.6.1.2), the authors demonstrated that ULBP3 protein levels reduced despite no change in mRNA expression levels, suggesting that JCV/BKV miRNA achieves this by inhibition of translation and not repression of mRNA expression (Bauman *et al.* 2011). Therefore, MCV-miR-M1-3p mimic was also included in the experiment to see whether SP100 protein expression is affected by the 3p strand of MCV-miR-M1. As can be seen in Figure 4.9 A, SP100 protein expression was significantly downregulated by more than 2-fold in the presence of MCV-miR-M1-5p mimic and not -3p mimic. To confirm whether SP100 protein expression was also downregulated in the context of MCV replication, western blotting was repeated for SP100 72h p.t. using total protein isolated from mock-, MCVSyn- and MCVSyn-hpko-transfected 293 cells. Similar to MCV-miR-M1 mimics experiment, SP100 protein expression demonstrated ~2-fold reduction at 72h p.t. in MCVSyn compared with MCVSyn-hpko and mock (Figure 4.9 B). Together, these data suggest that MCV drives downregulation of SP100 protein expression in an MCV-miR-M1-5p-dependent manner.

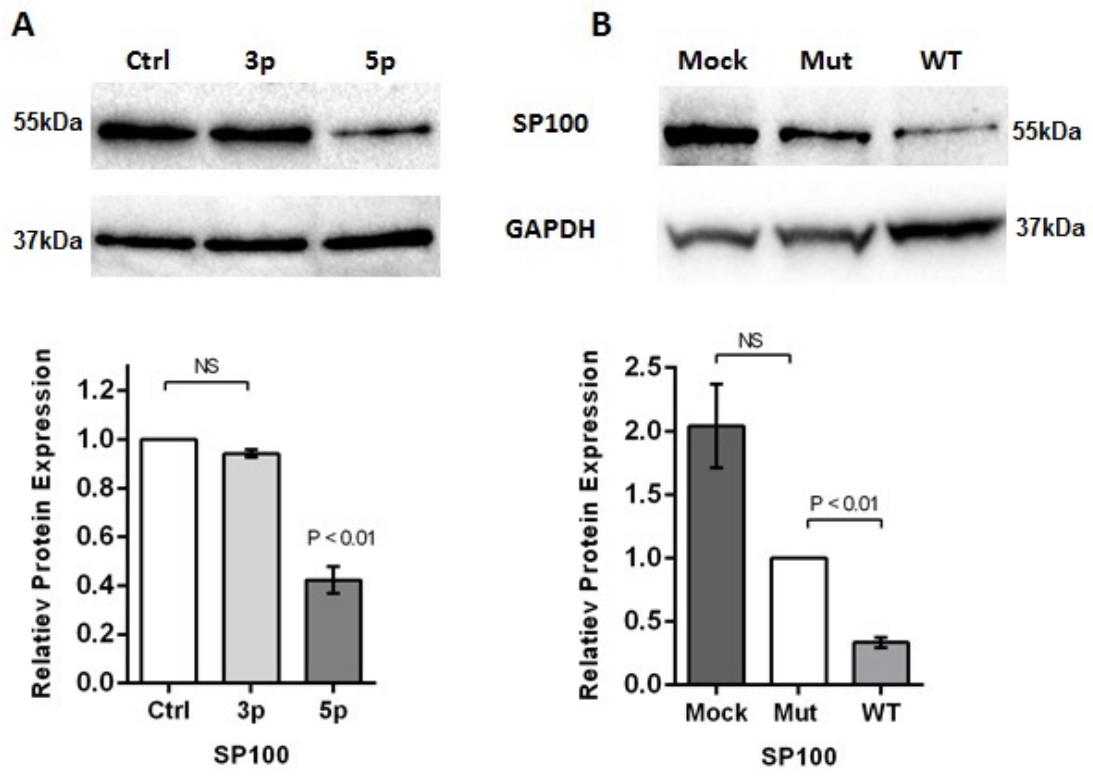

Figure 4.9. Protein expression of SP100 in total proteins of MCV-miR-M1-5p, -3p and control mimic-transfected (A) and mock-, MCVSyn- and MCVSyn-hpko-transfected (B) 293 cells. Densitometry analysis revealed more than 2-fold downregulation of SP100 with MCV-miR-M1-5p mimic and in MCVSyn versus MCVSyn-hpko and mock at 72h p.t. (p-value<0.01). NS, no significance. Immunoblots are representative of three independent biological repeats.

CXCL8 exhibited 16-fold downregulation in the MCV-miR-M1-3p RNA-Seq dataset and the highest frequency in immune-related pathways following GO analysis. Therefore, due to its key role in immune response and neutrophil activation and migration, I decided to investigate the impact of MCV-miR-M1 on the secreted levels of CXCL8 protein. Secreted levels of CXCL8 were

determined via ELISA analysis of growth media (Baggiolini *et al.* 1989) derived from TNF-α-stimulated 293 cells transfected with either MCV-miR-M1-3p or -5p mimic. As seen in Figure 4.10 A, growth media CXCL8 concentrations showed more than 25% reduction in the presence of MCV-miR-M1-3p mimic whereas secreted levels of CXCL8 protein remained unaltered in 293 cells transfected with the MCV-miR-M1-5p mimic. Next, to see if CXCL8 protein expression is also reduced in the presence of replicating MCVSyn, 293 cells were mock-transfected or transfected with MCVSyn and MCVSyn-hpko. Analysis via ELISA revealed that levels of secreted CXCL8 dropped by 70% in the growth media of MCVSyn-transfected cells compared to MCVSyn-hpko 72h p.t. (Figure 4.10 A & B). As expected, no CXCL8 was detected in mock-transfected cells due to lack of stimulation. These data suggest that secreted CXCL8 protein is downregulated in a MCV-miR-M1-dependent manner.

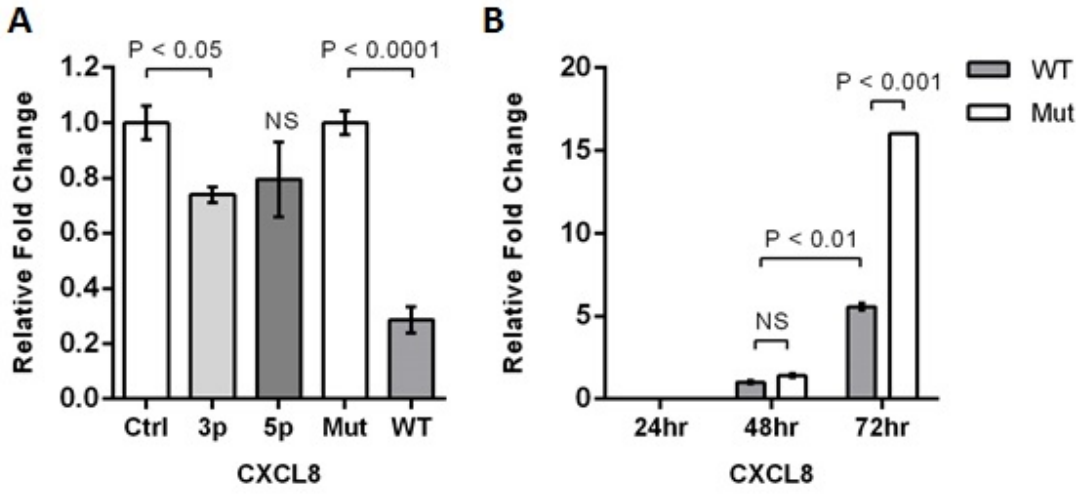

Figure 4.10. Secreted CXCL8 levels in growth media of 293 cells stimulated with TNF-α and transfected with MCV-miR-M1 mimics or transfected with MCVSyn and MCVSyn-hpko. Growth media CXCL8 was downregulated by more than 70% (3-fold) and 25% in MCVSyn- versus MCVSyn-hpko- and MCV-miR-M1-3p versus control mimic-transfected cells, respectively (A). Relative expression of CXCL8 in growth media of MCVsyn- and MCVSyn-hpko-transfected 293 cells increases by time. Downregulation of growth media CXCL8 in MCVSyn relative to MCVSyn-hpko is only detectable at 72h p.t. (B).

4.4. Discussion

Despite mounting evidence for the role of virus miRNAs in modulation of host cell transcripts (Kincaid and Sullivan 2012), thus far for most virus miRNAs there is a lack of global target identification. Recent studies have reported virus miRNA targetomes of KSHV and EBV in primary effusion lymphoma cell lines (Gottwein *et al.* 2011) and lymphoblastoid cell lines (Skalsky *et al.*

2012), respectively. In BKV and JCV, miRNA target identification has been limited to study of NKG2D ligands ULBP3, ULBP2 and MICA (Bauman *et al.* 2011). In MCV, currently there is no published data regarding cellular targets of MCV-miR-M1 and Lee *et al.*'s *in silico*-predicted cellular targets of MCV-miR-M1 (Lee *et al.* 2011) were based on incorrect MCV-miR-M1-5p seed sequence (Theiss *et al.* 2015). Therefore, there is an unmet need to identify potential targets of MCV-miR-M1 via an unbiased and global approach. It has been demonstrated that in the majority of cases (> 84%) miRNAs reduce the level of targeted mRNAs (Guo *et al.* 2010), suggesting mRNA expression level as a reliable indicator of miRNA impact. RNA-Seq has been used to measure differential transcriptomic changes induced by viruses such as KSHV (Viollet *et al.* 2015) or malignancies such as pancreatic cancer (Muller *et al.* 2015). In this project, using RNA-Seq in HEK293 cells I identified several hundred cellular transcripts with differential expression induced by MCV-miR-M1-5p and -3p mimics. To identify priority targets for downstream validation, GO analysis was carried out using DAVID software. A recent RNA-Seq-based comparative study of latent KSHV-infected cell line SLKK with non-infected SLK cell line has revealed differential expression of multiple pathways, among which are pathways associated with KSHV pathogenesis, such as regulation of the epithelial-to-mesenchymal transition pathway and CXCL8 signalling pathway (Viollet *et al.* 2015). Several studies have demonstrated that differential expression of pathways related to immune response are a common feature when investigating virus-host cell interaction (Juranic Lisnic *et al.* 2013; Rossetto *et al.* 2013; Mei *et al.* 2014; Wang *et al.* 2014b; Park *et al.* 2015; Richards *et al.* 2015; Hu *et al.* 2016). For instance,

the KSHV polyadenylated nuclear RNA (PAN RNA) dysregulates pathways involved in regulation of immune response and inflammatory cytokine production (Rossetto *et al.* 2013). EBV-B95-8 miRNAs target a number of pathways including interleukin signalling and IFN-γ signalling pathways (Skalsky *et al.* 2012). Of particular interest to this project, a recent study has revealed that MCV T Ags induce upregulation of pathways associated with cell cycle, DNA replication and immune response (Richards *et al.* 2015). In the present project, GO analysis placed a number of hits in immune-related GO terms (Figure 4.5). Cross-referencing top hits with significant GOs associated with processes known to be important in polyomavirus infection and replication led to the identified list of targets in Chapter 4. Strikingly, consistent with proposed function of viral miRNAs in virus-host interaction, several pathways with relevance to virus pathogenesis were highlighted in my GO analysis including, immune response, regulation of cell proliferation and cellular processes and cell communication pathways. In addition, several other pathways were identified such as, female gamete generation, response to steroid hormone stimulus, regulation of blood pressure and several neurological pathways such as, regulation of synaptic transmission and synaptic plasticity, learning or memory, sleep and behaviour. It is possible that some of the identified transcripts within these GOs might encode for proteins with diverse but as yet unidentified functions, however, due to currently unknown relevance to MCV pathogenesis or life cycle these transcripts were not included in target validation experiments. It should be noted that the starting number of RNA-Seq-identified targets for qRT-PCR validation was larger than the number of validated transcripts in Table 4.1.

Failure to validate some of the selected targets was largely due to none or very low qRT-PCR amplification of the non-validated transcripts with cDNA of 293 cells. In addition, in some cases target validation was not possible due to non-specific amplification of the transcripts, possibly as a result of alternate transcript variants. Importantly, at the end of my PhD project dermal fibroblasts were identified as the natural host of MCV (Liu *et al.* 2016) and it will be of interest and important to determine if key dysregulated cellular transcripts are also altered in response to MCV-miR-M1 expression in these cells.

Following target selection, a two-tiered approach was taken to RNA-Seq target validation. MCV-miR-M1 responsive cellular targets were initially analysed and validated via qRT-PCR following transfection of 293 cells with either MCV-miR-M1-5p or -3p mimics. Functional analysis of MCV-miR-M1 mimics demonstrated robust efficacy against their cognate target, MCV LT (Figure 3.5 B). However, it was important to establish if MCV-miR-M1 mimic-modulated cellular targets were also significantly altered by virus-encoded MCV-miR-M1 expressed during virus replication. To this end, the MCVSyn system was used to transfect 293 cells and expression of cellular targets was measured 72h p.t. due to higher expression and activity of MCV-miR-M1 at this time point (Figure 3.7 A & C). qRT-PCR analysis of the targets confirmed RNA-Seq and MCV-miR-M1 mimics data in all cases.

miRNAs are post-transcriptional regulators of gene expression and predominantly downregulate protein expression of their targeted transcripts (Guo *et al.* 2010). A hallmark of virus-encoded miRNAs is downregulation of their cognate viral proteins. Such effect has been demonstrated for KSHV-

miR-K12-9-5p suppression of KSHV RTA (Bellare and Ganem 2009), EBV-miR-BART-20-5p suppression of EBV RTA and ZTA (Jung *et al.* 2014) and HCMV miR-UL112-1 downregulation of IE1, UL112/113 and UL120/121 (Murphy *et al.* 2008). Polyomaviruses also express a miRNA which directly targets and downregulates protein expression of its cognate LT Ag (Sullivan *et al.* 2005; Seo *et al.* 2008). As discussed in section 1.6.1.3, it has been hypothesised that viruses use downregulation of their own proteins as a strategy to dampen lytic replication and avoid detection by the host immune system (Kincaid and Sullivan 2012). Therefore, LT Ag protein expression can be reliably used as a positive control in polyomavirus miRNA functional studies. With this view, 293 cells were transfected with MCVSyn system and expression of MCV LT was monitored for 72h at 24h intervals. Whilst MCV LT protein expression demonstrated 23-fold upregulation in MCVSyn-hpko-transfected cells within 72h time period, its expression remained constant in MCVSyn (Figure 4.7) despite its steady mRNA downregulation during same time period (Figure 3.7 C). This may be due to relatively stable steady-state expression of MCV LT in MCVSyn (Selbach *et al.* 2008), suggesting that a more prolonged transcriptional repression is required for significant downregulation of MCV LT protein.

In addition to their impact on the expression of viral proteins, there is mounting evidence for the key role of viral miRNAs in downregulation of proteins involved in host immune response. For instance, BKV and JCV identical miRNAs, BKV-miR-B1-3p and JCV-miR-J1-3p, directly target and downregulate immune ligand ULBP3 (Bauman *et al.* 2011). Although thus far there is no published data regarding cellular targets of MCV-miR-M1, a

recent study provided strong evidence for the involvement of MCV-miR-M1 in modulation of host immune response by showing *in vitro* that the miRNA-deficient MCVSyn-hpko fails to establish long term persistent infection (Theiss *et al.* 2015). In addition, it has been shown that SP100 acts as a negative regulator of MCV genome replication and its expression is abolished in the majority of cells with active MCV replication, however, the authors did not provide a mechanistic explanation for this observation (Neumann *et al.* 2016). Together, these observations suggest an association between MCV-miR-M1 and the antiviral immune response. In my RNA-Seq analysis, among the top MCV-miR-M1 hits in terms of differential expression was the immune-related transcript SP100 (>18-fold downregulation). Having confirmed mRNA downregulation of SP100 via MCV-miR-M1 mimic and MCVSyn systems, I investigated SP100 protein expression in the presence of MCV-miR-M1. Consistent with qRT-PCR data, western blotting confirmed downregulation of SP100 protein expression by MCV-miR-M1-5p mimic (Figure 4.9 A). In addition, it was crucial to determine whether endogenous expression of MCV-miR-M1 following MCV genome replication could also modulate SP100 protein expression. To this end, western blotting confirmed that MCVSyn replication diminishes SP100 protein expression compared to MCVSyn-hpko- and mock-transfected cells (Figure 4.9 B).

Importantly, Neumann *et al.*'s study about the relation of MCV replication and SP100 expression showed that while overexpression of sT or LT alone has no effect on SP100 expression, in cells with overexpressed early region where LT is expressed at substantially higher levels SP100 is significantly downregulated (Neumann *et al.* 2016). Therefore, Neumann *et al.*'s study

suggests that SP100 downregulation correlates with MCVSyn replication and level of LT expression, giving rise to the speculation that SP100 downregulation is MCV LT-mediated. However, my data argues strongly against this since increased genome replication and LT expression in MCVSyn-hpko does not downregulate SP100 relative to MCVSyn- or mock-transfected cells. Instead, I show SP100 downregulation independent of MCV LT and in the presence of MCV-miR-M1-5p mimic as well as in MCVSyn- versus MCVSyn-hpko- and mock-transfected cells (Figure 4.9). These data suggest a model where MCV-miR-M1 is expressed by MCV as a means to attenuate the host cell innate immune response via downregulation of SP100.

In addition to its role in immune response, dispersal of SP100 from PML-NB by tumourigenic viruses such as KSHV and EBV (Tavalai and Stamminger 2009) and its downregulation in MCV (Akhbari *et al*, in preparation) hint at a tumour suppressor role for SP100. This is supported by studies showing SP100 downregulation in laryngeal cancer (Li *et al.* 2010) and reduced proliferation and migration of glioma cells following SP100 overexpression (Held-Feindt *et al.* 2011). As described in section 4.2.1.2, this bifunctional immune-regulatory/tumour-suppressor characteristic is also relevant for other targets of MCV-miR-M1 including CYB5R2. Therefore, it is tempting to suggest that MCV modulates expression of transcripts which span the intersect of innate immunity and tumour suppression to establish a persistent infection necessary for MCV tumourigenesis. While my findings support this hypothesis whether this is the case requires further investigation.

SP100 is a cytokine-stimulating gene implicated in immune response against several dsDNA viruses such as HSV1, VZV, HCMV, EBV, KSHV, BKV and MCV (Tavalai and Stamminger 2009; Jiang *et al.* 2011; Tavalai *et al.* 2011; Wagenknecht *et al.* 2015; Neumann *et al.* 2016; Scherer and Stamminger 2016) and is a permanent constituent of PML-NB, a nuclear protein complex involved in various activities including, transcription regulation, apoptosis and cell cycle, response to stress and hormone signalling and development (Negorev and Maul 2001). To date, no one has demonstrated a direct regulatory role for SP100 on CXCL8 or NF-κB-induced chemokine expression, however, there is evidence implicating SP100 in trans via activating transcription of chemokine-inducing genes or potentiating their effect. For instance, SP100 has been shown to directly interact with and stimulate transcription of the transcription factor ETS-1 (Wasylyk *et al.* 2002), which is a stimulator of several cytokines such as IL-2, IL-4, IL-5 and IFN-γ and the monocyte and neutrophil chemoattractant chemokine (C-C motif) ligand 2 (CCL2) (Reichel *et al.* 2009; Russell and Garrett-Sinha 2010). Interestingly, ETS-1 has also been shown to upregulate CXCL8 expression and secretion in neuroblastoma cells (Qiao *et al.* 2007). It is possible, therefore, that SP100 might mediate expression of CCL2, CXCL8 and other chemokines and cytokines via ETS-1.

CXCL8 is a chemokine associated with various aspects of immune response such as, neutrophil activation, triggering neutrophil and IL-2-activated-NK cells chemotaxis (Sebok *et al.* 1993; DiVietro *et al.* 2001), mediating neutrophil endothelial arrest and binding via Lymphocyte function-associated antigen 1 (LFA1) and selectins (Lawrence and Springer 1991; Von Andrian *et*

al. 1992) and activating respiratory burst, rapid Ca++ release and degranulation of polymorphonuclear (PMN) cells (Lindley *et al.* 1988; Peveri *et al.* 1988; Carveth *et al.* 1989). Interestingly, several studies have emulated the CXCL8-mediated neutrophil recruitment *in vivo* by histological assessment of skin samples following intradermal injection of CXCL8 in human, rabbit and several other species (Colditz *et al.* 1990; Leonard *et al.* 1991; Rot 1991). It has also been shown that whilst CXCL8 is the major human neutrophil chemoattractant, CXCL8-activated neutrophils can release gelatinase B which in turn potentiates CXCL8 by catalysing its N-terminal truncation (Van den Steen *et al.* 2000; Starckx *et al.* 2002), suggesting a positive-feedback loop between CXCL8 and neutrophils. Several viruses have been shown to reduce CXCL8 expression. HSV-1 protein kinase US3 has been demonstrated to downregulate CXCL8 expression by inhibiting NF-κB activation (Wang *et al.* 2014a). Adenovirus dl922-947 E1A protein also dampens CXCL8 and CCL2 production by displacing NF-κB p65 subunit from their promoter in anaplastic thyroid carcinoma (ATC) cell line 8505-c (Passaro *et al.* 2016). HCMV miR-UL112-3p has been shown to inhibit NF-κB activation via directly targeting TLR2, leading to downregulation of CXCL8, IL-6 and IL-1β (Landais *et al.* 2015). A recent study has also shown that MCV sT prevents nuclear translocation of NF-κB leading to downregulation of NF-κB-stimulated genes including CXCL8, CXCL9 and CCL20 (Griffiths *et al.* 2013). In my RNA-Seq investigation, CXCL8 was a top hit in MCV-miR-M1-3p dataset by more than 16-fold downregulation. qRT-PCR confirmed CXCL8 reduced expression in MCV-miR-M1-3p mimic-transfected 293 cells (Figure 4.6 B). Having confirmed MCV-miR-M1-dependent downregulation of CXCL8

with MCV-miR-M1 mimic, CXCL8 mRNA expression using MCVSyn system also demonstrated significant CXCL8 downregulation 72h p.t. (Figure 4.6 B). Furthermore, to confirm whether downregulation of CXCL8 mRNA results in reduced protein expression secreted CXCL8 protein was measured in the growth media of MCV-miR-M1 mimic-transfected 293 cells. ELISA confirmed CXCL8 protein downregulation in MCV-miR-M1-3p mimic-transfected cells (Figure 4.10 A). Investigating growth media CXCL8 in MCVSyn-transfected cells corroborated MCV-miR-M1 mimic results at 72h p.t. (Figure 4.10 A & B). Whilst MCVSyn data confirm that CXCL8 is downregulated following MCV genome replication MCV-miR-M1 mimic data prove that this downregulation is MCV-miR-M1-dependent and independent of other MCV components, i.e. MCV LT proteins. Importantly, a recent study has shown that other components of MCV can modulate expression of cytokines. For instance, one study demonstrated downregulation of NF-κB-induced genes including CXCL8 using an expression vector and an inducible cell line expressing MCV sT (Griffiths *et al.* 2013). The authors showed that MCV sT interacts with IKKγ (NEMO), PP4C and PP2A Aβ in cytoplasmic puncta to prevent phosphorylation of IKKα and IKKβ and subsequent IkB degradation. This prevents NF-κB release and nuclear translocation which is required for transcription activation of NF-κB-inducible genes (Griffiths *et al.* 2013). Based on this model one would predict that we should see downregulation of CXCL8 in MCVSyn-hpko versus MCVSyn at 72h p.t., since at this time point MCV sT is upregulated in MCVSyn-hpko relative to MCVSyn (Figure 3.7 D). However, my findings show exactly the opposite where CXCL8 is downregulated at both mRNA and protein levels in MCVSyn versus

MCVSyn-hpko at 72h p.t. (Figures 4.6 B & 4.10). In addition, similar levels of secreted CXCL8 at 48h p.t. (Figure 4.10 B) do not correlate with higher levels of MCV sT transcripts in MCVSyn-hpko at this time point (Figure 3.7 D). Moreover, a recent study reported that MCV T Ags upregulate the expression of several inflammatory cytokines and chemokines including CXCL8 (Richards *et al.* 2015). Interestingly, the authors also demonstrate that while tumour-derived MCV LT upregulates CXCL8 expression, tumour-derived MCV LT+sT enhances this effect by more than 2.5-fold and 15-fold at mRNA and protein levels, respectively (Richards *et al.* 2015). Therefore, if MCV T Ags stimulate CXCL8 expression we expect to see increased levels of CXCL8 in MCVSyn-hpko relative to MCVSyn. This is in perfect agreement with my data where CXCL8 mRNA and protein levels are upregulated in MCVSyn-hpko-transfected cells (Figures 4.6 B & 4.10). Importantly, given the significantly low expression of MCV-miR-M1 in MCV-positive MCCs (Lee *et al.* 2011; Theiss *et al.* 2015) and that Richards *et al.* used tumour-derived truncated LT stable cell lines, elevated levels of CXCL8 in their study might be attributed to the absence of sufficient amounts of MCV-miR-M1. It is also possible that these differences are due to experimental set-up, as MCV LT was excluded in Griffiths *et al.*'s experiments. Moreover, neither of the studies considered MCV-miR-M1 expression and cytokine and chemokine expression in the context of MCV infection/replication.

TLR9 is an important PRR and unmethylated CpG ligand (Hemmi *et al.* 2000; Bauer *et al.* 2001) whose targeting and downregulation has been shown by EBV latent membrane protein 1 (LMP1) (Fathallah *et al.* 2010) and HPV16 E6 and E7 oncoproteins (Hasan *et al.* 2007). In addition, a recent study

showed that MCV T Ag locus can mediate TLR9 downregulation by negatively regulating C/EBPα and C/EBPβ expression (Shahzad *et al.* 2013), however, the authors did not provide conclusive evidence as to how MCV T Ag achieves this. A recent study has investigated cellular targets of EBV-B95-8 miRNAs in lymphoblastoid cell lines using Photoactivatable-Ribonucleoside-Enhanced Crosslinking and Immunoprecipitation (PAR-CLIP) (Skalsky *et al.* 2012). PAR-CLIP is a technique used for determining binding sites of RBPs such as miRISC at a transcriptome-wide scale (Hafner *et al.* 2010). Briefly, 4-thiouridine (4SU) is incorporated into cellular transcriptome to increase RNA-protein crosslinking efficiency via UV radiation (at 365nm). Cells are then lysed and RBPs are immunoprecipitated prior to protein removal by proteinase K. The remaining mRNAs are then reverse transcribed to cDNA and are subjected to deep sequencing to identify RBP-, i.e. miRISC-bound mRNAs (Corden 2010; Hafner *et al.* 2010). Therefore, PAR-CLIP has the advantage of identifying miRNA-targeted mRNAs with high resolution. Nevertheless, Skalsky *et al.* report that PAR-CLIP failed to identify several EBV-B95-8 miRNA cellular targets (Skalsky *et al.* 2012), demonstrating that the technology is not infallible. Similarly, several studies have shown that biases inherent to RNA-Seq library preparation may result in underrepresentation of some transcripts (Hafner *et al.* 2011; Jayaprakash *et al.* 2011; Huang *et al.* 2013; Theiss *et al.* 2015). Therefore, given the importance of TLR9, C/EBPα and C/EBPβ in antiviral immune response and the possibility of remaining undetected by RNA-Seq these transcripts were included in MCV-miR-M1 functional analysis. Interestingly, initial qRT-PCR analysis of TLR9 expression revealed significant downregulation in MCV-

miR-M1-3p and -5p mimic-transfected cells (Figure 4.6 L). Next, MCVSyn system was used to determine whether TLR9 expression is also impaired in the presence of MCV genome replication. qRT-PCR confirmed significant downregulation of TLR9 in the presence of MCVSyn 72h p.t. (Figure 4.6 L). Having confirmed MCV-miR-M1-dependent downregulation of TLR9 mRNA, western blotting was carried out to investigate changes at protein expression level. Whereas TLR9 protein expression remained unaltered with MCV-miR-M1-5p mimic, a ~40% decrease was consistently detected in the presence of MCV-miR-M1-3p mimic (Figure 4.8 A). This is in agreement with qRT-PCR data where MCV-miR-M1-3p mimic demonstrated a greater impact on TLR9 mRNA expression (>110-fold) compared to MCV-miR-M1-5p mimic (20-fold) (Figure 4.6 L). Furthermore, TLR9 protein expression was also probed in the MCVSyn system. Intriguingly, whilst TLR9 protein levels were increased in MCVSyn-hpko-transfected relative to MCVSyn- and mock-transfected cells, MCVSyn-transfected and mock-transfected cells showed similar levels of TLR9 protein expression (Figure 4.8 B). Thus, consistent with TLR9 recognition of unmethylated CpG, it is possible that increased genome replication in MCVSyn-hpko-transfected cells induced TLR9 expression, whereas in MCVSyn-transfected cells a combination of MCV-miR-M1 effect and lower amounts of replicated genome prevented TLR9 expression above the basal level detected in mock-transfected cells.

Given that the proposed model for TLR9 downregulation is that MCV T Ag locus mediates this via downregulation of C/EBPα and C/EBPβ expression (Shahzad *et al.* 2013), I also investigated the impact of MCV-miR-M1 on these transcripts. Data for C/EBPα was conflicting, with mimics

downregulating transcript levels and MCVSyn leading to increased expression in MCVSyn-transfected cells (Figure 4.6 M). For C/EBPβ, mRNA expression increased in MCV-miR-M1 mimics- and MCVSyn-transfected cells (Figure 4.6 N). These data show a negative correlation with TLR9 expression (Figures 4.6 L & 4.8) and are in contrast with Shahzad *et al.*'s findings where the MCV T Ag locus mediates downregulation of TLR9 via downregulation of C/EBPβ and C/EBPα (Shahzad *et al.* 2013). Thus, further investigation is required to fully delineate the relationship between MCV-miR-M1 and TLR9.

CHAPTER 5

Functional Studies

5. Functional significance and direct targets of MCV-miR-M1

In the previous chapter RNA-Seq analysis identified numerous cellular targets that display reduced expression in response to MCV-miR-M1. Several of these targets are key mediators of the host cell immune response and their presence in the RNA-Seq dataset was validated via qRT-PCR. Moreover, I demonstrated that several of these targets were reduced at the protein level in a MCV-miR-M1-dependent manner. In this chapter I describe experiments performed to determine if the observed effect on these targets is a result of direct activity of MCV-miR-M1 against the transcripts via DLA and whether the downregulation of host cell immune gene expression has a functional impact in terms of immune response.

5.1. *In silico* investigation of MCV-miR-M1-5p and -3p target sites

Having confirmed MCV-miR-M1-dependent downregulation of numerous cellular targets at the mRNA level and downregulation of several key immune-related genes (SP100, TLR9 and CXCL8) at both mRNA and protein levels, it was important to establish if these observed MCV-miR-M1-dependent effects were due to direct targeting of the host-cell mRNA transcript or via a secondary mechanism. To address this, I performed *in silico* investigation using the RNAhybrid online tool (Rehmsmeier *et al.* 2004) to search for MCV-miR-M1 recognition sites in the 3'UTRs of downregulated transcripts. RNAhybrid scan revealed putative recognition sites in 3'UTRs of SP100, TLR9, CXCL8 and several other targets identified via RNA-Seq and validated by qRT-PCR (Figure 5.1).

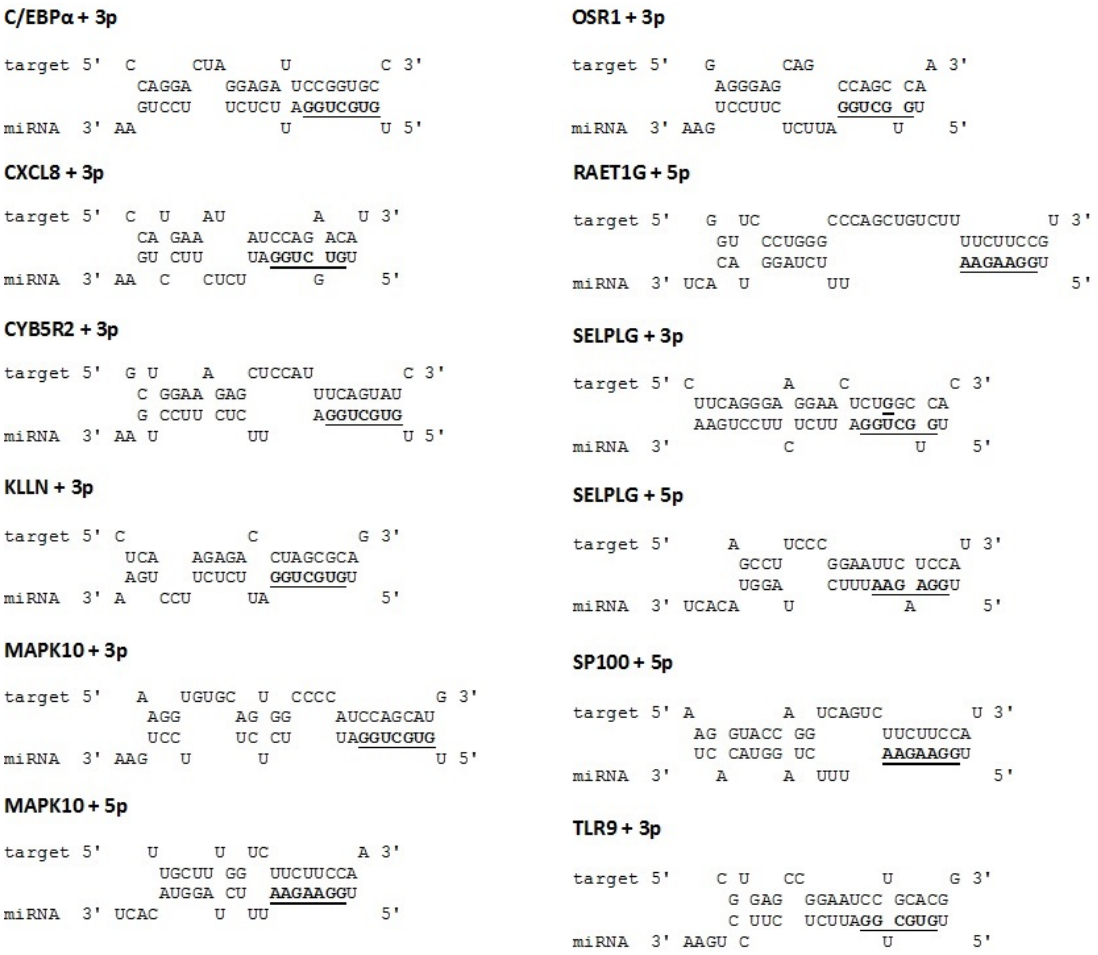

Figure 5.1. *In silico* investigation of MCV-miR-M1 target sites in 3'UTR of RNA-Seq-identified transcripts using RNAhybrid online tool (G:U matches allowed). MCV-miR-M1-5p and -3p seed sequences are underlined. For each transcript, only the hit with suitable seed sequence match (5p or 3p) and lowest minimum free energy is shown. qRT-PCR-validated targets with no seed sequence match, including ADRA1D, IFI30 and IFIH1 are not presented here.

5.2. Validating MCV-miR-M1-5p and -3p target sites by DLA

To determine if downregulation of qRT-PCR-validated transcripts was due to direct targeting of the *in silico*-identified sites by MCV-miR-M1, the 3'UTRs for each gene were PCR-amplified prior to cloning downstream of human *Renilla* luciferase (*hRluc*) in psiCHECK-2 plasmid (Figure 5.2).

Refer to Promega website at:
https://www.promega.co.uk/products/rna-purification-and-analysis/rna-interference/psicheck-1-and-psicheck-2-vectors/?catNum=C8011

Figure 5.2. Map of psiCHECK-2 plasmid vector. To determine whether RNAhybrid scan-identified cellular 3'UTRs were *bona fide* targets of MCV-miR-M1 (Figure 5.1), the 3'UTR sequences were PCR-amplified and inserted into XhoI/NotI, PmeI/NotI or XhoI/PmeI sites of psiCHECK-2 downstream of *hRluc* gene.

The resulting psiCHECK-2 constructs were co-transfected with MCV-miR-M1-5p mimic, -3p mimic or scramble mimic into 293 cells and cultured for 24h prior to DLA. Analysis of relative luciferase activity consistently revealed a statistically significant reduction in luminescence in cells transfected with MCV-miR-M1 compared to scramble mimic for SP100 and MAPK10 (Figure 5.3 A & C), whereas no significant reduction in luminescence was observed for CXCL8, KLLN, RAET1G and TLR9 across multiple independent experiments (Figure 5.3 E-H). To determine whether SP100 and MAPK10 results were reproducible in a more virus-relevant context, 293 cells were co-transfected with 3'UTR psiCHECK-2 constructs and MCVSyn or MCVSyn-hpko. Similar to results obtained in mimic transfected cells, normalised luciferase signal reduced in MCVSyn for SP100 and MAPK10 when compared to MCVSyn-hpko that does not express MCV-miR-M1 (Figure 5.3 B & D). Again, this effect was lost when MCVSyn was co-transfected with site-directed 3'UTR mutants lacking a seed-sequence match for MCV-miR-M1 (Figure 5.3 A-D). Collectively, these results demonstrate that SP100 and MAPK10 3'UTRs are directly targeted by MCV-miR-M1, leading to downregulation of the activity of SP100 and MAPK10 genes.

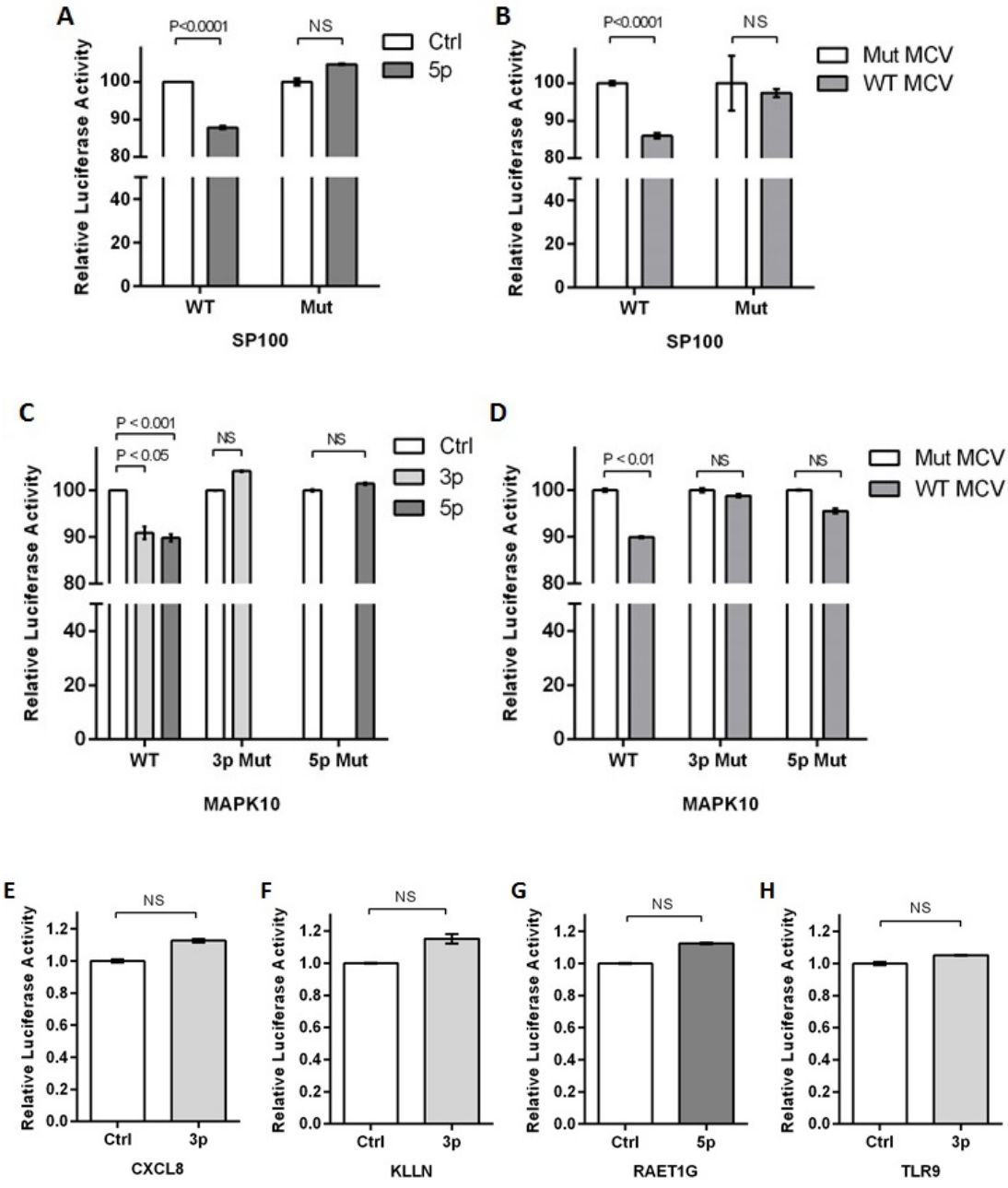
A
P<0.0001
NS
Ctrl
5p
Relative Luciferase Activity
100
90
80
40
20
0
WT
Mut
SP100
B
P<0.0001
NS
Mut MCV
WT MCV
Relative Luciferase Activity
100
90
80
40
20
0
WT
Mut
SP100
C
P < 0.001
P < 0.05
NS
NS
Ctrl
3p
5p
Relative Luciferase Activity
100
90
80
40
20
0
WT
3p Mut
5p Mut
MAPK10
D
P < 0.01
NS
NS
Mut MCV
WT MCV
Relative Luciferase Activity
100
90
80
40
20
0
WT
3p Mut
5p Mut
MAPK10
E
NS
Relative Luciferase Activity
1.2
1.0
0.8
0.6
0.4
0.2
0.0
Ctrl
3p
CXCL8
F
NS
Relative Luciferase Activity
1.2
1.0
0.8
0.6
0.4
0.2
0.0
Ctrl
3p
KLLN
G
NS
Relative Luciferase Activity
1.2
1.0
0.8
0.6
0.4
0.2
0.0
Ctrl
5p
RAET1G
H
NS
Relative Luciferase Activity
1.2
1.0
0.8
0.6
0.4
0.2
0.0
Ctrl
3p
TLR9

Figure 5.3. Dual luciferase assay (DLA) of cellular 3'UTR targets of MCV-miR-M1. Co-transfection of SP100 and MAPK10 3'UTR psiCHECK-2 constructs with miRNA mimics and MCVSyn led to downregulation of relative luciferase activity in the presence of MCV-miR-M1 in WT but not Mut constructs (A-D). Relative luciferase activity remained unchanged for CXCL8, KLLN, RAET1G and TLR9 3'UTRs in the presence of MCV-miR-M1 mimics (E-H). 5p and 3p Mut, mutated 3'UTR seed sequence matches of MCV-miR-M1-5p and -3p, respectively. NS, no statistical significance (p-value>0.05).

5.3. Investigating functional consequences of MCV-miR-M1-dependent CXCL8 downregulation on neutrophil migration

CXCL8 is a neutrophil chemoattractant and activator (Baggiolini *et al.* 1989; Modi *et al.* 1990; Harada *et al.* 1994) and therefore can modulate neutrophil migration. In order to establish if MCV-miR-M1-dependent downregulation of CXCL8 described in chapter 4 is significant in terms of attenuating neutrophil chemotaxis 293 cells were either transfected with MCVSyn or MCVSyn-hpko and cultured for 72h or stimulated with TNF-α prior to transfection with MCV-miR-M1 mimics or scramble mimic control and cultured for 24h prior to growth media being used as a chemoattractant in transwell migration assays with neutrophils isolated from blood. As can be seen in Figure 5.4, neutrophil migration was significantly impaired in both MCVSyn and MCV-miR-M1-5p and -3p mimic transfected cells compared to control, suggesting that MCV-miR-M1 negatively regulates neutrophil migration *in vitro*.

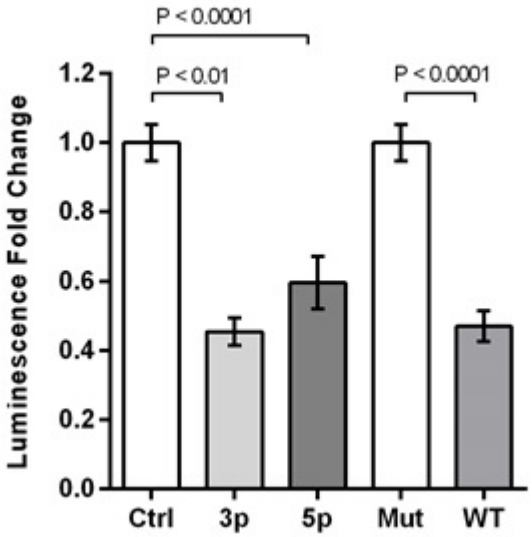

Figure 5.4. Transwell neutrophil migration assay. Neutrophils isolated from fresh blood were placed in upper chambers and growth media of MCVSyn- or miRNA mimic-transfected 293 cells were placed in lower chambers of a transwell plate. The plate was incubated for 2h at 37ºC with 5% CO2 prior to mixing the contents of lower chambers with CellTiter-Glo® 2.0 reagent (Promega). Luminescence of mixtures was recorded and chemotactic (migration) index was calculated by normalising the luminescence of MCVSyn (WT) to MCVSyn-hpko (Mut) and MCV-miR-M1 mimics to control mimic samples. Normalised luminescence showed 2-fold decrease in the presence of MCV-miR-M1 with statistical significance.

5.4. MCV-miR-M1-dependent downregulation of neutrophil migration is CXCL8-mediated

CXCL8 exerts its chemical effects via high affinity binding to C-X-C motif chemokine receptor 1 (CXCR1) and CXCR2 (Holmes *et al.* 1991; Murphy and Tiffany 1991). CXCR1 and CXCR2 are expressed on PMN leukocytes, monocytes, some T-cells (Chuntharapai *et al.* 1994), epithelial and endothelial cells and fibroblasts (Russo *et al.* 2014). It has been shown that antagonist driven inhibition of CXCR2 is sufficient to block CXCL8-induced neutrophil migration *in vitro* and *in vivo* (White *et al.* 1998). Having established that downregulation of neutrophil migration is MCV-miR-M1-dependent, it was crucial to determine if MCV-miR-M1 exerts this effect via CXCL8 downregulation. To this end, transwell migration assay was repeated in the presence and absence of the CXCR2 antagonist SB265610 (Bradley *et al.* 2009). As evidenced by Figure 5.5, blocking CXCR2 resulted in significant (p-value<0.05) downregulation of neutrophil migration towards growth media of both MCVSyn- and MCVSyn-hpko-transfected cells whereas no migration was observed towards DMEM (growth media used for 293 cell culture). This reduction was greater in MCVSyn-transfected cells where MCV-miR-M1 induces CXCL8 downregulation. These data suggest that MCV-miR-M1 mediates downregulation of neutrophil migration in a CXCL8-dependent manner.

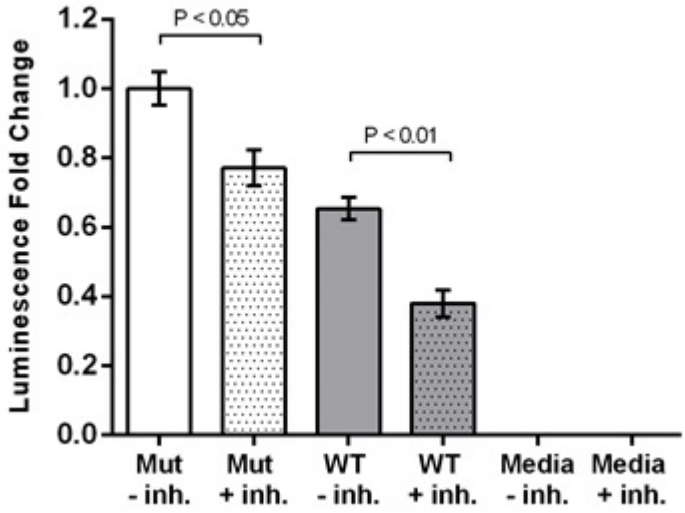

Figure 5.5. Transwell neutrophil migration assay in the presence or absence of CXCR2 antagonist. Neutrophil migration assay was repeated plus or minus CXCR2 antagonist SB265610 for MCVSyn- and MCVSyn-hpko-transfected 293 cells and cell growth media (DMEM) only. Addition of SB265610 to neutrophils resulted in ~20% and ~40% respective downregulation of neutrophil migration across transwell membrane towards growth media of MCVSyn-hpko- and MCVSyn-transfected 293 cells. No migration was detected towards DMEM. inh, SB265610; Media, DMEM; Mut, MCVSyn-hpko; WT, MCVSyn.

5.5. Discussion

miRNAs predominantly exert their effect by directing miRISC to the 3'UTR of target transcripts via seed sequence matching and supplementary binding (Lewis *et al.* 2003; Grimson *et al.* 2007). In this regard, various web-based tools have been devised to predict miRNA binding sites in the mRNAs of several species including, TargetScan (Agarwal *et al.* 2015), miRWalk

(Dweep and Gretz 2015) and RNAhybrid (Rehmsmeier *et al.* 2004). RNAhybrid has the advantage of predicting multiple putative target sites in any small to large RNA sequence by considering most favourable matches based on minimum free energy (mfe) and hence eliminating intramolecular hybridisations (Rehmsmeier *et al.* 2004). RNAhybrid has been widely used for predicting target binding of various miRNAs (Zhang *et al.* 2014; Khongnomnan *et al.* 2015; Yin *et al.* 2016) including the sequence match of BKV and JCV miRNA 3p strand in ULBP3 3'UTR (Bauman *et al.* 2011). Therefore, RNAhybrid was used to predict potential binding sites of MCV-miR-M1 in the 3'UTR of validated targets. Having identified putative sequence matches for MCV-miR-M1 (Figure 5.1), 3'UTRs of predicted targets were PCR-amplified from cDNA of 293 cells and cloned into psiCHECK-2 plasmid to generate response elements (RE) for MCV-miR-M1 (Figure 5.2).

MCV-miR-M1 mimics proved highly efficient in DLA against their cognate MCV LT RE (Figure 3.5 B). Therefore, MCV-miR-M1-5p and -3p mimics were initially used to assess binding of MCV-miR-M1 to the putative targets. DLA data revealed reduced luminescence signal in response to MCV-miR-M1-5p mimic in SP100 and in response to MCV-miR-M1-5p and -3p mimics in MAPK10 3'UTR RE-transfected cells (Figure 5.3 A & C). Other tested 3'UTR REs, including CXCL8 and TLR9, did not demonstrate any significant changes in luminescence signal in response to MCV-miR-M1 mimics across multiple independent repeats (Figure 5.3 E-H). To determine if downregulation of SP100 and MAPK10 signal was due to MCV-miR-M1 specific targeting of the respective REs, mutated REs were generated via

site-directed mutagenesis of seed match nucleotides. DLA of mutated REs for SP100 and MAPK10 showed a complete loss of reduction in luminescence signal in response to MCV-miR-M1 mimics (Figure 5.3 A & C). Having established binding of MCV-miR-M1 mimics to their RNAhybrid-predicted target sites in SP100 and MAPK10 REs, it was desirable to reproduce these data using endogenous MCV-miR-M1. To this end, DLA was repeated by co-transfecting wild type and mutated SP100 and MAPK10 REs with MCVSyn and MCVSyn-hpko and relative luminescence was measured 72h p.t. As shown in Figure 5.3 B & D, only in wild type SP100 and MAPK10 RE-transfected cells was luminescence signal downregulated in response to MCVSyn, confirming that MCV-miR-M1 directly targets SP100 and MAPK10 3'UTRs to downregulate mRNA and protein expression. Direct targeting of SP100 3'UTR has also been shown by EBV-BART1-3p in EBV-infected lymphoblastoid cell lines (Skalsky *et al.* 2012). SP100 data are of particular interest given that a negative correlation between MCV genome replication and SP100 expression has been shown by a recent study (Neumann *et al.* 2016). In this regard, whereas further analysis is required to determine the role of SP100 in regulating expression of cytokines and chemokines such as CXCL8, there is a possibility that MCV-miR-M1-5p downregulates neutrophil migration by directly targeting and downregulating SP100 expression.

Intriguingly, MAPK10 has also been implicated in regulating the expression of inflammatory cytokines. For instance, MAPK10 is an inducer of TNF-α (Kanehisa *et al.* 2016c) and has been shown to mediate CXCL8 expression (Biton and Ashkenazi 2011). In addition, MAPK10 downregulation or loss has

been reported in several cancers including, nasopharyngeal carcinoma (Li and Luo 2017), brain tumours (Yoshida *et al.* 2001), lymphomas, gastric and breast carcinomas and hepatocellular carcinoma, suggesting a tumour suppressor role for MAPK10 (Ying *et al.* 2006). Moreover, whilst thus far there is no data regarding MAPK10 expression in MCs, its expression has been demonstrated in human epidermis (Sextius *et al.* 2015) and mice basal epidermis (April and Barsh 2006) where MCs reside (Lucarz and Brand 2007). While I confirmed downregulation of MAPK10 in MCV-miR-M1-3p and -5p mimic-transfected cells via qRT-PCR (Figure 4.6 E), further studies are warranted for the impact of MCV-miR-M1 on MAPK10 protein expression and to determine whether MCV-miR-M1-3p mimic-dependent downregulation of CXCL8 is dictated via direct targeting of MAPK10.

CXCL8 is a mediator of endothelial arrest, oxidative burst and degranulation in PMN leukocytes (Lindley *et al.* 1988; Peveri *et al.* 1988; Lawrence and Springer 1991). In addition, CXCL8 is a potent activator and chemoattractant of PMN, especially neutrophils (Baggiolini *et al.* 1989; Carveth *et al.* 1989; Detmers *et al.* 1990). As discussed in Chapter 4, MCV-miR-M1 induces downregulation of CXCL8 mRNA and protein expression. Having established the effect of MCV-miR-M1 on CXCL8 expression, it was also important to determine whether these changes are sufficient to have a functional impact. Given the integral role of CXCL8 in inducing neutrophil activation and migration in the skin (Colditz *et al.* 1990; Leonard *et al.* 1991; Rot 1991), Boyden chamber assays were employed to investigate the impact of MCV-miR-M1-dependent CXCL8 downregulation on neutrophil migration. Initially, growth media of MCV-miR-M1 mimic-transfected cells revealed that

neutrophil migration is halved in the presence of MCV-miR-M1-5p and -3p mimics (Figure 5.4). Next, using 72h p.t. growth media of MCVSyn-transfected cells I confirmed that replicating MCVSyn also hinders neutrophil transwell migration by up to 50% compared with the MCVSyn-hpko mutant (Figure 5.4). These data indicate that MCV-miR-M1 expression in the context of MCV genome replication has a measurable impact on CXCL8 secretion and that this impact is functionally important in terms of modulating neutrophil migration. Importantly, experiments with MCV-miR-M1 mimics demonstrate that this effect occurs independently of MCV T Ags. Moreover, when CXCL8 stimulatory effect on neutrophils was blocked using the CXCR2 antagonist SB265610, neutrophil migration demonstrated a further downregulation compared to unblocked neutrophils. This effect was greater and more significant in MCVSyn-transfected cells where MCV-miR-M1 expression induced CXCL8 downregulation. Whilst CXCL8 does not exclusively bind to CXCR2 and CXCR2 is not specific to CXCL8 it has been shown that blockage of CXCR2 alone is sufficient to prevent CXCL8 chemotactic effect on neutrophils (White *et al.* 1998). Therefore, these observations strengthen the notion that MCV-miR-M1-dependent downregulation of neutrophil migration is mediated by CXCL8.

Intriguingly, neutrophil migration was also significantly hindered by MCV-miR-M1-5p mimic, which was somewhat surprising, as previous data demonstrated that CXCL8 mRNA and protein expression are only downregulated by MCV-miR-M1-3p mimic. This observation points at other contributing factors to neutrophil migration whose expression/function is modulated by MCV-miR-M1-5p. Interrogation of the RNA-Seq dataset

reveals two transcripts downregulated by MCV-miR-M1-5p mimic that have been associated with neutrophil activation and migration. Thrombopoietin (THPO) is an stimulator of megakaryocyte differentiation and platelet production (Kaushansky 2006). In mice, THPO triggers release of CXCR2 ligands CXCL1 and CXCL3 (Kanehisa *et al.* 2016a) by megakaryocytes which can then mobilise neutrophils from bone marrow (Kohler *et al.* 2011). Prostaglandin-endoperoxide synthase 2 (PTGS2) or cyclooxygenase-2 (COX-2) is an enzyme which plays an important role in inflammation by catalysing synthesis of prostaglandins (Hla and Neilson 1992). PTGS2 is induced by various factors such as TNF-α and NF-κB (Nakao *et al.* 2002), epidermal growth factor (EGF) and IL-1 (Hla and Neilson 1992). In PTGS2-defficient mice CXCL2 expression was downregulated, resulting in reduced neutrophil recruitment to site of liver injury (Hamada *et al.* 2008). Moreover, inhibition of PTGS2 *in vitro* significantly reduced IL-1β, CXCL6 and CXCL8 release from activated neutrophils (Kimura *et al.* 2003). THPO and PTGS2 were downregulated in MCV-miR-M1-5p mimic dataset, however, attempts to validate THPO and PTGS2 RNA-Seq data using qRT-PCR were unsuccessful due to low and inconsistent expression of the transcripts. It should be noted that analysis of CXCL8 secretion by ELISA did reveal a downregulation in CXCL8 protein in response to transfection with the MCV-miR-M1-5p mimic, however this was not significant. These data suggest that MCV-miR-M1-5p is able to indirectly modulate CXCL8 secretion presumably by targeting cellular transcripts that lead to changes in CXCL8 expression.

An alternative explanation for the observed reduction in neutrophil migration as a consequence of MCV-miR-M1-5p expression relates to 5p-depednent

downregulation of SP100. The SP100-mediated antiviral response has been associated with its role as a transcriptional repressor and its preferential binding affinity for unmethylated CpG DNA (Wilcox *et al.* 2005; Isaac *et al.* 2006). However, SP100 has also been shown to significantly increase IFN-β expression in a MAVS-dependent manner (Schmid *et al.* 2014). In addition, SP100 is induced by IRF7, a member of interferon regulatory factors (IRFs) which are involved in transcriptional regulation of IFNs and a number of other genes (Mamane *et al.* 1999; Barnes *et al.* 2004). An association between MAVS with IRFs and members of MAPK signalling pathway (Schmid *et al.* 2014) and MAVS-dependent induction of CXCL8 via activation of NF-κB (Kawai *et al.* 2005) has been described. Therefore, it seems that SP100 is closely associated with immune-related pathways which utilise IFNs, NF-κB and chemokines such as RIG-I-like receptor signalling and MAPK signalling pathways (Kanehisa *et al.* 2016b; Kanehisa *et al.* 2016d). In this regard, it is possible that SP100 downregulation leads to downregulation of neutrophil-stimulating cytokines and chemokines which manifestation is MCV-miR-M1-5p-dependent reduction of neutrophil migration.

CHAPTER 6

Discussion

6. Discussion

miRNAs act predominantly by repressing the expression of protein-coding transcripts (Guo *et al.* 2010) in a wide range of species, including mammals, plants, fungi and viruses (Sayed and Abdellatif 2011; Kincaid and Sullivan 2012) where they play a key role in development and disease (Sayed and Abdellatif 2011; Wilczynska and Bushell 2015). Virus-encoded miRNAs are involved in various aspects of the virus life cycle, including regulation of genome replication, pathogenesis and evasion of the host cell immune response via modulation of both virus and host cell transcripts. KSHV-miR-K12-9-5p prevents lytic replication by directly targeting and repressing KSHV RTA, a latent-to-lytic replication switch (Bellare and Ganem 2009). Such auto-regulatory effect has also been shown in BKV, JCV, SV40 and MCV where virus miRNA mediates LT Ag cleavage and hence negatively regulates genome replication (Sullivan *et al.* 2005; Seo *et al.* 2008; Lagatie *et al.* 2013). In accord with previous studies, my findings demonstrated that MCV-miR-M1 gives rise to two mature miRNAs (Figure 3.7 A & B) which directly target and downregulate MCV LT expression (Figure 3.4 C, 3.5 B and 4.7).

While a primary function of virus-encoded miRNAs is the auto-regulation of immunogenic virus-transcripts to limit host immune response, there is mounting evidence that virus-encoded miRNAs are also directly targeting key regulators of the host immune system. For example, EBV miR-BART2-5p and mir-BHRF1-3 directly target and downregulate MICB (NK ligand) and CXCL11 (T-cell chemoattractant), respectively (Xia *et al.* 2008; Nachmani *et al.* 2009). Moreover, these miRNAs also target innate immune-associated genes including PML-NB components SP100 and ZNF451 (Skalsky *et al.*

2012). BKV and JCV miRNA 3p strands repress host immune surveillance by directly targeting and downregulating ULBP3 (Bauman *et al.* 2011). In this project, RNA-Seq analysis of MCV-miR-M1 cellular targets uncovered a multitude of cellular transcripts modulated specifically by MCV-miR-M1-5p and -3p and GO analysis put most MCV-miR-M1-modulated targets in GO terms associated with immune response and regulation of various cellular processes.

Virus miRNA-mediated downregulation of chemokines as a strategy for host immune evasion has been described by several studies in other viruses. EBV-miR-BHRF1-3 suppresses the T-cell chemoattractant CXCL11 (Xia *et al.* 2008), whereas HCMV-miR-UL148D downregulates CCL5 by directly targeting its 3'UTR (Kim *et al.* 2012). In addition, KSHV miRNAs have been shown to target CXCL8 signalling pathway in SLKK cell line (Viollet *et al.* 2015) and KSHV-miR-K12-10a induces repression of CXCL8 and CCL2 by directly targeting TNF-like weak inducer of apoptosis receptor (TWEAKR) (Abend *et al.* 2010). Herein, I demonstrate that decreased levels of CXCL8 are secreted during MCV replication in an MCV-miR-M1-dependent manner. Moreover, this decrease in CXCL8 has a significant impact on neutrophil chemotaxis, suggesting a possible molecular mechanism for the observed association between MCV-miR-M1 and persistent infection (Figure 4.6 B & 4.10).

Data presented in this PhD thesis contribute to the emerging hypothesis that viral miRNAs are significant players in virus-host cell interaction and modulation of cellular processes. More specifically, the findings presented provide compelling and novel evidence supporting a role for MCV-miR-M1 in

the direct modulation of host immune response genes and suggest a mechanism for the observed dependency of MCV-miR-M1 in the establishment of persistent infection (Theiss *et al.* 2015; Neumann *et al.* 2016).

Much remains to be done in terms of investigating the role of MCV-miR-M1-modulated cellular transcripts and how these impact on MCV life cycle and pathogenesis. Initially, this can most easily be addressed via siRNA-mediated depletion and overexpression studies followed by assessment of virus replication using the MCVSyn system. These studies could be followed up with CRISPR/Cas9-mediated mutation of MCV-miR-M1 seed-recognition sequences in direct cellular targets, an approach that would also enable long-term infection studies to be carried out to assess the importance of MCV-miR-M1-modulated cellular targets in this process. A particularly interesting area to interrogate is the association between chemokine-stimulating factors such as SP100 and MAPK10 with CXCL8, for instance, by measuring CXCL8 expression following SP100 and MAPK10 knockdown and overexpression. Similar experiments could be used to investigate interplay between SP100 and components of other important immune-regulatory pathways such as TLR signalling, RIG-I-like receptor signalling and MAPK signalling pathways.

In addition, this project has produced a significant amount of data regarding the possible role of MCV-miR-M1 in virus replication and pathogenesis. Numerous cellular transcripts associated with cancer progression were dysregulated in response to MCV-miR-M1 expression including KLLN, CYB5R2 and OSR1. It will be of interest to determine if downregulation of these genes contributes to MCV tumourigenesis. Of note, several MCV-

positive MCC cell lines including MKL1, MKL2, WaGa, PeTa, BroLi and MS-1 were investigated for MCV-miR-M1 expression. While expression of MCV-miR-M1 was very low in these cells (data not shown), inhibition of MCV-miR-M1 using miRNA inhibitors resulted in inconsistent alterations in MCV LT expression (data not shown). The low expression levels of MCV-miR-M1 in these cell lines suggests that its functional importance in terms of cancer cell growth may be limited, however, a possible role for MCV-miR-M1 in transformation should not be disregarded. For instance, it will be of interest to determine if MCV-miR-M1 expression creates an environment in infected cells more conducive to LT truncation, MCV integration and inhibition of DNA damage response. This could be investigated by determining protein expression of these genes in the presence of MCV replication plus and minus MCV-miR-M1 inhibitors and by inducing DNA damage prior to measuring cell proliferation. In addition, expression of these tumour suppressor genes can be measured following transfection of MCV-miR-M1 inhibitors into MCV-positive MCCs prior to investigating alterations in cell phenotypes and proliferation. These experiments will be an important step in determining whether inhibition of MCV-miR-M1 can be used as a therapeutic approach in MCC treatment.

Finally, and of immediate importance are experiments to investigate the impact of MCV-miR-M1 inhibition on MCV replication and life cycle in dermal fibroblasts.

Appendix

Appendix 1. RNA-Seq-identified cellular transcripts with >2-fold downregulation (p-value<0.05) in MCV-miR-M1-5p and MCV-miR-M1-3p mimic-transfected 293 cells.

MCV-miR-M1-5p			
hgnc_symbol	hgnc_name	Fold decrease	p-value
LOC101926969	uncharacterized LOC101926969	23.32318149	0.007815
LOC729040	uncharacterized LOC729040	21.17838367	0.019171
CCDC85A	coiled-coil domain containing 85A	21.02701975	0.009823
SNAP25	synaptosomal-associated protein, 25kDa	18.43600523	0.017135
ARHGAP9	Rho GTPase activating protein 9	18.36259909	0.015628
MIR23B	microRNA 23b	18.36259909	0.015628
CFAP99	cilia and flagella associated protein 99	18.36249688	0.015628
KIF25	kinesin family member 25	18.36085228	0.015883
SP100	SP100 nuclear antigen	18.33236489	0.023567
LOC645434	uncharacterized LOC645434	18.20123777	0.038921
MIR1289-1	microRNA 1289-1	18.11842676	0.037724
TIGIT	T cell immunoreceptor with Ig and ITIM domains	16.15070759	0.038969
ADRA1D	adrenoceptor alpha 1D	15.9225359	0.032946
LOC100128006	uncharacterized LOC100128006	15.92241069	0.03294
LOC440700	carbonic anhydrase XIV (CA14) pseudogene	15.88210699	0.031255
CCNI2	cyclin I family, member 2	7.29635443	0.012677
SCARNA14	small Cajal body-specific RNA 14	6.648865129	0.022084
H2BFM	H2B histone family, member M	6.034934976	0.025776
PPIAP30	peptidylprolyl isomerase A (cyclophilin A) pseudogene 30	5.399180682	0.009798
DCX	doublecortin	5.370853191	0.039963
SNORD9	small nucleolar RNA, C/D box 9	5.24963838	0.000995
LOC100126784	uncharacterized LOC100126784	5.236600348	0.001712
IFI30	interferon, gamma-inducible protein 30	4.893713881	0.000237
SELPLG	selectin P ligand	4.561435997	0.049486
COX5BP6	cytochrome c oxidase subunit Vb pseudogene 6	4.470030356	0.004809
LOC101928809	uncharacterized LOC101928809	4.21176772	0.00829
LOC101927958	uncharacterized LOC101927958	4.180902341	0.03938
CYCSP52	cytochrome c, somatic pseudogene 52	4.169361804	0.042053
ZAN	zonadhesin (gene/pseudogene)	4.157606234	0.043871
LOC101927354	uncharacterized LOC101927354	4.146856746	0.045739
OTOA	otoancorin	3.985928911	0.024349
AOC1	amine oxidase, copper containing 1	3.845713397	0.048581
DENND2D	DENN/MADD domain containing 2D	3.546480352	0.000513
IGF2	insulin-like growth factor 2	3.506608739	0.031384
IQSEC3	IQ motif and Sec7 domain 3	3.456262465	0.039912
LOC102724329	uncharacterized LOC102724329	3.452484679	0.04126
THPO	thrombopoietin	3.452414669	0.038855
IL13RA2	interleukin 13 receptor, alpha 2	3.446991286	0.001034
LINC00102	long intergenic non-protein coding RNA 102	3.416540478	0.048763
MUC4	mucin 4, cell surface associated	3.324860584	0.046374
PARP9	poly (ADP-ribose) polymerase family, member 9	3.245221664	0.020743
ASIC4	acid sensing (proton gated) ion channel family member 4	3.242188227	0.043808
RGS9	regulator of G-protein signaling 9	3.125377015	0.011612
PMCH	pro-melanin-concentrating hormone	3.083517354	0.001901
LOC101927040	uncharacterized LOC101927040	3.062271519	0.034925
PTPRD-AS1	PTPRD antisense RNA 1	2.743992076	0.014845
DSEL	dermatan sulfate epimerase-like	2.739862866	0.028295
APOBEC3D	apolipoprotein B mRNA editing enzyme, catalytic polypeptide-like 3D	2.69685336	0.004953
TCTE1	t-complex-associated-testis-expressed 1	2.641885526	0.044148
ERBB4	erb-b2 receptor tyrosine kinase 4	2.631836973	0.045826
PTGS2	prostaglandin-endoperoxide synthase 2 (prostaglandin G/H synthase and cyclooxygenase)	2.617534968	0.022617
FAM131B	family with sequence similarity 131, member B	2.610855965	0.007753
TKTL1	transketolase-like 1	2.5251386	0.010798
TSKS	testis-specific serine kinase substrate	2.523453308	0.018217
GPR12	G protein-coupled receptor 12	2.508314979	0.038152
GNG3	guanine nucleotide binding protein (G protein), gamma 3	2.506780626	0.039491
TOLLIP-AS1	TOLLIP antisense RNA 1 (head to head)	2.411396587	0.045556
CLCNKB	chloride channel, voltage-sensitive Kb	2.38227796	0.012892
LOC100335030	FGFR1 oncogene partner 2 pseudogene	2.367547325	0.022862
KCNA1	potassium channel, voltage gated shaker related subfamily A, member 1	2.366154092	0.015645
LOC100996348	uncharacterized LOC100996348	2.33963014	0.037625
RAET1G	retinoic acid early transcript 1G	2.311296809	0.045665
BST2	bone marrow stromal cell antigen 2	2.255335835	0.015324
C6orf141	chromosome 6 open reading frame 141	2.15223303	0.03641
CRTAC1	cartilage acidic protein 1	2.102530982	0.037793
KLHL31	kelch-like family member 31	2.038972726	0.004805
ST7-OT4	ST7 overlapping transcript 4	2.037253381	0.001506
EGR1	early growth response 1	2.017910587	0.000125
HMGCLL1	3-hydroxymethyl-3-methylglutaryl-CoA lyase-like 1	2.012371342	0.023651

MCV-miR-M1-3p			
hgnc_symbol	hgnc_name	Fold decrease	p-value
CYB5R2	cytochrome b5 reductase 2	31.86143921	0.000556
SELPLG	selectin P ligand	31.71105286	0.003786
DMBT1	deleted in malignant brain tumors 1	27.24115832	0.007524
ARMC12	armadillo repeat containing 12	26.6735151	0.001954
LINC00403	long intergenic non-protein coding RNA 403	26.50008915	0.004961
ZNF20	zinc finger protein 20	24.08143507	0.004548
LMO3	LIM domain only 3 (rhombotin-like 2)	23.85258264	0.012588
LOC414300	uncharacterized LOC414300	22.88903319	0.018993
FAM198B	family with sequence similarity 198, member B	22.88709241	0.018993
LOC729040	uncharacterized LOC729040	21.84209876	0.018993
LOC100130502	uncharacterized LOC100130502	21.7091442	0.009713
LOC101928386	uncharacterized LOC101928386	21.538836	0.007815
ZNF542P	zinc finger protein 542, pseudogene	21.53872496	0.007815
LRAT	lecithin retinol acyltransferase (phosphatidylcholine--retinol O-acyltransferase)	21.0819763	0.022565
DPP6	dipeptidyl-peptidase 6	20.5483961	0.031044
OSR1	odd-skipped related transciption factor 1	19.0460116	0.017199
ENAM	enamelin	19.02696894	0.018658
MIR23B	microRNA 23b	18.97154203	0.015628
MIR320D1	microRNA 320d-1	18.97154138	0.015628
SCN1A	sodium channel, voltage gated, type I alpha subunit	18.96874175	0.015968
SLC26A3	solute carrier family 26 (anion exchanger), member 3	18.9461404	0.016328
LOC100507530	uncharacterized LOC100507530	16.47589039	0.048637
LOC102723716	uncharacterized LOC102723716	16.4699001	0.048541
CXCL8	chemokine (C-X-C motif) ligand 8	16.44218467	0.032909
CSTF3-AS1	CSTF3 antisense RNA 1 (head to head)	16.41003851	0.032218
MIR26A2	microRNA 26a-2	16.40414601	0.031255
CCDC27	coiled-coil domain containing 27	16.40406088	0.031255
ZNF311	zinc finger protein 311	16.40406088	0.031255
FLJ20712	uncharacterized FLJ20712	16.33340335	0.038877
DSCAS	DSC1/DSC2 antisense RNA	16.31101585	0.034749
RXFP2	relaxin/insulin-like family peptide receptor 2	16.31088565	0.034754
MIR5685	microRNA 5685	16.20201659	0.040122
SLC26A5	solute carrier family 26 (anion exchanger), member 5	9.165206746	0.002607
MIR933	microRNA 933	8.450804043	0.006343
CTSS	cathepsin S	7.749859678	0.006569
CYGB	cytoglobin	7.068989285	0.012354
H2BFM	H2B histone family, member M	6.423278063	0.025677
CDH8	cadherin 8, type 2	6.398904262	0.02313
MUC12	mucin 12, cell surface associated	5.910309589	0.003171
CPQ	carboxypeptidase Q	5.707089381	0.039368
RNU6-45P	RNA, U6 small nuclear 45, pseudogene	5.707084045	0.039363
LOC101927851	uncharacterized LOC101927851	5.704974568	0.039647
LINCR-0001	uncharacterized LINCR-0001	5.698306391	0.041469
IQSEC3	IQ motif and Sec7 domain 3	5.256871701	0.008324
CYBB	cytochrome b-245, beta polypeptide	5.247259977	0.013657
RBP5	retinol binding protein 5, cellular	4.887843638	0.01657
ERN2	endoplasmic reticulum to nucleus signaling 2	4.835137803	0.028395
RPSAP52	ribosomal protein SA pseudogene 52	4.484569713	0.02634
LINC01160	long intergenic non-protein coding RNA 1160	4.479431099	0.02665
CCNI2	cyclin I family, member 2	4.469754662	0.024197
MIR4766	microRNA 4766	4.464987282	0.02389
TMEM92	transmembrane protein 92	4.075622314	0.000143
LILRB5	leukocyte immunoglobulin-like receptor, subfamily B (with TM and ITIM domains), member 5	4.063009314	0.042756
REXO1L1P	REX1, RNA exonuclease 1 homolog (S. cerevisiae)-like 1, pseudogene	3.936316743	0.01141
APCDD1L	adenomatosis polyposis coli down-regulated 1-like	3.922722889	0.005784
COL15A1	collagen, type XV, alpha 1	3.705708019	0.008746
LINC00926	long intergenic non-protein coding RNA 926	3.691664983	0.022672
PAX1	paired box 1	3.548778641	0.002739
OR7E14P	olfactory receptor, family 7, subfamily E, member 14 pseudogene	3.548286131	0.002629
CGB7	chorionic gonadotropin, beta polypeptide 7	3.47791908	0.020251
LOC653786	otoancorin pseudogene	3.414433581	0.037531
C14orf105	chromosome 14 open reading frame 105	3.412437681	0.037596
PINLYP	phospholipase A2 inhibitor and LY6/PLAUR domain containing	3.382202175	0.010351
LOC101929787	uncharacterized LOC101929787	3.266647597	0.020703
LOC339666	uncharacterized LOC339666	3.197382258	0.003862
YBX2	Y box binding protein 2	3.16609967	0.018975
GPR182	G protein-coupled receptor 182	3.00035932	0.028224
TREH	trehalase (brush-border membrane glycoprotein)	2.974707187	0.010984
LOC101927972	uncharacterized LOC101927972	2.967128659	0.015942

hgnc_symbol	hgnc_name	Fold decrease	p-value
TRPV1	transient receptor potential cation channel, subfamily V, member 1	2.954869273	0.005262
LOC100133985	uncharacterized LOC100133985	2.83020859	0.028699
PNMT	phenylethanolamine N-methyltransferase	2.829296605	0.045771
C2	complement component 2	2.809585563	0.007884
LOC440934	cancer/testis antigen 75	2.692652084	0.021323
LINC00412	long intergenic non-protein coding RNA 412	2.657661475	0.045444
ANGPTL2	angiopoietin-like 2	2.656437287	0.045354
CDH4	cadherin 4, type 1, R-cadherin (retinal)	2.642838482	0.005286
PTPRD-AS1	PTPRD antisense RNA 1	2.590733708	0.018567
SLC9C1	solute carrier family 9, subfamily C (Na+-transporting carboxylic acid decarboxylase), member 1	2.56482099	0.002062
LOC100126784	uncharacterized LOC100126784	2.561759581	0.031376
MAGI1-AS1	MAGI1 antisense RNA 1	2.558998412	0.031541
ETV4	ets variant 4	2.541666435	0.002687
IFI30	interferon, gamma-inducible protein 30	2.477344461	0.007329
IFIH1	interferon induced with helicase C domain 1	2.477258707	0.012839
C1orf168	chromosome 1 open reading frame 168	2.475154854	0.007119
LOC100996455	uncharacterized LOC100996455	2.46427354	0.038391
PIANP	PILR alpha associated neural protein	2.45677274	0.006505
SOX10	SRY (sex determining region Y)-box 10	2.353775948	0.031266
CCDC176	coiled-coil domain containing 176	2.351070294	0.008777
PMCH	pro-melanin-concentrating hormone	2.314931455	0.01336
FBXO24	F-box protein 24	2.312735458	0.012818
KCNT1	potassium channel, sodium activated subfamily T, member 1	2.280249665	0.02204
MAGEC2	melanoma antigen family C2	2.26838522	0.043498
LOC101928553	uncharacterized LOC101928553	2.225790014	0.038184
CEACAM1	carcinoembryonic antigen-related cell adhesion molecule 1 (biliary glycoprotein)	2.218797953	0.013405
CPZ	carboxypeptidase Z	2.21703077	0.046289
GPR3	G protein-coupled receptor 3	2.212743491	0.046141
GAS8-AS1	GAS8 antisense RNA 1	2.203207714	0.008793
RPAP2	RNA polymerase II associated protein 2	2.202231139	0.031013
PLAC8L1	PLAC8-like 1	2.194711747	0.014284
KLLN	killin, p53-regulated DNA replication inhibitor	2.15711021	0.000993
TMPRSS5	transmembrane protease, serine 5	2.154639442	0.020967
MAPK10	mitogen-activated protein kinase 10	2.090909183	0.012
LOC101927768	uncharacterized LOC101927768	2.088550033	0.003877
TNFRSF10C	tumor necrosis factor receptor superfamily, member 10c, decoy without an intracellular domain	2.080275672	0.006939
BCO2	beta-carotene oxygenase 2	2.079840908	0.026661
CADM2	cell adhesion molecule 2	2.051700096	0.017937
LOC101929234	uncharacterized LOC101929234	2.040439642	0.000158
MMP25-AS1	MMP25 antisense RNA 1	2.027249103	0.000723
GXYLT1P3	glucoside xylosyltransferase 1 pseudogene 3	2.000756595	0.048459

References

Abend, J. R., Uldrick, T. and Ziegelbauer, J. M. (2010) Regulation of tumor necrosis factor-like weak inducer of apoptosis receptor protein (TWEAKR) expression by Kaposi's sarcoma-associated herpesvirus microRNA prevents TWEAK-induced apoptosis and inflammatory cytokine expression. *J Virol* 84 (23), 12139-51.

Afanasiev, O. K., Yelistratova, L., Miller, N., Nagase, K., Paulson, K., Iyer, J. G., Ibrani, D., Koelle, D. M. and Nghiem, P. (2013) Merkel polyomavirus-specific T cells fluctuate with merkel cell carcinoma burden and express therapeutically targetable PD-1 and Tim-3 exhaustion markers. *Clin Cancer Res* 19 (19), 5351-60.

Agarwal, V., Bell, G. W., Nam, J. W. and Bartel, D. P. (2015) Predicting effective microRNA target sites in mammalian mRNAs. *Elife* 4.

Agelli, M., Clegg, L. X., Becker, J. C. and Rollison, D. E. (2010) The etiology and epidemiology of merkel cell carcinoma. *Curr Probl Cancer* 34 (1), 14-37.

Akhoondi, S., Sun, D., von der Lehr, N., Apostolidou, S., Klotz, K., Maljukova, A., Cepeda, D., Fiegl, H., Dafou, D., Marth, C., Mueller-Holzner, E., Corcoran, M., Dagnell, M., Nejad, S. Z., Nayer, B. N., Zali, M. R., Hansson, J., Egyhazi, S., Petersson, F., Sangfelt, P., Nordgren, H., Grander, D., Reed, S. I., Widschwendter, M., Sangfelt, O. and Spruck, C. (2007) FBXW7/hCDC4 is a general tumor suppressor in human cancer. *Cancer Res* 67 (19), 9006-12.

Albores-Saavedra, J., Batich, K., Chable-Montero, F., Sagy, N., Schwartz, A. M. and Henson, D. E. (2010) Merkel cell carcinoma

demographics, morphology, and survival based on 3870 cases: a population based study. *J Cutan Pathol* 37 (1), 20-7.

Alfaro, C., Teijeira, A., Onate, C., Perez, G., Sanmamed, M. F., Andueza, M. P., Alignani, D., Labiano, S., Azpilikueta, A., Rodriguez-Paulete, A., Garasa, S., Fusco, J. P., Aznar, A., Inoges, S., De Pizzol, M., Allegretti, M., Medina-Echeverz, J., Berraondo, P., Perez-Gracia, J. L. and Melero, I. (2016) Tumor-Produced Interleukin-8 Attracts Human Myeloid-Derived Suppressor Cells and Elicits Extrusion of Neutrophil Extracellular Traps (NETs). *Clin Cancer Res* 22 (15), 3924-36.

Alvarez, F. J., Cervantes, C., Villalba, R., Blasco, I., Martinez-Murillo, R., Polak, J. M. and Rodrigo, J. (1988) Immunocytochemical analysis of calcitonin gene-related peptide and vasoactive intestinal polypeptide in Merkel cells and cutaneous free nerve endings of cats. *Cell Tissue Res* 254 (2), 429-37.

April, C. S. and Barsh, G. S. (2006) Skin layer-specific transcriptional profiles in normal and recessive yellow (Mc1re/Mc1re) mice. *Pigment Cell Res* 19 (3), 194-205.

Aravin, A. A., Lagos-Quintana, M., Yalcin, A., Zavolan, M., Marks, D., Snyder, B., Gaasterland, T., Meyer, J. and Tuschl, T. (2003) The small RNA profile during Drosophila melanogaster development. *Dev Cell* 5 (2), 337-50.

Arora, R., Shuda, M., Guastafierro, A., Feng, H., Toptan, T., Tolstov, Y., Normolle, D., Vollmer, L. L., Vogt, A., Domling, A., Brodsky, J. L., Chang, Y. and Moore, P. S. (2012) Survivin is a therapeutic target in Merkel cell carcinoma. *Sci Transl Med* 4 (133), 133ra56.

Arribas-Layton, M., Wu, D., Lykke-Andersen, J. and Song, H. (2013) Structural and functional control of the eukaryotic mRNA decapping machinery. *Biochim Biophys Acta* 1829 (6-7), 580-9.

Arvin, A., Campadelli-Fiume, G., Mocarski, E., Moore, P. S., Roizman, B., Whitley, R. and Yamanishi, K. (2007) *Human Herpesviruses: Biology, Therapy, and Immunoprophylaxis.* 1st edition*.* Cambridge: Cambridge University Press.

Auyeung, V. C., Ulitsky, I., McGeary, S. E. and Bartel, D. P. (2013) Beyond secondary structure: primary-sequence determinants license pri-miRNA hairpins for processing. *Cell* 152 (4), 844-58.

Backes, S., Shapiro, J. S., Sabin, L. R., Pham, A. M., Reyes, I., Moss, B., Cherry, S. and tenOever, B. R. (2012) Degradation of host microRNAs by poxvirus poly(A) polymerase reveals terminal RNA methylation as a protective antiviral mechanism. *Cell Host Microbe* 12 (2), 200-10.

Baggiolini, M., Walz, A. and Kunkel, S. L. (1989) Neutrophil-activating peptide-1/interleukin 8, a novel cytokine that activates neutrophils. *J Clin Invest* 84 (4), 1045-9.

Bain, B. J., Bates, I., Laffan, M. A. and Lewis, M. S. (2012) *$D_{acie\ and\ Lewis\ Practical\ Haematology}$.* 11 edition*.* Edinburgh: Elsevier Churchill Livingstone.

Bardot, E. S., Valdes, V. J., Zhang, J., Perdigoto, C. N., Nicolis, S., Hearn, S. A., Silva, J. M. and Ezhkova, E. (2013) Polycomb subunits Ezh1 and Ezh2 regulate the Merkel cell differentiation program in skin stem cells. *EMBO J* 32 (14), 1990-2000.

Bari, R., Datt Pant, B., Stitt, M. and Scheible, W. R. (2006) PHO2, microRNA399, and PHR1 define a phosphate-signaling pathway in plants. *Plant Physiol* 141 (3), 988-99.

Barisic, S., Strozyk, E., Peters, N., Walczak, H. and Kulms, D. (2008) Identification of PP2A as a crucial regulator of the NF-kappaB feedback loop: its inhibition by UVB turns NF-kappaB into a pro-apoptotic factor. *Cell Death Differ* 15 (11), 1681-90.

Barnes, B. J., Richards, J., Mancl, M., Hanash, S., Beretta, L. and Pitha, P. M. (2004) Global and distinct targets of IRF-5 and IRF-7 during innate response to viral infection. *J Biol Chem* 279 (43), 45194-207.

Bartel, D. P. (2004) MicroRNAs: genomics, biogenesis, mechanism, and function. *Cell* 116 (2), 281-97.

Bartel, D. P. (2009) MicroRNAs: target recognition and regulatory functions. *Cell* 136 (2), 215-33.

Basquin, J., Roudko, V. V., Rode, M., Basquin, C., Seraphin, B. and Conti, E. (2012) Architecture of the nuclease module of the yeast Ccr4-not complex: the Not1-Caf1-Ccr4 interaction. *Mol Cell* 48 (2), 207-18.

Bauer, S., Kirschning, C. J., Hacker, H., Redecke, V., Hausmann, S., Akira, S., Wagner, H. and Lipford, G. B. (2001) Human TLR9 confers responsiveness to bacterial DNA via species-specific CpG motif recognition. *Proc Natl Acad Sci U S A* 98 (16), 9237-42.

Bauman, Y. and Mandelboim, O. (2011) MicroRNA based immunoevasion mechanism of human polyomaviruses. *RNA Biol* 8 (4), 591-4.

Bauman, Y., Nachmani, D., Vitenshtein, A., Tsukerman, P., Drayman, N., Stern-Ginossar, N., Lankry, D., Gruda, R. and Mandelboim, O. (2011) An identical miRNA of the human JC and BK polyoma viruses targets the stress-induced ligand ULBP3 to escape immune elimination. *Cell Host Microbe* 9 (2), 93-102.

Bazzini, A. A., Lee, M. T. and Giraldez, A. J. (2012) Ribosome profiling shows that miR-430 reduces translation before causing mRNA decay in zebrafish. *Science* 336 (6078), 233-7.

Becker, J. C. (2010) Merkel cell carcinoma. *Ann Oncol* 21 Suppl 7, vii81-5.

Becker, J. C., Assaf, C., Vordermark, D., Reske, S. N., Hense, J., Dettenborn, T., Seitz, O. and Grabbe, S. (2013) Brief S2k guidelines--Merkel cell carcinoma. *J Dtsch Dermatol Ges* 11 Suppl 3, 29-36, 31-8.

Beiras, A., Garcia-Caballero, T., Espinosa, J. and Gallego, R. (1986) Staining of Merkel cells of pig snout epidermis using the uranaffin reaction. Morphometric analysis of neuroendocrine granules. *Differentiation* 32 (1), 89-92.

Bellare, P. and Ganem, D. (2009) Regulation of KSHV lytic switch protein expression by a virus-encoded microRNA: an evolutionary adaptation that fine-tunes lytic reactivation. *Cell Host Microbe* 6 (6), 570-5.

Ben-Arie, N., Hassan, B. A., Bermingham, N. A., Malicki, D. M., Armstrong, D., Matzuk, M., Bellen, H. J. and Zoghbi, H. Y. (2000) Functional conservation of atonal and Math1 in the CNS and PNS. *Development* 127 (5), 1039-48.

Betancur, J. G. and Tomari, Y. (2012) Dicer is dispensable for asymmetric RISC loading in mammals. *Rna* 18 (1), 24-30.

Bethune, J., Artus-Revel, C. G. and Filipowicz, W. (2012) Kinetic analysis reveals successive steps leading to miRNA-mediated silencing in mammalian cells. *EMBO Rep* 13 (8), 716-23.

Beutler, B. (2004) Inferences, questions and possibilities in Toll-like receptor signalling. *Nature* 430 (6996), 257-63.

Bihl, F., Mosam, A., Henry, L. N., Chisholm, J. V., 3rd, Dollard, S., Gumbi, P., Cassol, E., Page, T., Mueller, N., Kiepiela, P., Martin, J. N., Coovadia, H. M., Scadden, D. T. and Brander, C. (2007) Kaposi's sarcoma-associated herpesvirus-specific immune reconstitution and antiviral effect of combined HAART/chemotherapy in HIV clade C-infected individuals with Kaposi's sarcoma. *Aids* 21 (10), 1245-52.

Biton, S. and Ashkenazi, A. (2011) NEMO and RIP1 control cell fate in response to extensive DNA damage via TNF-alpha feedforward signaling. *Cell* 145 (1), 92-103.

Blaszczyk, J., Tropea, J. E., Bubunenko, M., Routzahn, K. M., Waugh, D. S., Court, D. L. and Ji, X. (2001) Crystallographic and modeling studies of RNase III suggest a mechanism for double-stranded RNA cleavage. *Structure* 9 (12), 1225-36.

Boeck, R., Tarun, S., Jr., Rieger, M., Deardorff, J. A., Muller-Auer, S. and Sachs, A. B. (1996) The yeast Pan2 protein is required for poly(A)-binding protein-stimulated poly(A)-nuclease activity. *J Biol Chem* 271 (1), 432-8.

Bohnsack, M. T., Czaplinski, K. and Gorlich, D. (2004) Exportin 5 is a RanGTP-dependent dsRNA-binding protein that mediates nuclear export of pre-miRNAs. *Rna* 10 (2), 185-91.

Boot, P. M., Rowden, G. and Walsh, N. (1992) The distribution of Merkel cells in human fetal and adult skin. *Am J Dermatopathol* 14 (5), 391-6.

Borchert, S., Czech-Sioli, M., Neumann, F., Schmidt, C., Wimmer, P., Dobner, T., Grundhoff, A. and Fischer, N. (2014) High-Affinity Rb Binding, p53 Inhibition, Subcellular Localization, and Transformation by Wild-Type or Tumor-Derived Shortened Merkel Cell Polyomavirus Large T Antigens. *J Virol* 88 (6), 3144-60.

Borowiec, J. A. and Hurwitz, J. (1988) ATP stimulates the binding of simian virus 40 (SV40) large tumor antigen to the SV40 origin of replication. *Proc Natl Acad Sci U S A* 85 (1), 64-8.

Bose, N., Wurst, L. R., Chan, A. S., Dudney, C. M., LeRoux, M. L., Danielson, M. E., Will, P. M., Nodland, S. E., Patchen, M. L., Dalle Lucca, J. J., Lebeda, F. J. and Vasilakos, J. P. (2014) Differential regulation of oxidative burst by distinct beta-glucan-binding receptors and signaling pathways in human peripheral blood mononuclear cells. *Glycobiology* 24 (4), 379-91.

Boss, I. W., Nadeau, P. E., Abbott, J. R., Yang, Y., Mergia, A. and Renne, R. (2011) A Kaposi's sarcoma-associated herpesvirus-encoded ortholog of microRNA miR-155 induces human splenic B-cell expansion in NOD/LtSz-scid IL2Rgammanull mice. *J Virol* 85 (19), 9877-86.

Boss, I. W., Plaisance, K. B. and Renne, R. (2009) Role of virus-encoded microRNAs in herpesvirus biology. *Trends Microbiol* 17 (12), 544-53.

Bradley, M. E., Bond, M. E., Manini, J., Brown, Z. and Charlton, S. J. (2009) SB265610 is an allosteric, inverse agonist at the human CXCR2 receptor. *Br J Pharmacol* 158 (1), 328-38.

Brahmer, J. R., Tykodi, S. S., Chow, L. Q., Hwu, W. J., Topalian, S. L., Hwu, P., Drake, C. G., Camacho, L. H., Kauh, J., Odunsi, K., Pitot, H. C., Hamid, O., Bhatia, S., Martins, R., Eaton, K., Chen, S., Salay, T. M., Alaparthy, S., Grosso, J. F., Korman, A. J., Parker, S. M., Agrawal, S., Goldberg, S. M., Pardoll, D. M., Gupta, A. and Wigginton, J. M. (2012) Safety and activity of anti-PD-L1 antibody in patients with advanced cancer. *N Engl J Med* 366 (26), 2455-65.

Braun, J. E., Huntzinger, E., Fauser, M. and Izaurralde, E. (2011) GW182 proteins directly recruit cytoplasmic deadenylase complexes to miRNA targets. *Mol Cell* 44 (1), 120-33.

Braun, J. E., Huntzinger, E. and Izaurralde, E. (2013) The role of GW182 proteins in miRNA-mediated gene silencing. *Adv Exp Med Biol* 768, 147-63.

Brechmann, M., Mock, T., Nickles, D., Kiessling, M., Weit, N., Breuer, R., Muller, W., Wabnitz, G., Frey, F., Nicolay, J. P., Booken, N., Samstag, Y., Klemke, C. D., Herling, M., Boutros, M., Krammer, P. H. and Arnold, R. (2012) A PP4 holoenzyme balances physiological and oncogenic nuclear factor-kappa B signaling in T lymphocytes. *Immunity* 37 (4), 697-708.

Brehm, A., Miska, E. A., McCance, D. J., Reid, J. L., Bannister, A. J. and Kouzarides, T. (1998) Retinoblastoma protein recruits histone deacetylase to repress transcription. *Nature* 391 (6667), 597-601.

Broekema, N. M. and Imperiale, M. J. (2013) miRNA regulation of BK polyomavirus replication during early infection. *Proc Natl Acad Sci U S A* 110 (20), 8200-5.

Brown, C. E., Tarun, S. Z., Jr., Boeck, R. and Sachs, A. B. (1996) PAN3 encodes a subunit of the Pab1p-dependent poly(A) nuclease in Saccharomyces cerevisiae. *Mol Cell Biol* 16 (10), 5744-53.

Buell, J. F., Trofe, J., Hanaway, M. J., Beebe, T. M., Gross, T. G., Alloway, R. R., First, M. R. and Woodle, E. S. (2002) Immunosuppression and Merkel cell cancer. *Transplant Proc* 34 (5), 1780-1.

Burack, J. and Altschuler, E. L. (2003) Sustained remission of metastatic Merkel cell carcinoma with treatment of HIV infection. *J R Soc Med* 96 (5), 238-9.

Cai, X., Hagedorn, C. H. and Cullen, B. R. (2004) Human microRNAs are processed from capped, polyadenylated transcripts that can also function as mRNAs. *Rna* 10 (12), 1957-66.

Cai, X., Li, G., Laimins, L. A. and Cullen, B. R. (2006) Human papillomavirus genotype 31 does not express detectable microRNA levels during latent or productive virus replication. *J Virol* 80 (21), 10890-3.

Calin, G. A., Dumitru, C. D., Shimizu, M., Bichi, R., Zupo, S., Noch, E., Aldler, H., Rattan, S., Keating, M., Rai, K., Rassenti, L., Kipps, T., Negrini, M., Bullrich, F. and Croce, C. M. (2002) Frequent deletions and down-

regulation of micro- RNA genes miR15 and miR16 at 13q14 in chronic lymphocytic leukemia. *Proc Natl Acad Sci U S A* 99 (24), 15524-9.

Calin, G. A., Ferracin, M., Cimmino, A., Di Leva, G., Shimizu, M., Wojcik, S. E., Iorio, M. V., Visone, R., Sever, N. I., Fabbri, M., Iuliano, R., Palumbo, T., Pichiorri, F., Roldo, C., Garzon, R., Sevignani, C., Rassenti, L., Alder, H., Volinia, S., Liu, C. G., Kipps, T. J., Negrini, M. and Croce, C. M. (2005) A MicroRNA signature associated with prognosis and progression in chronic lymphocytic leukemia. *N Engl J Med* 353 (17), 1793-801.

Campeau, E., Ruhl, V. E., Rodier, F., Smith, C. L., Rahmberg, B. L., Fuss, J. O., Campisi, J., Yaswen, P., Cooper, P. K. and Kaufman, P. D. (2009) A versatile viral system for expression and depletion of proteins in mammalian cells. *PLoS One* 4 (8), e6529.

Cann, A. J. (2012) *Principles of Molecular Virology.* 5th edition edition. Oxford: Academic Press.

Caplan, S., Hartnell, L. M., Aguilar, R. C., Naslavsky, N. and Bonifacino, J. S. (2001) Human Vam6p promotes lysosome clustering and fusion in vivo. *J Cell Biol.* Vol. 154. 109-22.

Carter, J. J., Daugherty, M. D., Qi, X., Bheda-Malge, A., Wipf, G. C., Robinson, K., Roman, A., Malik, H. S. and Galloway, D. A. (2013) Identification of an overprinting gene in Merkel cell polyomavirus provides evolutionary insight into the birth of viral genes. *Proc Natl Acad Sci U S A* 110 (31), 12744-9.

Carveth, H. J., Bohnsack, J. F., McIntyre, T. M., Baggiolini, M., Prescott, S. M. and Zimmerman, G. A. (1989) Neutrophil activating factor (NAF) induces polymorphonuclear leukocyte adherence to endothelial cells

and to subendothelial matrix proteins. *Biochem Biophys Res Commun* 162 (1), 387-93.

Caudy, A. A., Ketting, R. F., Hammond, S. M., Denli, A. M., Bathoorn, A. M., Tops, B. B., Silva, J. M., Myers, M. M., Hannon, G. J. and Plasterk, R. H. (2003) A micrococcal nuclease homologue in RNAi effector complexes. *Nature* 425 (6956), 411-4.

Cavaloc, Y., Popielarz, M., Fuchs, J. P., Gattoni, R. and Stevenin, J. (1994) Characterization and cloning of the human splicing factor 9G8: a novel 35 kDa factor of the serine/arginine protein family. *Embo j* 13 (11), 2639-49.

Chang, K., Elledge, S. J. and Hannon, G. J. (2006) Lessons from Nature: microRNA-based shRNA libraries. *Nat Methods* 3 (9), 707-14.

Chelbi-Alix, M. K. and de The, H. (1999) Herpes virus induced proteasome-dependent degradation of the nuclear bodies-associated PML and Sp100 proteins. *Oncogene* 18 (4), 935-41.

Cheloufi, S., Dos Santos, C. O., Chong, M. M. and Hannon, G. J. (2010) A dicer-independent miRNA biogenesis pathway that requires Ago catalysis. *Nature* 465 (7298), 584-9.

Chen, C. J., Cox, J. E., Kincaid, R. P., Martinez, A. and Sullivan, C. S. (2013) Divergent MicroRNA targetomes of closely related circulating strains of a polyomavirus. *J Virol* 87 (20), 11135-47.

Chen, C. Y., Zheng, D., Xia, Z. and Shyu, A. B. (2009) Ago-TNRC6 triggers microRNA-mediated decay by promoting two deadenylation steps. *Nat Struct Mol Biol* 16 (11), 1160-6.

Chen, C. Z., Li, L., Lodish, H. F. and Bartel, D. P. (2004) MicroRNAs modulate hematopoietic lineage differentiation. *Science* 303 (5654), 83-6.

Chen, L., Hodges, R. R., Funaki, C., Zoukhri, D., Gaivin, R. J., Perez, D. M. and Dartt, D. A. (2006) Effects of alpha1D-adrenergic receptors on shedding of biologically active EGF in freshly isolated lacrimal gland epithelial cells. *Am J Physiol Cell Physiol* 291 (5), C946-56.

Chen, Y., Boland, A., Kuzuoglu-Ozturk, D., Bawankar, P., Loh, B., Chang, C. T., Weichenrieder, O. and Izaurralde, E. (2014) A DDX6-CNOT1 complex and W-binding pockets in CNOT9 reveal direct links between miRNA target recognition and silencing. *Mol Cell* 54 (5), 737-50.

Chendrimada, T. P., Gregory, R. I., Kumaraswamy, E., Norman, J., Cooch, N., Nishikura, K. and Shiekhattar, R. (2005) TRBP recruits the Dicer complex to Ago2 for microRNA processing and gene silencing. *Nature* 436 (7051), 740-4.

Chiang, H. R., Schoenfeld, L. W., Ruby, J. G., Auyeung, V. C., Spies, N., Baek, D., Johnston, W. K., Russ, C., Luo, S., Babiarz, J. E., Blelloch, R., Schroth, G. P., Nusbaum, C. and Bartel, D. P. (2010) Mammalian microRNAs: experimental evaluation of novel and previously annotated genes. *Genes Dev* 24 (10), 992-1009.

Cho, Y. J. and Liang, P. (2008) Killin is a p53-regulated nuclear inhibitor of DNA synthesis. *Proc Natl Acad Sci U S A* 105 (14), 5396-401.

Choy, E. Y., Siu, K. L., Kok, K. H., Lung, R. W., Tsang, C. M., To, K. F., Kwong, D. L., Tsao, S. W. and Jin, D. Y. (2008) An Epstein-Barr virus-encoded microRNA targets PUMA to promote host cell survival. *J Exp Med* 205 (11), 2551-60.

Chu, I. M., Hengst, L. and Slingerland, J. M. (2008) The Cdk inhibitor p27 in human cancer: prognostic potential and relevance to anticancer therapy. *Nat Rev Cancer* 8 (4), 253-67.

Chuntharapai, A., Lee, J., Hebert, C. A. and Kim, K. J. (1994) Monoclonal antibodies detect different distribution patterns of IL-8 receptor A and IL-8 receptor B on human peripheral blood leukocytes. *J Immunol* 153 (12), 5682-8.

Ciccia, A. and Elledge, S. J. (2010) The DNA damage response: making it safe to play with knives. *Mol Cell* 40 (2), 179-204.

Cifuentes, D., Xue, H., Taylor, D. W., Patnode, H., Mishima, Y., Cheloufi, S., Ma, E., Mane, S., Hannon, G. J., Lawson, N. D., Wolfe, S. A. and Giraldez, A. J. (2010) A novel miRNA processing pathway independent of Dicer requires Argonaute2 catalytic activity. *Science* 328 (5986), 1694-8.

Colditz, I. G., Zwahlen, R. D. and Baggiolini, M. (1990) Neutrophil accumulation and plasma leakage induced in vivo by neutrophil-activating peptide-1. *J Leukoc Biol* 48 (2), 129-37.

Collier, L., Kellam, P. and Oxford, J. (2010) *Human Virology.* 4th edition edition. Oxford: Oxford University Press.

Comerford, S. A., Schultz, N., Hinnant, E. A., Klapproth, S. and Hammer, R. E. (2012) Comparative analysis of SV40 17kT and LT function in vivo demonstrates that LT's C-terminus re-programs hepatic gene expression and is necessary for tumorigenesis in the liver. *Oncogenesis* 1, e28.

Corden, J. L. (2010) Shining a new light on RNA-protein interactions. *Chem Biol* 17 (4), 316-8.

Cosman, D., Mullberg, J., Sutherland, C. L., Chin, W., Armitage, R., Fanslow, W., Kubin, M. and Chalupny, N. J. (2001) ULBPs, novel MHC class I-related molecules, bind to CMV glycoprotein UL16 and stimulate NK cytotoxicity through the NKG2D receptor. *Immunity* 14 (2), 123-33.

Costinean, S., Sandhu, S. K., Pedersen, I. M., Tili, E., Trotta, R., Perrotti, D., Ciarlariello, D., Neviani, P., Harb, J., Kauffman, L. R., Shidham, A. and Croce, C. M. (2009) Src homology 2 domain-containing inositol-5-phosphatase and CCAAT enhancer-binding protein beta are targeted by miR-155 in B cells of Emicro-MiR-155 transgenic mice. *Blood* 114 (7), 1374-82.

Crane, A. M. and Bhattacharya, S. K. (2013) The use of bromodeoxyuridine incorporation assays to assess corneal stem cell proliferation. *Methods Mol Biol* 1014, 65-70.

Czech, B., Zhou, R., Erlich, Y., Brennecke, J., Binari, R., Villalta, C., Gordon, A., Perrimon, N. and Hannon, G. J. (2009) Hierarchical rules for Argonaute loading in Drosophila. *Mol Cell* 36 (3), 445-56.

Czimmerer, Z., Hulvely, J., Simandi, Z., Varallyay, E., Havelda, Z., Szabo, E., Varga, A., Balazs, D., Balogh, M., Horvath, A., Domokos, B., Torok, Z., Nagy, L. and Balint, B. (2013) A Versatile Method to Design Stem-Loop Primer-Based Quantitative PCR Assays for Detecting Small Regulatory RNA Molecules. *Plos One* 8 (1).

Dahl, J., You, J. and Benjamin, T. L. (2005) Induction and utilization of an ATM signaling pathway by polyomavirus. *J Virol* 79 (20), 13007-17.

Dang, D. T., Chen, X., Feng, J., Torbenson, M., Dang, L. H. and Yang, V. W. (2003) Overexpression of Kruppel-like factor 4 in the human colon

cancer cell line RKO leads to reduced tumorigenecity. *Oncogene* 22 (22), 3424-30.

Daniels, R., Sadowicz, D. and Hebert, D. N. (2007) A very late viral protein triggers the lytic release of SV40. *PLoS Pathog* 3 (7), e98.

DeCaprio, J. A. and Garcea, R. L. (2013) A cornucopia of human polyomaviruses. *Nat Rev Microbiol* 11 (4), 264-76.

Demetriou, S. K., Ona-Vu, K., Sullivan, E. M., Dong, T. K., Hsu, S. W. and Oh, D. H. (2012) Defective DNA repair and cell cycle arrest in cells expressing Merkel cell polyomavirus T antigen. *Int J Cancer* 131 (8), 1818-27.

Dent, A. L., Yewdell, J., Puvion-Dutilleul, F., Koken, M. H., de The, H. and Staudt, L. M. (1996) LYSP100-associated nuclear domains (LANDs): description of a new class of subnuclear structures and their relationship to PML nuclear bodies. *Blood* 88 (4), 1423-6.

Detmers, P. A., Lo, S. K., Olsen-Egbert, E., Walz, A., Baggiolini, M. and Cohn, Z. A. (1990) Neutrophil-activating protein 1/interleukin 8 stimulates the binding activity of the leukocyte adhesion receptor CD11b/CD18 on human neutrophils. *J Exp Med* 171 (4), 1155-62.

Devaney, J. M., Wang, S., Funda, S., Long, J., Taghipour, D. J., Tbaishat, R., Furbert-Harris, P., Ittmann, M. and Kwabi-Addo, B. (2013) Identification of novel DNA-methylated genes that correlate with human prostate cancer and high-grade prostatic intraepithelial neoplasia. *Prostate Cancer Prostatic Dis* 16 (4), 292-300.

DiVietro, J. A., Smith, M. J., Smith, B. R., Petruzzelli, L., Larson, R. S. and Lawrence, M. B. (2001) Immobilized IL-8 triggers progressive activation

of neutrophils rolling in vitro on P-selectin and intercellular adhesion molecule-1. *J Immunol* 167 (7), 4017-25.

Djuranovic, S., Nahvi, A. and Green, R. (2012) miRNA-mediated gene silencing by translational repression followed by mRNA deadenylation and decay. *Science* 336 (6078), 237-40.

Du, P., Wu, J., Zhang, J., Zhao, S., Zheng, H., Gao, G., Wei, L. and Li, Y. (2011) Viral infection induces expression of novel phased microRNAs from conserved cellular microRNA precursors. *PLoS Pathog* 7 (8), e1002176.

Dweep, H. and Gretz, N. (2015) miRWalk2.0: a comprehensive atlas of microRNA-target interactions. *Nat Methods* 12 (8), 697.

Eash, S. and Atwood, W. J. (2005) Involvement of cytoskeletal components in BK virus infectious entry. *J Virol* 79 (18), 11734-41.

Eash, S., Querbes, W. and Atwood, W. J. (2004) Infection of vero cells by BK virus is dependent on caveolae. *J Virol* 78 (21), 11583-90.

Ebert, M. S., Neilson, J. R. and Sharp, P. A. (2007) MicroRNA sponges: competitive inhibitors of small RNAs in mammalian cells. *Nat Methods* 4 (9), 721-6.

Elkayam, E., Kuhn, C. D., Tocilj, A., Haase, A. D., Greene, E. M., Hannon, G. J. and Joshua-Tor, L. (2012) The structure of human argonaute-2 in complex with miR-20a. *Cell* 150 (1), 100-10.

Elphick, G. F., Querbes, W., Jordan, J. A., Gee, G. V., Eash, S., Manley, K., Dugan, A., Stanifer, M., Bhatnagar, A., Kroeze, W. K., Roth, B. L. and Atwood, W. J. (2004) The human polyomavirus, JCV, uses serotonin receptors to infect cells. *Science* 306 (5700), 1380-3.

Engels, E. A., Frisch, M., Goedert, J. J., Biggar, R. J. and Miller, R. W. (2002) Merkel cell carcinoma and HIV infection. *Lancet* 359 (9305), 497-8.

Etienne-Manneville, S. (2013) Microtubules in cell migration. *Annu Rev Cell Dev Biol* 29, 471-99.

Eulalio, A., Huntzinger, E. and Izaurralde, E. (2008) GW182 interaction with Argonaute is essential for miRNA-mediated translational repression and mRNA decay. *Nat Struct Mol Biol* 15 (4), 346-53.

Ewers, H., Romer, W., Smith, A. E., Bacia, K., Dmitrieff, S., Chai, W., Mancini, R., Kartenbeck, J., Chambon, V., Berland, L., Oppenheim, A., Schwarzmann, G., Feizi, T., Schwille, P., Sens, P., Helenius, A. and Johannes, L. (2010) GM1 structure determines SV40-induced membrane invagination and infection. *Nat Cell Biol* 12 (1), 11-8; sup pp 1-12.

Eystathioy, T., Chan, E. K., Tenenbaum, S. A., Keene, J. D., Griffith, K. and Fritzler, M. J. (2002) A phosphorylated cytoplasmic autoantigen, GW182, associates with a unique population of human mRNAs within novel cytoplasmic speckles. *Mol Biol Cell* 13 (4), 1338-51.

Eystathioy, T., Jakymiw, A., Chan, E. K., Seraphin, B., Cougot, N. and Fritzler, M. J. (2003) The GW182 protein colocalizes with mRNA degradation associated proteins hDcp1 and hLSm4 in cytoplasmic GW bodies. *RNA.* Vol. 9. 1171-3.

Fabian, M. R., Mathonnet, G., Sundermeier, T., Mathys, H., Zipprich, J. T., Svitkin, Y. V., Rivas, F., Jinek, M., Wohlschlegel, J., Doudna, J. A., Chen, C. Y., Shyu, A. B., Yates, J. R., 3rd, Hannon, G. J., Filipowicz, W., Duchaine, T. F. and Sonenberg, N. (2009) Mammalian miRNA RISC recruits

CAF1 and PABP to affect PABP-dependent deadenylation. *Mol Cell* 35 (6), 868-80.

Faraoni, I., Antonetti, F. R., Cardone, J. and Bonmassar, E. (2009) miR-155 gene: a typical multifunctional microRNA. *Biochim Biophys Acta* 1792 (6), 497-505.

Fathallah, I., Parroche, P., Gruffat, H., Zannetti, C., Johansson, H., Yue, J., Manet, E., Tommasino, M., Sylla, B. S. and Hasan, U. A. (2010) EBV latent membrane protein 1 is a negative regulator of TLR9. *J Immunol* 185 (11), 6439-47.

Fehon, R. G., McClatchey, A. I. and Bretscher, A. (2010) Organizing the cell cortex: the role of ERM proteins. *Nat Rev Mol Cell Biol* 11 (4), 276-87.

Feng, H., Kwun, H. J., Liu, X., Gjoerup, O., Stolz, D. B., Chang, Y. and Moore, P. S. (2011) Cellular and viral factors regulating Merkel cell polyomavirus replication. *PLoS One* 6 (7), e22468.

Feng, H., Shuda, M., Chang, Y. and Moore, P. S. (2008) Clonal integration of a polyomavirus in human Merkel cell carcinoma. *Science* 319 (5866), 1096-100.

Flynt, A. S., Greimann, J. C., Chung, W. J., Lima, C. D. and Lai, E. C. (2010) MicroRNA biogenesis via splicing and exosome-mediated trimming in Drosophila. *Mol Cell* 38 (6), 900-7.

Foster, K. W., Frost, A. R., McKie-Bell, P., Lin, C. Y., Engler, J. A., Grizzle, W. E. and Ruppert, J. M. (2000) Increase of GKLF messenger RNA and protein expression during progression of breast cancer. *Cancer Res* 60 (22), 6488-95.

Franco-Zorrilla, J. M., Valli, A., Todesco, M., Mateos, I., Puga, M. I., Rubio-Somoza, I., Leyva, A., Weigel, D., Garcia, J. A. and Paz-Ares, J. (2007) Target mimicry provides a new mechanism for regulation of microRNA activity. *Nat Genet* 39 (8), 1033-7.

Frank, F., Sonenberg, N. and Nagar, B. (2010) Structural basis for 5'-nucleotide base-specific recognition of guide RNA by human AGO2. *Nature* 465 (7299), 818-22.

French, C. A., Miyoshi, I., Aster, J. C., Kubonishi, I., Kroll, T. G., Dal Cin, P., Vargas, S. O., Perez-Atayde, A. R. and Fletcher, J. A. (2001) BRD4 bromodomain gene rearrangement in aggressive carcinoma with translocation t(15;19). *Am J Pathol* 159 (6), 1987-92.

Frolov, M. V. and Dyson, N. J. (2004) Molecular mechanisms of E2F-dependent activation and pRB-mediated repression. *J Cell Sci* 117 (Pt 11), 2173-81.

Fukaya, T. and Tomari, Y. (2011) PABP is not essential for microRNA-mediated translational repression and deadenylation in vitro. *Embo j* 30 (24), 4998-5009.

Fukuda, Y., Kawasaki, H. and Taira, K. (2006) Construction of microRNA-containing vectors for expression in mammalian cells. *Methods Mol Biol* 338, 167-73.

Fukunaga, R., Han, B. W., Hung, J. H., Xu, J., Weng, Z. and Zamore, P. D. (2012) Dicer partner proteins tune the length of mature miRNAs in flies and mammals. *Cell* 151 (3), 533-46.

Gallego Romero, I., Pai, A. A., Tung, J. and Gilad, Y. (2014) RNA-seq: impact of RNA degradation on transcript quantification. *BMC Biol* 12, 42.

Garcia-Caballero, T., Gallego, R., Roson, E., Basanta, D., Morel, G. and Beiras, A. (1989) Localization of serotonin-like immunoreactivity in the Merkel cells of pig snout skin. *Anat Rec* 225 (4), 267-71.

Garrod, D. and Chidgey, M. (2008) Desmosome structure, composition and function. *Biochim Biophys Acta* 1778 (3), 572-87.

Geng, J. G., Bevilacqua, M. P., Moore, K. L., McIntyre, T. M., Prescott, S. M., Kim, J. M., Bliss, G. A., Zimmerman, G. A. and McEver, R. P. (1990) Rapid neutrophil adhesion to activated endothelium mediated by GMP-140. *Nature* 343 (6260), 757-60.

Ghildiyal, M., Xu, J., Seitz, H., Weng, Z. and Zamore, P. D. (2010) Sorting of Drosophila small silencing RNAs partitions microRNA* strands into the RNA interference pathway. *Rna* 16 (1), 43-56.

Giffin, L. and Damania, B. (2014) KSHV: pathways to tumorigenesis and persistent infection. *Adv Virus Res* 88, 111-59.

Gilbert, J. and Benjamin, T. (2004) Uptake pathway of polyomavirus via ganglioside GD1a. *J Virol* 78 (22), 12259-67.

Goon, P. K., Greenberg, D. C., Igali, L. and Levell, N. J. (2016) Merkel Cell Carcinoma: rising incidence in the East of England. *J Eur Acad Dermatol Venereol*.

Gooptu, C., Woollons, A., Ross, J., Price, M., Wojnarowska, F., Morris, P. J., Wall, S. and Bunker, C. B. (1997) Merkel cell carcinoma arising after therapeutic immunosuppression. *Br J Dermatol* 137 (4), 637-41.

Gosert, R., Rinaldo, C. H., Funk, G. A., Egli, A., Ramos, E., Drachenberg, C. B. and Hirsch, H. H. (2008) Polyomavirus BK with rearranged noncoding control region emerge in vivo in renal transplant

patients and increase viral replication and cytopathology. *J Exp Med* 205 (4), 841-52.

Gottwein, E., Corcoran, D. L., Mukherjee, N., Skalsky, R. L., Hafner, M., Nusbaum, J. D., Shamulailatpam, P., Love, C. L., Dave, S. S., Tuschl, T., Ohler, U. and Cullen, B. R. (2011) Viral microRNA targetome of KSHV-infected primary effusion lymphoma cell lines. *Cell Host Microbe* 10 (5), 515-26.

Gottwein, E., Mukherjee, N., Sachse, C., Frenzel, C., Majoros, W. H., Chi, J. T., Braich, R., Manoharan, M., Soutschek, J., Ohler, U. and Cullen, B. R. (2007) A viral microRNA functions as an orthologue of cellular miR-155. *Nature* 450 (7172), 1096-9.

Gould, V. E., Moll, R., Moll, I., Lee, I. and Franke, W. W. (1985) Neuroendocrine (Merkel) cells of the skin: hyperplasias, dysplasias, and neoplasms. *Lab Invest* 52 (4), 334-53.

Gredell, J. A., Dittmer, M. J., Wu, M., Chan, C. and Walton, S. P. (2010) Recognition of siRNA asymmetry by TAR RNA binding protein. *Biochemistry* 49 (14), 3148-55.

Grey, F., Tirabassi, R., Meyers, H., Wu, G., McWeeney, S., Hook, L. and Nelson, J. A. (2010) A viral microRNA down-regulates multiple cell cycle genes through mRNA 5'UTRs. *PLoS Pathog* 6 (6), e1000967.

Griffiths, D. A., Abdul-Sada, H., Knight, L. M., Jackson, B. R., Richards, K., Prescott, E. L., Peach, A. H. S., Blair, G. E., Macdonald, A. and Whitehouse, A. (2013) Merkel Cell Polyomavirus Small T Antigen Targets the NEMO Adaptor Protein To Disrupt Inflammatory Signaling. *Journal of Virology* 87 (24), 13853-13867.

Grifo, J. A., Tahara, S. M., Morgan, M. A., Shatkin, A. J. and Merrick, W. C. (1983) New initiation factor activity required for globin mRNA translation. *J Biol Chem* 258 (9), 5804-10.

Grim, M. and Halata, Z. (2000) Developmental origin of avian Merkel cells. *Anat Embryol (Berl)* 202 (5), 401-10.

Grimson, A., Farh, K. K., Johnston, W. K., Garrett-Engele, P., Lim, L. P. and Bartel, D. P. (2007) MicroRNA targeting specificity in mammals: determinants beyond seed pairing. *Mol Cell* 27 (1), 91-105.

Grotzinger, T., Jensen, K. and Will, H. (1996) The interferon (IFN)-stimulated gene Sp100 promoter contains an IFN-gamma activation site and an imperfect IFN-stimulated response element which mediate type I IFN inducibility. *J Biol Chem* 271 (41), 25253-60.

Grundhoff, A. and Sullivan, C. S. (2011) Virus-encoded microRNAs. *Virology* 411 (2), 325-43.

Gu, W., An, J., Ye, P., Zhao, K. N. and Antonsson, A. (2011) Prediction of conserved microRNAs from skin and mucosal human papillomaviruses. *Arch Virol* 156 (7), 1161-71.

Guldner, H. H., Szostecki, C., Schroder, P., Matschl, U., Jensen, K., Luders, C., Will, H. and Sternsdorf, T. (1999) Splice variants of the nuclear dot-associated Sp100 protein contain homologies to HMG-1 and a human nuclear phosphoprotein-box motif. *J Cell Sci* 112 (Pt 5), 733-47.

Guo, H., Ingolia, N. T., Weissman, J. S. and Bartel, D. P. (2010) Mammalian microRNAs predominantly act to decrease target mRNA levels. *Nature* 466 (7308), 835-40.

Ha, M. and Kim, V. N. (2014) Regulation of microRNA biogenesis. *Nat Rev Mol Cell Biol* 15 (8), 509-24.

Haas, G., Braun, J. E., Igreja, C., Tritschler, F., Nishihara, T. and Izaurralde, E. (2010) HPat provides a link between deadenylation and decapping in metazoa. *J Cell Biol* 189 (2), 289-302.

Haase, A. D., Jaskiewicz, L., Zhang, H., Laine, S., Sack, R., Gatignol, A. and Filipowicz, W. (2005) TRBP, a regulator of cellular PKR and HIV-1 virus expression, interacts with Dicer and functions in RNA silencing. *EMBO Rep* 6 (10), 961-7.

Hafner, C., Houben, R., Baeurle, A., Ritter, C., Schrama, D., Landthaler, M. and Becker, J. C. (2012) Activation of the PI3K/AKT pathway in Merkel cell carcinoma. *PLoS One* 7 (2), e31255.

Hafner, M., Landthaler, M., Burger, L., Khorshid, M., Hausser, J., Berninger, P., Rothballer, A., Ascano, M., Jungkamp, A. C., Munschauer, M., Ulrich, A., Wardle, G. S., Dewell, S., Zavolan, M. and Tuschl, T. (2010) Transcriptome-wide identification of RNA-binding protein and microRNA target sites by PAR-CLIP. *Cell* 141 (1), 129-41.

Hafner, M., Renwick, N., Brown, M., Mihailovic, A., Holoch, D., Lin, C., Pena, J. T., Nusbaum, J. D., Morozov, P., Ludwig, J., Ojo, T., Luo, S., Schroth, G. and Tuschl, T. (2011) RNA-ligase-dependent biases in miRNA representation in deep-sequenced small RNA cDNA libraries. *Rna* 17 (9), 1697-712.

Hagan, J. P., Piskounova, E. and Gregory, R. I. (2009) Lin28 recruits the TUTase Zcchc11 to inhibit let-7 maturation in mouse embryonic stem cells. *Nat Struct Mol Biol* 16 (10), 1021-5.

Halata, Z., Grim, M. and Bauman, K. I. (2003) Friedrich Sigmund Merkel and his "Merkel cell", morphology, development, and physiology: review and new results. *Anat Rec A Discov Mol Cell Evol Biol* 271 (1), 225-39.

Hamada, T., Tsuchihashi, S., Avanesyan, A., Duarte, S., Moore, C., Busuttil, R. W. and Coito, A. J. (2008) Cyclooxygenase-2 deficiency enhances Th2 immune responses and impairs neutrophil recruitment in hepatic ischemia/reperfusion injury. *J Immunol* 180 (3), 1843-53.

Hammond, S. M., Boettcher, S., Caudy, A. A., Kobayashi, R. and Hannon, G. J. (2001) Argonaute2, a link between genetic and biochemical analyses of RNAi. *Science* 293 (5532), 1146-50.

Han, B. W., Hung, J. H., Weng, Z., Zamore, P. D. and Ameres, S. L. (2011) The 3'-to-5' exoribonuclease Nibbler shapes the 3' ends of microRNAs bound to Drosophila Argonaute1. *Curr Biol* 21 (22), 1878-87.

Han, J., Lee, Y., Yeom, K. H., Kim, Y. K., Jin, H. and Kim, V. N. (2004) The Drosha-DGCR8 complex in primary microRNA processing. *Genes Dev* 18 (24), 3016-27.

Han, Y. C., Park, C. Y., Bhagat, G., Zhang, J., Wang, Y., Fan, J. B., Liu, M., Zou, Y., Weissman, I. L. and Gu, H. (2010) microRNA-29a induces aberrant self-renewal capacity in hematopoietic progenitors, biased myeloid development, and acute myeloid leukemia. *J Exp Med* 207 (3), 475-89.

Harada, A., Sekido, N., Akahoshi, T., Wada, T., Mukaida, N. and Matsushima, K. (1994) Essential involvement of interleukin-8 (IL-8) in acute inflammation. *J Leukoc Biol* 56 (5), 559-64.

Harrison, C. J., Meinke, G., Kwun, H. J., Rogalin, H., Phelan, P. J., Bullock, P. A., Chang, Y., Moore, P. S. and Bohm, A. (2011) Asymmetric assembly of Merkel cell polyomavirus large T-antigen origin binding domains at the viral origin. *J Mol Biol* 409 (4), 529-42.

Hartschuh, W. and Grube, D. (1979) The Merkel cell--a member of the APUD cell system. Fluorescence and electron microscopic contribution to the neurotransmitter function of the Merkel cell granules. *Arch Dermatol Res* 265 (2), 115-22.

Hasan, U. A., Bates, E., Takeshita, F., Biliato, A., Accardi, R., Bouvard, V., Mansour, M., Vincent, I., Gissmann, L., Iftner, T., Sideri, M., Stubenrauch, F. and Tommasino, M. (2007) TLR9 expression and function is abolished by the cervical cancer-associated human papillomavirus type 16. *J Immunol* 178 (5), 3186-97.

Hata, Y., Matsuka, K., Ito, O., Matsuda, H., Furuichi, H., Konstantinos, A. and Nuri, B. (1997) Two cases of Merkel cell carcinoma cured by intratumor injection of natural human tumor necrosis factor. *Plast Reconstr Surg* 99 (2), 547-53.

Heath, M., Jaimes, N., Lemos, B., Mostaghimi, A., Wang, L. C., Penas, P. F. and Nghiem, P. (2008) Clinical characteristics of Merkel cell carcinoma at diagnosis in 195 patients: the AEIOU features. *J Am Acad Dermatol* 58 (3), 375-81.

Held-Feindt, J., Hattermann, K., Knerlich-Lukoschus, F., Mehdorn, H. M. and Mentlein, R. (2011) SP100 reduces malignancy of human glioma cells. *Int J Oncol* 38 (4), 1023-30.

Hemmi, H., Takeuchi, O., Kawai, T., Kaisho, T., Sato, S., Sanjo, H., Matsumoto, M., Hoshino, K., Wagner, H., Takeda, K. and Akira, S. (2000) A Toll-like receptor recognizes bacterial DNA. *Nature* 408 (6813), 740-5.

Hengst, L. and Reed, S. I. (1996) Translational control of p27Kip1 accumulation during the cell cycle. *Science* 271 (5257), 1861-4.

Heo, I., Ha, M., Lim, J., Yoon, M. J., Park, J. E., Kwon, S. C., Chang, H. and Kim, V. N. (2012) Mono-uridylation of pre-microRNA as a key step in the biogenesis of group II let-7 microRNAs. *Cell* 151 (3), 521-32.

Heo, I., Joo, C., Cho, J., Ha, M., Han, J. and Kim, V. N. (2008) Lin28 mediates the terminal uridylation of let-7 precursor MicroRNA. *Mol Cell* 32 (2), 276-84.

Hesbacher, S., Pfitzer, L., Wiedorfer, K., Angermeyer, S., Borst, A., Haferkamp, S., Scholz, C. J., Wobser, M., Schrama, D. and Houben, R. (2016) RB1 is the crucial target of the Merkel cell polyomavirus Large T antigen in Merkel cell carcinoma cells. *Oncotarget*.

Hislop, A. D. and Sabbah, S. (2008) CD8+ T cell immunity to Epstein-Barr virus and Kaposi's sarcoma-associated herpes virus. *Semin Cancer Biol* 18 (6), 416-22.

Hla, T. and Neilson, K. (1992) Human cyclooxygenase-2 cDNA. *Proc Natl Acad Sci U S A* 89 (16), 7384-8.

Hodgson, N. C. (2005) Merkel cell carcinoma: changing incidence trends. *J Surg Oncol* 89 (1), 1-4.

Holmes, W. E., Lee, J., Kuang, W. J., Rice, G. C. and Wood, W. I. (1991) Structure and functional expression of a human interleukin-8 receptor. *Science* 253 (5025), 1278-80.

Houben, R., Adam, C., Baeurle, A., Hesbacher, S., Grimm, J., Angermeyer, S., Henzel, K., Hauser, S., Elling, R., Brocker, E. B., Gaubatz, S., Becker, J. C. and Schrama, D. (2012) An intact retinoblastoma protein-binding site in Merkel cell polyomavirus large T antigen is required for promoting growth of Merkel cell carcinoma cells. *Int J Cancer* 130 (4), 847-56.

Houben, R., Angermeyer, S., Haferkamp, S., Aue, A., Goebeler, M., Schrama, D. and Hesbacher, S. (2014) Characterization of functional domains in the Merkel cell polyoma virus Large T antigen. *Int J Cancer*.

Houben, R., Shuda, M., Weinkam, R., Schrama, D., Feng, H., Chang, Y., Moore, P. S. and Becker, J. C. (2010) Merkel cell polyomavirus-infected Merkel cell carcinoma cells require expression of viral T antigens. *J Virol* 84 (14), 7064-72.

Hough, R. F. and Bass, B. L. (1994) Purification of the Xenopus laevis double-stranded RNA adenosine deaminase. *J Biol Chem* 269 (13), 9933-9.

Hu, Y., Song, J., Liu, L., Li, J., Tang, B., Wang, J., Zhang, X., Zhang, Y., Wang, L., Liao, Y., He, Z. and Li, Q. (2016) Different microRNA alterations contribute to diverse outcomes following EV71 and CA16 infections: Insights from high-throughput sequencing in rhesus monkey peripheral blood mononuclear cells. *Int J Biochem Cell Biol* 81 (Pt A), 20-31.

Huang, X., Yuan, T., Tschannen, M., Sun, Z., Jacob, H., Du, M., Liang, M., Dittmar, R. L., Liu, Y., Kohli, M., Thibodeau, S. N., Boardman, L. and Wang, L. (2013) Characterization of human plasma-derived exosomal RNAs by deep sequencing. *BMC Genomics* 14, 319.

Hubert, L., Darbousset, R., Panicot-Dubois, L., Robert, S., Sabatier, F., Fallague, K., Dignat-George, F. and Dubois, C. (2014) Neutrophils recruit and activate human endothelial colony-forming cells at the site of vessel injury via P-selectin glycoprotein ligand-1 and L-selectin. *J Thromb Haemost* 12 (7), 1170-81.

Hughes, M. P., Hardee, M. E., Cornelius, L. A., Hutchins, L. F., Becker, J. C. and Gao, L. (2014) Merkel Cell Carcinoma: Epidemiology, Target, and Therapy. *Curr Dermatol Rep.* Vol. 3. 46-53.

Hutvagner, G. and Zamore, P. D. (2002) A microRNA in a multiple-turnover RNAi enzyme complex. *Science* 297 (5589), 2056-60.

Hynes, R. O. (2002) Integrins: bidirectional, allosteric signaling machines. *Cell* 110 (6), 673-87.

Imataka, H., Gradi, A. and Sonenberg, N. (1998) A newly identified N-terminal amino acid sequence of human eIF4G binds poly(A)-binding protein and functions in poly(A)-dependent translation. *Embo j* 17 (24), 7480-9.

Ingelfinger, D., Arndt-Jovin, D. J., Luhrmann, R. and Achsel, T. (2002) The human LSm1-7 proteins colocalize with the mRNA-degrading enzymes Dcp1/2 and Xrnl in distinct cytoplasmic foci. *Rna* 8 (12), 1489-501.

Iorio, M. V., Ferracin, M., Liu, C. G., Veronese, A., Spizzo, R., Sabbioni, S., Magri, E., Pedriali, M., Fabbri, M., Campiglio, M., Menard, S., Palazzo, J. P., Rosenberg, A., Musiani, P., Volinia, S., Nenci, I., Calin, G. A., Querzoli, P., Negrini, M. and Croce, C. M. (2005) MicroRNA gene expression deregulation in human breast cancer. *Cancer Res* 65 (16), 7065-70.

Isaac, A., Wilcox, K. W. and Taylor, J. L. (2006) SP100B, a repressor of gene expression preferentially binds to DNA with unmethylated CpGs. *J Cell Biochem* 98 (5), 1106-22.

Iwasaki, S., Kobayashi, M., Yoda, M., Sakaguchi, Y., Katsuma, S., Suzuki, T. and Tomari, Y. (2010) Hsc70/Hsp90 chaperone machinery mediates ATP-dependent RISC loading of small RNA duplexes. *Mol Cell* 39 (2), 292-9.

Izikson, L., Nornhold, E., Iyer, J. G., Nghiem, P. and Zeitouni, N. C. (2011) Merkel cell carcinoma associated with HIV: review of 14 patients. *Aids* 25 (1), 119-21.

Jayaprakash, A. D., Jabado, O., Brown, B. D. and Sachidanandam, R. (2011) Identification and remediation of biases in the activity of RNA ligases in small-RNA deep sequencing. *Nucleic Acids Res* 39 (21), e141.

Jiang, M., Abend, J. R., Johnson, S. F. and Imperiale, M. J. (2009) The role of polyomaviruses in human disease. *Virology* 384 (2), 266-73.

Jiang, M., Entezami, P., Gamez, M., Stamminger, T. and Imperiale, M. J. (2011) Functional reorganization of promyelocytic leukemia nuclear bodies during BK virus infection. *MBio* 2 (1), e00281-10.

Jiang, M., Zhao, L., Gamez, M. and Imperiale, M. J. (2012) Roles of ATM and ATR-mediated DNA damage responses during lytic BK polyomavirus infection. *PLoS Pathog* 8 (8), e1002898.

Jiang, Y., Saavedra, H. I., Holloway, M. P., Leone, G. and Altura, R. A. (2004) Aberrant regulation of survivin by the RB/E2F family of proteins. *J Biol Chem* 279 (39), 40511-20.

Jopling, C. L., Yi, M., Lancaster, A. M., Lemon, S. M. and Sarnow, P. (2005) Modulation of hepatitis C virus RNA abundance by a liver-specific MicroRNA. *Science* 309 (5740), 1577-81.

Jourdain, L., Curmi, P., Sobel, A., Pantaloni, D. and Carlier, M. F. (1997) Stathmin: a tubulin-sequestering protein which forms a ternary T2S complex with two tubulin molecules. *Biochemistry* 36 (36), 10817-21.

Jung, Y. J., Choi, H., Kim, H. and Lee, S. K. (2014) MicroRNA miR-BART20-5p stabilizes Epstein-Barr virus latency by directly targeting BZLF1 and BRLF1. *J Virol* 88 (16), 9027-37.

Juranic Lisnic, V., Babic Cac, M., Lisnic, B., Trsan, T., Mefferd, A., Das Mukhopadhyay, C., Cook, C. H., Jonjic, S. and Trgovcich, J. (2013) Dual analysis of the murine cytomegalovirus and host cell transcriptomes reveal new aspects of the virus-host cell interface. *PLoS Pathog* 9 (9), e1003611.

Kanehisa, M. S., Y., Kawashima, M., Furumichi, M. and Tanabe, M. (2016a) *Cytokine-Cytokine receptor interaction*.

Kanehisa, M. S., Y., Kawashima, M., Furumichi, M. and Tanabe, M. (2016b) *MAPK signalling pathway*.

Kanehisa, M. S., Y., Kawashima, M., Furumichi, M. and Tanabe, M. (2016c) *NOD-like receptor signalling pathway*.

Kanehisa, M. S., Y., Kawashima, M., Furumichi, M. and Tanabe, M. (2016d) *RIG-I-like receptor signalling pathway*.

Kanehisa, M. S., Y., Kawashima, M., Furumichi, M. and Tanabe, M. (2016e) ***Toll-like receptor signaling pathway****Toll-like receptor signaling pathway*.

Kansas, G. S. (1996) Selectins and their ligands: current concepts and controversies. *Blood* 88 (9), 3259-87.

Kasof, G. M., Goyal, L. and White, E. (1999) Btf, a novel death-promoting transcriptional repressor that interacts with Bcl-2-related proteins. *Mol Cell Biol* 19 (6), 4390-404.

Katoh, T., Sakaguchi, Y., Miyauchi, K., Suzuki, T., Kashiwabara, S. and Baba, T. (2009) Selective stabilization of mammalian microRNAs by 3' adenylation mediated by the cytoplasmic poly(A) polymerase GLD-2. *Genes Dev* 23 (4), 433-8.

Kaushansky, K. (2006) Lineage-specific hematopoietic growth factors. *N Engl J Med* 354 (19), 2034-45.

Kaverina, I. and Straube, A. (2011) Regulation of cell migration by dynamic microtubules. *Semin Cell Dev Biol* 22 (9), 968-74.

Kawahara, Y., Zinshteyn, B., Chendrimada, T. P., Shiekhattar, R. and Nishikura, K. (2007) RNA editing of the microRNA-151 precursor blocks cleavage by the Dicer-TRBP complex. *EMBO Rep* 8 (8), 763-9.

Kawai, T., Takahashi, K., Sato, S., Coban, C., Kumar, H., Kato, H., Ishii, K. J., Takeuchi, O. and Akira, S. (2005) IPS-1, an adaptor triggering RIG-I- and Mda5-mediated type I interferon induction. *Nat Immunol* 6 (10), 981-8.

Kedde, M., van Kouwenhove, M., Zwart, W., Oude Vrielink, J. A., Elkon, R. and Agami, R. (2010) A Pumilio-induced RNA structure switch in p27-3' UTR controls miR-221 and miR-222 accessibility. *Nat Cell Biol* 12 (10), 1014-20.

Keller, J. M. and Alwine, J. C. (1984) Activation of the SV40 late promoter: direct effects of T antigen in the absence of viral DNA replication. *Cell* 36 (2), 381-9.

Kennedy, R. B., Ovsyannikova, I. G., Pankratz, V. S., Haralambieva, I. H., Vierkant, R. A., Jacobson, R. M. and Poland, G. A. (2012) Genome-wide genetic associations with IFNgamma response to smallpox vaccine. *Hum Genet* 131 (9), 1433-51.

Khalili, K., White, M. K., Sawa, H., Nagashima, K. and Safak, M. (2005) The agnoprotein of polyomaviruses: a multifunctional auxiliary protein. *J Cell Physiol* 204 (1), 1-7.

Khongnomnan, K., Makkoch, J., Poomipak, W., Poovorawan, Y. and Payungporn, S. (2015) Human miR-3145 inhibits influenza A viruses replication by targeting and silencing viral PB1 gene. *Exp Biol Med (Maywood)* 240 (12), 1630-9.

Kim, Y., Lee, S., Kim, S., Kim, D., Ahn, J. H. and Ahn, K. (2012) Human cytomegalovirus clinical strain-specific microRNA miR-UL148D targets the human chemokine RANTES during infection. *PLoS Pathog* 8 (3), e1002577.

Kim, Y. E., Lee, J. H., Kim, E. T., Shin, H. J., Gu, S. Y., Seol, H. S., Ling, P. D., Lee, C. H. and Ahn, J. H. (2011) Human cytomegalovirus infection causes degradation of Sp100 proteins that suppress viral gene expression. *J Virol* 85 (22), 11928-37.

Kimura, T., Iwase, M., Kondo, G., Watanabe, H., Ohashi, M., Ito, D. and Nagumo, M. (2003) Suppressive effect of selective cyclooxygenase-2

inhibitor on cytokine release in human neutrophils. *Int Immunopharmacol* 3 (10-11), 1519-28.

Kincaid, R. P., Burke, J. M. and Sullivan, C. S. (2012) RNA virus microRNA that mimics a B-cell oncomiR. *Proc Natl Acad Sci U S A* 109 (8), 3077-82.

Kincaid, R. P. and Sullivan, C. S. (2012) Virus-encoded microRNAs: an overview and a look to the future. *PLoS Pathog* 8 (12), e1003018.

Kiss, A. L. and Botos, E. (2009) Endocytosis via caveolae: alternative pathway with distinct cellular compartments to avoid lysosomal degradation? *J Cell Mol Med* 13 (7), 1228-37.

Knight, L. M., Stakaityte, G., Wood, J. J., Abdul-Sada, H., Griffiths, D. A., Howell, G. J., Wheat, R., Blair, G. E., Steven, N. M., Macdonald, A., Blackbourn, D. J. and Whitehouse, A. (2014) Merkel cell polyomavirus small T antigen mediates microtubule destabilisation to promote cell motility and migration. *J Virol*.

Koepp, D. M., Schaefer, L. K., Ye, X., Keyomarsi, K., Chu, C., Harper, J. W. and Elledge, S. J. (2001) Phosphorylation-dependent ubiquitination of cyclin E by the SCFFbw7 ubiquitin ligase. *Science* 294 (5540), 173-7.

Kohler, A., De Filippo, K., Hasenberg, M., van den Brandt, C., Nye, E., Hosking, M. P., Lane, T. E., Mann, L., Ransohoff, R. M., Hauser, A. E., Winter, O., Schraven, B., Geiger, H., Hogg, N. and Gunzer, M. (2011) G-CSF-mediated thrombopoietin release triggers neutrophil motility and mobilization from bone marrow via induction of Cxcr2 ligands. *Blood* 117 (16), 4349-57.

Kong, Y. W., Cannell, I. G., de Moor, C. H., Hill, K., Garside, P. G., Hamilton, T. L., Meijer, H. A., Dobbyn, H. C., Stoneley, M., Spriggs, K. A., Willis, A. E. and Bushell, M. (2008) The mechanism of micro-RNA-mediated translation repression is determined by the promoter of the target gene. *Proc Natl Acad Sci U S A* 105 (26), 8866-71.

Krug, A., French, A. R., Barchet, W., Fischer, J. A., Dzionek, A., Pingel, J. T., Orihuela, M. M., Akira, S., Yokoyama, W. M. and Colonna, M. (2004) TLR9-dependent recognition of MCMV by IPC and DC generates coordinated cytokine responses that activate antiviral NK cell function. *Immunity* 21 (1), 107-19.

Krug, A., Veeraswamy, R., Pekosz, A., Kanagawa, O., Unanue, E. R., Colonna, M. and Cella, M. (2003) Interferon-producing cells fail to induce proliferation of naive T cells but can promote expansion and T helper 1 differentiation of antigen-experienced unpolarized T cells. *J Exp Med* 197 (7), 899-906.

Kuwamoto, S. (2011) Recent advances in the biology of Merkel cell carcinoma. *Hum Pathol* 42 (8), 1063-77.

Kwun, H. J., Guastafierro, A., Shuda, M., Meinke, G., Bohm, A., Moore, P. S. and Chang, Y. (2009) The minimum replication origin of merkel cell polyomavirus has a unique large T-antigen loading architecture and requires small T-antigen expression for optimal replication. *J Virol* 83 (23), 12118-28.

Kwun, H. J., Shuda, M., Feng, H., Camacho, C. J., Moore, P. S. and Chang, Y. (2013) Merkel cell polyomavirus small T antigen controls viral

replication and oncoprotein expression by targeting the cellular ubiquitin ligase SCFFbw7. *Cell Host Microbe* 14 (2), 125-35.

Kyratsous, C. A., Walters, M. S., Panagiotidis, C. A. and Silverstein, S. J. (2009) Complementation of a Herpes Simplex Virus ICP0 Null Mutant by Varicella-Zoster Virus ORF61p.

Lagatie, O., Tritsmans, L. and Stuyver, L. J. (2013) The miRNA world of polyomaviruses. *Virology Journal* 10.

Landais, I., Pelton, C., Streblow, D., DeFilippis, V., McWeeney, S. and Nelson, J. A. (2015) Human Cytomegalovirus miR-UL112-3p Targets TLR2 and Modulates the TLR2/IRAK1/NFkappaB Signaling Pathway. *PLoS Pathog* 11 (5), e1004881.

Larsen, E., Celi, A., Gilbert, G. E., Furie, B. C., Erban, J. K., Bonfanti, R., Wagner, D. D. and Furie, B. (1989) PADGEM protein: a receptor that mediates the interaction of activated platelets with neutrophils and monocytes. *Cell* 59 (2), 305-12.

Lau, M. E. and Hunstad, D. A. (2013) Quantitative assessment of human neutrophil migration across a cultured bladder epithelium. *J Vis Exp* (81), e50919.

Lawrence, M. B. and Springer, T. A. (1991) Leukocytes roll on a selectin at physiologic flow rates: distinction from and prerequisite for adhesion through integrins. *Cell* 65 (5), 859-73.

Lebbe, C., Becker, J. C., Grob, J. J., Malvehy, J., Del Marmol, V., Pehamberger, H., Peris, K., Saiag, P., Middleton, M. R., Bastholt, L., Testori, A., Stratigos, A. and Garbe, C. (2015) Diagnosis and treatment of Merkel Cell

Carcinoma. European consensus-based interdisciplinary guideline. *Eur J Cancer* 51 (16), 2396-403.

Lee, H. Y., Zhou, K., Smith, A. M., Noland, C. L. and Doudna, J. A. (2013) Differential roles of human Dicer-binding proteins TRBP and PACT in small RNA processing. *Nucleic Acids Res* 41 (13), 6568-76.

Lee, S., Paulson, K. G., Murchison, E. P., Afanasiev, O. K., Alkan, C., Leonard, J. H., Byrd, D. R., Hannon, G. J. and Nghiem, P. (2011) Identification and validation of a novel mature microRNA encoded by the Merkel cell polyomavirus in human Merkel cell carcinomas. *Journal of Clinical Virology* 52 (3), 272-275.

Lee, S. H., Kalejta, R. F., Kerry, J., Semmes, O. J., O'Connor, C. M., Khan, Z., Garcia, B. A., Shenk, T. and Murphy, E. (2012) BclAF1 restriction factor is neutralized by proteasomal degradation and microRNA repression during human cytomegalovirus infection. *Proc Natl Acad Sci U S A* 109 (24), 9575-80.

Lee, Y., Hur, I., Park, S. Y., Kim, Y. K., Suh, M. R. and Kim, V. N. (2006) The role of PACT in the RNA silencing pathway. *Embo j* 25 (3), 522-32.

Lei, C. Q., Zhang, Y., Li, M., Jiang, L. Q., Zhong, B., Kim, Y. H. and Shu, H. B. (2015) ECSIT bridges RIG-I-like receptors to VISA in signaling events of innate antiviral responses. *J Innate Immun* 7 (2), 153-64.

Lei, X., Bai, Z., Ye, F., Xie, J., Kim, C. G., Huang, Y. and Gao, S. J. (2010) Regulation of NF-kappaB inhibitor IkappaBalpha and viral replication by a KSHV microRNA. *Nat Cell Biol* 12 (2), 193-9.

Leifer, C. A., Kennedy, M. N., Mazzoni, A., Lee, C., Kruhlak, M. J. and Segal, D. M. (2004) TLR9 is localized in the endoplasmic reticulum prior to stimulation. *J Immunol* 173 (2), 1179-83.

Lemos, B. D., Storer, B. E., Iyer, J. G., Phillips, J. L., Bichakjian, C. K., Fang, L. C., Johnson, T. M., Liegeois-Kwon, N. J., Otley, C. C., Paulson, K. G., Ross, M. I., Yu, S. S., Zeitouni, N. C., Byrd, D. R., Sondak, V. K., Gershenwald, J. E., Sober, A. J. and Nghiem, P. (2010) Pathologic nodal evaluation improves prognostic accuracy in Merkel cell carcinoma: analysis of 5823 cases as the basis of the first consensus staging system. *J Am Acad Dermatol* 63 (5), 751-61.

Lentz, S. R., Krewson, L. and Zutter, M. M. (1993) Recurrent neuroendocrine (Merkel cell) carcinoma of the skin presenting as marrow failure in a man with systemic lupus erythematosus. *Med Pediatr Oncol* 21 (2), 137-41.

Leonard, E. J., Yoshimura, T., Tanaka, S. and Raffeld, M. (1991) Neutrophil recruitment by intradermally injected neutrophil attractant/activation protein-1. *J Invest Dermatol* 96 (5), 690-4.

Leuschner, P. J., Ameres, S. L., Kueng, S. and Martinez, J. (2006) Cleavage of the siRNA passenger strand during RISC assembly in human cells. *EMBO Rep* 7 (3), 314-20.

Lewis, B. P., Shih, I. H., Jones-Rhoades, M. W., Bartel, D. P. and Burge, C. B. (2003) Prediction of mammalian microRNA targets. *Cell* 115 (7), 787-98.

Li, L. and Luo, Z. (2017) Dysregulated miR-27a-3p promotes nasopharyngeal carcinoma cell proliferation and migration by targeting Mapk10. *Oncol Rep* 37 (5), 2679-2687.

Li, W., Shang, C., Guan, C., Zhang, Y., Sun, K. and Fu, W. (2010) Low expression of Sp100 in laryngeal cancer: correlation with cell differentiation. *Med Sci Monit* 16 (6), Br174-8.

Li, Y., Long, X., Huang, L., Yang, M., Yuan, Y., Wang, Y., Delecluse, H. J. and Kuang, E. (2016) Epstein-Barr Virus BZLF1-Mediated Downregulation of Proinflammatory Factors Is Essential for Optimal Lytic Viral Replication. *J Virol* 90 (2), 887-903.

Lillis, J., Ceilley, R. I. and Nelson, P. (2005) Merkel cell carcinoma in a patient with autoimmune hepatitis. *J Drugs Dermatol* 4 (3), 357-9.

Lin, A., Wang, S., Nguyen, T., Shire, K. and Frappier, L. (2008) The EBNA1 protein of Epstein-Barr virus functionally interacts with Brd4. *J Virol* 82 (24), 12009-19.

Lin, C. C., Liu, L. Z., Addison, J. B., Wonderlin, W. F., Ivanov, A. V. and Ruppert, J. M. (2011) A KLF4-miRNA-206 autoregulatory feedback loop can promote or inhibit protein translation depending upon cell context. *Mol Cell Biol* 31 (12), 2513-27.

Linder, P. (2003) Yeast RNA helicases of the DEAD-box family involved in translation initiation. *Biol Cell* 95 (3-4), 157-67.

Lindley, I., Aschauer, H., Seifert, J. M., Lam, C., Brunowsky, W., Kownatzki, E., Thelen, M., Peveri, P., Dewald, B., von Tscharner, V. and et al. (1988) Synthesis and expression in Escherichia coli of the gene encoding monocyte-derived neutrophil-activating factor: biological equivalence

between natural and recombinant neutrophil-activating factor. *Proc Natl Acad Sci U S A* 85 (23), 9199-203.

Liu, J., Carmell, M. A., Rivas, F. V., Marsden, C. G., Thomson, J. M., Song, J. J., Hammond, S. M., Joshua-Tor, L. and Hannon, G. J. (2004) Argonaute2 is the catalytic engine of mammalian RNAi. *Science* 305 (5689), 1437-41.

Liu, W., Yang, R., Payne, A. S., Schowalter, R. M., Spurgeon, M. E., Lambert, P. F., Xu, X., Buck, C. B. and You, J. (2016) Identifying the Target Cells and Mechanisms of Merkel Cell Polyomavirus Infection. *Cell Host Microbe* 19 (6), 775-87.

Liu, X., Hein, J., Richardson, S. C., Basse, P. H., Toptan, T., Moore, P. S., Gjoerup, O. V. and Chang, Y. (2011) Merkel cell polyomavirus large T antigen disrupts lysosome clustering by translocating human Vam6p from the cytoplasm to the nucleus. *J Biol Chem* 286 (19), 17079-90.

Liu, X., Jin, D. Y., McManus, M. T. and Mourelatos, Z. (2012) Precursor microRNA-programmed silencing complex assembly pathways in mammals. *Mol Cell* 46 (4), 507-17.

Liu, Y., Ye, X., Jiang, F., Liang, C., Chen, D., Peng, J., Kinch, L. N., Grishin, N. V. and Liu, Q. (2009) C3PO, an endoribonuclease that promotes RNAi by facilitating RISC activation. *Science* 325 (5941), 750-3.

Low, J. A., Magnuson, B., Tsai, B. and Imperiale, M. J. (2006) Identification of gangliosides GD1b and GT1b as receptors for BK virus. *J Virol* 80 (3), 1361-6.

Lu, C. C., Li, Z., Chu, C. Y., Feng, J., Sun, R. and Rana, T. M. (2010a) MicroRNAs encoded by Kaposi's sarcoma-associated herpesvirus regulate viral life cycle. *EMBO Rep* 11 (10), 784-90.

Lu, F., Stedman, W., Yousef, M., Renne, R. and Lieberman, P. M. (2010b) Epigenetic regulation of Kaposi's sarcoma-associated herpesvirus latency by virus-encoded microRNAs that target Rta and the cellular Rbl2-DNMT pathway. *J Virol* 84 (6), 2697-706.

Lucarz, A. and Brand, G. (2007) Current considerations about Merkel cells. *Eur J Cell Biol* 86 (5), 243-51.

Lund, E., Guttinger, S., Calado, A., Dahlberg, J. E. and Kutay, U. (2004) Nuclear export of microRNA precursors. *Science* 303 (5654), 95-8.

Lund, J., Sato, A., Akira, S., Medzhitov, R. and Iwasaki, A. (2003) Toll-like receptor 9-mediated recognition of Herpes simplex virus-2 by plasmacytoid dendritic cells. *J Exp Med* 198 (3), 513-20.

Lytle, J. R., Yario, T. A. and Steitz, J. A. (2007) Target mRNAs are repressed as efficiently by microRNA-binding sites in the 5' UTR as in the 3' UTR. *Proc Natl Acad Sci U S A* 104 (23), 9667-72.

Macrae, I. J., Zhou, K. and Doudna, J. A. (2007) Structural determinants of RNA recognition and cleavage by Dicer. *Nat Struct Mol Biol* 14 (10), 934-40.

Macrae, I. J., Zhou, K., Li, F., Repic, A., Brooks, A. N., Cande, W. Z., Adams, P. D. and Doudna, J. A. (2006) Structural basis for double-stranded RNA processing by Dicer. *Science* 311 (5758), 195-8.

Mahrle, G. and Orfanos, C. E. (1974) Merkel cells as human cutaneous neuroreceptor cells. Their presence in dermal neural corpuscles

and in the external hair root sheath of human adult skin. *Arch Dermatol Forsch* 251 (1), 19-26.

Mamane, Y., Heylbroeck, C., Genin, P., Algarte, M., Servant, M. J., LePage, C., DeLuca, C., Kwon, H., Lin, R. and Hiscott, J. (1999) Interferon regulatory factors: the next generation. *Gene* 237 (1), 1-14.

Maricich, S. M., Wellnitz, S. A., Nelson, A. M., Lesniak, D. R., Gerling, G. J., Lumpkin, E. A. and Zoghbi, H. Y. (2009) Merkel Cells are Essential for Light Touch Responses. *Science* 324 (5934), 1580-2.

Marquitz, A. R., Mathur, A., Nam, C. S. and Raab-Traub, N. (2011) The Epstein-Barr Virus BART microRNAs target the pro-apoptotic protein Bim. *Virology* 412 (2), 392-400.

Maser, R. S., Choudhury, B., Campbell, P. J., Feng, B., Wong, K. K., Protopopov, A., O'Neil, J., Gutierrez, A., Ivanova, E., Perna, I., Lin, E., Mani, V., Jiang, S., McNamara, K., Zaghlul, S., Edkins, S., Stevens, C., Brennan, C., Martin, E. S., Wiedemeyer, R., Kabbarah, O., Nogueira, C., Histen, G., Aster, J., Mansour, M., Duke, V., Foroni, L., Fielding, A. K., Goldstone, A. H., Rowe, J. M., Wang, Y. A., Look, A. T., Stratton, M. R., Chin, L., Futreal, P. A. and DePinho, R. A. (2007) Chromosomally unstable mouse tumours have genomic alterations similar to diverse human cancers. *Nature* 447 (7147), 966-71.

Mathonnet, G., Fabian, M. R., Svitkin, Y. V., Parsyan, A., Huck, L., Murata, T., Biffo, S., Merrick, W. C., Darzynkiewicz, E., Pillai, R. S., Filipowicz, W., Duchaine, T. F. and Sonenberg, N. (2007) MicroRNA inhibition of translation initiation in vitro by targeting the cap-binding complex eIF4F. *Science* 317 (5845), 1764-7.

Mathys, H., Basquin, J., Ozgur, S., Czarnocki-Cieciura, M., Bonneau, F., Aartse, A., Dziembowski, A., Nowotny, M., Conti, E. and Filipowicz, W. (2014) Structural and biochemical insights to the role of the CCR4-NOT complex and DDX6 ATPase in microRNA repression. *Mol Cell* 54 (5), 751-65.

McLoone, N. M., McKenna, K., Edgar, D., Walsh, M. and Bingham, A. (2005) Merkel cell carcinoma in a patient with chronic sarcoidosis. *Clin Exp Dermatol.* Vol. 30. England: 580-2.

Mei, B., Ding, X., Xu, H. Z. and Wang, M. T. (2014) Global gene expression changes in human peripheral blood after H7N9 infection. *Gene* 551 (2), 255-60.

Meijer, H. A., Kong, Y. W., Lu, W. T., Wilczynska, A., Spriggs, R. V., Robinson, S. W., Godfrey, J. D., Willis, A. E. and Bushell, M. (2013) Translational repression and eIF4A2 activity are critical for microRNA-mediated gene regulation. *Science* 340 (6128), 82-5.

Meister, G., Landthaler, M., Patkaniowska, A., Dorsett, Y., Teng, G. and Tuschl, T. (2004) Human Argonaute2 mediates RNA cleavage targeted by miRNAs and siRNAs. *Mol Cell* 15 (2), 185-97.

Merrick, W. C. (2015) eIF4F: a retrospective. *J Biol Chem* 290 (40), 24091-9.

Mishima, Y., Fukao, A., Kishimoto, T., Sakamoto, H., Fujiwara, T. and Inoue, K. (2012) Translational inhibition by deadenylation-independent mechanisms is central to microRNA-mediated silencing in zebrafish. *Proc Natl Acad Sci U S A* 109 (4), 1104-9.

Mochizuki, K., Nishiyama, A., Jang, M. K., Dey, A., Ghosh, A., Tamura, T., Natsume, H., Yao, H. and Ozato, K. (2008) The bromodomain protein Brd4 stimulates G1 gene transcription and promotes progression to S phase. *J Biol Chem* 283 (14), 9040-8.

Modi, W. S., Dean, M., Seuanez, H. N., Mukaida, N., Matsushima, K. and O'Brien, S. J. (1990) Monocyte-derived neutrophil chemotactic factor (MDNCF/IL-8) resides in a gene cluster along with several other members of the platelet factor 4 gene superfamily. *Hum Genet* 84 (2), 185-7.

Moldovan, G. L., Pfander, B. and Jentsch, S. (2007) PCNA, the maestro of the replication fork. *Cell* 129 (4), 665-79.

Moll, I., Kuhn, C. and Moll, R. (1995) Cytokeratin 20 is a general marker of cutaneous Merkel cells while certain neuronal proteins are absent. *J Invest Dermatol* 104 (6), 910-5.

Moll, I., Moll, R. and Franke, W. W. (1986) Formation of epidermal and dermal Merkel cells during human fetal skin development. *J Invest Dermatol* 87 (6), 779-87.

Moll, I., Roessler, M., Brandner, J. M., Eispert, A. C., Houdek, P. and Moll, R. (2005) Human Merkel cells--aspects of cell biology, distribution and functions. *Eur J Cell Biol* 84 (2-3), 259-71.

Morrison, K. M., Miesegaes, G. R., Lumpkin, E. A. and Maricich, S. M. (2009) Mammalian Merkel cells are descended from the epidermal lineage. *Dev Biol* 336 (1), 76-83.

Motley, A., Bright, N. A., Seaman, M. N. and Robinson, M. S. (2003) Clathrin-mediated endocytosis in AP-2-depleted cells. *J Cell Biol* 162 (5), 909-18.

Mourelatos, Z., Dostie, J., Paushkin, S., Sharma, A., Charroux, B., Abel, L., Rappsilber, J., Mann, M. and Dreyfuss, G. (2002) miRNPs: a novel class of ribonucleoproteins containing numerous microRNAs. *Genes Dev* 16 (6), 720-8.

Muller, S., Raulefs, S., Bruns, P., Afonso-Grunz, F., Plotner, A., Thermann, R., Jager, C., Schlitter, A. M., Kong, B., Regel, I., Roth, W. K., Rotter, B., Hoffmeier, K., Kahl, G., Koch, I., Theis, F. J., Kleeff, J., Winter, P. and Michalski, C. W. (2015) Next-generation sequencing reveals novel differentially regulated mRNAs, lncRNAs, miRNAs, sdRNAs and a piRNA in pancreatic cancer. *Mol Cancer* 14, 94.

Munde, P. B., Khandekar, S. P., Dive, A. M. and Sharma, A. (2013) Pathophysiology of merkel cell. *J Oral Maxillofac Pathol.* Vol. 17. 408-412.

Murchison, E. P., Partridge, J. F., Tam, O. H., Cheloufi, S. and Hannon, G. J. (2005) Characterization of Dicer-deficient murine embryonic stem cells. *Proc Natl Acad Sci U S A* 102 (34), 12135-40.

Murphree, A. L. and Benedict, W. F. (1984) Retinoblastoma: clues to human oncogenesis. *Science* 223 (4640), 1028-33.

Murphy, E., Vanicek, J., Robins, H., Shenk, T. and Levine, A. J. (2008) Suppression of immediate-early viral gene expression by herpesvirus-coded microRNAs: implications for latency. *Proc Natl Acad Sci U S A* 105 (14), 5453-8.

Murphy, P. M. and Tiffany, H. L. (1991) Cloning of complementary DNA encoding a functional human interleukin-8 receptor. *Science* 253 (5025), 1280-3.

Nachmani, D., Stern-Ginossar, N., Sarid, R. and Mandelboim, O. (2009) Diverse herpesvirus microRNAs target the stress-induced immune ligand MICB to escape recognition by natural killer cells. *Cell Host Microbe* 5 (4), 376-85.

Nair, V. and Zavolan, M. (2006) Virus-encoded microRNAs: novel regulators of gene expression. *Trends Microbiol* 14 (4), 169-75.

Nakamura, T., Sato, Y., Watanabe, D., Ito, H., Shimonohara, N., Tsuji, T., Nakajima, N., Suzuki, Y., Matsuo, K., Nakagawa, H., Sata, T. and Katano, H. (2010) Nuclear localization of Merkel cell polyomavirus large T antigen in Merkel cell carcinoma. *Virology* 398 (2), 273-9.

Nakanishi, K., Weinberg, D. E., Bartel, D. P. and Patel, D. J. (2012) Structure of yeast Argonaute with guide RNA. *Nature* 486 (7403), 368-74.

Nakao, S., Ogtata, Y., Shimizu, E., Yamazaki, M., Furuyama, S. and Sugiya, H. (2002) Tumor necrosis factor alpha (TNF-alpha)-induced prostaglandin E2 release is mediated by the activation of cyclooxygenase-2 (COX-2) transcription via NFkappaB in human gingival fibroblasts. *Mol Cell Biochem* 238 (1-2), 11-8.

Nakatani, M., Maksimovic, S., Baba, Y. and Lumpkin, E. A. (2015) Mechanotransduction in epidermal Merkel cells. *Pflugers Arch* 467 (1), 101-8.

Nardi, V., Song, Y., Santamaria-Barria, J. A., Cosper, A. K., Lam, Q., Faber, A. C., Boland, G. M., Yeap, B. Y., Bergethon, K., Scialabba, V. L., Tsao, H., Settleman, J., Ryan, D. P., Borger, D. R., Bhan, A. K., Hoang, M. P., Iafrate, A. J., Cusack, J. C., Engelman, J. A. and Dias-Santagata, D. (2012) Activation of PI3K signaling in Merkel cell carcinoma. *Clin Cancer Res* 18 (5), 1227-36.

Negorev, D. and Maul, G. G. (2001) Cellular proteins localized at and interacting within ND10/PML nuclear bodies/PODs suggest functions of a nuclear depot. *Oncogene* 20 (49), 7234-42.

Negorev, D. G., Vladimirova, O. V., Ivanov, A., III, F. R. and Maul, G. G. (2006) Differential Role of Sp100 Isoforms in Interferon-Mediated Repression of Herpes Simplex Virus Type 1 Immediate-Early Protein Expression.

Negorev, D. G., Vladimirova, O. V. and Maul, G. G. (2009) Differential functions of interferon-upregulated Sp100 isoforms: herpes simplex virus type 1 promoter-based immediate-early gene suppression and PML protection from ICP0-mediated degradation. *J Virol* 83 (10), 5168-80.

Nemoto, I., Sato-Matsumura, K. C., Fujita, Y., Natsuga, K., Ujiie, H., Tomita, Y., Kato, N., Kondo, M. and Ohnishi, K. (2008) Leukaemic dissemination of Merkel cell carcinoma in a patient with systemic lupus erythematosus. *Clin Exp Dermatol* 33 (3), 270-2.

Neu, U., Hengel, H., Blaum, B. S., Schowalter, R. M., Macejak, D., Gilbert, M., Wakarchuk, W. W., Imamura, A., Ando, H., Kiso, M., Arnberg, N., Garcea, R. L., Peters, T., Buck, C. B. and Stehle, T. (2012) Structures of Merkel cell polyomavirus VP1 complexes define a sialic acid binding site required for infection. *PLoS Pathog* 8 (7), e1002738.

Neumann, F., Borchert, S., Schmidt, C., Reimer, R., Hohenberg, H., Fischer, N. and Grundhoff, A. (2011) Replication, gene expression and particle production by a consensus Merkel Cell Polyomavirus (MCPyV) genome. *PLoS One* 6 (12), e29112.

Neumann, F., Czech-Sioli, M., Schmidt, C., Dobner, T., Grundhoff, A., Schreiner, S. and Fischer, N. (2016) Replication of merkel cell polyomavirus induces reorganization of promyelocytic leukemia nuclear bodies. *J Gen Virol*.

Ngiow, S. F., von Scheidt, B., Akiba, H., Yagita, H., Teng, M. W. and Smyth, M. J. (2011) Anti-TIM3 antibody promotes T cell IFN-gamma-mediated antitumor immunity and suppresses established tumors. *Cancer Res* 71 (10), 3540-51.

Nickeleit, V., Hirsch, H. H., Binet, I. F., Gudat, F., Prince, O., Dalquen, P., Thiel, G. and Mihatsch, M. J. (1999) Polyomavirus infection of renal allograft recipients: from latent infection to manifest disease. *J Am Soc Nephrol* 10 (5), 1080-9.

Noland, C. L., Ma, E. and Doudna, J. A. (2011) siRNA repositioning for guide strand selection by human Dicer complexes. *Mol Cell* 43 (1), 110-21.

Norkin, L. C., Anderson, H. A., Wolfrom, S. A. and Oppenheim, A. (2002) Caveolar endocytosis of simian virus 40 is followed by brefeldin A-sensitive transport to the endoplasmic reticulum, where the virus disassembles. *J Virol* 76 (10), 5156-66.

Obeidy, P. and Sharland, A. F. (2009) NKG2D and its ligands. *Int J Biochem Cell Biol* 41 (12), 2364-7.

Okada, C., Yamashita, E., Lee, S. J., Shibata, S., Katahira, J., Nakagawa, A., Yoneda, Y. and Tsukihara, T. (2009) A high-resolution structure of the pre-microRNA nuclear export machinery. *Science* 326 (5957), 1275-9.

Okamura, K., Hagen, J. W., Duan, H., Tyler, D. M. and Lai, E. C. (2007) The mirtron pathway generates microRNA-class regulatory RNAs in Drosophila. *Cell* 130 (1), 89-100.

Okamura, K., Liu, N. and Lai, E. C. (2009) Distinct mechanisms for microRNA strand selection by Drosophila Argonautes. *Mol Cell* 36 (3), 431-44.

Orba, Y., Suzuki, T., Makino, Y., Kubota, K., Tanaka, S., Kimura, T. and Sawa, H. (2010) Large T antigen promotes JC virus replication in G2-arrested cells by inducing ATM- and ATR-mediated G2 checkpoint signaling. *J Biol Chem* 285 (2), 1544-54.

Orom, U. A., Nielsen, F. C. and Lund, A. H. (2008) MicroRNA-10a binds the 5'UTR of ribosomal protein mRNAs and enhances their translation. *Mol Cell* 30 (4), 460-71.

Otani, K., Dong, Y., Li, X., Lu, J., Zhang, N., Xu, L., Go, M. Y., Ng, E. K., Arakawa, T., Chan, F. K., Sung, J. J. and Yu, J. (2014) Odd-skipped related 1 is a novel tumour suppressor gene and a potential prognostic biomarker in gastric cancer. *J Pathol* 234 (3), 302-15.

Ottinger, M., Christalla, T., Nathan, K., Brinkmann, M. M., Viejo-Borbolla, A. and Schulz, T. F. (2006) Kaposi's sarcoma-associated herpesvirus LANA-1 interacts with the short variant of BRD4 and releases cells from a BRD4- and BRD2/RING3-induced G1 cell cycle arrest. *J Virol* 80 (21), 10772-86.

Pallas, D. C., Shahrik, L. K., Martin, B. L., Jaspers, S., Miller, T. B., Brautigan, D. L. and Roberts, T. M. (1990) Polyoma small and middle T

antigens and SV40 small t antigen form stable complexes with protein phosphatase 2A. *Cell* 60 (1), 167-76.

Pandya, A. Y., Talley, L. I., Frost, A. R., Fitzgerald, T. J., Trivedi, V., Chakravarthy, M., Chhieng, D. C., Grizzle, W. E., Engler, J. A., Krontiras, H., Bland, K. I., LoBuglio, A. F., Lobo-Ruppert, S. M. and Ruppert, J. M. (2004) Nuclear localization of KLF4 is associated with an aggressive phenotype in early-stage breast cancer. *Clin Cancer Res* 10 (8), 2709-19.

Park, J. E., Heo, I., Tian, Y., Simanshu, D. K., Chang, H., Jee, D., Patel, D. J. and Kim, V. N. (2011) Dicer recognizes the 5' end of RNA for efficient and accurate processing. *Nature* 475 (7355), 201-5.

Park, S. J., Kumar, M., Kwon, H. I., Seong, R. K., Han, K., Song, J. M., Kim, C. J., Choi, Y. K. and Shin, O. S. (2015) Dynamic changes in host gene expression associated with H5N8 avian influenza virus infection in mice. *Sci Rep* 5, 16512.

Parker, J. S., Roe, S. M. and Barford, D. (2005) Structural insights into mRNA recognition from a PIWI domain-siRNA guide complex. *Nature* 434 (7033), 663-6.

Passaro, C., Borriello, F., Vastolo, V., Di Somma, S., Scamardella, E., Gigantino, V., Franco, R., Marone, G. and Portella, G. (2016) The oncolytic virus dl922-947 reduces IL-8/CXCL8 and MCP-1/CCL2 expression and impairs angiogenesis and macrophage infiltration in anaplastic thyroid carcinoma. *Oncotarget* 7 (2), 1500-15.

Patel, P. H., Barbee, S. A. and Blankenship, J. T. (2016) GW-Bodies and P-Bodies Constitute Two Separate Pools of Sequestered Non-Translating RNAs. *PLoS One* 11 (3), e0150291.

Paulson, K. G., Iyer, J. G., Tegeder, A. R., Thibodeau, R., Schelter, J., Koba, S., Schrama, D., Simonson, W. T., Lemos, B. D., Byrd, D. R., Koelle, D. M., Galloway, D. A., Leonard, J. H., Madeleine, M. M., Argenyi, Z. B., Disis, M. L., Becker, J. C., Cleary, M. A. and Nghiem, P. (2011) Transcriptome-wide studies of merkel cell carcinoma and validation of intratumoral CD8+ lymphocyte invasion as an independent predictor of survival. *J Clin Oncol* 29 (12), 1539-46.

Pelkmans, L. and Helenius, A. (2002) Endocytosis via caveolae. *Traffic* 3 (5), 311-20.

Pelkmans, L., Kartenbeck, J. and Helenius, A. (2001) Caveolar endocytosis of simian virus 40 reveals a new two-step vesicular-transport pathway to the ER. *Nat Cell Biol* 3 (5), 473-83.

Penn, I. and First, M. R. (1999) Merkel's cell carcinoma in organ recipients: report of 41 cases. *Transplantation* 68 (11), 1717-21.

Peveri, P., Walz, A., Dewald, B. and Baggiolini, M. (1988) A novel neutrophil-activating factor produced by human mononuclear phagocytes. *J Exp Med* 167 (5), 1547-59.

Pfeffer, S. and Voinnet, O. (2006) Viruses, microRNAs and cancer. *Oncogene* 25 (46), 6211-9.

Pham, J. W., Pellino, J. L., Lee, Y. S., Carthew, R. W. and Sontheimer, E. J. (2004) A Dicer-2-dependent 80s complex cleaves targeted mRNAs during RNAi in Drosophila. *Cell* 117 (1), 83-94.

Pho, M. T., Ashok, A. and Atwood, W. J. (2000) JC virus enters human glial cells by clathrin-dependent receptor-mediated endocytosis. *J Virol* 74 (5), 2288-92.

Piedade, D. and Azevedo-Pereira, J. M. (2016) The Role of microRNAs in the Pathogenesis of Herpesvirus Infection. *Viruses* 8 (6).

Pillai, R. S., Bhattacharyya, S. N., Artus, C. G., Zoller, T., Cougot, N., Basyuk, E., Bertrand, E. and Filipowicz, W. (2005) Inhibition of translational initiation by Let-7 MicroRNA in human cells. *Science* 309 (5740), 1573-6.

Poulin, D. L., Kung, A. L. and DeCaprio, J. A. (2004) p53 targets simian virus 40 large T antigen for acetylation by CBP. *J Virol* 78 (15), 8245-53.

Qiao, J., Kang, J. H., Cree, J., Evers, B. M. and Chung, D. H. (2007) Ets1 transcription factor mediates gastrin-releasing peptide-induced IL-8 regulation in neuroblastoma cells. *Neoplasia* 9 (3), 184-91.

Qiao, M., Luo, D., Kuang, Y., Feng, H., Luo, G. and Liang, P. (2015) Cell cycle specific distribution of killin: evidence for negative regulation of both DNA and RNA synthesis. *Cell Cycle* 14 (12), 1823-9.

Querbes, W., Benmerah, A., Tosoni, D., Di Fiore, P. P. and Atwood, W. J. (2004) A JC virus-induced signal is required for infection of glial cells by a clathrin- and eps15-dependent pathway. *J Virol* 78 (1), 250-6.

Rand, T. A., Petersen, S., Du, F. and Wang, X. (2005) Argonaute2 cleaves the anti-guide strand of siRNA during RISC activation. *Cell* 123 (4), 621-9.

Raulet, D. H. (2003) Roles of the NKG2D immunoreceptor and its ligands. *Nat Rev Immunol* 3 (10), 781-90.

Ray, B. K., Lawson, T. G., Kramer, J. C., Cladaras, M. H., Grifo, J. A., Abramson, R. D., Merrick, W. C. and Thach, R. E. (1985) ATP-dependent

unwinding of messenger RNA structure by eukaryotic initiation factors. *J Biol Chem* 260 (12), 7651-8.

Rehmsmeier, M., Steffen, P., Hochsmann, M. and Giegerich, R. (2004) Fast and effective prediction of microRNA/target duplexes. *Rna* 10 (10), 1507-17.

Reichel, C. A., Rehberg, M., Lerchenberger, M., Berberich, N., Bihari, P., Khandoga, A. G., Zahler, S. and Krombach, F. (2009) Ccl2 and Ccl3 mediate neutrophil recruitment via induction of protein synthesis and generation of lipid mediators. *Arterioscler Thromb Vasc Biol* 29 (11), 1787-93.

Richards, K. F., Guastafierro, A., Shuda, M., Toptan, T., Moore, P. S. and Chang, Y. (2015) Merkel Cell Polyomavirus T Antigens Promote Cell Proliferation and Inflammatory Cytokine Gene Expression. *J Gen Virol*.

Richards, K. H. and Macdonald, A. (2011) Putting the brakes on the anti-viral response: negative regulators of type I interferon (IFN) production. *Microbes Infect* 13 (4), 291-302.

Riley, K. J., Rabinowitz, G. S., Yario, T. A., Luna, J. M., Darnell, R. B. and Steitz, J. A. (2012) EBV and human microRNAs co-target oncogenic and apoptotic viral and human genes during latency. *Embo j* 31 (9), 2207-21.

Ro, S., Park, C., Young, D., Sanders, K. M. and Yan, W. (2007) Tissue-dependent paired expression of miRNAs. *Nucleic Acids Res* 35 (17), 5944-53.

Roberts, A. P., Lewis, A. P. and Jopling, C. L. (2011) miR-122 activates hepatitis C virus translation by a specialized mechanism requiring particular RNA components. *Nucleic Acids Res* 39 (17), 7716-29.

Ross, M. H. and Wojciech, P. (2010) *Histology: A Text and Atlas.* 6th edition. Philadelphia: Lippincott Williams & Wilkins.

Rossetto, C. C., Tarrant-Elorza, M., Verma, S., Purushothaman, P. and Pari, G. S. (2013) Regulation of viral and cellular gene expression by Kaposi's sarcoma-associated herpesvirus polyadenylated nuclear RNA. *J Virol* 87 (10), 5540-53.

Rot, A. (1991) Chemotactic potency of recombinant human neutrophil attractant/activation protein-1 (interleukin-8) for polymorphonuclear leukocytes of different species. *Cytokine* 3 (1), 21-7.

Rouya, C., Siddiqui, N., Morita, M., Duchaine, T. F., Fabian, M. R. and Sonenberg, N. (2014) Human DDX6 effects miRNA-mediated gene silencing via direct binding to CNOT1. *Rna* 20 (9), 1398-409.

Ruby, J. G., Jan, C. H. and Bartel, D. P. (2007) Intronic microRNA precursors that bypass Drosha processing. *Nature* 448 (7149), 83-6.

Rumi, M., Ishihara, S., Aziz, M., Kazumori, H., Ishimura, N., Yuki, T., Kadota, C., Kadowaki, Y. and Kinoshita, Y. (2006) RNA polymerase II mediated transcription from the polymerase III promoters in short hairpin RNA expression vector. *Biochem Biophys Res Commun* 339 (2), 540-7.

Russell, L. and Garrett-Sinha, L. A. (2010) Transcription factor Ets-1 in cytokine and chemokine gene regulation. *Cytokine* 51 (3), 217-26.

Russo, R. C., Garcia, C. C., Teixeira, M. M. and Amaral, F. A. (2014) The CXCL8/IL-8 chemokine family and its receptors in inflammatory diseases. *Expert Rev Clin Immunol* 10 (5), 593-619.

Sakuishi, K., Apetoh, L., Sullivan, J. M., Blazar, B. R., Kuchroo, V. K. and Anderson, A. C. (2010) Targeting Tim-3 and PD-1 pathways to reverse T

cell exhaustion and restore anti-tumor immunity. *J Exp Med* 207 (10), 2187-94.

Salunke, D. M., Caspar, D. L. and Garcea, R. L. (1986) Self-assembly of purified polyomavirus capsid protein VP1. *Cell* 46 (6), 895-904.

Santanam, U., Zanesi, N., Efanov, A., Costinean, S., Palamarchuk, A., Hagan, J. P., Volinia, S., Alder, H., Rassenti, L., Kipps, T., Croce, C. M. and Pekarsky, Y. (2010) Chronic lymphocytic leukemia modeled in mouse by targeted miR-29 expression. *Proc Natl Acad Sci U S A* 107 (27), 12210-5.

Sapp, M. and Day, P. M. (2009) Structure, attachment and entry of polyoma- and papillomaviruses. *Virology* 384 (2), 400-9.

Sarras, H., Alizadeh Azami, S. and McPherson, J. P. (2010) In search of a function for BCLAF1. *ScientificWorldJournal* 10, 1450-61.

Satolli, F., Venturi, C., Vescovi, V., Morrone, P. and De Panfilis, G. (2005) Merkel-cell carcinoma in Behcet's disease. *Acta Derm Venereol.* Vol. 85. Norway: 79.

Sayed, D. and Abdellatif, M. (2011) MicroRNAs in development and disease. *Physiol Rev* 91 (3), 827-87.

Schelhaas, M. (2010) Come in and take your coat off - how host cells provide endocytosis for virus entry. *Cell Microbiol* 12 (10), 1378-88.

Scherer, M. and Stamminger, T. (2016) Emerging Role of PML Nuclear Bodies in Innate Immune Signaling. *J Virol* 90 (13), 5850-4.

Schirle, N. T. and MacRae, I. J. (2012) The crystal structure of human Argonaute2. *Science* 336 (6084), 1037-40.

Schmid, S., Sachs, D. and tenOever, B. R. (2014) Mitogen-activated protein kinase-mediated licensing of interferon regulatory factor 3/7 reinforces the cell response to virus. *J Biol Chem* 289 (1), 299-311.

Schowalter, R. M. and Buck, C. B. (2013) The Merkel cell polyomavirus minor capsid protein. *PLoS Pathog* 9 (8), e1003558.

Schowalter, R. M., Pastrana, D. V. and Buck, C. B. (2011) Glycosaminoglycans and sialylated glycans sequentially facilitate Merkel cell polyomavirus infectious entry. *PLoS Pathog* 7 (7), e1002161.

Schowalter, R. M., Pastrana, D. V., Pumphrey, K. A., Moyer, A. L. and Buck, C. B. (2010) Merkel cell polyomavirus and two previously unknown polyomaviruses are chronically shed from human skin. *Cell Host Microbe* 7 (6), 509-15.

Schrama, D. and Becker, J. C. (2011) Merkel cell carcinoma--pathogenesis, clinical aspects and treatment. *J Eur Acad Dermatol Venereol* 25 (10), 1121-9.

Schroeder, A., Mueller, O., Stocker, S., Salowsky, R., Leiber, M., Gassmann, M., Lightfoot, S., Menzel, W., Granzow, M. and Ragg, T. (2006) The RIN: an RNA integrity number for assigning integrity values to RNA measurements. *BMC Mol Biol* 7, 3.

Schwarz, D. S., Hutvagner, G., Du, T., Xu, Z., Aronin, N. and Zamore, P. D. (2003) Asymmetry in the assembly of the RNAi enzyme complex. *Cell* 115 (2), 199-208.

Scott, M. P. and Helm, K. F. (1999) Cytokeratin 20: a marker for diagnosing Merkel cell carcinoma. *Am J Dermatopathol* 21 (1), 16-20.

Screpanti, I., Romani, L., Musiani, P., Modesti, A., Fattori, E., Lazzaro, D., Sellitto, C., Scarpa, S., Bellavia, D., Lattanzio, G. and et al. (1995) Lymphoproliferative disorder and imbalanced T-helper response in C/EBP beta-deficient mice. *Embo j* 14 (9), 1932-41.

Sebok, K., Woodside, D., al-Aoukaty, A., Ho, A. D., Gluck, S. and Maghazachi, A. A. (1993) IL-8 induces the locomotion of human IL-2-activated natural killer cells. Involvement of a guanine nucleotide binding (Go) protein. *J Immunol* 150 (4), 1524-34.

Seeler, J. S., Marchio, A., Losson, R., Desterro, J. M., Hay, R. T., Chambon, P. and Dejean, A. (2001) Common properties of nuclear body protein SP100 and TIF1alpha chromatin factor: role of SUMO modification. *Mol Cell Biol* 21 (10), 3314-24.

Seely, A. J., Naud, J. F., Campisi, G., Giannias, B., Liu, S., DiCarlo, A., Ferri, L. E., Pascual, J. L., Tchervenkov, J. and Christou, N. V. (2002) Alteration of chemoattractant receptor expression regulates human neutrophil chemotaxis in vivo. *Ann Surg* 235 (4), 550-9.

Seitz, H. (2009) Redefining microRNA targets. *Curr Biol* 19 (10), 870-3.

Selbach, M., Schwanhausser, B., Thierfelder, N., Fang, Z., Khanin, R. and Rajewsky, N. (2008) Widespread changes in protein synthesis induced by microRNAs. *Nature* 455 (7209), 58-63.

Seo, G. J., Chen, C. J. and Sullivan, C. S. (2009) Merkel cell polyomavirus encodes a microRNA with the ability to autoregulate viral gene expression. *Virology* 383 (2), 183-7.

Seo, G. J., Fink, L. H., O'Hara, B., Atwood, W. J. and Sullivan, C. S. (2008) Evolutionarily conserved function of a viral microRNA. *J Virol* 82 (20), 9823-8.

Sextius, P., Marionnet, C., Tacheau, C., Bon, F. X., Bastien, P., Mauviel, A., Bernard, B. A., Bernerd, F. and Dubertret, L. (2015) Analysis of gene expression dynamics revealed delayed and abnormal epidermal repair process in aged compared to young skin. *Arch Dermatol Res* 307 (4), 351-64.

Shah, M. H., Lorigan, P., O'Brien, M. E., Fossella, F. V., Moore, K. N., Bhatia, S., Kirby, M. and Woll, P. J. (2016) Phase I study of IMGN901, a CD56-targeting antibody-drug conjugate, in patients with CD56-positive solid tumors. *Invest New Drugs* 34 (3), 290-9.

Shahzad, N., Shuda, M., Gheit, T., Kwun, H. J., Cornet, I., Saidj, D., Zannetti, C., Hasan, U., Chang, Y., Moore, P. S., Accardi, R. and Tommasino, M. (2013) The T antigen locus of Merkel cell polyomavirus downregulates human Toll-like receptor 9 expression. *J Virol* 87 (23), 13009-19.

Sheng, Q., Denis, D., Ratnofsky, M., Roberts, T. M., DeCaprio, J. A. and Schaffhausen, B. (1997) The DnaJ domain of polyomavirus large T antigen is required to regulate Rb family tumor suppressor function. *J Virol* 71 (12), 9410-6.

Shuda, M., Arora, R., Kwun, H. J., Feng, H., Sarid, R., Fernandez-Figueras, M. T., Tolstov, Y., Gjoerup, O., Mansukhani, M. M., Swerdlow, S. H., Chaudhary, P. M., Kirkwood, J. M., Nalesnik, M. A., Kant, J. A., Weiss, L. M., Moore, P. S. and Chang, Y. (2009) Human Merkel cell polyomavirus

infection I. MCV T antigen expression in Merkel cell carcinoma, lymphoid tissues and lymphoid tumors. *Int J Cancer* 125 (6), 1243-9.

Shuda, M., Feng, H., Kwun, H. J., Rosen, S. T., Gjoerup, O., Moore, P. S. and Chang, Y. (2008) T antigen mutations are a human tumor-specific signature for Merkel cell polyomavirus. *Proc Natl Acad Sci U S A* 105 (42), 16272-7.

Shuda, M., Guastafierro, A., Geng, X., Shuda, Y., Ostrowski, S. M., Lukianov, S., Jenkins, F. J., Honda, K., Maricich, S. M., Moore, P. S. and Chang, Y. (2015) Merkel Cell Polyomavirus Small T Antigen Induces Cancer and Embryonic Merkel Cell Proliferation in a Transgenic Mouse Model. *PLoS One* 10 (11), e0142329.

Shuda, M., Kwun, H. J., Feng, H., Chang, Y. and Moore, P. S. (2011) Human Merkel cell polyomavirus small T antigen is an oncoprotein targeting the 4E-BP1 translation regulator. *J Clin Invest* 121 (9), 3623-34.

Sihto, H., Bohling, T., Kavola, H., Koljonen, V., Salmi, M., Jalkanen, S. and Joensuu, H. (2012) Tumor infiltrating immune cells and outcome of Merkel cell carcinoma: a population-based study. *Clin Cancer Res* 18 (10), 2872-81.

Sihto, H. and Joensuu, H. (2012) Tumor-infiltrating lymphocytes and outcome in Merkel cell carcinoma, a virus-associated cancer. *Oncoimmunology* 1 (8), 1420-1421.

Skalsky, R. L., Corcoran, D. L., Gottwein, E., Frank, C. L., Kang, D., Hafner, M., Nusbaum, J. D., Feederle, R., Delecluse, H. J., Luftig, M. A., Tuschl, T., Ohler, U. and Cullen, B. R. (2012) The viral and cellular

microRNA targetome in lymphoblastoid cell lines. *PLoS Pathog* 8 (1), e1002484.

Skalsky, R. L., Samols, M. A., Plaisance, K. B., Boss, I. W., Riva, A., Lopez, M. C., Baker, H. V. and Renne, R. (2007) Kaposi's sarcoma-associated herpesvirus encodes an ortholog of miR-155. *J Virol* 81 (23), 12836-45.

Somers, W. S., Tang, J., Shaw, G. D. and Camphausen, R. T. (2000) Insights into the molecular basis of leukocyte tethering and rolling revealed by structures of P- and E-selectin bound to SLe(X) and PSGL-1. *Cell* 103 (3), 467-79.

Song, J. J., Smith, S. K., Hannon, G. J. and Joshua-Tor, L. (2004) Crystal structure of Argonaute and its implications for RISC slicer activity. *Science* 305 (5689), 1434-7.

Sowd, G. A., Li, N. Y. and Fanning, E. (2013) ATM and ATR activities maintain replication fork integrity during SV40 chromatin replication. *PLoS Pathog* 9 (4), e1003283.

Spurgeon, M. E. and Lambert, P. F. (2013) Merkel cell polyomavirus: a newly discovered human virus with oncogenic potential. *Virology* 435 (1), 118-30.

Stakaityte, G., Wood, J. J., Knight, L. M., Abdul-Sada, H., Adzahar, N. S., Nwogu, N., Macdonald, A. and Whitehouse, A. (2014) Merkel cell polyomavirus: molecular insights into the most recently discovered human tumour virus. *Cancers (Basel)* 6 (3), 1267-97.

Starckx, S., Van den Steen, P. E., Wuyts, A., Van Damme, J. and Opdenakker, G. (2002) Neutrophil gelatinase B and chemokines in leukocytosis and stem cell mobilization. *Leuk Lymphoma* 43 (2), 233-41.

Stepp, W. H., Meyers, J. M. and McBride, A. A. (2013) Sp100 provides intrinsic immunity against human papillomavirus infection. *MBio* 4 (6), e00845-13.

Stergiou, L., Bauer, M., Mair, W., Bausch-Fluck, D., Drayman, N., Wollscheid, B., Oppenheim, A. and Pelkmans, L. (2013) Integrin-mediated signaling induced by simian virus 40 leads to transient uncoupling of cortical actin and the plasma membrane. *PLoS One* 8 (2), e55799.

Stewart, S. E., Eddy, B. E. and Borgese, N. (1958) Neoplasms in mice inoculated with a tumor agent carried in tissue culture. *J Natl Cancer Inst* 20 (6), 1223-43.

Strohmaier, H., Spruck, C. H., Kaiser, P., Won, K. A., Sangfelt, O. and Reed, S. I. (2001) Human F-box protein hCdc4 targets cyclin E for proteolysis and is mutated in a breast cancer cell line. *Nature* 413 (6853), 316-22.

Subramanian, S. and Steer, C. J. (2010) MicroRNAs as gatekeepers of apoptosis. *J Cell Physiol* 223 (2), 289-98.

Suffert, G., Malterer, G., Hausser, J., Viiliainen, J., Fender, A., Contrant, M., Ivacevic, T., Benes, V., Gros, F., Voinnet, O., Zavolan, M., Ojala, P. M., Haas, J. G. and Pfeffer, S. (2011) Kaposi's sarcoma herpesvirus microRNAs target caspase 3 and regulate apoptosis. *PLoS Pathog* 7 (12), e1002405.

Sullivan, C. S., Cantalupo, P. and Pipas, J. M. (2000) The molecular chaperone activity of simian virus 40 large T antigen is required to disrupt Rb-E2F family complexes by an ATP-dependent mechanism. *Mol Cell Biol* 20 (17), 6233-43.

Sullivan, C. S., Grundhoff, A. T., Tevethia, S., Pipas, J. M. and Ganem, D. (2005) SV40-encoded microRNAs regulate viral gene expression and reduce susceptibility to cytotoxic T cells. *Nature* 435 (7042), 682-6.

Sullivan, C. S., Sung, C. K., Pack, C. D., Grundhoff, A., Lukacher, A. E., Benjamin, T. L. and Ganem, D. (2009) Murine Polyomavirus encodes a microRNA that cleaves early RNA transcripts but is not essential for experimental infection. *Virology* 387 (1), 157-67.

Sun, R., Lin, S. F., Gradoville, L., Yuan, Y., Zhu, F. and Miller, G. (1998) A viral gene that activates lytic cycle expression of Kaposi's sarcoma-associated herpesvirus. *Proc Natl Acad Sci U S A* 95 (18), 10866-71.

Sun, Z., Jha, H. C., Pei, Y. G. and Robertson, E. S. (2016) The MHC II HLA-DRalpha is Downregulated by KSHV encoded lytic transactivator RTA and MARCH8. *J Virol*.

Swartz, J. E., Bor, Y. C., Misawa, Y., Rekosh, D. and Hammarskjold, M. L. (2007) The shuttling SR protein 9G8 plays a role in translation of unspliced mRNA containing a constitutive transport element. *J Biol Chem* 282 (27), 19844-53.

Szeder, V., Grim, M., Halata, Z. and Sieber-Blum, M. (2003) Neural crest origin of mammalian Merkel cells. *Dev Biol* 253 (2), 258-63.

Szostecki, C., Guldner, H. H., Netter, H. J. and Will, H. (1990) Isolation and characterization of cDNA encoding a human nuclear antigen

predominantly recognized by autoantibodies from patients with primary biliary cirrhosis. *J Immunol* 145 (12), 4338-47.

Tai, P. T., Yu, E., Winquist, E., Hammond, A., Stitt, L., Tonita, J. and Gilchrist, J. (2000) Chemotherapy in neuroendocrine/Merkel cell carcinoma of the skin: case series and review of 204 cases. *J Clin Oncol* 18 (12), 2493-9.

Tang, S., Bertke, A. S., Patel, A., Wang, K., Cohen, J. I. and Krause, P. R. (2008) An acutely and latently expressed herpes simplex virus 2 viral microRNA inhibits expression of ICP34.5, a viral neurovirulence factor. *Proc Natl Acad Sci U S A* 105 (31), 10931-6.

Tang, S., Patel, A. and Krause, P. R. (2009) Novel less-abundant viral microRNAs encoded by herpes simplex virus 2 latency-associated transcript and their roles in regulating ICP34.5 and ICP0 mRNAs. *J Virol* 83 (3), 1433-42.

Tavalai, N., Adler, M., Scherer, M., Riedl, Y. and Stamminger, T. (2011) Evidence for a dual antiviral role of the major nuclear domain 10 component Sp100 during the immediate-early and late phases of the human cytomegalovirus replication cycle. *J Virol* 85 (18), 9447-58.

Tavalai, N. and Stamminger, T. (2009) Interplay between Herpesvirus Infection and Host Defense by PML Nuclear Bodies. *Viruses* 1 (3), 1240-64.

Theiss, J. M., Gunther, T., Alawi, M., Neumann, F., Tessmer, U., Fischer, N. and Grundhoff, A. (2015) A Comprehensive Analysis of Replicating Merkel Cell Polyomavirus Genomes Delineates the Viral Transcription Program and Suggests a Role for mcv-miR-M1 in Episomal Persistence. *PLoS Pathog* 11 (7), e1004974.

Thermo Fisher Scientific, A. (2014) *mirVana™ Mimics & Inhibitors. http://www.lifetechnologies.com/uk/en/home/life-science/epigenetics-noncoding-rna-research/mirna-profiling-/mirvana-mimics-inhibitors.html* Accessed 10/05/2014.

Thomson, D. W., Bracken, C. P., Szubert, J. M. and Goodall, G. J. (2013) On measuring miRNAs after transient transfection of mimics or antisense inhibitors. *PLoS One* 8 (1), e55214.

Tian, Y., Simanshu, D. K., Ma, J. B., Park, J. E., Heo, I., Kim, V. N. and Patel, D. J. (2014) A phosphate-binding pocket within the platform-PAZ-connector helix cassette of human Dicer. *Mol Cell* 53 (4), 606-16.

Tili, E., Croce, C. M. and Michaille, J. J. (2009) miR-155: on the crosstalk between inflammation and cancer. *Int Rev Immunol* 28 (5), 264-84.

Toker, C. (1972) Trabecular carcinoma of the skin. *Arch Dermatol* 105 (1), 107-10.

Tolstov, Y. L., Knauer, A., Chen, J. G., Kensler, T. W., Kingsley, L. A., Moore, P. S. and Chang, Y. (2011) Asymptomatic primary Merkel cell polyomavirus infection among adults. *Emerg Infect Dis* 17 (8), 1371-80.

Tomari, Y., Du, T. and Zamore, P. D. (2007) Sorting of Drosophila small silencing RNAs. *Cell* 130 (2), 299-308.

Topalian, S. L., Hodi, F. S., Brahmer, J. R., Gettinger, S. N., Smith, D. C., McDermott, D. F., Powderly, J. D., Carvajal, R. D., Sosman, J. A., Atkins, M. B., Leming, P. D., Spigel, D. R., Antonia, S. J., Horn, L., Drake, C. G., Pardoll, D. M., Chen, L., Sharfman, W. H., Anders, R. A., Taube, J. M., McMiller, T. L., Xu, H., Korman, A. J., Jure-Kunkel, M., Agrawal, S., McDonald, D., Kollia, G. D., Gupta, A., Wigginton, J. M. and Sznol, M. (2012)

Safety, activity, and immune correlates of anti-PD-1 antibody in cancer. *N Engl J Med* 366 (26), 2443-54.

Topalis, D., Andrei, G. and Snoeck, R. (2013) The large tumor antigen: a "Swiss Army knife" protein possessing the functions required for the polyomavirus life cycle. *Antiviral Res* 97 (2), 122-36.

Tsai, B., Gilbert, J. M., Stehle, T., Lencer, W., Benjamin, T. L. and Rapoport, T. A. (2003) Gangliosides are receptors for murine polyoma virus and SV40. *Embo j* 22 (17), 4346-55.

Tsang, S. H., Wang, X., Li, J., Buck, C. B. and You, J. (2014) Host DNA damage response factors localize to merkel cell polyomavirus DNA replication sites to support efficient viral DNA replication. *J Virol* 88 (6), 3285-97.

Tsutsumi, A., Kawamata, T., Izumi, N., Seitz, H. and Tomari, Y. (2011) Recognition of the pre-miRNA structure by Drosophila Dicer-1. *Nat Struct Mol Biol* 18 (10), 1153-8.

Tucker, M., Valencia-Sanchez, M. A., Staples, R. R., Chen, J., Denis, C. L. and Parker, R. (2001) The transcription factor associated Ccr4 and Caf1 proteins are components of the major cytoplasmic mRNA deadenylase in Saccharomyces cerevisiae. *Cell* 104 (3), 377-86.

Tybulewicz, V. L. and Henderson, R. B. (2009) Rho family GTPases and their regulators in lymphocytes. *Nat Rev Immunol* 9 (9), 630-44.

Uchida, N., Hoshino, S. and Katada, T. (2004) Identification of a human cytoplasmic poly(A) nuclease complex stimulated by poly(A)-binding protein. *J Biol Chem* 279 (2), 1383-91.

Uchigasaki, S., Suzuki, H. and Inoue, K. (2004) Merkel cells in the vellus hair follicles of human facial skin: a study using confocal laser microscopy. *J Dermatol* 31 (3), 218-22.

Umbach, J. L., Nagel, M. A., Cohrs, R. J., Gilden, D. H. and Cullen, B. R. (2009) Analysis of human alphaherpesvirus microRNA expression in latently infected human trigeminal ganglia. *J Virol* 83 (20), 10677-83.

Ungewickell, E. J. and Hinrichsen, L. (2007) Endocytosis: clathrin-mediated membrane budding. *Curr Opin Cell Biol* 19 (4), 417-25.

Van den Steen, P. E., Proost, P., Wuyts, A., Van Damme, J. and Opdenakker, G. (2000) Neutrophil gelatinase B potentiates interleukin-8 tenfold by aminoterminal processing, whereas it degrades CTAP-III, PF-4, and GRO-alpha and leaves RANTES and MCP-2 intact. *Blood* 96 (8), 2673-81.

van Gent, M., Griffin, B. D., Berkhoff, E. G., van Leeuwen, D., Boer, I. G., Buisson, M., Hartgers, F. C., Burmeister, W. P., Wiertz, E. J. and Ressing, M. E. (2011) EBV lytic-phase protein BGLF5 contributes to TLR9 downregulation during productive infection. *J Immunol* 186 (3), 1694-702.

Van Keymeulen, A., Mascre, G., Youseff, K. K., Harel, I., Michaux, C., De Geest, N., Szpalski, C., Achouri, Y., Bloch, W., Hassan, B. A. and Blanpain, C. (2009) Epidermal progenitors give rise to Merkel cells during embryonic development and adult homeostasis. *J Cell Biol* 187 (1), 91-100.

Vincent, I. E., Zannetti, C., Lucifora, J., Norder, H., Protzer, U., Hainaut, P., Zoulim, F., Tommasino, M., Trepo, C., Hasan, U. and Chemin, I. (2011) Hepatitis B virus impairs TLR9 expression and function in plasmacytoid dendritic cells. *PLoS One* 6 (10), e26315.

Viollet, C., Davis, D. A., Reczko, M., Ziegelbauer, J. M., Pezzella, F., Ragoussis, J. and Yarchoan, R. (2015) Next-Generation Sequencing Analysis Reveals Differential Expression Profiles of MiRNA-mRNA Target Pairs in KSHV-Infected Cells. *PLoS One* 10 (5), e0126439.

Von Andrian, U. H., Hansell, P., Chambers, J. D., Berger, E. M., Torres Filho, I., Butcher, E. C. and Arfors, K. E. (1992) L-selectin function is required for beta 2-integrin-mediated neutrophil adhesion at physiological shear rates in vivo. *Am J Physiol* 263 (4 Pt 2), H1034-44.

Voog, E., Biron, P., Martin, J. P. and Blay, J. Y. (1999) Chemotherapy for patients with locally advanced or metastatic Merkel cell carcinoma. *Cancer* 85 (12), 2589-95.

Wagenknecht, N., Reuter, N., Scherer, M., Reichel, A., Muller, R. and Stamminger, T. (2015) Contribution of the Major ND10 Proteins PML, hDaxx and Sp100 to the Regulation of Human Cytomegalovirus Latency and Lytic Replication in the Monocytic Cell Line THP-1. *Viruses* 7 (6), 2884-907.

Wagner, H. (2002) Interactions between bacterial CpG-DNA and TLR9 bridge innate and adaptive immunity. *Curr Opin Microbiol* 5 (1), 62-9.

Wagner, H. (2004) The immunobiology of the TLR9 subfamily. *Trends Immunol* 25 (7), 381-6.

Wagner, R. W., Smith, J. E., Cooperman, B. S. and Nishikura, K. (1989) A double-stranded RNA unwinding activity introduces structural alterations by means of adenosine to inosine conversions in mammalian cells and Xenopus eggs. *Proc Natl Acad Sci U S A* 86 (8), 2647-51.

Wahid, F., Shehzad, A., Khan, T. and Kim, Y. Y. (2010) MicroRNAs: synthesis, mechanism, function, and recent clinical trials. *Biochim Biophys Acta* 1803 (11), 1231-43.

Wahl, R. U., Braunschweig, T., Ghassemi, A. and Rubben, A. (2016) Immunotherapy with imiquimod and interferon alfa for metastasized Merkel cell carcinoma. *Curr Oncol* 23 (2), e150-3.

Wahle, E. and Winkler, G. S. (2013) RNA decay machines: deadenylation by the Ccr4-not and Pan2-Pan3 complexes. *Biochim Biophys Acta* 1829 (6-7), 561-70.

Wang, K., Ni, L., Wang, S. and Zheng, C. (2014a) Herpes simplex virus 1 protein kinase US3 hyperphosphorylates p65/RelA and dampens NF-kappaB activation. *J Virol* 88 (14), 7941-51.

Wang, X., Li, J., Schowalter, R. M., Jiao, J., Buck, C. B. and You, J. (2012) Bromodomain protein Brd4 plays a key role in Merkel cell polyomavirus DNA replication. *PLoS Pathog* 8 (11), e1003021.

Wang, Y., He, X., Yu, Q. and Eng, C. (2013a) Androgen receptor-induced tumor suppressor, KLLN, inhibits breast cancer growth and transcriptionally activates p53/p73-mediated apoptosis in breast carcinomas. *Hum Mol Genet* 22 (11), 2263-72.

Wang, Y., Juranek, S., Li, H., Sheng, G., Tuschl, T. and Patel, D. J. (2008a) Structure of an argonaute silencing complex with a seed-containing guide DNA and target RNA duplex. *Nature* 456 (7224), 921-6.

Wang, Y., Juranek, S., Li, H., Sheng, G., Wardle, G. S., Tuschl, T. and Patel, D. J. (2009) Nucleation, propagation and cleavage of target RNAs in Ago silencing complexes. *Nature* 461 (7265), 754-61.

Wang, Y., Lupiani, B., Reddy, S. M., Lamont, S. J. and Zhou, H. (2014b) RNA-seq analysis revealed novel genes and signaling pathway associated with disease resistance to avian influenza virus infection in chickens. *Poult Sci* 93 (2), 485-93.

Wang, Y., Radhakrishnan, D., He, X., Peehl, D. M. and Eng, C. (2013b) Transcription factor KLLN inhibits tumor growth by AR suppression, induces apoptosis by TP53/TP73 stimulation in prostate carcinomas, and correlates with cellular differentiation. *J Clin Endocrinol Metab* 98 (3), E586-94.

Wang, Y., Sheng, G., Juranek, S., Tuschl, T. and Patel, D. J. (2008b) Structure of the guide-strand-containing argonaute silencing complex. *Nature* 456 (7219), 209-13.

Wasylyk, C., Schlumberger, S. E., Criqui-Filipe, P. and Wasylyk, B. (2002) Sp100 interacts with ETS-1 and stimulates its transcriptional activity. *Mol Cell Biol* 22 (8), 2687-702.

Welcker, M. and Clurman, B. E. (2008) FBW7 ubiquitin ligase: a tumour suppressor at the crossroads of cell division, growth and differentiation. *Nature Reviews Cancer* 8 (2), 83-93.

Wessel, R., Schweizer, J. and Stahl, H. (1992) Simian virus 40 T-antigen DNA helicase is a hexamer which forms a binary complex during bidirectional unwinding from the viral origin of DNA replication. *J Virol* 66 (2), 804-15.

West, L. C. and Cresswell, P. (2013) Expanding roles for GILT in immunity. *Curr Opin Immunol* 25 (1), 103-8.

White, J. R., Lee, J. M., Young, P. R., Hertzberg, R. P., Jurewicz, A. J., Chaikin, M. A., Widdowson, K., Foley, J. J., Martin, L. D., Griswold, D. E. and Sarau, H. M. (1998) Identification of a potent, selective non-peptide CXCR2 antagonist that inhibits interleukin-8-induced neutrophil migration. *J Biol Chem* 273 (17), 10095-8.

Wilcox, K. W., Sheriff, S., Isaac, A. and Taylor, J. L. (2005) SP100B is a repressor of gene expression. *J Cell Biochem* 95 (2), 352-65.

Wilczynska, A. and Bushell, M. (2015) The complexity of miRNA-mediated repression. *Cell Death Differ* 22 (1), 22-33.

Wold, M. S. (1997) Replication protein A: a heterotrimeric, single-stranded DNA-binding protein required for eukaryotic DNA metabolism. *Annu Rev Biochem* 66, 61-92.

Wold, M. S. and Kelly, T. (1988) Purification and characterization of replication protein A, a cellular protein required for in vitro replication of simian virus 40 DNA. *Proc Natl Acad Sci U S A* 85 (8), 2523-7.

Wood, L. D., Parsons, D. W., Jones, S., Lin, J., Sjoblom, T., Leary, R. J., Shen, D., Boca, S. M., Barber, T., Ptak, J., Silliman, N., Szabo, S., Dezso, Z., Ustyanksky, V., Nikolskaya, T., Nikolsky, Y., Karchin, R., Wilson, P. A., Kaminker, J. S., Zhang, Z., Croshaw, R., Willis, J., Dawson, D., Shipitsin, M., Willson, J. K., Sukumar, S., Polyak, K., Park, B. H., Pethiyagoda, C. L., Pant, P. V., Ballinger, D. G., Sparks, A. B., Hartigan, J., Smith, D. R., Suh, E., Papadopoulos, N., Buckhaults, P., Markowitz, S. D., Parmigiani, G., Kinzler, K. W., Velculescu, V. E. and Vogelstein, B. (2007) The genomic landscapes of human breast and colorectal cancers. *Science* 318 (5853), 1108-13.

Woolford, L., Rector, A., Van Ranst, M., Ducki, A., Bennett, M. D., Nicholls, P. K., Warren, K. S., Swan, R. A., Wilcox, G. E. and O'Hara, A. J. (2007) A novel virus detected in papillomas and carcinomas of the endangered western barred bandicoot (Perameles bougainville) exhibits genomic features of both the Papillomaviridae and Polyomaviridae. *J Virol* 81 (24), 13280-90.

Wu, H., Ye, C., Ramirez, D. and Manjunath, N. (2009) Alternative processing of primary microRNA transcripts by Drosha generates 5' end variation of mature microRNA. *PLoS One* 4 (10), e7566.

Wu, S. Y., Lee, A. Y., Hou, S. Y., Kemper, J. K., Erdjument-Bromage, H., Tempst, P. and Chiang, C. M. (2006) Brd4 links chromatin targeting to HPV transcriptional silencing. *Genes Dev* 20 (17), 2383-96.

Xhemalce, B., Robson, S. C. and Kouzarides, T. (2012) Human RNA methyltransferase BCDIN3D regulates microRNA processing. *Cell* 151 (2), 278-88.

Xia, T., O'Hara, A., Araujo, I., Barreto, J., Carvalho, E., Sapucaia, J. B., Ramos, J. C., Luz, E., Pedroso, C., Manrique, M., Toomey, N. L., Brites, C., Dittmer, D. P. and Harrington, W. J., Jr. (2008) EBV microRNAs in primary lymphomas and targeting of CXCL-11 by ebv-mir-BHRF1-3. *Cancer Res* 68 (5), 1436-42.

Xiao, X., Zhao, W., Tian, F., Zhou, X., Zhang, J., Huang, T., Hou, B., Du, C., Wang, S., Mo, Y., Yu, N., Zhou, S., You, J., Zhang, Z., Huang, G. and Zeng, X. (2014) Cytochrome b5 reductase 2 is a novel candidate tumor suppressor gene frequently inactivated by promoter hypermethylation in human nasopharyngeal carcinoma. *Tumour Biol* 35 (4), 3755-63.

Xie, M., Li, M., Vilborg, A., Lee, N., Shu, M. D., Yartseva, V., Sestan, N. and Steitz, J. A. (2013) Mammalian 5'-capped microRNA precursors that generate a single microRNA. *Cell* 155 (7), 1568-80.

Xu, L. G., Wang, Y. Y., Han, K. J., Li, L. Y., Zhai, Z. and Shu, H. B. (2005) VISA is an adapter protein required for virus-triggered IFN-beta signaling. *Mol Cell* 19 (6), 727-40.

Xu, S., Xue, C., Li, J., Bi, Y. and Cao, Y. (2011) Marek's disease virus type 1 microRNA miR-M3 suppresses cisplatin-induced apoptosis by targeting Smad2 of the transforming growth factor beta signal pathway. *J Virol* 85 (1), 276-85.

Yada, M., Hatakeyama, S., Kamura, T., Nishiyama, M., Tsunematsu, R., Imaki, H., Ishida, N., Okumura, F., Nakayama, K. and Nakayama, K. I. (2004) Phosphorylation-dependent degradation of c-Myc is mediated by the F-box protein Fbw7. *Embo j* 23 (10), 2116-25.

Yamashita, A., Chang, T. C., Yamashita, Y., Zhu, W., Zhong, Z., Chen, C. Y. and Shyu, A. B. (2005) Concerted action of poly(A) nucleases and decapping enzyme in mammalian mRNA turnover. *Nat Struct Mol Biol* 12 (12), 1054-63.

Yang, W., Chendrimada, T. P., Wang, Q., Higuchi, M., Seeburg, P. H., Shiekhattar, R. and Nishikura, K. (2006) Modulation of microRNA processing and expression through RNA editing by ADAR deaminases. *Nat Struct Mol Biol* 13 (1), 13-21.

Yang, Z., Jakymiw, A., Wood, M. R., Eystathioy, T., Rubin, R. L., Fritzler, M. J. and Chan, E. K. (2004) GW182 is critical for the stability of GW

bodies expressed during the cell cycle and cell proliferation. *J Cell Sci* 117 (Pt 23), 5567-78.

Yekta, S., Shih, I. H. and Bartel, D. P. (2004) MicroRNA-directed cleavage of HOXB8 mRNA. *Science* 304 (5670), 594-6.

Yeom, K. H., Lee, Y., Han, J., Suh, M. R. and Kim, V. N. (2006) Characterization of DGCR8/Pasha, the essential cofactor for Drosha in primary miRNA processing. *Nucleic Acids Res* 34 (16), 4622-9.

Yi, R., Qin, Y., Macara, I. G. and Cullen, B. R. (2003) Exportin-5 mediates the nuclear export of pre-microRNAs and short hairpin RNAs. *Genes Dev* 17 (24), 3011-6.

Yin, Y., Song, M., Gu, B., Qi, X., Hu, Y., Feng, Y., Liu, H., Zhou, L., Bian, Z., Zhang, J., Zuo, X. and Huang, Z. (2016) Systematic analysis of key miRNAs and related signaling pathways in colorectal tumorigenesis. *Gene* 578 (2), 177-84.

Ying, J., Li, H., Cui, Y., Wong, A. H., Langford, C. and Tao, Q. (2006) Epigenetic disruption of two proapoptotic genes MAPK10/JNK3 and PTPN13/FAP-1 in multiple lymphomas and carcinomas through hypermethylation of a common bidirectional promoter. *Leukemia.* Vol. 20. England: 1173-5.

Yoda, M., Cifuentes, D., Izumi, N., Sakaguchi, Y., Suzuki, T., Giraldez, A. J. and Tomari, Y. (2013) Poly(A)-specific ribonuclease mediates 3'-end trimming of Argonaute2-cleaved precursor microRNAs. *Cell Rep* 5 (3), 715-26.

Yoda, M., Kawamata, T., Paroo, Z., Ye, X., Iwasaki, S., Liu, Q. and Tomari, Y. (2010) ATP-dependent human RISC assembly pathways. *Nat Struct Mol Biol* 17 (1), 17-23.

Yoshida, S., Fukino, K., Harada, H., Nagai, H., Imoto, I., Inazawa, J., Takahashi, H., Teramoto, A. and Emi, M. (2001) The c-Jun NH2-terminal kinase3 (JNK3) gene: genomic structure, chromosomal assignment, and loss of expression in brain tumors. *J Hum Genet* 46 (4), 182-7.

Young, J. L., Roffers, S. D., Gloeckler Ries, L. A., Fritz, A. G. and Hurlbut, A. A. (2000) *SEER SUMMARY STAGING MANUAL-2000*

CODES AND CODING INSTRUCTIONS. National Cancer Institute. *http://seer.cancer.gov/tools/ssm/intro.pdf*

Zahler, A. M., Neugebauer, K. M., Stolk, J. A. and Roth, M. B. (1993) Human SR proteins and isolation of a cDNA encoding SRp75. *Mol Cell Biol* 13 (7), 4023-8.

Zdanowicz, A., Thermann, R., Kowalska, J., Jemielity, J., Duncan, K., Preiss, T., Darzynkiewicz, E. and Hentze, M. W. (2009) Drosophila miR2 primarily targets the m7GpppN cap structure for translational repression. *Mol Cell* 35 (6), 881-8.

Zee, J. M., Shideler, K. K., Eystathioy, T., Bruecks, A. K., Fritzler, M. J. and Mydlarski, P. R. (2008) GW bodies: cytoplasmic compartments in normal human skin. *J Invest Dermatol* 128 (12), 2909-12.

Zeng, Y. and Cullen, B. R. (2005) Efficient processing of primary microRNA hairpins by Drosha requires flanking nonstructured RNA sequences. *J Biol Chem* 280 (30), 27595-603.

Zeng, Y., Wagner, E. J. and Cullen, B. R. (2002) Both natural and designed micro RNAs can inhibit the expression of cognate mRNAs when expressed in human cells. *Mol Cell* 9 (6), 1327-33.

Zeng, Y., Yi, R. and Cullen, B. R. (2003) MicroRNAs and small interfering RNAs can inhibit mRNA expression by similar mechanisms. *Proc Natl Acad Sci U S A* 100 (17), 9779-84.

Zerrahn, J., Knippschild, U., Winkler, T. and Deppert, W. (1993) Independent expression of the transforming amino-terminal domain of SV40 large I antigen from an alternatively spliced third SV40 early mRNA. *Embo j* 12 (12), 4739-46.

Zhang, H., Kolb, F. A., Brondani, V., Billy, E. and Filipowicz, W. (2002) Human Dicer preferentially cleaves dsRNAs at their termini without a requirement for ATP. *Embo j* 21 (21), 5875-85.

Zhang, H., Kolb, F. A., Jaskiewicz, L., Westhof, E. and Filipowicz, W. (2004) Single processing center models for human Dicer and bacterial RNase III. *Cell* 118 (1), 57-68.

Zhang, Y., Guo, X., Xiong, L., Yu, L., Li, Z., Guo, Q., Li, B. and Lin, N. (2014) Comprehensive analysis of microRNA-regulated protein interaction network reveals the tumor suppressive role of microRNA-149 in human hepatocellular carcinoma via targeting AKT-mTOR pathway. *Mol Cancer* 13, 253.

Zhao, W., Hisamuddin, I. M., Nandan, M. O., Babbin, B. A., Lamb, N. E. and Yang, V. W. (2004) Identification of Kruppel-like factor 4 as a potential tumor suppressor gene in colorectal cancer. *Oncogene* 23 (2), 395-402.

Zhao, Y., Xu, H., Yao, Y., Smith, L. P., Kgosana, L., Green, J., Petherbridge, L., Baigent, S. J. and Nair, V. (2011) Critical role of the virus-encoded microRNA-155 ortholog in the induction of Marek's disease lymphomas. *PLoS Pathog* 7 (2), e1001305.

Zhou, H., Xia, X. G. and Xu, Z. (2005) An RNA polymerase II construct synthesizes short-hairpin RNA with a quantitative indicator and mediates highly efficient RNAi. *Nucleic Acids Res* 33 (6), e62.

Zhu, H., Qiu, H., Yoon, H. W. P., Huang, S. and Bunn, H. F. (1999) Identification of a cytochrome b-type NAD(P)H oxidoreductase ubiquitously expressed in human cells. *Proc Natl Acad Sci U S A* 96 (26), 14742-7.

Ziegelbauer, J. M., Sullivan, C. S. and Ganem, D. (2009) Tandem array-based expression screens identify host mRNA targets of virus-encoded microRNAs. *Nat Genet* 41 (1), 130-4.

Zuber, J., Shi, J., Wang, E., Rappaport, A. R., Herrmann, H., Sison, E. A., Magoon, D., Qi, J., Blatt, K., Wunderlich, M., Taylor, M. J., Johns, C., Chicas, A., Mulloy, J. C., Kogan, S. C., Brown, P., Valent, P., Bradner, J. E., Lowe, S. W. and Vakoc, C. R. (2011) RNAi screen identifies Brd4 as a therapeutic target in acute myeloid leukaemia. *Nature* 478 (7370), 524-8.